



HAL
open science

Regulation of adult muscle stem cell quiescence by Notch signalling

Meryem Baghdadi

► **To cite this version:**

Meryem Baghdadi. Regulation of adult muscle stem cell quiescence by Notch signalling. Development Biology. Université Pierre et Marie Curie - Paris VI, 2017. English. NNT : 2017PA066461 . tel-01878356

HAL Id: tel-01878356

<https://theses.hal.science/tel-01878356>

Submitted on 21 Sep 2018

HAL is a multi-disciplinary open access archive for the deposit and dissemination of scientific research documents, whether they are published or not. The documents may come from teaching and research institutions in France or abroad, or from public or private research centers.

L'archive ouverte pluridisciplinaire **HAL**, est destinée au dépôt et à la diffusion de documents scientifiques de niveau recherche, publiés ou non, émanant des établissements d'enseignement et de recherche français ou étrangers, des laboratoires publics ou privés.

Université Pierre et Marie Curie

Complexité du vivant - ED515

Equipe Cellules Souches et Développement, CNRS URA 3738

Institut Pasteur, 25 rue du Docteur Roux, 75015 Paris

Régulation de la quiescence des cellules souches du muscle squelettique par la voie Notch

Regulation of adult muscle stem cell quiescence by Notch signalling

Par Meryem Baghdadi

Thèse de doctorat de Cellules souches et Médecine Régénérative

Dirigée par Shhragim Tajbakhsh

Présentée et soutenue publiquement le 19 Septembre 2017

Devant un jury composé de :

M. le Pr. Thierry Jaffredo	Président du jury
Mme la Dr. Jyotsna Dhawan	Rapportrice
M. le Pr. Freddy Radtke	Rapporteur
Mme. la Dr. Silvia Fre	Examinatrice
Mme la Pr. Maria Dominguez	Examinatrice
M. le Pr. Shhragim Tajbakhsh	Directeur de thèse



*We will either find a way, or make one
Hannibal*

Acknowledgements

First and foremost, I would like to express my sincere gratitude to all the jury members for accepting to evaluate my thesis and for their precious time especially at this time of the year. I would like to thank Pr. Freddy Radtke and Dr. Jyotsna Dhawan for evaluating my manuscripts, their precious comments and for coming all the way from Switzerland and India respectively to attend my defence.

Also, Pr. Thierry Jaffredo that first evaluated me as a Master 2 student in 2013 and for accepting to be the president of the PhD jury today. I hope you are satisfied by the evolution of the master student I was.

My sincere thanks also go to Dr. Maria Dominguez for accepting to evaluate my thesis as a micro-RNA expert, and for travelling from Spain to be present at my defence.

And finally, I would like to thank Dr. Silvia Fre for accepting to be in my PhD committee before being part of my PhD jury today. Thank you so much for all the advices and support for these past four years. You were more than a tutor to me.

“Mentor: noun, experienced and trusted adviser”. I was lucky enough to have two of them!

Firstly, I would like to thank my PhD supervisor Shahragim for “rescuing” me when I quit my first Masters lab. Thank you Shahragim, for your trust during these past 4 years, and for the freedom you gave me. Freedom to try, to fail, try again and eventually succeed. Thank you for the freedom to disagree with you and be myself. I have learnt so much with you, scientifically speaking but also in life: “You are never dead until you are dead”, right? You always have been very demanding but that was really stimulating and challenging. Your support and trust were a driving force all along this tough road. Thank you again for all the opportunities and cards you gave me for the future, I will do my best to use them wisely.

Secondly, I want to sincerely thank my “unofficial” supervisor/other mentor and friend Philippos, for his trust and support. Thank you for involving me in the Collagen project: we did such a nice work together! I cut my teeth working with you at the bench and you contributed to the scientist I am today. Thank you, for caring about me when I work too much, and for pushing me when I lose motivation. I will never thank you enough for the trust you put in me; it gave me the fuel to keep going.

I hope that both of you, Shah and Pmour are proud of the scientist I became and of the work that we have done together.

Je souhaiterais remercier tous les membres, passés et présents, du Tajbakhsh Lab; je vous souhaite à tous beaucoup de réussite. A ceux qui ont cru en moi qui ont quitté le labo, j'espère vous revoir bientôt et partager encore avec vous.

Je souhaiterais remercier David Castel pour m'avoir légué la suite de son projet microRNA, j'espère que tu es satisfait de ce que j'en ai fait.

Je remercie également Barbara et Gérard Dumas qui m'ont appris tous les basiques du muscle, et du labo lorsque je suis arrivée et bien après.

Merci Eglantine pour ton aide lors de l'écriture de ma première revue, j'ai autant appris de la phylogénie que de la gestion de la frustration. Merci Brendan pour tout ce que tu m'as appris en biologie moléculaire et toutes les discussions que nous avons eu; j'espère ne pas avoir été trop nulle comme élève. Zuza, merci pour tes attentions quotidiennes et ton aide spontanée. In addition to these very talented postdoc, I also want to deeply thank the fireball Daniela, for your involvement in the miR project, your energy and ideas. Sylvain, même si ça n'a pas toujours été facile entre nous, je te remercie pour ton aide technique quand tu le pouvais. Merci à toi Marc pour ton énergie, ton aide constante et ta bonne humeur (après la banane de 10h). Francesca, things have not always been easy but you always tried to help me the way you could! Thank you.

Je vous souhaite à tous beaucoup de succès et la réussite à laquelle vous aspirez.

Je remercie ceux qui sont devenus plus que des collègues; Glenda, ma superwoman Juanita! Merci d'avoir partagé avec moi cette force que tu as et que j'admire tant. Merci de me comprendre autant et de m'avoir soutenu au labo et en dehors. Merci à au brillant technicien, Gilles pour son aide technique. Ta bienveillance et ta gentillesse me redonnent le sourire et m'apaise quand tout va mal. J'aimerais te mettre dans une Pokeball et t'emmener avec moi.

Merci Clémire pour le travail fabuleux que tu fais dans la joie et la bonne humeur. J'adore venir dans ton jardin secret ou règne musique et bonnes ondes.

Merci à Sophie et Sandrine du CIH pour votre aide technique et aussi pour m'avoir allumer le FACS tant de fois! Grâce à vous j'ai gagné énormément de temps et beaucoup rit !

*Je remercie certains membres de l'équipe Chrétien : David B, David H, Pierre, Patricia et Franck pour leur aide technique et les vannes à chaque fois que je passe au slide-scanner !
Je remercie aussi tous les membres du département et plus particulièrement les membres de Miria team, pour les discussions stimulantes et l'aide lors de manip' ponctuelles.*

Merci Chloé pour ton soutien infailible lors de ce parcours que l'on a fait l'une à côté de l'autre.

Merci Léo pour ton aide technique et pour ton soutien quand je « craque ».

Merci du fond du cœur à ma dimère d'enzyme, Céline, de venir d'aussi loin pour moi ! Tout comme Marielle, qui m'a appris à utiliser une pipette en 3^e année et qui est aujourd'hui une post-doc brillante. J'espère que tu es fière du moi maintenant !

Elodie, Quynh-Lan, Emmanuelle et Marie, vous êtes encore mieux que les sœurs dont j'ai pu rêver. Merci pour votre amitié/amour qui me rappelle que je ne suis jamais seule. Merci de me sortir de mon labo et de mon lit ! Je vous adore.

Merci Joao pour ton soutien et ta force. J'ai pu avancer grâce à toi et à la confiance que tu m'infuses. Je suis tellement fière de partager ma vie avec un scientifique si brillant et homme qui m'a toujours poussé à respecter mes valeurs. Tu m'as appris l'acceptation et l'amour de soi malgré le monde extérieur. J'ai hâte de te retrouver.

Merci à mon père d'adoption, Gabriel pour son soutien depuis toujours.

Et pour terminer, tout cela n'aurait jamais été possible sans ton soutien inconditionnel Maman. Merci d'être toujours là pour moi, dans les bons et mauvais moments. J'espère un jour n'être pour mes enfants que la moitié de la mère que tu as été pour moi. Que Dieu te garde auprès de moi.

Table of Contents

Abstract	1
Résumé	3
INTRODUCTION	5
Chapter 1.	7
Skeletal muscle and its resident stem cells.....	7
1. Skeletal muscle structure and function	9
1.1. Skeletal muscle as a contractile unit	9
1.2. Muscle regeneration.....	10
2. Satellite cells as adult skeletal muscle stem cells	13
2.1. A brief history	13
2.2. Molecular regulation of muscle stem cell emergence	14
2.3. Heterogeneity in the muscle stem cell population	17
3. Functions of muscle stem cells	19
3.1. Adult myogenesis	19
3.1.1. Satellite cell activation and differentiation	21
3.1.2. Satellite cell self-renewal	22
Chapter 2.	25
Stem cell niche is essential for quiescence.....	25
1. Stem cell quiescence	27
1.1. Identification of quiescent stem cells.....	27
1.2. <i>Ex vivo</i> induction of quiescence.....	28
1.3. Molecular signature of quiescence	28
1.3.1. Epigenetic control	28
1.3.2. Cell cycle regulators	29
2. Molecular signature of MuSCs	29
2.1.1. Calcitonin receptor.....	30
2.1.2. Teneurin-4 or Odz4.....	32
2. The stem cell niche	33
2.1. Extracellular matrix: powerful modulator of cell behaviour	34
2.2. ECM-cell interaction.....	36
2.3. Biophysical properties of ECM	36
2.4. Collagens constitute a major component of the ECM	38
2.4.1. Insights from Collagen V.....	38
3. The MuSCs niche	39
3.1. Extracellular matrix and associated factors	40
Chapter 3.	43
Post-transcriptional regulation of myogenesis: a role for microRNAs	43

1. The discovery of microRNAs	45
2. MicroRNAs: Genomics, biogenesis, mechanism and function	45
2.1. Biogenesis of microRNAs	45
2.2. MicroRNAs arise from distinct genomic loci.....	47
2.3. MicroRNA prediction tools	48
3. MicroRNAs in cell and tissue regulation.....	49
4. Regulation of myogenesis by microRNAs	50
5. Inhibition of microRNAs using “Antagomirs”	53
Chapter 4.	55
Notch signalling is a pleiotropic regulator of stem cells	55
1. An introduction to the world of Notch	57
2. Notch receptors, ligands and the cascade	57
3. Notch targets genes and their regulation	61
4. Notch signalling in the regulation of stem cell fate.....	62
5. Notch signalling in skeletal muscle and satellite cells.....	63
RESULTS	69
Part I:	71
Notch-induced Collagen V maintains muscle stem cells by reciprocal activation of the Calcitonin Receptor	71
Part II:.....	111
The Notch-induced microRNA-708 maintains quiescence and regulates migratory behavior of adult muscle stem cells	111
CONCLUSIONS AND PERSPECTIVES	153
1. Context of this thesis project	155
2. Notch signalling regulates ECM niche components.....	156
3. Notch signalling positions MuSCs in their niche	158
4. Potential regulation of Notch signalling by microRNAs.....	161
ANNEX 1: Review	163
Regulation and phylogeny of muscle regeneration	163
ANNEX 2: Resource paper	175
Comparison of multiple transcriptomes using a new analytical pipeline <i>Sherpa</i> exposes unified and divergent features of quiescent and activated skeletal muscle stem cells.....	175
ANNEX 3:	213
Small-RNA sequencing identifies dynamic microRNA deregulation during muscle lineage progression.....	213
REFERENCES	245

Abstract

Adult skeletal muscles can regenerate after repeated trauma, yet our understanding of how adult muscle satellite (stem) cells (MuSCs) restore muscle integrity and homeostasis after regeneration is limited. In the adult mouse, MuSCs are quiescent and located between the basal lamina and the myofibre. After injury, they re-enter the cell cycle, proliferate, differentiate and fuse to restore the damaged fibre. A subpopulation of myogenic cells then self-renews and replenishes the stem cell pool for future repair. The paired/homeodomain transcription factor Pax7 is expressed all skeletal muscle stem and progenitor cells and various genetically modified mice have exploited this locus for isolation and analysis of MuSCs. When MuSCs are removed from their niche, they rapidly express the commitment marker Myod and proliferate. The basal lamina that ensheaths MuSCs is rich in collagens, non-collagenous glycoproteins and proteoglycans. Whether these and other extracellular matrix (ECM) proteins constitute functional components of MuSCs niche remains unclear. Moreover, although signalling pathways that maintain MuSCs quiescence have been identified, how these regulate stem cell properties and niche composition remains largely unknown. Sustained, high activity of the Notch signalling pathway is critical for the maintenance of MuSCs in a quiescence state. Of interest, whole-genome ChIP for direct Notch/Rbpj transcriptional targets identified specific micro-RNAs and collagen genes in satellite cells. Using genetic tools to conditionally activate or abrogate Notch signalling, we demonstrate that the expression of these target genes is controlled by the Notch pathway *in vitro* and *in vivo*. Further, we propose that Collagen V and miR708 can contribute cell-autonomously to the generation of the MuSC niche via a Notch signalling-regulated mechanism.

Résumé

Le muscle squelettique adulte est capable de se régénérer à plusieurs reprises après blessure grâce à sa population de cellules souches résidentes : les cellules satellites. Cependant, les mécanismes impliquant les cellules satellite dans la recouvrement de l'homéostasie et de l'intégrité musculaire ne sont toujours pas clairs. Chez l'adulte, les cellules satellites sont quiescentes et localisées dans une niche entre la lame basale et la fibre musculaire. Après blessure, elles entrent à nouveau dans le cycle cellulaire, prolifèrent, se différencient et fusionnent afin de restaurer les fibres endommagées. Le pair-homeo domaine facteur de transcription Pax7 marque les cellules souches périnatales et postnatales et permet l'isolation de ces cellules à l'état souche et activé. Lorsque la niche des cellules satellite est altérée elles expriment rapidement le marqueur d'activation *Myod* puis prolifèrent. La lame basale des cellules souches est riche en collagène, glycoprotéines qui ne font pas partie de la famille des collagènes et de protéoglycan. Cependant, le mécanisme de fonction de ces protéines de la matrice extracellulaire (MEC) dans le maintien de la cellule satellite dans sa niche est toujours inconnu. De plus, l'interaction entre la MEC et des voies de signalisation cellulaire essentielles au maintien des cellules souches quiescentes sont toujours un mystère. Nous avons identifiés la voie Notch comme effecteur indispensable à la quiescence des cellules satellites. Un ChIP screening dans des cellules musculaires nous a permis d'identifier des micro-RNAs et collagènes spécifiques comme des gènes cibles de la voie Notch. L'utilisation d'outils génétiques permettant de moduler l'activité de la voie Notch démontrent que ces micro-RNAs et collagènes sont régulés transcriptionnellement par la voie Notch *in vitro* et *in vivo*. Nous proposons que le Collagène de type V et miR-708, induits par Notch, peuvent autoréguler la niche des cellules souches.

INTRODUCTION

Chapter 1.

Skeletal muscle and its resident stem cells

1. Skeletal muscle structure and function

1.1. Skeletal muscle as a contractile unit

Skeletal muscle is one of the largest tissues in mammals. It allows voluntary movement and plays a key role in regulating metabolism and homeostasis of the organism. Throughout evolution, skeletal muscle is essentially defined by the succession of motor units which consists of a motoneuron and all of the muscle fibres innervated by that motoneuron (**Figure 1**). Myofibres are multinucleated cells and compose the cellular units of mature skeletal muscles. The structure of myofibres is strikingly repetitive at all sites in the organism, and the basic principles that govern the development of myofibres are conserved from *Drosophila* to humans. This structure is illustrated by the linear and repetitive arrangement of sarcomeres composed by an actin and myosin network together with associated proteins that enable muscle contraction (**Figure 1**). Different fibre types have been described, and these can be classified as slow-oxidative, fast-oxidative-glycolytic, and fast-glycolytic (Peter et al., 1972). The inherent contractile speed of each fibre-type cluster is determined essentially by the myosin motor protein isoform that is expressed predominantly. For example, the slow-oxidative unit expresses primarily a slow myosin heavy chain (MyHC) gene designated as slow or type I. The fast-oxidative unit expresses a combination of the fast type IIa and IIx MyHC genes, whereas the fast-glycolytic unit expresses both the fast IIb and IIx MyHC genes (Larsson et al., 1991). The accessibility of the hind limb *Tibialis anterior* muscle (below the knee), a mix of slow and fast fibres, has made it one of the major sites for experimentation in studies on muscle homeostasis and regeneration. Finally, skeletal muscle allows the study of plasticity at the tissue and cellular level in different conditions such as overload (exercise), sarcopenia (muscle loss), ageing, and disease (myopathies).

The resident stem cells of skeletal muscle, historically called satellite cells, are located between the basement membrane containing a basal lamina, and the plasmalemma of the muscle fibre (Mauro, 1961) (**Figure 1**). Importantly, $\approx 90\%$ of Muscle stem cells (MuSCs) are located in tight proximity with vessels (within $21\mu\text{m}$) (Christov et al., 2007) (**Figure 1**), suggesting a communication between the vasculature and the MuSCs.

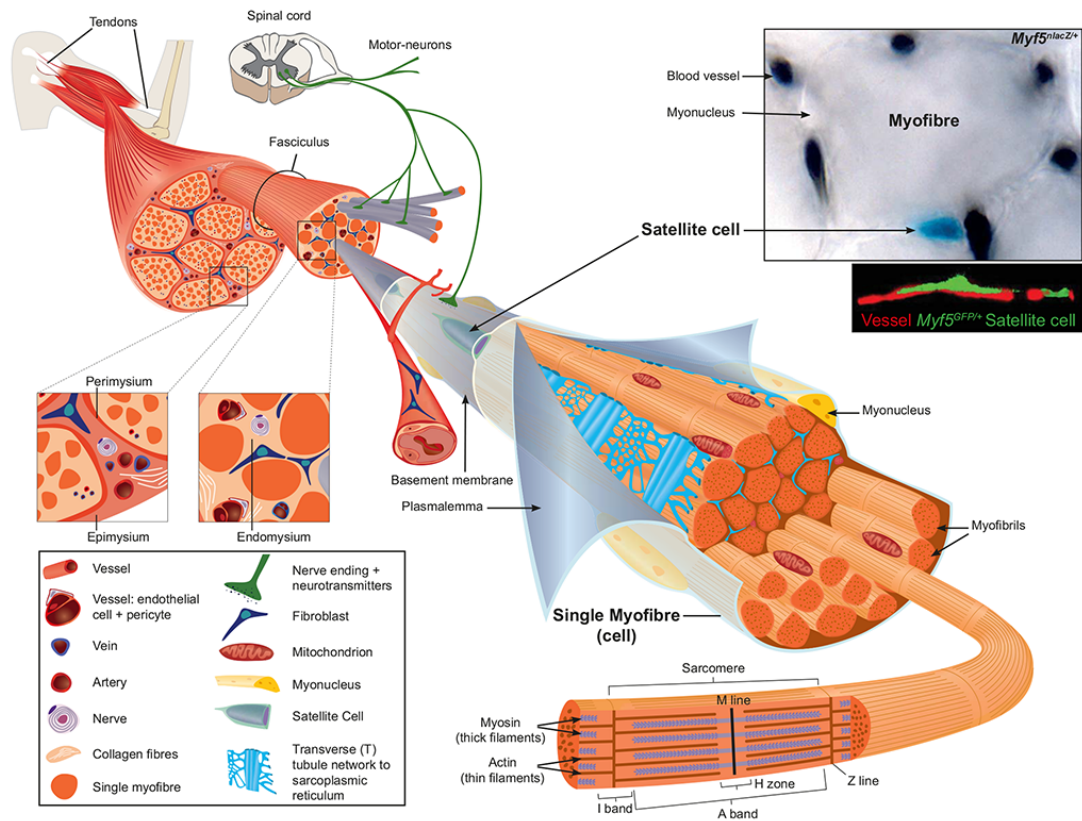


Figure 1. Scheme of skeletal muscle and associated structures. Skeletal muscles in general are attached at each end to the bone via tendons. Three connective tissue layers can be distinguished in skeletal muscle. The epimysium is the deep fascia component that encloses the entire muscle and it is contiguous with the tendon and endosteum (fascia surrounding bone). The perimysium encloses individual muscle fibers into fasciculi (bundles). The endomysium is located between fibers and it encloses individual muscle fibers. Within the muscle cell (myofibre) the major intracellular source of calcium needed for muscle contraction is the sarcoplasmic reticulum, which connects to the transverse (T) tubules, and these surround the sarcomeres. Satellite cells are located between the basement membrane and the plasmalemma of the myofibre. Note the close proximity of the vessel, stained with India ink on the muscle section, and satellite cell from adult *Myf5^{nlacZ+}* mouse stained with X-gal (upper image), or immunostained with GFP from a *Myf5^{GFP/+}* adult mouse. (Tajbakhsh, 2009)

1.2. Muscle regeneration

The remarkable regenerative ability of skeletal muscle was shown several decades ago in rats that had received weekly injections of bupivacaine (anaesthetic drug that blocks sodium channels (see, (Gayraud-Morel et al., 2009)) for 6 months, and did not show reduction or exhaustion of muscle fibres repair capacity (Sadeh et al., 1985). Similarly in mouse, after 50 bupivacaine injections into the TA muscle mice regenerated their muscle without loss of myofibres or gain of fibrotic areas (Luz

et al., 2002). In human, skeletal muscle injuries resulting from direct trauma (contusions), partial tears, fatigue, following surgical procedures or myopathies are common and present a challenge in traumatology, as therapy and recuperation are not well supported. The most commonly used acute murine injury models involve intramuscular injection of myotoxins (cardiotoxin and notexin), BaCl₂, and mechanical injury (freeze, needle or crush injuries) (Gayraud-Morel et al., 2009; Hardy et al., 2016) (see also Annex 1). For the purpose of our study, we will focus on the injury following the injection of myotoxins. Cardiotoxin (CTX, protein kinase C inhibitor) and Notexin (NTX, phospholipaseA2) are isolated from snake venom, and they trigger an increase in Ca²⁺ influx followed by fibre depolarization and consequently myofibre hypercontraction and necrosis (Gayraud-Morel et al., 2009; Hardy et al., 2016). After trauma, skeletal muscle regeneration follows three distinguishable and overlapping phases (**Figure 2**). The first phase of degeneration following severe injury is characterized by necrosis and significant inflammation (0 to 5 days post-injury (dpi)). After clearance of cellular debris, new fibres form and they transiently express embryonic and neonatal Myosin Heavy Chain (MyHC) from 3-14 dpi. The remodelling phase is characterized by hyperplasia and hypertrophy regulated in part by the IGF-1/Akt and TGFβ /Smad pathways. IGF-1 affects the balance between protein synthesis and protein degradation thus inducing muscle hypertrophy, whereas TGFβ negatively controls muscle growth (Schiaffino et al., 2013).

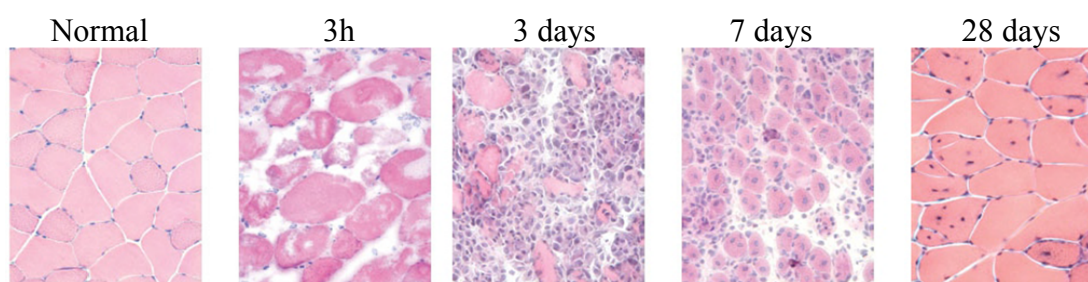


Figure 2. Regeneration of *Tibialis anterior* (TA) muscle after myotoxin injury. Three hours after injury with the snake venom notexin, severe necrosis is apparent. After 3 days, most of the necrotic fibres are cleared by immune infiltrate and empty spaces are colonized by new myoblasts derived from satellite cells after activation and proliferation. Seven days post-injury, myoblasts continue to proliferate and fuse to restore fibre homeostasis (central nuclei). By 28 days, muscle regeneration appears to be complete histologically with the presence of centrally located myonuclei, a hallmark of regeneration. (Gayraud-Morel et al., 2009)

Although satellite cells play a crucial role in restoring myofibres following injury, it is clear that other cells types impact on the regeneration process (**Figure 3**) (see Annex 1). For example, fibro-adipogenic progenitors (FAPs) reside in the muscle interstitium and they play a significant myogenic and trophic role in muscle physiology during regeneration (Fiore et al., 2016; Joe et al., 2010; Lemos et al., 2015; Uezumi et al., 2010). Similarly, macrophages play a critical role during the initial stages following tissue damage as they are required for phagocytosis and cytokines release. The first wave of macrophages (peak at 3dpi) promotes myoblast proliferation via the secretion of pro-inflammatory molecules such as TNF α (Tumor Necrosis Factor α), INF α (Interferon α) and IL6 (Interleukin 6) (Lu et al., 2011a). Subsequently, macrophages undergo a phenotypical and functional switch toward an anti-inflammatory fate characterized by the production of IL4 and IL10, for example (Arnold et al., 2007). As mentioned previously, this anti-inflammatory response stimulates FAPs, mesoangioblasts, and also directly myoblasts to promote differentiation and fusion (Chazaud et al., 2003; Saclier et al., 2013). In addition, pericytes, located peripheral to the endothelium of microvessels, are known to be involved in blood vessel growth, remodelling, homeostasis, and permeability (Armulik et al., 2011) (**Figure 3**). The integrity of vessels is essential for muscle repair and homeostasis and it has been proposed that microvascular insufficiency could be responsible for the local inflammation and necrosis observed in both dystrophin-deficient mouse and human (Cazzato, 1968). Moreover, pericytes in skeletal muscles are constituents of the satellite cell niche where they secrete molecules such as IGF1 (insulin growth factor-1) or ANGPT1 (angiopoetin-1) to modulate postnatal myofibres growth and satellite cell entry in quiescence, respectively (Kostallari et al., 2015).

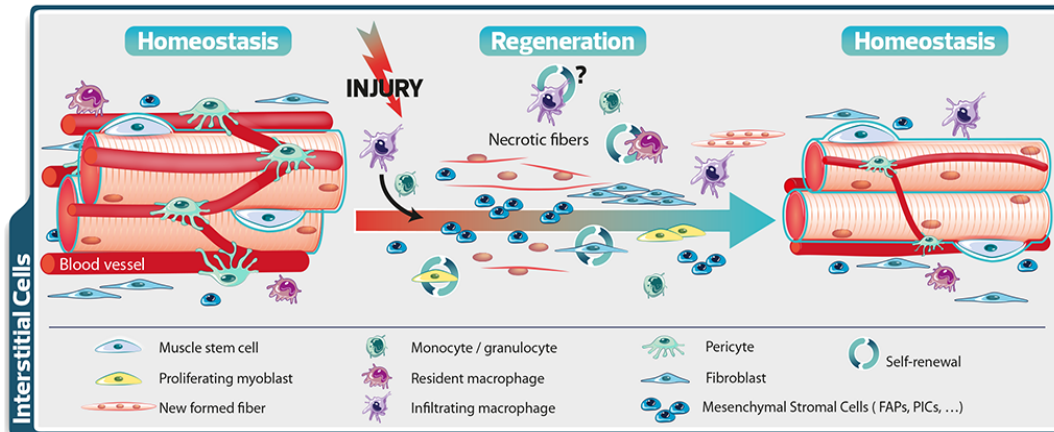


Figure 3. Synoptic view of the different cell populations involved in muscle repair. Although the generation of new fibres is dependent on MuSCs, other cell types such as macrophages, monocytes, mesenchymal stromal cells (including FAPs, mesoangioblasts and PICs), pericytes and fibroblasts are also critical for the regeneration process. (Baghdadi and Tajbakhsh, Annex 1).

2. Satellite cells as adult skeletal muscle stem cells

2.1. A brief history

The regenerative potential of muscle was first shown in the 1860s, but almost a century elapsed before the satellite cell was discovered. Using electron microscopy, Alexander Mauro observed a group of mononucleated cells located at the periphery of the adult skeletal muscle fibres from the *Tibialis anticus* of the *Xenopus* and rat (Mauro, 1961). These cells were named satellite cells due to their localisation on the periphery of the myofibres (**Figure 4**).

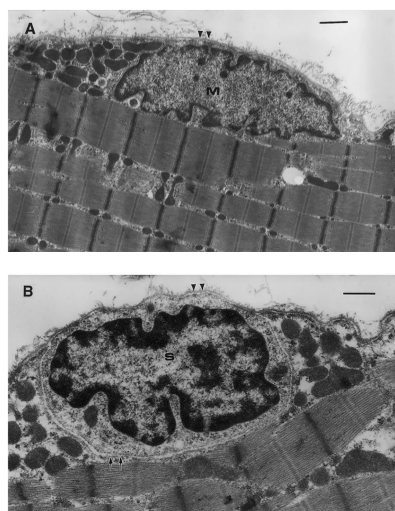


Figure 4. Electron micrograph of a typical myonucleus (A) and satellite cells (B) in mouse. Muscle satellite cell (S) is inside the basal lamina (arrowheads) and outside the sarcolemma (arrows) with an independent cytoplasm. In contrast, a myonucleus (M) is located inside the sarcolemma of the muscle fibre. Bar: 1µm. (Sinha-Hikim et al., 2003)

The absence of satellite cells in cardiac muscle prompted him to speculate a role for these cells as skeletal-muscle specific precursor cells: "satellite cells are merely

dormant myoblasts that failed to fuse with other myoblasts and are ready to recapitulate the embryonic development of skeletal muscle fibre when the main multinucleate cell is damaged" (Mauro, 1961). Interestingly, the position of this cell adjacent to the myofibre appears to be highly conserved in evolution, and similar satellite cells have been observed in multiple species, from the arthropods to mammals (see Baghdadi and Tajbakhsh, Annex 1). Electron microscopy also revealed other morphological characteristics of satellite cells: large nuclear-to-cytoplasmic ratio, few organelles, small nucleus, and condensed interphase chromatin.

The role of satellite cells in regeneration was first assessed after crush injury to the small web muscles of the East African fruit bat, *Eidolon helvum* (Church and Noronha, 1965). This study reported that satellite cells disappear from the highly injured area at the same time as the emergence of mitotic myoblasts, then reappear on myotubes after repair. Authors provided evidence that satellite cells were skeletal muscle “reserve cells”, capable of generating new fibres upon injury and replenishing the initial pool of cells. Additional [³H]-Thymidine tracing experiments combined with electron microscopy demonstrated that satellite cells are mitotically quiescent in adult muscle contribute to myofibre nuclei upon injury (Moss and Leblond, 1970; Reznik, 1969). The same studies also demonstrated that satellite cells give rise to proliferating myoblasts (myogenic progenitors cells), which were previously shown to form multinucleated myotubes *in vitro* (Konigsberg, 1963; Snow, 1977; Yaffe, 1969). Moreover, *in vivo* [³H]-Thymidine donor satellite cells specific labelling after free grafting of the muscle showed the presence of labelled nuclei on the periphery of regenerated myofibres in the host (Gutmann et al., 1976).

2.2. Molecular regulation of muscle stem cell emergence

During early development, muscle stem/progenitor cells migrate underneath the dorsal part of the somites called the dermomyotome (DM) and differentiate into mononucleated myocytes to form the myotome. In response to key transcription factors, committed myocytes align and fuse to generate small multinucleated myofibres during primary myogenesis in the embryo (from E11-E14.5), then myofibres containing a few hundred myonuclei during secondary myogenesis (from E14.5-to birth). During the early and late perinatal period that lasts about 4 weeks,

continued myoblast fusion, or hyperplasia, is followed by muscle hypertrophy (Sambasivan and Tajbakhsh, 2007; Tajbakhsh, 2009; White et al., 2010) (**Figure 5**).

The developmental origin of satellite cells was first shown in a chick-quail chimera study: satellite cells of quail origin were found after replacement of chick somitic mesoderm by one from quail. In addition, electroporation of the central dermomyotome (the dorsal somite) in the trunk with a molecular marker showed that marked cells gave rise to Pax7⁺ satellite cells after hatching, thereby establishing the dermomyotome origin of satellite cells, in chick (Armand et al., 1983; Gros et al., 2005). Further evidences that satellite cells also originate from Pax3/7⁺ cells coming from the somites have been reported in the mouse (Kassar-Duchossoy et al., 2005; Relaix et al., 2005).

Emerging satellite cells are found underneath a basement membrane from about 2 days before birth in mice and they further proliferate until the mid-perinatal stage (Kassar-Duchossoy et al., 2005). The majority of quiescent MuSCs are established from about 2-4 weeks after birth (Tajbakhsh, 2009; White et al., 2010). During prenatal and postnatal myogenesis, stem cell self-renewal and commitment are governed by a gene regulatory network that includes the paired/homeodomain transcription factors *Pax3* and *Pax7*, and basic helix-loop-helix (bHLH) myogenic regulatory factors (MRFs), *Myf5*, *Mrf4*, *Myod* and *Myogenin* (**Figure 5**). *Pax3* plays a critical role in establishing MuSCs during embryonic development (except in cranial-derived muscles) and *Pax7* during late foetal and perinatal growth. Indeed, *Pax3:Pax7* double mutant mice exhibit severe hypoplasia due to a loss of stem and progenitor cells from mid embryonic stages, and these *Pax* genes appear to regulate apoptosis (Relaix et al., 2006; Relaix et al., 2005; Sambasivan et al., 2009). During perinatal growth, *Pax7* null mice are deficient in the number of MuSCs and fail to regenerate muscle after injury in adult mice (Lepper et al., 2009; Oustanina et al., 2004; Seale et al., 2000; von Maltzahn et al., 2013).

Experiments using simple or double knockout mice have shown the temporal and functional roles of these different factors during myogenesis. *Myf5*, *Mrf4* and *Myod* assign myogenic cell fate of muscle progenitor cells to give rise to myoblasts

(Kassar-Duchossoy et al., 2004; Rudnicki et al., 1993; Tajbakhsh et al., 1996) whereas *Myogenin* plays a crucial role in myoblast differentiation prenatally (Hasty et al., 1993; Nabeshima et al., 1993) but not postnatally as the conditional mutation of *Myogenin* in the adult has a relatively mild phenotype (Knapp et al., 2006; Meadows et al., 2008; Venuti et al., 1995). In the adult, *Myod* deficient mice that survive have increased precursor cell numbers accompanied by a delay in regeneration (Megency et al., 1996; White et al., 2000); whereas *Myf5* null mice display a slight delay in repair (Gayraud-Morel et al., 2007). These studies suggested that *Myf5*, *Mrf4* and *Myod* could in some cases compensate for each other's function. Whereas *Mrf4* plays a role in embryonic progenitors, *Myf5* and *Myod* continue to regulate muscle progenitor cell fate throughout foetal and postnatal life. Interestingly, additional transcription factors have been shown to interact with MYOD to regulate myogenesis. For instance, ChIP-seq data demonstrated that KLF5 (Kruppel-like factor, member of a subfamily of zinc-finger transcription factors) (Hayashi et al., 2016) as well as RUNX1 (Umansky et al., 2015) binding to *Myod*-regulated enhancers is necessary to activate a set of myogenic differentiation genes.

The MRFs form heterodimers with members of the E-protein bHLH family (E2A, E2-2 and HEB) and bind to a consensus E-box sequence (CANNTG) to activate muscle-specific gene expression. Although there are millions of consensus E-boxes in the genome that can bind of the myogenic bHLH factors, the productivity of this occupancy and the specificity of binding is determined by flanking nucleotides in the E-box, thereby effectively reducing the number of sites that are functional (Cao et al., 2010).

It is likely that MRFs combined with other transcription factors fine-tune the myogenesis process and it would be important to further explore the set of co-activators/repressors required for each step of muscle repair.

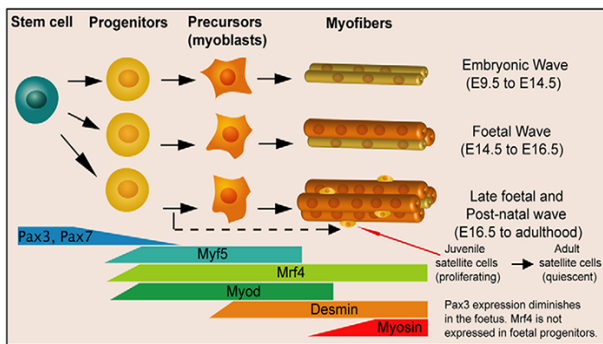


Figure 5. Expression of MRFs during lineage progression of myogenesis. *Pax3* and *Pax7* expressions decline in the foetus. *Myf5*, *MyoD* and *Mrf4* expressing instruct to the progenitors cell a myogenic program. Desmin is an intermediate filament protein express in the muscle and Myosin is a component of the contractile apparatus. Around E16.5 *Pax7*⁺ cells appear in satellite cell position (see also Fig. 6). (Sambasivan and Tajbakhsh, 2007)

2.3. Heterogeneity in the muscle stem cell population

Compelling evidence from several studies has demonstrated that the satellite cell population is heterogeneous regarding their gene set of expression, proliferation rate, differentiation potential, stemness and even survival.

One remarkable example is demonstrated by the heterogeneity in satellite cells derived from skeletal muscle arising from different developmental origins: head (non-segmented paraxial mesoderm) versus limb (somites) that showed distinct molecular signatures. Cranial mesoderm derived muscles (except extraoculars) are *Tbx1*-dependent, whereas somite-derived muscles are *Pax3*-dependent (Sambasivan et al., 2011a). Furthermore, *Alx4*, *Pitx1/2* are specifically expressed in the cranial mesoderm-derived extraocular muscles (EOM) (Sambasivan et al., 2009). In addition, EOM-derived satellite cells showed greater *ex vivo* growth, self-renewal capacities and *in vivo* transplantation efficiency (Stuelsatz et al., 2015).

Similarly, single fibre transplantation experiments suggested that heterogeneity exists in muscles with the same developmental origin, but different anatomical location: MuSCs isolated from EDL (*Extensor digitorum longus*) or soleus muscles have superior engraftment potential compared to MuSCs from TA (*Tibialis anterior*) (Collins et al., 2005). Given that the MuSCs were grafted with their adjacent fibre in those experiments, this result could also be explained by the heterogeneity in the stem cell niche rather than cell-autonomous properties of the satellite cells.

Strikingly, even within a single muscle cell population, heterogeneity has been reported. Continuous *in vivo* labelling with the thymidine analogue BrdU (5'-bromo-2'-deoxyuridine) in 4weeks-old rats revealed two populations: about $\approx 80\%$ of satellite cells readily marked over the first 5 days and a slow cycling minority of cells not fully saturated upon 2 weeks of treatment. This second population named “reserve cells” was proposed to maintain quiescence during muscle growth/homeostasis and enter cell-cycle only upon trauma (Schultz, 1996). Furthermore, freshly isolated single myofibres from *Myf5^{nlacZ}* and *Myf5^{Cre};R26R^{YFP}* mice showed $\approx 13\%$ of MuSCs that never express *Myf5* (*Pax7⁺/ β -gal⁻*; *Pax7⁺/YFP⁻*, respectively), suggesting a more stem-like fate (Kuang et al., 2007). This *Myf5*— population is capable of asymmetric cell division and replenish the stem cell pool upon engraftment, whereas the *Myf5⁺* undergo differentiation. These results suggest a hierarchical organisation of quiescent MuSCs: with a more stem population that will give rise to the more committed cells upon activation while self-renew to repopulate the quiescent niche. However, this phenotype is less pronounced with another *Myf5^{Cre}* allele, and eventually all satellite cells experience *Myf5* expression, therefore it is unclear how the genetically modified mice reflect stem-like behaviour over time (Sambasivan et al., 2013). Indeed, the presence/absence of labelling relies on the efficiency of the Cre-recombinase that has been shown to not faithfully represent *Myf5* expression in every condition, a phenomenon that has been reported also for other tissues (Comai et al., 2014).

To address some of these issues, a *Tg:Pax7-nGFP* mouse has been used to fractionate the satellite cell population in both quiescent and injured muscles based on the nGFP intensity. Interestingly, fractionation of the *Pax7-nGFP* population by FACS into *Pax7^{High}* (Top 10%) and *Pax7^{Low}* (Bottom 10%) revealed that the *Pax7^{High}* population displays more stem-like features such as lower metabolic activity, longer time to enter cell cycle compared to *Pax7^{Low}* that express more activation/differentiation genes (e.g: *Myod*, *Myogenin*, see below section 3.1.2), and higher expression of stem cell markers. Notably, *Pax7^{High}* cells were considered to be in a more dormant cell state (deeper quiescence), however serial transplantation of these subpopulations did not show dramatic differences in contribution to the niche (Rocheteau et al., 2012).

Recent technological advancements in single cell RNAseq, methylome analysis and mass cytometry now permit investigations of cellular heterogeneity within specific cell populations (Angermueller et al., 2016; Grun et al., 2016; Spitzer and Nolan, 2016). For example, analysis of single cells by multiparameter sequencing-based analysis, specifically RNAseq and bisulfite based methylome analysis, allows the investigation of epigenetic, genomic and transcriptional heterogeneities. Although powerful, some limitations include sequence depth and coverage of the genome. On the other hand, CyTOF based mass cytometry is based on a combination of markers conjugated to metal isotopes, and this led to the identification and classification of subpopulations of myogenic cells following muscle injury (Porpiglia et al., 2017). These emerging technologies can be used to assess the relative potential and role of a whole population at the single cell level and promise to give further insights into understanding MuSC heterogeneities.

3. Functions of muscle stem cells

3.1. Adult myogenesis

The absolute requirement for MuSCs was shown by genetic elimination of satellite cells postnatally using an inducible diphtheria toxin system that leads to an arrest in translation and subsequent cell death. This resulted in failed regeneration and replacement of the damaged muscle tissue with inflammatory and adipogenic cells (Lepper et al., 2011; Murphy et al., 2011; Sambasivan et al., 2011b). Nevertheless, some outstanding questions remain regarding the potential role of other interstitial cells in muscle repair (see Baghdadi and Tajbakhsh, Annex 1).

Examination of β -galactosidase activity in *Myf5^{nlacZ}* mice indicated that the *Myf5* locus is active in 90% of quiescent satellite cells, which suggests that most satellite cells are committed to the myogenic lineage (Beauchamp et al., 2000). Satellite cell physiology and progression throughout the myogenic program are tightly controlled by a hierarchy of transcription factors (Yablonka-Reuveni and Rivera, 1994) (**Figure 6**). At homeostasis, MuSCs remain quiescent and reside in G₀-phase within their sublaminal niche contiguous to the myofibre (Schultz et al., 1978). It is thought that all adult quiescent satellite cells express the transcription factor *Pax7* (Seale et al.,

2000); its paralogue *Pax3* is also expressed in a subset of satellite cells of certain muscles (Relaix et al., 2006). While *Pax3* plays a critical role during embryonic myogenesis, most satellite cells, however, downregulate *Pax3* before birth (Kassar-Duchossoy et al., 2005). As mentioned above, in myogenesis, *Pax7* and *Pax3* play overlapping but non-redundant roles. These functional differences can be explained by differential binding affinities for paired versus homeobox motifs, suggesting differences in DNA binding and chromatin status affinities (Soleimani et al., 2012). Upon injury, MuSCs activate, re-enter the cell cycle and undergo cellular division to give rise to myoblasts, a highly proliferative transient amplifying cell population (Figure 6). In the adult, MRFs are also responsible for both myogenic lineage specification as well as for the regulation differentiation. Although MYF5, but not MYOD protein is expressed in satellite cells, *Myod* and *Myf5* genes are both rapidly upregulated upon activation (Cooper et al., 1999; Gayraud-Morel et al., 2012). Finally, terminal differentiation is initiated by the downregulation of *Pax7* (Olguin and Olwin, 2004) and the upregulation of *Myogenin* and *Mrf4* to generate elongated myocytes that will further fuse into myotubes (Cornelison et al., 2000; Cornelison and Wold, 1997) (Figure 6). Essentially, a subpopulation of activated satellite cells, exit the cell cycle and return to quiescence in order to maintain the stem cell pool for future regeneration (Figure 6).

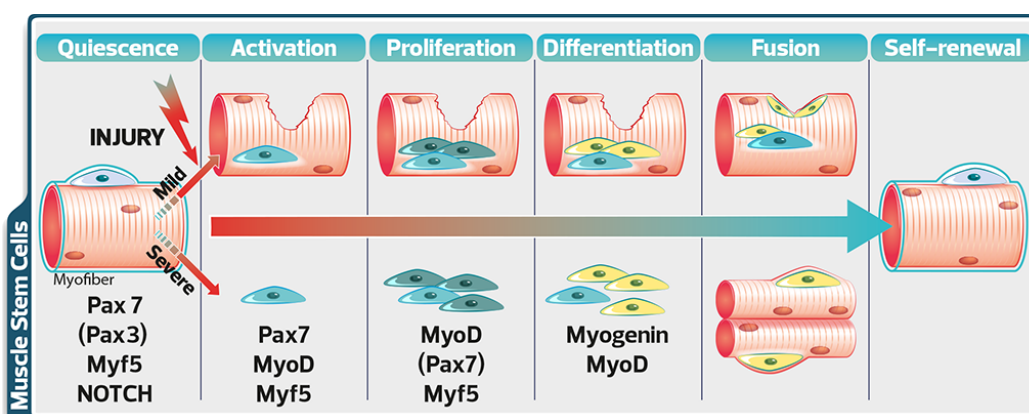


Figure 6. Muscle regeneration following different forms of injury. Following mild or severe injury, quiescent muscle stem cells (MuSCs) activate, differentiate and fuse to repair the damaged fibre. The myogenic process is tightly regulated by the action of key transcription factors and regulators. (Baghdadi and Tajbakhsh, Annex 1)

3.1.1. Satellite cell activation and differentiation

Immediately following muscle injury, *Myod* expression is rapidly upregulated and MYOD protein is already detectable within satellite cells as early as 12 h after injury, before the first cell division that takes place from about 20h (Rocheteau et al., 2012; Smith et al., 1994). This early expression of *Myod* is proposed to be associated with a subpopulation of committed satellite cells, which are poised to differentiate without proliferation (Rantanen et al., 1995). In contrast, the majority of satellite cells express either *Myod* or *Myf5* by 24h following injury and subsequently co-express both factors (Cornelison and Wold, 1997; Gayraud-Morel et al., 2012; Zammit et al., 2002) (**Figure 6**). Interestingly, ectopic expression of *Myod* in NIH-3T3 and C3H10T1/2 fibroblasts is sufficient to activate the complete myogenic program in these cells (Hollenberg et al., 1993); thus expression of *Myod* is an important determinant of myogenic commitment and differentiation, and its absence promotes proliferation and delayed differentiation (*Myod*^{-/-})(Sabourin et al., 1999). During satellite cell activation, *Pax7* and *Pax3* target genes to promote proliferation and commitment to the myogenic lineage, while repressing genes that induce terminal myogenic differentiation (Soleimani et al., 2012). For example, PAX7 and PAX3 induce the expression of *Myf5* by direct binding to distal enhancer elements and *Myod* by binding to the proximal promoter (Bajard et al., 2006; Hu et al., 2008). Moreover, p38 kinase (p38 γ) also negatively regulates the transcriptional potential of *Myod* by phosphorylation, which leads to a repressive *Myod* complex occupying the *Myogenin* promoter (Gillespie et al., 2009). This observation is supported by the premature expression of *Myogenin* and reduced proliferation of myoblasts in *p38*-deficient muscle (Gillespie et al., 2009).

Terminal differentiation is initiated by the expression of *Myogenin* and later *Mrf4* (Smith et al., 1994; Yablonka-Reuveni and Rivera, 1994) (**Figure 6**). ChIP-on-chip experiments (Bergstrom et al., 2002; Cao et al., 2006) and ChIP-Seq analysis (Cao et al., 2010) revealed MYOD and MYOGENIN specific target genes. These studies suggested a hierarchical organization involved in satellite cell activation and differentiation with regard to MRFs. MYOD directly activates *Myogenin* and *Mef2* transcription factors, a large portion of downstream targets are muscle-specific

structural and contractile genes, such as those encoding actins, myosins, and troponins, essential for proper myofibres function.

p38 α / β kinase stimulates the binding of MYOD and MEF2s to the promoters of muscle-specific genes, leading to the recruitment of chromatin remodelling complexes promoting myogenesis (Cox et al., 2003; Wu et al., 2000).

Besides MRFs and their regulators, other post-transcriptional factors have been shown to be involved in myogenic differentiation such as micro-RNAs (see Chapter 3).

3.1.2. Satellite cell self-renewal

The self-renewing capability of MuSCs has been demonstrated by series of transplantation experiments and clearly showed their remarkable ability to sustain the capacity for muscle repair. For example, transplantation of a single myofibre and its resident MuSCs (7-22/fibre) into irradiated muscles of immunodeficient dystrophic mice (*nude; mdx*) showed that MuSCs can give rise to over 100 new myofibres, expand and support further rounds of muscle regeneration (Collins et al., 2005). Similarly, purification of MuSCs followed by transplantation showed that they both contribute to muscle repair of *nude; mdx* mice and colonize the stem cell niche (Montarras et al., 2005). The self-renewing capability of satellite cells was further shown by serial transplantations of isolated Pax7-nGFP cells in pre-injured immunocompromised mice (Rocheteau et al., 2012); GFP+ cells were collected up to seven rounds of transplantations. Finally, single cell transplant experiments demonstrated that a single freshly isolated MuSC is capable to give rise to progeny cells and to self-renew upon injury (Sacco et al., 2008).

To study self-renewal *ex vivo*, two models are generally used: 1) floating isolated single myofibres where MuSCs will proliferate in clusters formed by activated, differentiated and self-renewed cells within 72h in the absence of cell fusion (**Figure 7**); 2) reserve cell model, where cells plated at high density will form myotubes and this is accompanied by the emergence of non-proliferative single cells (Pax7⁺) adjacent to the myotubes (**Figure 7**).

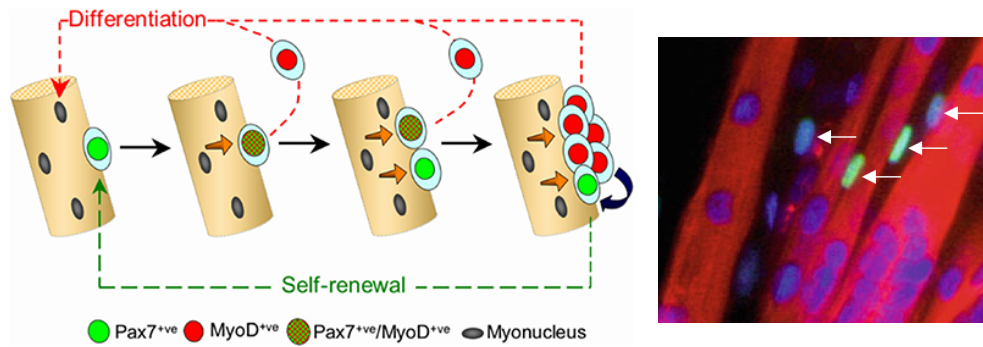


Figure 7. *Ex vivo* study of satellite cell self-renewal. Left: Schematic representation of single myofiber satellite cell renewal model. Within 72h after isolation, a single MuSC will give rise to a cluster composed by self-renewed cells Pax7⁺ (green), differentiated cells Myod⁺/Pax7⁻ (red) (Zammit *et al.*, 2006). Right: Culture of murine cells showing differentiated MyHC⁺ myotubes (red) and tightly associated Pax7⁺ satellite cells (green; arrows) that returned to quiescence: reserve cells (Abou-Khalil *et al.*, 2013).

Stem cells can divide, commit to differentiation and self-renew in two fashions: asymmetrically (one daughter stem cell and one daughter committed cell) or symmetrically (two identical daughter cells, either renewed or committed). The balance between asymmetric versus symmetric division depends on several intrinsic and extrinsic cues, however how this is regulated, during growth and regeneration remains largely unknown (Collins *et al.*, 2005; Motohashi and Asakura, 2014; Yennek *et al.*, 2014). Asymmetric cell divisions have been reported in myogenic cells in several studies by following the differential distribution of transcription factors (Pax7, Myod, Myogenin), non-random DNA segregation (NRDS) of old and new DNA strands using nucleotide analogues, reporter gene expression, and dystrophin/Par complex (Kuang *et al.*, 2007; Rocheteau *et al.*, 2012; Shinin *et al.*, 2006; Yennek *et al.*, 2014).

For example, when myogenic cells were isolated on myofibers, asymmetric divisions were reported to occur when the mitotic spindle is perpendicular to the myofiber axis with the satellite stem cell (Pax7⁺/Myf5⁻) in close contact with the basal lamina and the committed cell (Pax7⁺/Myf5⁺) adjacent to the myofiber plasma membrane (Kuang *et al.*, 2007). Furthermore, Wnt7a, through its receptor Frizzled-7, was reported to be upregulated in Pax7⁺/Myf5⁺ cells, and it induced polarized expression of *Vangl2*, an

effector of the planar cell polarity pathway, which was required for Wnt7a-mediated satellite cell expansion (Le Grand, Jones, Seale, Scime, & Rudnicki, 2009).

In other studies, NRDS was reported in satellite cells *ex vivo* and *in vivo* (Yennek and Tajbakhsh, 2013). Semiconservative replication of DNA can result in random or non-random segregation of older template and nascent DNA strands in daughter cells during cell division. Pulse-chase DNA labelling experiments using thymidine analogues (BrdU, EdU (5'-ethynyl-2'-deoxyuridine)) in injured muscle showed that up to 80% of the Pax7^{High} activated population (by extrapolation, 8% of total GFP population) performs non-random or template DNA segregation (NRDS or TDSS) (Rocheteau et al., 2012; Shinin et al., 2006; Yennek et al., 2014). Interestingly, NRDS was directly associated with cell fates: the more stem cell Pax7⁺/Myogenin⁻ retains the old strand while the committed cell Pax7⁻/Myogenin⁺ inherits the newly synthesized strand (**Figure 8**) (Conboy et al., 2007; Rocheteau et al., 2012; Yennek et al., 2014).

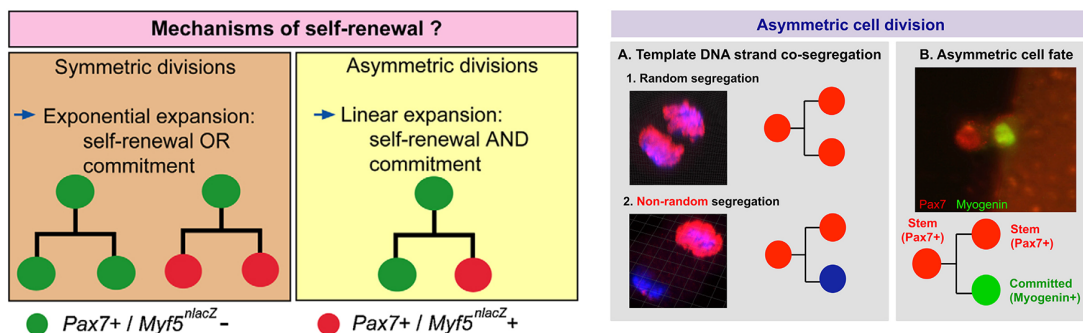


Figure 8. Proposed models for satellite cell self-renewal via asymmetric cell division. Left: Satellite cell self-renewal can be achieved by either symmetric or asymmetric cell division. Symmetric divisions can amplify the stem cell pool, or generate differentiated cells whereas asymmetric divisions result in maintenance of one stem cell and the generation of one differentiated daughter cell (*Sambasivan and Tajbakhsh, 2007*). Right: (A) Random DNA segregation where daughter cells inherit old and new DNA strands (1) or only one cell is labelled with BrdU indicating non-random DNA segregation (2). (B) Asymmetric division and cell fate: the division of one Pax7⁺ cell gives rise to one stem (red) and one committed (green) daughter cell. (*Yennek and Tajbakhsh, 2013*)

Chapter 2.

Stem cell niche is essential for quiescence

1. Stem cell quiescence

Cellular quiescence is a reversible, non-proliferative G_0 -arrested state characterized by the ability to re-enter the cell cycle and generate progenitor cells in response stimuli, such as trauma. The quiescence state was extensively studied in the budding yeast *Saccharomyces cerevisiae* as a mode of survival that can be induced by nutrient deprivation (Herman, 2002). Similar conditions were noted in mammalian cells *in vitro* (Zetterberg and Larsson, 1985). The presence of quiescent adult stem cells in multiple tissues and organs highlights the essential role of this cell state.

1.1. Identification of quiescent stem cells

Due to the low numbers of quiescent stem cells (QSCs) in a given tissue, our understanding of this cell state has been limited to the absence of markers associated with proliferation and differentiation. For example, nucleotide analogues (^3H -TdR, BrdU, EdU), endogenous markers of proliferation (PCNA, a DNA polymerase accessory protein expressed in S-phase), Ki67 (ribosomal RNA transcription associated protein), MCM-2 (protein involved in replication origins, S-phase) and phospho-Histone3 (M-phase specific) can be detected by autoradiography or immunofluorescence (Conboy et al., 2007; Shinin et al., 2006). More recently, histone tagged proteins (H2B-GFP/YFP) have been used as their association with DNA is replication-dependent thereby allowing live imaging by videomicroscopy (Foudi et al., 2009; Tumber et al., 2004). QSCs have also been identified based on label retention. Label retention is based on the premise that a dividing cell will dilute away an incorporated label (e.g. nucleotide analogue, H2B-GFP), whereas a QSC, or slow-cycling cell, will retain the label for longer periods of time. The presence or absence of label-retaining cells (LRCs) has been for a long time the only tool to determine if a population of stem cells was quiescent; however, it has become increasingly clear that this approach is not sufficient. In high-turnover tissues such as the small intestinal epithelium, lineage-tracing experiments allow the distinction of at least two populations with stem cell potential: the long-retaining reserve cells (+4) and the proliferating stem cells (Lgr5+) (Buczacki et al., 2013). Similarly, the skin houses a first proliferative stem population at the basal layer of the epidermis and a quiescent population in the bulge of the hair follicle (HFSC) (Ito et al., 2005). Interestingly, in both cases, the active stem population was proposed to be involved

in tissue homeostasis whereas the quiescent, LRCs appear to be mobilized upon injury (Li and Clevers, 2010).

1.2. *Ex vivo* induction of quiescence

Cellular quiescence can be mimicked *in vitro* by modulating cell culture conditions such as the nutrient concentration or adherence cues. The loss of adherence has been shown to induce both mouse and human myoblasts back to quiescence by culture in suspension in a methylcellulose gel (Milasincic et al., 1996; Sellathurai et al., 2013). Similarly, culture on soft substrate induces the loss of contractile property and can trigger a quiescent-like state (Gilbert et al., 2010). Although fibroblasts respond well to the deprivation of nutrients/mitogens, myoblasts tend to differentiate rather than go back to quiescence (Arora et al., 2017; Rumman et al., 2015).

1.3. Molecular signature of quiescence

1.3.1. Epigenetic control

Recent epigenetic studies showed that during development, chromatin configuration becomes more and more restrictive as cells commit and differentiate into specific lineages. One key determinant of gene expression is the landscape of histone modifications often associated with gene activation or repression. For example, actively transcribed genes are commonly marked by trimethylation of histone 3 lysine 4 (H3K4me3) around their transcription start sites (TSSs) and H3K36me3 in the gene body, whereas Polycomb group (PcG) complex-mediated H3K27me3 is associated with transcriptional repression (Jenuwein and Allis, 2001). Some chromatin regions, referred to as bivalent domains are marked by both H3K4me3 and H3K27me3. They are frequently located in close proximity to TSS and have been shown to mark master regulators of cell lineage, maintaining ES cell in this poised state mentioned above (Bernstein et al., 2007; Li et al., 2012).

Regarding MuSCs, histone profiles in quiescent versus activated (2, 3, and 5dpi) satellite cells has been performed by mass-spectrometry-based proteomics and highlighted a time-dependent shift towards a heterochromatic state during activation (Schworer et al., 2016). Complementary to this study, chromatin

immunoprecipitation sequencing (ChIP-seq) combined with transcriptomic analysis in quiescent and activated satellite cells also showed a switch from permissive state in quiescence to a more repressed state in activation (Liu et al., 2013a). Quiescence to activation transition is marked by the retention of H3K4me3 and a dramatic increase of H3K27me3 mark at the TSSs. Finally, the fine-tuned epigenetic regulation of establishment and/or maintenance of the reversible quiescent state has been recently demonstrated in MuSCs, where the H3K9 methyl-transferase PRDM2 binds to thousands of promoters mostly marked by the repressive H3K9me2 mark such as the G₀-arrest inducing gene *Ccna2* (Cheedipudi et al., 2015).

1.3.2. Cell cycle regulators

Cyclin-dependent kinase inhibitors (CKIs) such as p21, p27 inhibit CDK2, and CDK4 respectively are expressed in QSCs to block cell cycle progression (Sherr and Roberts, 1999). The genetic loss of *p21* or *p27* induces exhaustion of HSCs due to a high proliferative capacity (Zou et al., 2011). Similarly, MuSCs deficient for *p21* (p21 KO) increase their proliferation rate but fail to undergo differentiation (Hawke et al., 2003); meaning that different CKIs are involved in the exit from the cell cycle triggered by differentiation (Mohan and Asakura, 2017).

Rb family proteins (Rb, p130 and p107) are guardians of the G1/S transition and inhibit cell cycle progression by controlling S-phase transcription factors (Weinberg, 1995). HSCs deficient for Rb proteins have an enhanced proliferation and fail to replenish the stem cell pool in the bone marrow after transplantation (Viatour et al., 2008). Rb proteins are highly expressed in quiescent MuSCs, and their genetic inactivation induce accelerated cell cycle entry, loss of myogenic differentiation and ultimately cell death (Hosoyama et al., 2011). Interestingly, p300 has been shown to suppress myogenic differentiation genes; thus Rb proteins block cell cycle progression and differentiation of MuSCs (Carnac et al., 2000).

2. Molecular signature of MuSCs

Transcriptomic analysis comparing quiescent and activated satellite cells have been done by several labs (Farina et al., 2012; Fukada et al., 2007; Garcia-Prat et al., 2016; Liu et al., 2013a; Lukjanenko et al., 2016; Pallafacchina et al., 2010). Although many quiescence specific genes are found in all data sets, the variations in the

experimental procedures raise questions regarding reproducibility. For instance, for *in vivo* satellite cell activation, several techniques were used to induce the injuries including BaCl₂, or myotoxins. Cell extraction protocols also varied among the different studies: i) using transgenic mice expressing a reporter gene that marks satellite cells and ii) using a combination of antibodies targeting surface cell antigens specific to satellites cells (see Annex 2). In an attempt to normalize these differences, we developed a standardized pipeline for comparing quiescent versus activation data sets. An initial analysis of 11 samples revealed a quiescent transcriptional signature that includes already known genes such as Calcitonin receptor, Teneurin-4 and Collagen genes (type 5 and 6) (see Annex 2; manuscript in preparation).

Furthermore, histone landscape analysis coupled with microarray in quiescent versus activated satellite cells showed that genes expressed at high levels in quiescence were marked only by H3K4me3 (Liu et al., 2013a). This list of genes included a large number of known quiescent-specific genes such as *Pax7*, *Cd34*, *Odz4* and Calcitonin receptor (*Calcr*), and Notch target genes *Hey1*, *Hey2*, and *HeyL*. Notably, this list of genes was dominated by genes encoding glycoproteins. Given that glycoproteins are integral membrane proteins that often play an important role in cell-cell and cell-matrix interactions (Moremen et al., 2012), these glycoproteins that expressed at high levels in QSCs may be important mediators of interactions within the niche (see Section 2 below). In the context of our work, we focus on two quiescent-specific genes: Calcitonin receptor and Teneurin-4.

[2.1.1. Calcitonin receptor](#)

The calcitonin receptor (*Calcr*) belongs to the secretin-like family of is a G-protein- coupled seven transmembrane protein (GPCR) arising from a 70kb gene composed of 12 encoding exons. In human and rodents, alternative splicing gives rise to two *Calcr* isoforms: *Calcr-C1 α* and *Calcr-C1 β* . As the *Calcr* is widely expressed, it has been proposed that its tissue-specific expression is regulated by the single transmembrane co-receptor of the RAMPs: RAMP1-3 (receptor activity modifying protein) (Russell et al., 2014). Upon glycosylation, the heterodimerization of both CALCR and one of the RAMP peptides is required for the mature protein to be exported from the endoplasmic reticulum to the plasma membrane (McLatchie et al.,

1998). It is still unclear how the dimerization of RAMPs with the CALCR is regulated, especially in cell types that coexpress several RAMP isoforms (**Figure 9**).

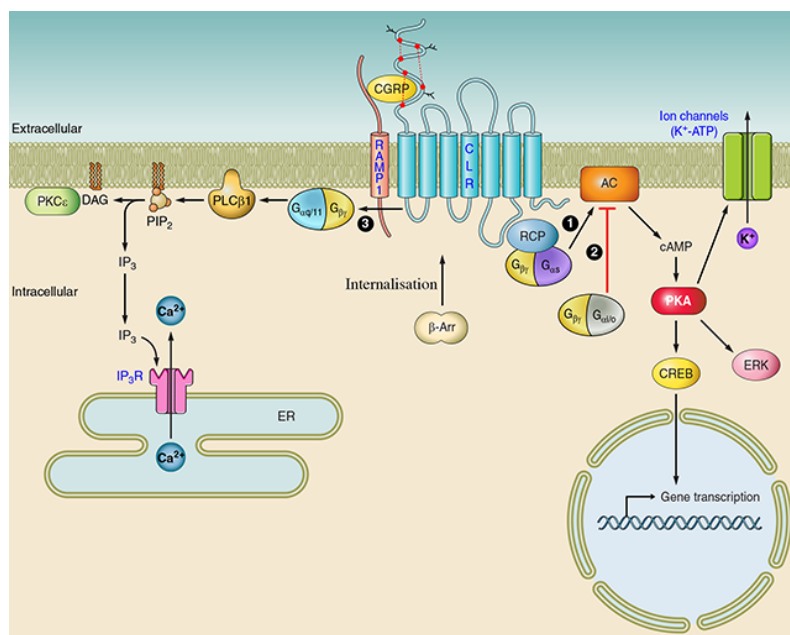


Figure 9. Intracellular mediated signalling of calcitonin receptor. Binding of CGRP ligand to the CALCR/RAMP receptor can activate multiple signalling pathways. (1) The activation of adenylate cyclase (AC) by $G_{\alpha s}$ G-protein subunit, triggers the elevation of intracellular cAMP, thereby activating protein kinase A (PKA), resulting in the phosphorylation of multiple downstream targets. These targets may include potassium-sensitive ATP channels (K_{ATP} channels), extracellular signal-related kinases (ERKs), or transcription factors, such as cAMP response element-binding protein (CREB). (3) Reports in osteoblasts have also shown evidence of $G_{\alpha q/11}$ -mediated signalling, involving activation of PLC-1, cleaving phosphatidylinositol 4,5-bisphosphate (PIP_2) to form inositol trisphosphate (IP_3) and diacylglycerol (DAG). IP_3 binds to the IP_3 receptor (IP_3R) on the endoplasmic reticulum (ER), causing calcium release and thus raising cytoplasmic concentrations. DAG may activate PKC_{ϵ} , which in turn phosphorylates proteins further downstream. Upon activation, GPCR forms a complex with β -arrestins (β -Arr), that undergoes dynamin/clathrin dependent endocytosis for further lysosomal degradation or endosome recycling (Walker et al., 2010). Adapted from (Russell et al., 2014)

To date, the only known ligand of CALCR is the polypeptide hormone calcitonin (CT), synthesized by the thyroid gland and known to regulate serum calcium levels. The main targets of CT are the osteoclasts where it inhibits bone resorption via interaction with CALCR. Although it has other roles in the blood, kidney, CNS, respiratory system, gastrointestinal system and sperm, whether its function is mediated by CT is unclear (Russell et al., 2014). Upon activation, CALCR triggers a downstream pathway involving $G_{\alpha s}$ protein described in **Figure 9**.

Quiescent MuSCs specifically express the C1 α isoform and all three RAMP isoforms. *Calcr* is downregulated during activation and is absent in activated cells (2, 5 and 7d post-injury), then it is re-expressed by 14dpi when the majority of satellite cells return to quiescence (Yamaguchi et al., 2015). Interestingly, the specific ablation of *Calcr* in satellite cells (*Pax7^{CreERT2}; Calcr^{fllox}*) induces an exit of satellite cells from the quiescence niche followed by apoptosis, resulting in partial a loss of the stem cell pool (Yamaguchi et al., 2015). Furthermore, *in vitro* activation of CALCR with the synthetic peptide Elcatonin induces the cAMP-PKA pathway to inhibit the expression of cyclin-related genes (like *Ccnd1*, *Ccna2*, and *Skp2*) resulting in the active maintenance of the G0-quiescent state (Yamaguchi et al., 2015).

2.1.2. Teneurin-4 or Odz4

Odz is the vertebrate homologue of the *Drosophila odd Oz* pair-rule gene and encodes a large type II transmembrane protein family: teneurins (Tenm). In vertebrates, there are four *Odz/Tenm* numbered 1-4 mainly expressed in the CNS (Tucker et al., 2007). Although Odz4 function has been studied in chick embryo neuron patterning (Kenzelmann-Broz et al., 2010) and mouse oligodendrocyte differentiation (Suzuki et al., 2012), the role of the teneurins and their mechanisms of action remain largely unknown. When the intracellular domain of teneurins are targeted by immunostaining on cells *in vitro*, they localize to the nucleus whereas the extracellular domain remains at the membrane, suggesting that they might be cleaved and act as transcription factors similar to Notch (see Chapter 4)(Bagutti et al., 2003). However, whether ODZ/TENM binds to DNA and activates transcription of specific genes has yet to be demonstrated.

Odz4 and *Odz3* are both present in satellite cells, however only *Odz4* expression shows a clear restriction to quiescent satellite cells, and its expression reappears between 5-7 days post-injury (Fukada et al., 2007). *Odz4* contains 33 exons that can give rise to 12 different coding proteins by alternative splicing. Interestingly, in the study reporting the role of *Odz4* in oligodendrocyte differentiation, the authors also indicated that focal adhesion kinase (FAK), a key regulator of cell adhesion, is activated downstream of *Odz4* (Suzuki et al., 2012); therefore, in quiescent MuSCs, *Odz4* might control cell adhesion and/or differentiation.

The only study involving *Odz4* in muscle used a transgenic mouse originally designed to study the role of a recombinant FLAG-tagged perlecan (heparin sulfate proteoglycan) specifically in cartilage under the control of *Col2a1* promoter (Suzuki et al., 2012). Homozygous null mice developed severe tremors in the hindlimbs and paralysis due to hypomyelination in the CNS, hereafter named “furue” (japanese term for tremor): *Furue*^{Tg(Hspg2)2Yy}. Because this phenotype was likely caused by the transgene insertion, FISH (fluorescent in situ hybridization) and screening of a bacterial artificial chromosome library prepared from *Furue* mice allowed the identification of a transgene insertion into intron 5 of *Odz4*, located on chromosome 7 (Suzuki et al., 2012). The analysis of *Furue* mice showed hypoplasia in perinatal and adult animals in addition to a decrease in MuSCs number, subsequently inducing a delay in regeneration upon injury (Ishii et al., 2015). Moreover, upon injury, *Odz4*-deficient satellite cells atypically maintained high proliferation capacities and the activation marker MYOD 7dpi (Ishii et al., 2015). However, the constitutive repression of *Odz4* raises questions about the specificity of its action in the satellite cell population as muscle growth and repair involve the collaboration of diverse cell regulators. Furthermore, the innervation of muscle is critical for its proper development and regeneration, thus the hypomyelination of the CNS showed by Suzuki and colleagues has high probability to affect muscle function in general as nervous input is altered (Suzuki et al., 2012).

Finally, in the mutant embryos *Pax3*^{Cre/+}; *Rbpj*^{flox/flox}; *Myod*^{-/-} a decrease of *Odz4* expression was observed in isolated myoblasts suggesting that *Odz4* and Notch functions might be correlated (Brohl et al., 2012). Accordingly, we showed that *Odz4* is a Notch pathway target genes (see Results, part II).

2. The stem cell niche

The concept of the “niche” proposed to represent the specific microenvironment that maintains and instructs stem cells (Schofield, 1978). Extensive studies that investigated *Drosophila* and *Caenorhabditis elegans* (*C. elegans*) adult SC niches *in vivo* have confirmed the critical role of the niche in modulating stem cell behaviour (Byrd and Kimble, 2009; de Cuevas and Matunis,

2011). Recent work has since confirmed in multiple invertebrate and mammalian organ systems that adult stem cells reside in tissue specific niches providing structural support and molecular signals to regulate quiescence, self-renewal, and proliferation instructions essential for tissue homeostasis and regeneration (Blanpain et al., 2004; Jones and Wagers, 2008; Kai and Spradling, 2003; Song et al., 2002; Wilson et al., 2008; Wilson and Trumpp, 2006). Increasing evidence of deregulation of the stem cell niche has been associated with aging, tissue degeneration and cancer (Voog and Jones, 2010).

Although each stem cell type resides in a specific niche, in most systems, the organization and components of niche have similar features: (1) the stem cell and progeny themselves, as they provide autocrine and paracrine regulation, respectively, within their own lineage; (2) neighbouring mesenchymal or stromal cells providing paracrine signals; (3) extracellular matrix (ECM) or cell–cell contacts involving adhesion molecules; and (4) external cues from distant sources within the tissue or outside the tissue, such as from blood vessels, neurons, or immune cells (**Figure 10**). Thus, it is the synergy of all this elements that creates a discretely localized niche.

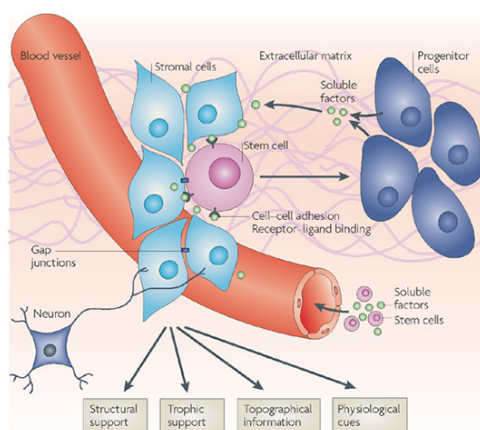


Figure 10. Components and functions of stem cell niches. Scheme depicting a hypothetical niche composite that all together provide structure and trophic support, topographical information and physiological cues to instruct stem cell behaviour. (*Jones and Wagers, 2008*)

2.1. Extracellular matrix: powerful modulator of cell behaviour

ECM was initially considered to be an inert supportive scaffold, however, it is now clear that by either direct or indirect action, ECM regulates cell behaviour and it plays essential roles during development (Hynes, 2002). Indeed, the dynamism of ECM is provided by its capacities to adapt the production, degradation, and remodelling of its components. First, the ECM possesses both direct and indirect signalling properties, since it can act directly by binding cell surface receptors or by

growth factor presentation (Hynes, 2002). Second, ECM components confer biomechanical properties to the ECM such as rigidity, porosity, topography and insolubility that can influence various anchorage-related biological functions, like cell division, tissue polarity and cell migration (Lu et al., 2011b). Indeed, ECM stiffness is an essential property by which cells sense the external forces and respond to the environment in an appropriate manner, a process known as mechanotransduction (DuFort et al., 2011; Mammoto and Ingber, 2010). Experiments performed with decellularized tissues, in which the ECM is preserved, showed capacity to guide stem cell differentiation into the cell types residing in the tissue from which the ECM was derived (Nakayama et al., 2010) (Webster et al., 2016). Despite the well-investigated cellular stem cell niche, details are lacking regarding the specific roles of ECM components (**Figure 11**).

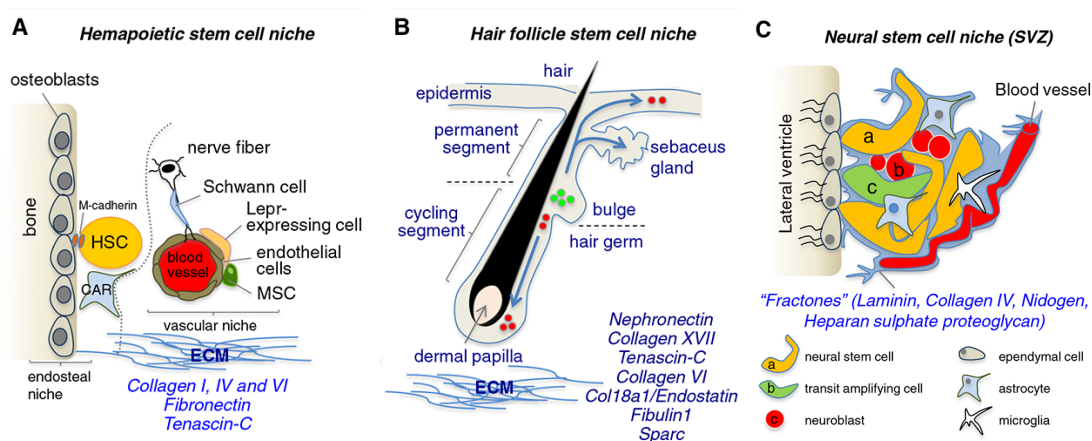


Figure 11. Stem cell niches and their ECM. (A) the HSC niche is composed of distinct cellular entities including the endosteal niche populated by osteoblasts, and the vascular niche. To date, no evidence for ECM regulation has been demonstrated. (B) HFSCs deposit nephronectin in the bulge that interact with $\alpha 8\beta 1$ integrin promoting stem cell anchorage. Collagen XVII synthesized by HFSC is essential for their maintenance by providing an additional niche for melanocyte stem cells; thus maintaining self-renewal of both populations. (C) The subventricular zone (SVZ) of the lateral ventricle is composed of three cell populations that lie immediately beneath a monolayer of ependymal cells and corresponding to NSC, mitotically active transit amplifying cells and neuroblasts. NSCs in the niche are associated with heparan sulfate proteoglycan which regulates the proliferation and differentiation by presenting growth factors (EGF, FGF). (Rezza et al., 2014)

2.2. ECM-cell interaction

Interactions between ECM and stem cells can be directly mediated by a number of cell receptors, however, most of the studies have focused on integrins. Integrins are the main family of ECM receptors for cell adhesion as they connect the extracellular compartment to the intracellular cytoskeleton (Hynes, 2002). They constitute a large family of heterodimeric transmembrane receptors composed of non-covalently associated α and β subunits. In vertebrates, 18 α subunits and 8 β subunits combine to form 24 distinct type of integrins. The large variety of integrins makes them potent receptor to a large number of ECM components or other cell surface adhesion molecules and receptors (Arnaout et al., 2007; Barczyk et al., 2010; Hynes, 2002). They have been found to be essential for the homing of HSCs in the bone marrow niche ($\alpha 4$, $\alpha 6$, $\alpha 9$ and $\beta 1$) (Potocnik et al., 2000; Qian et al., 2006), spermatogonial stem cells in the testicular niche by binding to laminin ($\alpha 6\beta 1$) (Kanatsu-Shinohara et al., 2008) and NSCs to their vascular niche (Shen et al., 2008). In addition, follicular stem cells of *Drosophila* ovary require integrin-mediated interaction for their anchorage to the niche and for their proper self-renewal and asymmetric cell division (O'Reilly et al., 2008). Finally, in the mouse hair follicle, bulge stem cells produce the ECM protein nephronectin, which interacts with the $\alpha 8\beta 1$ integrin receptor present on the arrector pili muscle to maintain the appropriate position and function of HFSCs (Fujiwara et al., 2011).

Integrins can directly activate downstream signalling via focal adhesion kinase (FAK) and phosphoinositide 3-kinase (PI3K) (Lu et al., 2011b) or interact with other pathways such as Notch, EGF receptor or Hedgehog signalling (Brisken and Duss, 2007; Campos et al., 2006; Jones et al., 2006) thus regulating self-renewal, proliferation and differentiation of a large variety of stem cells.

2.3. Biophysical properties of ECM

As mentioned above, ECM biophysical properties also influence the stem cell niche by regulating the internal forces that are transmitted to the environment by adhesion sites (DuFort et al., 2011). The focal adhesion complexes, which include integrins, adaptors and signalling proteins, physically link the actomyosin cytoskeleton with the ECM. Together with cytoskeleton, nuclear matrix, nuclear envelope and chromatin, the focal adhesion complexes constitute a complex

machinery that determines how cells respond to forces generated from the ECM. A number of mechanotransduction pathways have emerged as key downstream mediators of ECM elasticity, cell shape and cytoskeletal organization: Ras/MAPK, PI3K/Akt, RhoA/ ROCK, Wnt/ β -catenin, TGF- β pathways and more recently YAP/TAZ (Halder et al., 2012; Sun et al., 2012).

The stiffness of the extracellular microenvironment, mainly expressed by the elastic modulus (or Young's modulus), is usually several orders of magnitude lower in many organs compared to what cells experience when cultured directly onto a plastic or glass dish. Because of the difficulties in manipulating tissue stiffness *in vivo*, researchers have developed *in vitro* engineered stem cell niches, with the aim to mimic the *in vivo* niche and study stem cells in less artificial conditions. To date, those bioengineering tools include synthesizing novel biomaterials for stem cell culture, fabricating scaffolds in three dimensions with micro/nanoscale topography, micropatterning ECM in two dimensions, and performing high-throughput ECM microarrays (Lutolf and Blau, 2009; Peerani and Zandstra, 2010). Interestingly, when human mesenchymal stem cells are cultured on different stiffnesses of ECM that mimic the elastic moduli of brain, muscle or bone, they undergo tissue-specific cell fate switches into neurons, myoblasts and osteoblasts, respectively (Engler et al., 2006). Adult NSCs cultured on fibronectin-hydrogel with the stiffness of brain tissue differentiate into neurons, whereas stiffer gels promote their differentiation into glial cells (Saha et al., 2008). This biomechanical regulation of cell fate is confirmed *in vivo* by the finding of stiffness gradients in the hippocampus. Regarding MuSCs, modulating substrate elasticity was found to regulate their self-renewal in culture (Gilbert et al., 2010; Urciuolo et al., 2013), and asymmetric micropatterns were able to switch a subpopulation of satellite cells from symmetric to asymmetric division (Yennek et al., 2014). Notably, in *Col6* mutant mice that model the human Bethlem/Ulrich myopathy, muscle stiffness is decreased (from 12 to 7kPa) leading to an indirect defect of MuSC self-renewal. Of interest, the engraftment of COLVI-synthesizing fibroblasts partially restores the stiffness and consequently MuSC properties (Urciuolo et al., 2013).

2.4. Collagens constitute a major component of the ECM

One key component of the ECM is collagen, the most abundant protein in animals. In light of what has been described above, collagens provide essential structural support for connective tissues but they can also directly interact with cells through cell surface receptors or via intermediary molecules. Collagens have a triple helical structure composed of three genetically distinct polypeptide chains termed α -chains ($\alpha 1$, $\alpha 2$, $\alpha 3$), characterized by repeating glycine-X-X' sequence with X and X' being any amino acid. Looping of the three α -chains requires every third amino acid to be a glycine whereas 4-hydroxyproline-proline confers stability. In vertebrates 46 distinct collagen α -chains assemble to form 29 homodimer or heterodimer collagen types. Most triple helices assemble collagen into macromolecules to form fibrils and fibres that are essential components of tissues and bones. Collagen families include fibrillar collagen (eg. type I, III, V), network-forming collagen (COLIV, major component of basement membranes), fibril-associated collagens with interruptions in their helices (FACIT; eg IX, XII) and filamentous (COLVI; beaded microfibrils) (Mouw et al., 2014).

Upon synthesis, collagens α -chains are targeted to the ER where they assemble and undergo post-transcriptional modifications to form a precursor procollagen molecule. Note that the $\alpha 1$ -chain is necessarily present in every collagen form. Procollagens are then secreted by cells into the extracellular space and converted into mature collagen by the removal of the N- and C-propeptides via collagen type-specific metalloproteinase enzymes (Mouw et al., 2014).

2.4.1. Insights from Collagen V

For the purpose of this thesis, we will focus on one specific type of collagen: type V Collagen. Collagen V is a fibrillar collagen involved in the regulation of fibril assembly and it can be classified as a regulatory fibril-forming collagen. The major isoform of Collagen V, $[\alpha 1(V)]_2\alpha 2(V)$ (two $\alpha 1$ chains and one $\alpha 2$), co-assembles with Collagen I to form heterotypic fibrils (Birk et al., 1988). The constitutive deletion of Collagen V in mouse (*Col5a1*^{-/-}) is lethal at embryonic day E8.5. Interestingly, in the embryonic mesenchyme, even if the number of COLI fibrils is altered, the amount of Collagen I remains normal, suggesting that Collagen V is

critical for fibril assembly (Wenstrup et al., 2004). Moreover, *Col5a1* heterozygous mice are haploinsufficient and present a phenotype mimicking the human Ehlers-Danlos syndrome (EDS) that is characterized by a connective tissue disorder with broad tissue involvement typified by fragile, hyperextensible skin, widened atrophic scars, joint laxity, a high prevalence of aortic root dilation, and other manifestations of connective tissue (Malfait et al., 2010; Wenstrup et al., 2006). This mouse model of EDS of heterozygous *Col5a1* ablation ultimately provides an explanation for the haploinsufficiency observed in *Col5a1* mice (Wenstrup et al., 2006).

Native collagen triple helix can interact directly with cells via cell transmembrane receptors triggering diverse functions such as stable adhesion or migration. To date, four classes of vertebrate receptors have been described: collagen-binding integrins ($\alpha1\beta1$, $\alpha2\beta1$, $\alpha11\beta1$, $\alpha10\beta1$), discoidin domain receptors (DDR), glycoprotein VI (GPVI), and leukocyte-associated immunoglobulin-like receptor-1 (LAIR-1). Although collagen-binding integrins and DDRs have different structures, they both bind to specific amino acid motifs within the collagen triple helix, and have overlapping cellular functions (Leitinger, 2011). In contrast, the structurally related receptors GPVI and LAIR-1 have similar collagen-binding motifs but mediate opposing functions: GPVI is an activating receptor on platelets, and LAIR-1 is an inhibitory receptor on immune cells (Leitinger, 2011).

Intriguingly, G-protein coupled receptors (GPCRs) have been shown to bind to collagen as well; to date, only two examples have been described *in vitro*: 1) Collagen III (COL3A1) interacts with GPR56 and induces RhoA downstream pathway to inhibit neural migration (Luo et al., 2011); and 2) Collagen IV binds to GPR126 and activates the cAMP downstream pathway (Paavola et al., 2014) in HEK293T cells.

3. The MuSCs niche

As noted with other adult stem cells, MuSCs are localized in a highly specific niche, composed of ECM, a vascular network, different types of surrounding cells, and various diffusible molecules. Furthermore, satellite cells, acting as niche

components, have been suggested to influence each other by means of cell-cell interaction and autocrine or paracrine signals (Jones and Wagers, 2008).

Due to the direct physical contact with MuSCs, myofibres represent the first critical component of the MuSC niche. Selective killing of myofibres with Marcaine resulted in greater numbers of proliferating satellite cells, thus demonstrating their requirement for MuSC homing and quiescence (Bischoff, 1990). Myofibres are likely to be the main source of the transmembrane Notch ligand Delta-like 1, thereby inducing the Notch signalling cascade in MuSCs, which in turn is critical for their maintenance (Bjornson et al., 2012; Mourikis et al., 2012b)(see Chapter 4, Section 5). According to the context, myofibres can release numerous modulators that impact on satellite cell behaviour, such as TGF β to maintain quiescence or Wnt to stimulate proliferation and expansion by symmetric division of myoblasts following injury (Bentzinger et al., 2013).

3.1. Extracellular matrix and associated factors

Resident fibroblasts are considered to be the main producers of ECM in skeletal muscle. The ECM surrounding the myofibres is composed of laminin, fibronectin (Fn), collagen and proteoglycans; all together these constituents form the basal lamina (BL) and the reticular lamina (RL) (Sanes, 2003) (**Figure 12**). Importantly, at homeostasis, MuSC is not in contact with the RL. MuSCs sit on top of the fibre and are surrounded by the BL, whose two primary components are collagen IV and laminin-2 ($\alpha 2\beta 1\gamma$), which form a network that will further link the BL to the glycoprotein nidogen (Sanes, 2003). Notably, the BL also contains type I and type VI Collagens that make the connection with the RL. COLIV and laminin-2 concentrations vary with the muscle type; slow-type *Soleus* muscle has twice more COLIV and twice less laminin-2 than the fast-type *Rectus femoris* (Kovanen et al., 1988; Schultz, 1984). Perlecan, decorin and biglycan are negatively-charged proteoglycans capable of binding and sequestering several growth factors, such as TGF β or Wnt ligands (Thorsteinsdottir et al., 2011). Perlecan binds to COLIV while decorin binds to COLIV and laminin-2 with COLI in the RL (**Figure 12**). Fibronectin is another important ECM regulator located in the RL. Finally, the structure of the satellite cell niche is stabilized by the direct binding of the BL with dystroglycan

complex proteins that are connected to the myofibres via membrane proteins such as dystrophin (**Figure 12**).

Integrins play important signalling roles in the regulation of myogenesis. Although satellite cells express almost all of the integrin subtypes (Siegel et al., 2009), quiescent MuSCs express mainly integrin $\alpha7$ and $\beta1$ that form a complex with laminin-2 in the BL. Interestingly, MuSCs deficient for integrin- $\beta1$ (*Pax7^{CreERT2}; Itgb1^{Flox}*) cannot maintain quiescence and they differentiate spontaneously without extensive proliferation (Rozo et al., 2016). Moreover, integrin- $\beta1$ has been shown to cooperate with the growth factor Fgf2 to maintain the cell in the niche.

Furthermore, $\beta1$ integrins were found to be essential in preserving the pool of different types of stem cells, by controlling the balance between symmetric and asymmetric divisions (similarly in NSCs), as well as stem cell self-renewal and differentiation (Boppart et al., 2006). However, their expression decreases with activation and is replaced by other types of integrins like $\alpha5\beta3$ that bind to proteins with RGD exposed domain (Arg-Gly-Asp) such as fibronectin or some degraded laminins and collagens (Goetsch et al., 2003). This temporal variation of integrin expression reflects the dynamic remodelling of the ECM from developing muscle to resting and injured states.

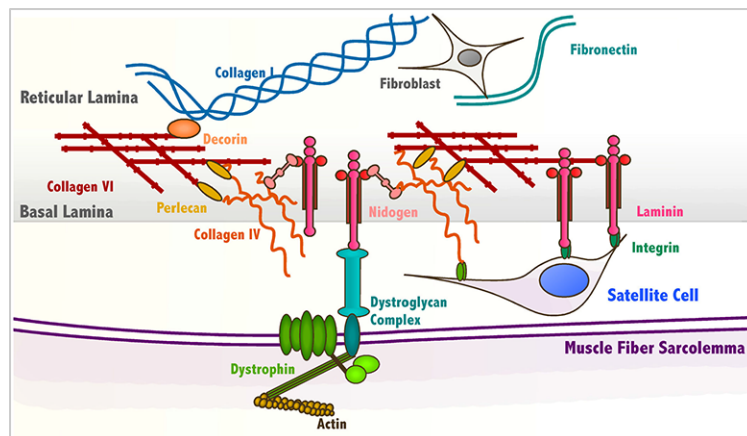


Figure 12. Satellite cell immediate niche.
(Thomas et al., 2015)

Injury involves the destruction of the BL structure by proteases inducing ECM fragmentation and growth factor release essential for recruitment of immune cells, endothelial cells and myoblasts. Metalloproteases (MMP2 and MMP9) expression peaks upon damage, followed by an upregulation of the ECM components

of the BL in a total muscle extract and in purified satellite cells (Kherif et al., 1999); These observations suggest that satellite cells are involved in the breakdown of their own niche, allowing them to migrate to the site of injury.

Given that fibroblasts are a major contributor to niche (Zou et al., 2008) to what extent do satellite cells participate to the remodelling of their own microenvironment? Interestingly, co-culture of mouse fibroblasts with quail myoblasts showed COLIV incorporation into the BL of myotubes of both mouse and quail origin, suggesting that both fibro- and myo-blasts contribute to COLIV in the niche (Kuhl et al., 1984). In addition, transcriptome analysis in quiescent and activated satellite cells showed a clear ECM signature characteristic of each cell state. Similarly, MuSCs from foetal (E.16.5), perinatal (P8) and adult (8weeks) showed an ECM stage-specific ECM signature with a progressive acquisition of the adult characteristics (Tierney et al., 2016). *Col6a1*, *Col6a2*, *Col6a3*, *Fn* and *Tenascin C* (TnC) were the more upregulated ECM genes in foetal MuSCs; however, only TnC showed a foetal-specific expression. Loss of function experiments of TnC followed by transplantation showed inhibition of cell expansion resulting in a decrease of engraftment potency. Interestingly, Fn is rapidly upregulated upon injury, and it binds to Syndecan-4 together with the Wnt ligand Frizzled-7 to form a functional Wnt activating complex that promotes symmetric expansion of myoblasts (Bentzinger et al., 2013). However, these assays rely on *in vitro* gain and loss of function experiments with purified MuSCs, and they do not address which proportion of ECM proteins produced by the fibroblasts or the satellite cells *in vivo* is sufficient for proper function.

Chapter 3.

Post-transcriptional regulation of myogenesis: a role for microRNAs

1. The discovery of microRNAs

Studies in the 1990s revealed the existence of an endogenous regulatory RNA ~22nt in size in *C. elegans*, *lin-4*, as a regulator of developmental timing (Lee et al., 1993; Wightman et al., 1993). The identification of a second small RNA, *let-7*, that is highly conserved in bilaterians was a major breakthrough as it strongly suggested the post-transcriptional regulation of gene expression by small RNAs in other organisms (Pasquinelli et al., 2000). The development of high throughput next-generation sequencing methods for small RNAs, combined with computational analysis, allowed detailed investigations of microRNAs (miRNAs). From a phylogenetic perspective, miRNAs are found early in evolution in eumetazoans (cnidarians) and expansion of miRNAs is observed at the base of vertebrate lineage and the lineage leading to mammals (Campo-Paysaa et al., 2011; Christodoulou et al., 2010; Grimson et al., 2008; Hertel et al., 2006). Remarkably, there is a direct correlation between the number of miRNAs and morphological complexity, suggesting that expansion of miRNAs may have been a key event in the emergence of complex organisms (Prochnik et al., 2007; Sempere et al., 2006; Wheeler et al., 2009). A comprehensive description of microRNAs is listed in miRBase the online database that catalogues more than 30,000 miRNAs from 206 species including mouse and human (<http://mirbase.org>). As an example, the human genome comprises >1500 hairpin structures that produce detectable small RNAs. Although their functions remain to be established, it suggests that more than half of all human protein-coding genes are under the control of small-RNAs (Bartel, 2004; Chiang et al., 2010).

2. MicroRNAs: Genomics, biogenesis, mechanism and function

2.1. Biogenesis of microRNAs

Mature miRNAs are endogenous single-stranded non-coding RNAs 20-23 nucleotides in length generated by multiple processing steps (**Figure 13**). First, RNA polymerase II produces the primary miRNAs (pri-miRNAs), a long double-stranded hairpin-shaped RNA (Lee et al., 2004) with a 5' cap structure and poly-A tail (Cai et al., 2004). In the canonical pathway, the microprocessor complex, composed of the

RNAse III Droscha and its double strand RNA binding domain partner DGCR8 (DiGeorge syndrome critical region gene 8, in mammals and Pasha in flies)(Han et al., 2004; Han et al., 2006), recognizes and cleaves ~11nt from the base of the stem-loop to produce a ~60bp hairpin structure, designated as the precursor RNA (pre-miRNA)(Gregory et al., 2004; Lee et al., 2003; Lee et al., 2002). The pre-miRNA is actively transported from the nucleus to the cytoplasm by a nuclear export receptor Exportin 5 coupled to Ran-GTP (Lund et al., 2004; Yi et al., 2003) where it undergoes a second cleavage by Dicer, another RNAse III enzyme (Bernstein et al., 2001; Grishok et al., 2001; Hutvagner et al., 2001; Ketting et al., 2001). Cleavage of the terminal loop end of pre-miRNAs leaves the 5' phosphate (miRNA-5p) and ~2nt 3' overhang (miRNA-3p) of a ~22nt double stranded duplex miRNA-miRNA* (miRNA* for passenger strand) (Lau et al., 2001). Following processing, the strand of the duplex with a less thermodynamically stable 5' end, the guide RNA, is preferentially loaded with one of the Argonaute proteins (AGO) to form the miRNA-induced silencing complex (RISC)(Hammond et al., 2000; Kawamata and Tomari, 2010). The other strand (miRNA*) is usually degraded, however, in some cases it can also be incorporated into the RISC to function as miRNA (Khvorova et al., 2003; Schwarz et al., 2003). The mature miRNA associated with the RICS binds to the 3'UTR of the target mRNA based on their complementarity (Elbashir et al., 2001a; Elbashir et al., 2001b). The primary determinant of binding specificity to complementary target mRNA is determined by Watson-Crick base-pairing of nucleotides 2-8 at the 5' end of the miRNA, referred as to "seed sequence" (Bartel, 2009; Lai, 2002). When the complementarity is perfect, the miRNA induces degradation of the target mRNA through AGO endonuclease activity. In contrast, partial paring results in repression of target mRNA translation at the initiation or elongation steps and/or sequestration of target mRNAs into cytoplasmic processing bodies (P-bodies) where mRNA is degraded through deadenylation pathways (**Figure 13**) (Parker and Sheth, 2007). Because near-perfect complementary is thought to be required for RISC-mediated cleavage but not translational repression, the lower degree of complementary seen in animals suggests that translational repression is more prevalent in animals than in plants. And to date only one example in mammalian cells of miRNA inducing cleavage of a target has been shown (Yekta et al., 2004).

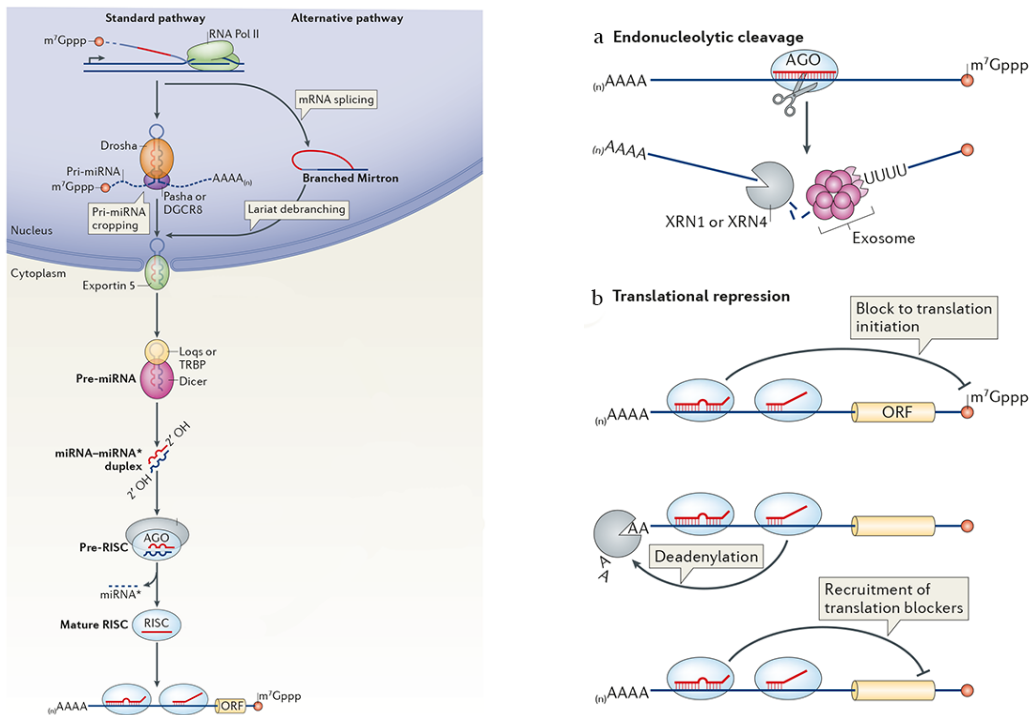


Figure 13. microRNA biogenesis and function. Left: miRNA genes are transcribed by RNA polymerase II and processed in two steps. The first step involves either the microprocessor Drosha/DGCR8 (canonical pathway, Pasha in flies) or the splicing machinery (mirtron pathway). After transport to the nucleus, the pri-miRNA is cleaved a second time by Dicer together with its ds-RNA-binding partners TRBP (mammals; Loqs in flies). Mature miRNAs assemble with the RISC complex and regulate gene expression by inhibiting translation, inducing mRNA degradation, while the passenger strand miRNA* is degraded. See text for more details. Right: (a) Perfect pairing induces endonucleolytic cleavage of the target mRNA; the 5'-to-3' exoribonuclease XRN1 (XRN4 in plant) and the 3'-to-5' exonucleolytic complex, the exosome subsequently degrade the sliced mRNA. (b) Imperfect pairing induces translation inhibition by blocking its initiation, deadenylation or recruitment of translation blockers. *Adapted from (Ameres and Zamore, 2013)*

2.2. MicroRNAs arise from distinct genomic loci

As mentioned earlier, miRNA emerge from different genomic sources that determine their spatiotemporal pattern. miRNAs can be encoded in genomes as independent transcriptional units with their own promoters (solo miRNAs) (**Figure 14a**) or as clusters of several miRNA genes transcribed as a single pri-miRNA (Ambros et al., 2003) (**Figure 14b**). miRNAs produced from a polycistronic unit arise from local gene duplication, thus they have identical seed sequences and are grouped into the same family (Ambros et al., 2003). It is estimated that 33% of the

human and 38% of mouse miRNAs are grouped into 141 families (Ambros et al., 2003). A substantial fraction of animal miRNA genes are located in introns of protein-coding genes (Rodriguez et al., 2004). For example, almost half of human miRNAs are located in introns in the same orientation of the host gene (Campo-Paysaa et al., 2011). Intronic miRNAs can have their own promoter (**Figure 14c**) or depend on the expression the host gene, thus refer to as mirtron (Isik et al., 2010; Ozsolak et al., 2008). Mirtrons are released during the alternative splicing of the host gene following debranching of the branched lariat intermediate (Ruby et al., 2007) (**Figure 13 and Figure 14d**).

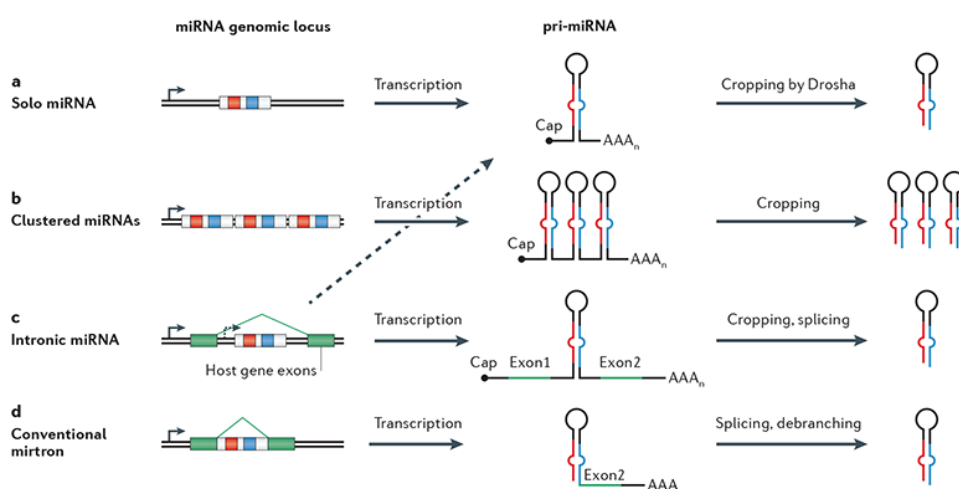


Figure 14. RNA gene structure. miRNA transcripts emerge from the genome either as independent transcriptional units with their own promoters (a) or clusters of multiple miRNAs transcribed as a single pri-miRNA (b). An important fraction of miRNAs in animals is located within introns with their own promoter (c) or do not rely on Drosha processing but rather use the host gene splicing events machinery to generate pre-miRNA (d). (Berezikov, 2011)

2.3. MicroRNA prediction tools

Micro-RNAs comprise 1-2% of all genes in worms, flies and mammals (Bartel, 2009), and because each miRNA is predicted to regulate hundreds of targets, the majority of coding proteins is thought to be under their control (Friedman et al., 2009). Thus, target identification and validation required for phenotypical analysis remains a major challenge in the field. Prediction algorithms based on diverse methods and performance have been generated where the major criterium is based on the type of pairing between the seed sequence and its potential targets (**Figure 15**). Additional features such as the conservation across species, the positioning within the 3'UTR (away from centre, 15nt from stop codon), and AU-rich nucleotide

composition near the binding site, are also used for determination of predicted target genes (Agarwal et al., 2015; Bartel, 2009). **Figure 15** shows a non-exhaustive list of prediction tools in metazoans.

Tool	Criteria for Prediction and Ranking	Website URL
Site conservation considered		
TargetScan	Stringent seed pairing, site number, site type, site context (which includes factors that influence site accessibility); option of ranking by likelihood of preferential conservation rather than site context	targetscan.org
PicTar	Stringent seed pairing for at least one of the sites for the miRNA, site number, overall predicted pairing stability	pictar.mdc-berlin.de
EIMMo	Stringent seed pairing, site number, likelihood of preferential conservation	mirz.unibas.ch/EIMMo2
Miranda	Moderately stringent seed pairing, site number, pairing to most of the miRNA	microRNA.org
miRBase Targets	Moderately stringent seed pairing, site number, overall pairing	microrna.sanger.ac.uk
PITA Top	Moderately stringent seed pairing, site number, overall predicted pairing stability, predicted site accessibility	genie.weizmann.ac.il/pubs/mir07/mir07_data.html

Figure 15. Target prediction tools. (Bartel, 2009)

3. MicroRNAs in cell and tissue regulation

The absolute requirement of miRNAs for mouse development has been shown by the germinal loss of *Dicer* which leads to lethality during gastrulation (Bernstein et al., 2003), and *Dgcr8* knock-out (KO) mice that die early in development (E6.5)(Wang et al., 2007). To bypass the lethality associated with inactivation of *Dicer*, generation of conditional KO mice using inducible Cre-recombinase has been essential to study the role of miRNAs in specific adult tissues. Interestingly, blocking the miRNA biogenesis pathway in adult mice through ubiquitous KO of *Dicer* ($R26^{CreERT2}; Dicer^{flox}$) results in defects in several tissues; the mice rapidly developed intestinal decline and died within 10 days with additional defects in bone marrow, spleen and thymus (Huang et al., 2012a). These phenotypes point to the continuous requirement of miRNAs in tissues that undergo turnover and are maintained by stem cells. For example, the deletion of *Dicer* in HSCs in adult mice (*Mx1-Cre* combined with interferon or polyinosinic-polycytidylic acid (pI:pC) treatment) induces apoptosis of HSCs following irradiation. In adult skin, deletion of *Dicer* from the basal epidermal layer (*K14-CT2; Dicer^{flox}*) showed epidermal thickening and presence

of ectopic suprabasal cells (Teta et al., 2012). Hair follicles are known to undergo cycles of growth (anagen), regression (catagen) and rest (telogen), which can be experimentally induced by hair plucking. Deletion of *Dicer* and *Drosha* at different time points during the hair follicle cycle using a doxycycline-inducible Cre (*Krt5-rtTA* and *tetO-Cre*) that is active throughout the basal epidermis and in hair follicle cells, showed that loss of miRNAs in telogen did not affect resting hair follicles (Teta et al., 2012). Interestingly, after hair plucking, mutant follicles undergo apoptosis and degradation of hair follicles. These findings underscore the temporal requirement of the miRNA pathway specifically in the growth phase in adult skin.

4. Regulation of myogenesis by microRNAs

The essential role of miRNAs for muscle development was demonstrated by the conditional deletion of *Dicer* in *Myod*-expressing cells in embryos (*Myod^{Cre}; Dicer^{fllox}*) that results in perinatal lethality due to muscle hypoplasia (O'Rourke et al., 2007). In the adult, the requirement of miRNAs in skeletal muscle regeneration has been demonstrated where the conditional deletion of *Dicer* in the Pax7+ population results in depletion of MuSCs and a quasi-absence of repair following injury (Cheung et al., 2012).

Almost immediately after the discovery that miRNAs are conserved across species, it became apparent that some miRNAs are not ubiquitously expressed as let-7, but are expressed only in certain tissues. The initial finding that some miRNAs were expressed in a tissue-specific fashion was confirmed in a study showing that miR-1, miR-122a and miR-124a expression was restricted to striated muscle, liver and brain, respectively (Lagos-Quintana et al., 2002). In an effort to identify new miRNAs, 30 miRNAs were found to be enriched or specifically expressed in skeletal muscle (Sempere et al., 2006). In addition, several studies identified other skeletal muscle specific miRNAs defined as myomirs. Interestingly, myomirs appear to have either uniform expression throughout the muscle (miR-1 and miR-133a)(McCarthy and Esser, 2007; van Rooij et al., 2009), or are enriched in slow-twitch, type I muscles (miR-206, miR-208b and miR-499)(Liu et al., 2013b; Muroya et al., 2013). To date, no myomir has been reported to be enriched specifically in fast-twitch, type II muscle. However, several miRNAs have been experimentally shown to regulate

myogenesis; these miRNAs and their respective targets are listed in Table 1. Most of the published studies contributing to our understanding of miRNAs during myogenesis have been performed using the immortalized myogenic C2C12 cell line, which recapitulates the proliferation and differentiation processes of myogenesis *in vitro* (Yaffe and Saxel, 1977), while *in vivo* studies are still missing. Due to the technical limitations to study quiescence *in vitro*, only one report has emerged implicating miR-489 regulating quiescence by the suppression of the oncogene *Dek* (Cheung et al., 2012). Thus, the regulation of MuSC quiescence and/or self-renewal by miRs remains largely unexplored.

Table 1: miRNAs controlling adult myogenesis

miRNA	Target	Biological role	Reference
miR-489	<i>Dek</i>	Regulation of proliferation of daughter cells following asymmetrical division	(Cheung et al., 2012)
miR-133a	<i>Srf</i>	Promotes differentiation	(Chen et al., 2006)
miR-27a	<i>Myostatin</i> <i>Pax3</i>	Relieves the negative regulation of Myostatin Promotes migration of myogenic progenitors	(Huang et al., 2012b) (Crist et al., 2009)
miR-27b	<i>Mef2c</i>	Promotes proliferation and differentiation by suppressing <i>Mef2c</i> which cannot associate with MRF	(Chinchilla et al., 2011)
miR-1/206	<i>Pax7</i> <i>Connexin43</i> <i>CyclinD1</i> <i>Hdac4</i> <i>Notch3</i> <i>DNA Polα</i> <i>Hmgb3</i>	Induces differentiation Inhibits formation of gap junctions Promotes cell cycle arrest Relieves HDAC repression on the chromatin associated with myogenic genes Promotes differentiation Cell cycle arrest Relieves inhibitory effects of Hmgb3 chromatin binding protein, that inhibits expression of myogenic genes	(Chen et al., 2010; Dey et al., 2011) (Anderson et al., 2006) (Zhang et al., 2012) (Chen et al., 2006) (Gagan et al., 2012) (Kim et al., 2006) (Maciotta et al., 2012)
miR-133	<i>Sp1</i> <i>Fgfr1</i>	Cell cycle arrest by relief of SP1 target, CyclinD1 Inhibition proliferation by suppression ERK1/2 signalling	(Zhang et al., 2012) (Feng et al., 2013)
miR-486	<i>Pax7</i> <i>Pten</i>	Induces differentiation Relieves Pten inhibition of mTOR signalling	(Dey et al., 2011) (Alexander et al., 2011)
miR-26a	<i>Ezh2</i> <i>Smad1/4</i>	Relieves the repressive effects of Polycomb complex on myogenic genes Inhibits TGF-β signalling to promote myogenesis	(Wong and Tellam, 2008) (Dey et al., 2012)
miR-214	<i>Ezh2</i> <i>N-ras</i>	Relieves the repressive effects of Polycomb complex on myogenic genes Cell cycle arrest	(Juan et al., 2009) (Liu et al., 2010)
miR-503	<i>Cdc25a</i>	Cell cycle arrest	(Sarkar et al., 2010)
miR-29	<i>Yy1</i> <i>Hdac4</i> <i>Akt3</i>	Relieves inhibitory effect of NFκB on myogenesis Relieves HDAC repression on the chromatin associated with myogenic genes Inhibits Akt/mTOR signalling	(Wang et al., 2008) (Winbanks et al., 2011) (Wei et al., 2013)
miR-675	<i>Smad1/5/6</i> <i>Cdc6</i>	Inhibits TGF-β signalling Cell cycle arrest	(Dey et al., 2014) (Dey et al., 2014)
miR-155	<i>Mef2c</i>	Suppresses <i>Mef2c</i> which cannot associate with MRF	(Seok et al., 2011)
miR-199a	<i>Igf1</i> <i>Pi3kr1</i> <i>mTOR</i>	Inhibition of mTOR signalling	(Jia et al., 2013)
miR-181	<i>Hox-A11</i>	Promotes upregulation <i>Myod</i> that inhibits <i>Hox-A11</i>	(Naguibneva et al., 2006)
miR-23a	<i>Myh 1,2,4</i>	Suppresses expression of contractile proteins required for the terminally differentiation	(Wang et al., 2012)
miR-148a	<i>Rock1</i>	Cytoskeleton stability	(Zhang et al., 2012)

Table 1. Recapitulation of miRNAs regulating quiescence (red), proliferation (blue) and differentiation (black). Abbreviations : Akt (RAC-alpha serine/threonine-protein kinase); DNA Pol α (DNA polymerase); Ezh2 (Enhancer of zeste homolog 2); Fgfr (foetal growth factor recetor); Hdac4 (Histone deacetylase 4); Hmgb (High mobility group box); Igf (Insulin growth factor); Mef2 (Myocyte enhancing factor); Mrf4 (Myogenic regulator factor 4); mTor (Mechanical target of rapamycin); Myf5 (Myogenic regulatory factor 5); Myod (Myogenic differentiation); Pax3/7 (Paired-box 3/7); Pten (Phosphatase and tensin homolog); Rock (Rho-associated protein kinase); Srf (Serum response factor); TGF- β (Transforming growth factor); Yy (Ying yang).

5. Inhibition of microRNAs using “Antagomirs”

A traditional approach for selective *in vivo* miRNA inhibition is to perform a knockout. Considering that about half of miRNAs are located in introns (mirtron or intronic) care will need to be taken to avoid disruption of host mRNA processing. To date, no mirtrons have yet been specifically deleted, thus *in vivo* evidence of mirtron functions from knockouts remain to be studied.

Other strategies to selectively block miRNAs *in vivo* include employing various complementary oligonucleotides which bind miRNAs and render them non-functional, or destabilize them. The most commonly used are antagomirs: 20-25 nucleotide long, single stranded RNA molecules, with a sequence complementary to an entire mature miRNA. Their backbone consists of 2'-O-methyl (2'-O-Me) single stranded oligoribonucleotides and partially modified phosphorothioate (PS) linkers. Antagomirs have a cholesterol-tag at their 3' end, which enables their efficient direct uptake via the cell membrane. Antagomirs cannot cross the blood-brain barrier and silencing was detectable up to one month after treatment even at low doses (Krutzfeldt et al., 2005). However, the systemic delivery of antagomirs induces a lack of specific cellular targeting thus secondary effects should be taken into account in the analysis of a given phenotype (Krutzfeldt et al., 2005).

Over the past fifteen years, miRNAs have emerged as key components of gene regulation; *in vitro* and *in vivo* studies uncovered their important role in myogenesis, however, whether they function to maintain muscle throughout adulthood is less clear. Moreover, future research should focus on the miRNAs involved in maintenance of adult skeletal muscle, and whether the dysregulation of miRNA

expression is responsible of the progressive loss of muscle mass with disease or ageing (Chen et al., 2009; Goljanek-Whysall et al., 2012; Williams et al., 2009). Furthermore, miRNA have been shown to be dysregulated in various myopathies, therefore both cases represent possibilities where miRNAs may be therapeutic targets or biomarkers of specific disorders (Cacchiarelli et al., 2011; Li et al., 2014). Similarly, antagomirs could be used as potential therapeutics by controlling the ability of a given miRNA to post-transcriptionally regulate gene targets that are dysfunctional resulting in a disease phenotype.

Chapter 4.

Notch signalling is a pleiotropic regulator of stem cells

1. An introduction to the world of Notch

Almost a century ago, the first description of a mutant in *Drosophila* named Notch emerged because it generated serrations (“notches”) on the wing margin (Mohr, 1919). Since then, the study of Notch has contributed to the progress of genetics as a fundamental link with developmental biology. The study of lethal phenotypes of chromosomal deficiencies unveiled a small X-linked deficiency surrounding the Notch locus (Notch⁸) that was haploinsufficient: heterozygous females had characteristic “Notch” wings, while homozygous Notch females or hemizygous Notch males died as embryos (Dexter, 1914). Finally, the analysis of the Notch lethal allele revealed a specific and reproducible neurogenic phenotype (hypertrophy of the nervous system at the expense of ectoderm). Shortly thereafter, Notch proteins were cloned in *C. elegans* and in the vertebrate *Xenopus* (Coffman et al., 1990). The wide array of tissues throughout ontogeny and the fundamental developmental processes it affects, make the *Notch* locus pleiotropic, a rare feature in metazoans.

However, it was the cloning of vertebrate Notch proteins (Coffman et al., 1990) that established the pathway logic biochemically, starting with the suggestion that truncated receptors were constitutively active (Coffman et al., 1993; Ellisen et al., 1991), identification of Notch/RBPJ complexes in nuclear extracts and the characterization of Notch cleavage sites (Jarriault et al., 1995). After twenty-five years of research, it is now clear that Notch is a fundamental, evolutionarily conserved, cell-cell interaction signalling pathways that govern metazoan cell fate determination. Not surprisingly, dysregulated signalling has also been implicated in a number of different human diseases ranging from neurodegeneration to cancer, most notably in the case of T-cell acute lymphoblastic leukemia/lymphoma (T-ALL) (Aster et al., 2008; Weng et al., 2004).

2. Notch receptors, ligands and the cascade

The binding of a specific Notch receptor to a given ligand directs the specification of cell type behaviour toward differentiation, proliferation, survival, and apoptosis – events that are essential for tissue patterning and morphogenesis (Bray,

2006; Fiuza and Arias, 2007). Notch receptors are large transmembrane proteins that transfer signals upon binding to transmembrane ligands expressed on adjacent cells. Evolution induces divergence of invertebrates as flies possess a single *Notch* gene, worms two (GLP-1 and LIN-12), and mammals four (NOTCH1-4). Regarding the canonical ligands, *Drosophila* has two prototypes, Delta and Serrate, while mammals have three Delta-like proteins (DLL1, 3 and 4) and two homologues of Serrate, Jagged-1 and 2 (JAG1-2) (Figure 16) grouped in the DSL (Delta/Serrate/LAG-2) nomenclature.

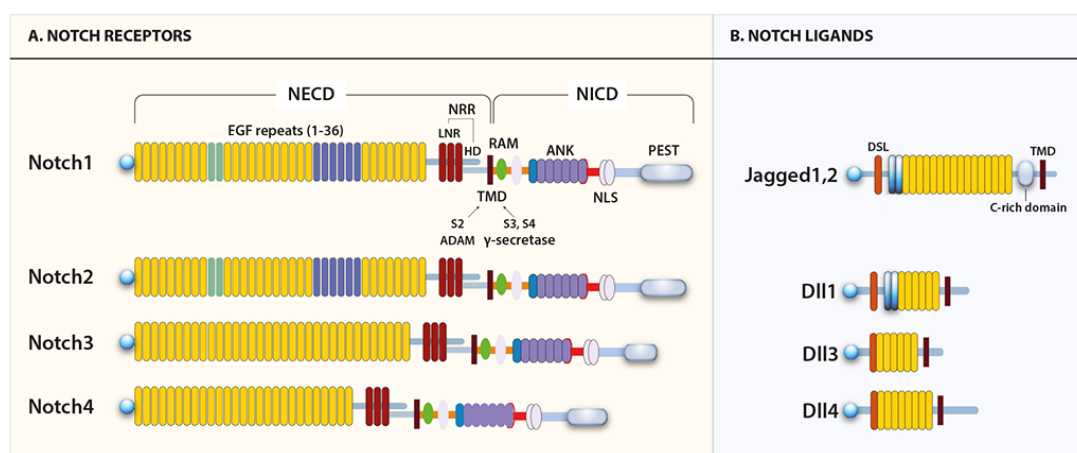


Figure 16. Structural domains of canonical Notch receptors and ligands. (A) Notch receptors are all composed of an extracellular domain (NECD), a transmembrane domain (TMD) and an intracellular domain (NICD). The four mammalian Notch receptors (Notch1-4) differ in their NECD by the number of epidermal growth factor (EGF) repeats arranged in tandems (1-36), followed by the negative regulatory region (NRR), which is composed of three cysteine-rich Lin repeats (LNR) and a heterodimerization domain (HD). EGF repeats 11-12 (green) and 24-29 (blue) mediate ligand interactions. The TMD is targeted by ADAM and γ -secretase proteolytic cleavages at S2 and S3/S4 respectively. NICD contains a RAM (RBPj κ association module) domain, nuclear localization sequences (NLSs), a seven ankyrin repeats (ANK) domain, and a transactivation domain (TAD) that harbors conserved proline/glutamic acid/serine/threonine-rich motifs (PEST). (B) Mammalian canonical ligands, Delta (Dll1/2/3) and Jagged (JAG1/2), are characterized by the presence of a Delta/Serrate/LAG-2 (DSL) domain and multiple EGF repeats. The DSL domain together with the first two EGF repeats (blue) are required for canonical binding to receptors. (Yavropoulou and Yovos, 2014)

In the absence of ligand, Notch receptors are maintained in a resting, proteolytically resistant conformation on the cell surface. DSL ligand binding induces a proteolytic cascade that releases the Notch intracellular domain of the receptor (NICD) from the membrane. The first cleavage step is achieved by ADAM metalloproteases at the S2

site located ≈ 12 amino acids before the plasma membrane and generates the membrane-anchored Notch extracellular truncation (NEXT) fragment (Brou et al., 2000; Mumm et al., 2000). This truncated receptor NEXT remains at the membrane until it is processed at site S3 and S4 by γ -secretase, a multiprotein enzyme complex (De Strooper et al., 1999; Struhl and Greenwald, 1999; Wolfe et al., 1999). After γ -secretase cleavage, NICD translocates to the nucleus, where it assembles a transcriptional activation complex containing a DNA-binding transcription factor called CSL [CBF1 (yeast)/RBPJ (vertebrates)/Su(H) (*Drosophila*)/Lag-1 (*C. elegans*)] and a co-activator of the Mastermind family (MAML) (Petcherski and Kimble, 2000) to induce the transcription of specific genes (**Figure 17**). Interestingly, genome-wide Chromatin immunoprecipitation (ChIP) sequencing experiment performed on myogenic cells unravelled a dynamic recruitment of RBPJ on DNA upon Notch activation. Moreover, in the majority of cases, RBPJ was not statically occupying gene regulatory sequences and the absence of expression was essentially due to the absence of RBPJ rather than an active transcriptional repression (Castel et al., 2013) (**Figure 18**). This new model, that complemented similar findings in *Drosophila* (Krejci and Bray, 2007), modified our view on how Notch signalling activation/repression modulates cell behaviour; however future work on other cell types needs to be performed to define whether this is a general phenomenon.

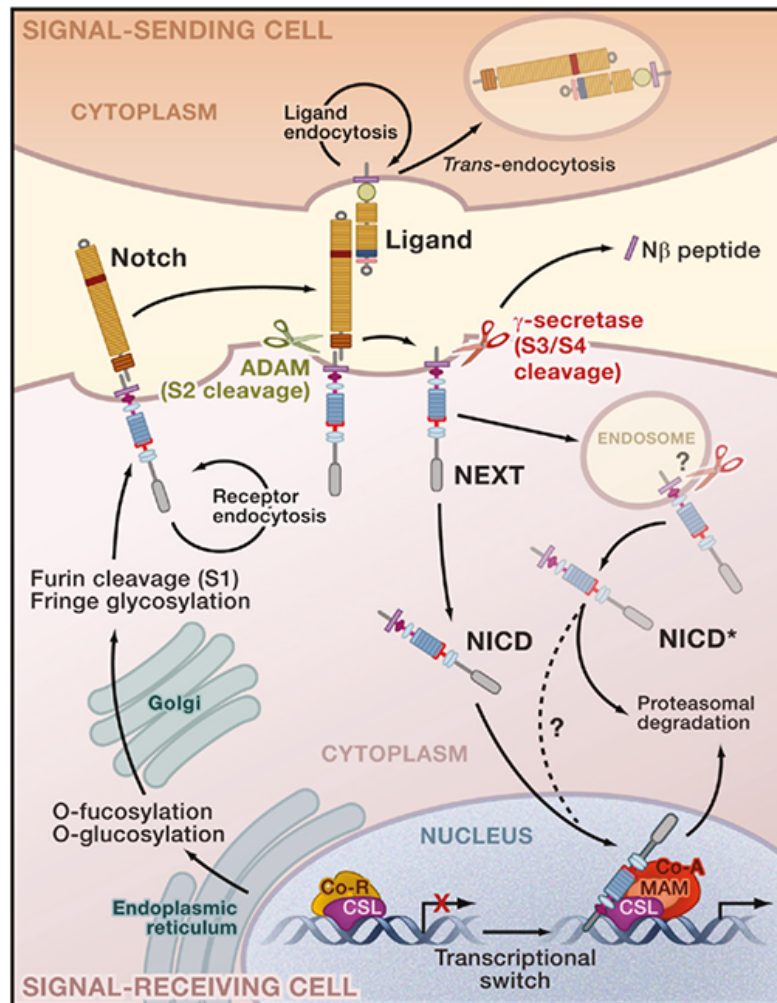


Figure 17. Canonical Notch signalling. Notch signalling is involved in short-range communication between juxtaposed cells with the signal-sending cell expressing ligand (Dll, Jag) and the signal-receiving cell expressing Notch receptor. Activation of the receptor is mediated by proteolytic cleavage events, but optimal Notch signalling also depends on post-translational modifications and proper membrane trafficking of Notch receptors and ligands. In the receiving cell, newly synthesized receptor undergoes O-fucosylation and O-glycosylation within the endoplasmic reticulum (ER). Upon transit through the Golgi, fucose moieties are further modified through the addition of N-acetylglucosamine by Fringe O-glycosyltransferases, which can alter ligand-binding specificity. In addition, the Notch receptor is cleaved by furin-like protease (S1 cleavage) to generate heterodimers held together by non-covalent interaction. Mature receptor is then delivered to the plasma membrane. Upon ligand binding, the Notch receptor is cleaved by ADAM (S2 cleavage), which release Notch extracellular truncation fragment (NEXT) that will further be cleaved by γ -secretase (S3/S4 cleavage) and produce the Notch intracellular domain (NICD) and N β peptide. Studies have shown that this cleavage occurs in an endosome structure as well. In the absence of signalling, CSL interacts with co-repressors molecules (Co-R) to suppress transcription of specific genes. However, upon Notch activation, NICD is translocated to the nucleus where it binds to CSL, MAM and other co-activators (Co-A) to activate transcription. NICD signalling is terminated by rapid phosphorylation of its PEST domain and targeting for proteosomal degradation by E3 ubiquitin ligases. (Kopan and Ilagan, 2009)

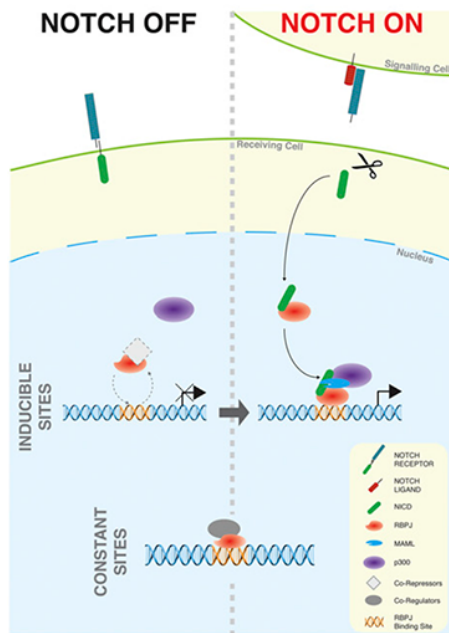


Figure 18. Inducible Rbpj-binding model in response to Notch activation. Upon Notch receptor activation and cleavage, NICD (green) is translocated to the nucleus, where it binds to RBPJ (red). This model proposes an absence of RBPJ occupancy on DNA in absence of NICD. Instead, NICD binds to RBPJ off the DNA and subsequently recruits the co-activators to induce gene transcription on the inducible sites. On the constant sites, RBPJ is present on DNA and inhibits transcription by binding to co-repressors. (Castel et al., 2013)

3. Notch targets genes and their regulation

The diversity in Notch signalling outputs covers proliferation, apoptosis, cell fates or activation of other signalling pathways. However, only a fairly limited set of Notch target genes have been identified in various cellular and developmental contexts. The first and best-characterized Notch targets are the highly conserved basic helix-loop-helix (bHLH) genes of the hairy/enhancer of split (*Hes*) and its related *Hey* genes families, like the *E(spl)* genes in *Drosophila* and *Hes1* in mouse (Fischer and Gessler, 2007). Several lines of evidence have suggested that these genes are indeed direct Notch target genes: a) Their promoters (*Hes*, *Hey* and *HeyL*) can be activated by a constitutive active form of *Notch1* (Iso et al., 2003), b) endogenous expression is upregulated by NICD in several different cell lines (Iso et al., 2003), c) similarly in co-culture experiments with Notch-ligand expressing cells, that reach a more physiological level of Notch signalling (Jarriault et al., 1998; Shawber et al., 1996); d) microarray analysis on γ -secretase (inhibitor DAPT) treated cells identified again members of this transcription factor family as direct Notch target genes (Weng et al., 2004). Finally, Notch signalling such as oscillations of *Hes* expression that have been observed and are thought to contribute to clocks that regulates somitogenesis, limb segmentation, and neural progenitor maintenance (Brend and Holley, 2009; Kageyama et al., 2010; Lewis et al., 2009; Pascoal et al., 2007; Shimojo et al., 2008).

All HES/HEY proteins appear to function as transcriptional repressors as they share a C-terminal motif sufficient to recruit transcriptional co-repressors of the Groucho family (Paroush et al., 1994). However, *Hes/Hey* genes alone are not sufficient to explain all *Notch* functions as demonstrated by the elimination of *E(spl)* genes in the *Drosophila* wing that fails to mimic the classic wing "notching" caused by *Notch* mutation. This includes *Nrarp* (Lamar et al., 2001) and *Deltex-1* (Izon et al., 2002), *c-myc* (Palomero et al., 2006), *cyclinD1* (Ronchini and Capobianco, 2001), *Notch1* itself and *Notch3* (Weng et al., 2004), *bcl-2* (Deftos et al., 1998) and *E2Ac* (Ordentlich et al., 1998) and *HoxA5*, *9* and *10* (Weerkamp et al., 2006). Interestingly, recent genome-wide studies in human T-ALL cells and in *Drosophila* myogenic precursor-related cells revealed that, even within a specific cell type, Notch regulates a diverse array of direct targets at every step during lineage progression (Krejci et al., 2009; Palomero et al., 2006).

4. Notch signalling in the regulation of stem cell fate

As mentioned in the previous chapter, maintenance and differentiation of stem cells depend intimately on cellular interactions between stem cells themselves, and between stem cells and the stromal cell components of their niche. As a consequence, the pleiotropic influence of Notch on tissue-specific stem cells is highly context dependent, and its biological outcomes vary from stem cell maintenance or expansion, to promotion of differentiation (**Table 2**) (Brack et al., 2008; Casali and Batlle, 2009; Dreesen and Brivanlou, 2007; Farnie and Clarke, 2006). Advances in inducible Cre-loxP targeting technologies that allow cell-specific *in vivo* tracing and gain/loss of function have demonstrated the critical role of Notch signalling in tissue renewal and maintenance in many organs, including blood, intestine, central nervous system, bone, skin and muscle (**Table 2**).

Stem/Progenitor cells	Function	Reference
<i>Small intestinal</i> ISC	Maintenance Proliferation and terminal differentiation to absorptive lineage	(Fre et al., 2011; Fre et al., 2005; Pellegrinet et al., 2011)
<i>Skin</i> Bulge SC Epidermal SC	Tumour suppressor Lineage determination toward hair follicle cells	(Blanpain et al., 2006; Demehri et al., 2008; Nowell and Radtke, 2013; Okuyama et al., 2008)
<i>Hair follicle</i> Melanocyte SC	Survival of immature melanoblasts Luminal lineage differentiation	(Lee et al., 2007; Nowell and Radtke, 2013; Okuyama et al., 2008; Rizvi et al., 2002)
<i>Nervous system</i> NPC, NSC	Maintenance of quiescence Inhibit differentiation	(Carlen et al., 2009; Chapouton et al., 2010; Ge et al., 2002; Imayoshi et al., 2010; Kazanis et al., 2010; Mizutani et al., 2007)
<i>Mammary gland</i> MaSC	Oncogene Proliferation and differentiation of MaSC	(Bouras et al., 2008; Dontu et al., 2004; Farnie and Clarke, 2007; Visvader and Stingl, 2014)
<i>Bone</i> MSC	Maintenance of mesenchymal progenitors to promote osteogenesis	(Yavropoulou and Yovos, 2014)
<i>Blood</i> HSC	Dispensable for maintenance Expansion of multipotent progenitors High Notch > T-cell Absence Notch > B-cell	(Han et al., 2002; Izon et al., 2002; Maillard et al., 2008; Pear and Radtke, 2003; Weerkamp et al., 2006)
<i>Eye</i> Corneal epithelial SC	Maintenance of SCs during repair	(Nowell and Radtke, 2017; Vauclair et al., 2007)

Table 2. Summary of Notch signalling in mammalian adult stem cells. ISC: Intestinal stem cell; SC: Stem cell; NPC: Neural progenitor cell; NSC: Neural stem cell; MaSC: Mammary stem cell; MSC: Mesenchymal "stem" cell; HSC: Hematopoietic stem cell.

5. Notch signalling in skeletal muscle and satellite cells

In the dermomyotome, lineage-tracing experiments showed that Notch activity is necessary for smooth muscle production while inhibiting striated muscle differentiation by influencing lineage diversification in the multipotent cells (Ben-Yair and Kalcheim, 2008). Moreover, activated Notch signalling has long been known to suppress myogenic differentiation before muscle cell commitment and muscle structural gene activation by suppressing *Myod* and to lesser extent *Myf5*

(Kopan et al., 1994). Moreover, Notch was shown to be essential for myogenic stem cell fate regulation and differentiation throughout embryogenesis as conditional mutation of *Rbpj* or *Dll1* results in uncontrolled myogenic differentiation associated with depletion of the myogenic precursor pool and severe muscle hypotrophy (Schuster-Gossler et al., 2007; Vasyutina et al., 2007). This block of myogenic differentiation appears to be mediated by repression of MRF expression by *Hes1* (Jarriault et al., 1998) as well as by direct interaction of activated Notch with Mef2c (Wilson-Rawls et al., 1999). Interestingly, in dorsal somitic muscle progenitor cells in the avian embryo, transient, but not sustained Notch activation is necessary for the expression of *Myod* and *Myf5* and for lineage commitment and differentiation (Rios et al., 2011) showing differences among vertebrates.

Emerging MuSCs are found underneath a basement membrane from about 2 days before birth in mice and they continue to proliferate until the mid-perinatal stage (Tajbakhsh, 2009). Consistent with this notion, previous studies have indicated that the muscle stem cell population requires the presence of differentiating cells for their maintenance, such that a lack of differentiated cells results in the loss of upstream Pax7⁺ cells in the foetus (Kassar-Duchossoy et al., 2005). Furthermore, deletion of *Rbpj* in myogenic progenitor pool results in depletion of progenitors accompanied by upregulation of *Myod* (Vasyutina et al., 2007). Interestingly, the double elimination of both *Rbpj* and *Myod* in myogenic progenitors (*Pax3^{Cre}; Rbpj^{flox/flox}; Myod^{-/-}*) rescues the loss of the myogenic stem cell pool. However, those cells fail to adopt a satellite cell phenotype and do not colonize the stem cell niche (Brohl et al., 2012). The transcriptomic analysis of *Pax3^{Cre}; Rbpj^{flox/flox}; Myod^{-/-}* isolated cells showed deregulated expression of genes encoding cell adhesion (e.g. *Megf10*, *Gpc1*, *Mcam*) and basal lamina molecules (e.g. *Itga7*, *Col18a1*, *Sgca*, *Col4a2*). Additional immunostaining experiments showed defects in the assembly of the basal lamina surrounding emerging cKO satellite cells highlighting the requirement of Notch in the homing and anchorage of future satellite cells in the embryos (Brohl et al., 2012).

In contrast, constitutive overexpression of NICD in myoblast precursors (*Myf5^{Cre}; R26^{stop-NICD}*) results in adoption of a premature MuSC fate (under basal lamina, EdU-negative, Calcitonin receptor-positive) (Mourikis et al., 2012a). Taken together, these

studies showed an essential role of Notch, initiated by Dll1 ligand and transduced by RBPJ, for establishing the muscle stem cell pool during development, however, the mechanisms underlying those events remain unclear.

In addition to its key significance in developing skeletal muscle, Notch signalling plays a continuous and essential role in satellite cell quiescence and proliferation during muscle regeneration. Notch activity is high in the more upstream progenitors, and it decreases with commitment (Mourikis et al., 2012b). Satellite cells express Notch 1, 2, and 3 receptors and the ligand, Dll, is most likely provided by the myofibres. The involvement of Notch in satellite cell behaviour has been shown first *in vitro* by overexpression of the *Dll1* in signal-sending cells, or constitutive expression of *Notch1* in satellite cells that also showed inhibition of myogenic differentiation (Conboy et al., 2003; Conboy and Rando, 2002; Sun et al., 2008).

However, the role of Numb as a negative regulator of Notch in this process remains unclear; although it has been shown to have a role in the asymmetric cell division in primary myoblasts (Shinin et al., 2006), Numb does not appear to regulate Notch in satellite cells (Le Roux et al., 2015) (George et al., 2013). Ultimately, it was the *in vivo* conditional depletion of *Rbpj* in MuSCs (*Tg:Pax7-CT2; Rbpj^{flox}*) that revealed the absolute requirement for Notch activity in maintaining satellite cell quiescence and maintenance. In these studies, the absence of Notch induces the MuSCs spontaneous exit from quiescence and premature differentiation leading to the depletion of the stem cell pool and quasi-absence of regeneration upon injury (Bjornson et al., 2012; Mourikis et al., 2012b) (**Figure 19**). Surprisingly, overexpression of NICD in MuSCs induces a fate switch from myogenic to brown adipogenic lineage (*Pax7^{CreET2/+}; R26^{stop-NICD}*), while it rescues the loss of satellite cells in adult *Pax7*-deficient mice (*Pax7^{CreET2/flox}; R26^{stop-NICD}*) (Pasut et al., 2016).

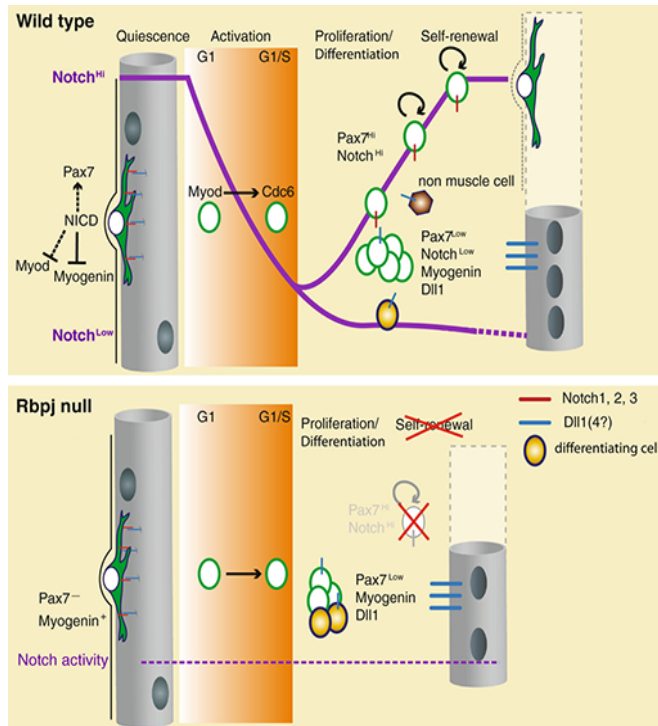


Figure 19. Notch regulation of muscle stem cells. Top: Quiescent, G₀-arrested MuSCs express high level of Notch (Notch^{High}), which directly inhibits *Myogenin* (via *Hey1*) and indirectly *Myod* to maintain *Pax7*. Upon activation, Notch level rapidly decreases, *Myod* expression is released to promote expression of *Cd6* and S-phase entry. During amplification, Notch is restricted to upstream Pax7^{High} population that will self-renew. Bottom: The majority of *Rbpj* null MuSCs spontaneously differentiate without injury, bypass S-phase and fuse with the pre-existing fibre. (Mourikis and Tajbakhsh, 2014)

As mentioned above, the activation of Notch in muscle cells results in the transcription activation of specific genes, notably members of the Hes/Hey family (Castel et al., 2013; Jarriault et al., 1998; Kopan and Ilagan, 2009). Intriguingly, the constitutive double *Hey1* and *HeyL* knock-out triggers a progressive loss of MuSCs (<20% in 20 weeks) similar to depletion of *Rbpj* (Fukada et al., 2011), whereas the absence of Notch3 receptor (*Notch3*^{-/-}) results in an increase in satellite cell number (+140% in 4 months) (Kitamoto and Hanaoka, 2010). Although those studies used constitutive mutants, they provide insightful information on the role of Notch in muscle physiology and repair. For example, aged (*Tg:MCK-Cre; R26*^{stop-NICD}) and dystrophic mice (*Tg:MCK-Cre; R26*^{stop-NICD}; *mdx*) that experienced NICD specifically in myofibres have been shown to improve muscle function and repair (Bi et al., 2016).

To control muscle stem and progenitor cell activity, Notch signals must be integrated with a host of other intrinsic and extrinsic inputs, which ultimately determine cell fate. Indeed, genetic and pharmacological analyses indicate significant cross talk between this pathway and several other key regulators of muscle development and regeneration (Buas and Kadesch, 2010). Interestingly, Notch signals can either

reinforce or counteract these additional tissue regulators in a developmental and tissue-dependent manner. Similar to Notch, induction of BMP signalling appears to block differentiation of myogenic cells (Kopan et al., 1994; Kuroda et al., 1999). Addition of BMP4 in satellite cells *in vitro* dramatically reduces the number of differentiated myoblasts and simultaneously induces Notch responsive genes (*Hey1* and *Hes1*), suggesting that BMP4 may inhibit myogenic differentiation through upregulation of Notch signalling (Dahlgqvist et al., 2003). Consistent with this notion, concomitant blockade of Notch signalling in BMP4-treated cell cultures, either by addition of GSI or by introduction of a dominant-negative version of CSL, can restore myogenic differentiation (Dahlgqvist et al., 2003). Thus, functional Notch signalling appears to act in concert with BMP4 to restrict myogenic differentiation and promote a more primitive stem cell fate among muscle satellite cells.

Similarly, TGF- β also instructs a signalling cascade that intersects with Notch pathway, however, in contrast to BMP4, TGF- β appears to restrain myogenic differentiation. For example, aged muscle produces excessive TGF- β which induces abnormal high levels of phosphorylated Smad3 in satellite cells that appears to impair muscle regenerative capacity through direct antagonism of endogenous Notch signals. Thus, inhibition of TGF- β /Smad3 or, conversely, activation of Notch signalling in the injured muscle of aged mice can restore muscle regenerative potential (Carlson et al., 2008; Derynck and Zhang, 2003; Massague and Wotton, 2000).

RESULTS

Part I:

Notch-induced Collagen V maintains muscle
stem cells by reciprocal activation of the
Calcitonin Receptor

Nature, under revision

1 **Notch-induced collagen V maintains muscle stem cells by reciprocal activation of the**
2 **Calcitonin Receptor**

3

4 Meryem B. Baghdadi^{1,2,3}, David Castel^{4,5}, So-ichiro Fukada⁶, David E. Birk⁷, Frederic
5 Relaix⁸, Shahragim Tajbakhsh^{1,2*} and Philippos Mourikis^{8*}.

6 *1: Stem Cells and Development, Department of Developmental & Stem Cell Biology, Institut Pasteur,*
7 *Paris 75015, France.*

8 *2 : CNRS UMR 3738, Institut Pasteur, Paris 75015, France.*

9 *3: Sorbonne Universités, UPMC, University of Paris 06, IFD-ED 515, 4 Place Jussieu, Paris 75252,*
10 *France.*

11 *4: UMR8203 Vectorologie et Thérapeutiques Anticancéreuses," CNRS, Gustave Roussy, Univ. Paris-*
12 *Sud, Université Paris-Saclay, 94805, Villejuif, France*

13 *5: Département de Cancérologie de l'Enfant et de l'Adolescent, Gustave Roussy, Univ. Paris-Sud,*
14 *Université Paris- Saclay, 94805, Villejuif, France*

15 *6: Laboratory of Molecular and Cellular Physiology, Graduate School of Pharmaceutical Sciences,*
16 *Osaka University, Osaka 565-0871, Japan.*

17 *7: Department of Molecular Pharmacology & Physiology, University of South Florida, Morsani*
18 *College of Medicine, Tampa, Florida 33612.*

19 *8: INSERM IMRB U955-E10, UPEC, ENVA, EFS, Creteil 94000, France.*

20 ** Correspondence: shahragim.tajbakhsh@pasteur.fr and philippos.mourikis@inserm.fr*

21

22

23

24

25

26

27

28

29

30

31

32 **Abstract**

33 **The stem cell microenvironment is critical for their maintenance and can be of cellular**
34 **and non-cellular nature, including secreted growth factors and extracellular matrix**
35 **(ECM)¹⁻³. Although certain signalling pathways that regulate quiescence have been**
36 **identified⁴⁻⁷, the composition and source of niche molecules remain largely unknown. By**
37 **ChIP-sequencing we identified Notch/RBPJ-bound regulatory elements adjacent to**
38 **specific collagen genes in adult muscle stem cells (MuSCs), whose products are linked to**
39 **the ECM and constitute putative niche components. Using genetically modified mice, we**
40 **show that the expression of these collagens is controlled by Notch activity *in vivo*.**
41 **Notably, we find that MuSC-produced collagen V (COLV) is a critical component of the**
42 **quiescent niche, as conditional deletion of *Col5a1* leads to anomalous cell cycle entry**
43 **and differentiation of MuSCs. The G-protein coupled Calcitonin receptor (CALCR) is**
44 **critical for MuSC maintenance and its ligand is expressed systemically⁸. Strikingly,**
45 **COLV, but not collagen I and VI, specifically interacts with and activates CALCR,**
46 **thereby acting as a local surrogate ligand to retain MuSCs in their niche. Finally,**
47 **functional studies on *Rbpj* null MuSCs demonstrate that COLV-CALCR activity is**
48 **epistatic to Notch signalling. This study unveils a Notch/COLV/CALCR signalling**
49 **cascade that cell-autonomously maintains the MuSC quiescent state, and raises the**
50 **possibility of a similar reciprocal mechanism acting in diverse stem cell populations.**

51

52 Using ChIP-seq screening we identified ECM collagens as direct targets of Notch signalling,
53 a pathway critical for maintaining MuSCs in a quiescent state⁴. Sequences bound by
54 intracellular Notch (NICD) and its downstream effector RBPJ were found close to collagens
55 *Col5a1*, *Col5a*, *Col6a1* and *Col6a2* (Figure 1A; data available at Gene Expression Omnibus,
56 Accession no. GSE37184), which are amongst the most highly expressed collagen types in
57 MuSCs (Figure S1A). The epigenetic signature of these sequences by the histone
58 modifications H3K4me1, H3K27ac and the acetyltransferase p300 that are associated with
59 enhancer elements (Figure 1A), the presence of RBPJ binding consensus, and their ability to
60 induce transcription upon Notch activation in cell-based luciferase assays, demonstrated that
61 these are *bona fide* NICD/RBPJ-regulated enhancers⁹⁻¹¹ (Figure 1B-C). Accordingly, RNA-

62 seq in the murine myogenic C2C12 cell line showed that following Notch activation, 4 out of
63 the 5 upregulated collagen genes corresponded to those associated with NICD/RBPJ
64 regulated enhancers (Figure S1B)¹².

65

66 We then investigated the transcriptional response of the collagen genes to Notch activity
67 modulations *in vivo*. First, we analysed distinct subpopulations of MuSCs from *Tg:Pax7-*
68 *nGFP* E17.5 fetuses, in which endogenous Notch activity gradually declines as cells transit
69 from an upstream Pax7^{Hi} to a committed Pax7^{Lo} state^{4,13} (Figure S1C-C'). Accordingly, we
70 found that *Col5a1*, *Col5a3*, *Col6a1*, and *Col6a2* were highly expressed in the Pax7-
71 nGFP^{Hi}/Notch-high population and drastically decreased in the differentiating, Pax7-nGFP^{Lo}
72 cells (Figure 1D). Analysis of quiescent MuSCs in which Notch signalling was abrogated by
73 combining the *Pax7^{CreERT2}* driver and the conditionally null *Rbpj^{flox}* allele^{4,14} showed a
74 marked reduction of the candidate collagen targets in *Rbpj* null compared to control cells
75 (Figure 1E and S1D). In a complementary gain-of-function approach, we expressed NICD
76 (*R26^{stop-NICD-nGFP}*) conditionally in embryonic¹⁵ and adult MuSCs, using *Myf5^{Cre}* and
77 *Pax7^{CreERT2}*, respectively. All collagen target transcripts tested were significantly upregulated
78 in MuSCs isolated from E17.5 *Myf5^{Cre}-NICD* fetuses (Figure 1F) and the COLV protein
79 isoform [(a1(V)a2(V)a3(V))] (α 3-COLV) was drastically increased both in foetal forelimb
80 (Figure 1G) and resting adult *Tibialis anterior* (TA) muscle sections (Figure 1H and S1E). To
81 determine if Notch drives *de novo* COLV synthesis in MuSCs, we isolated and
82 immunolabelled single myofibres from *Pax7^{CT2}-NICD* mice. Expectedly, as collagenase is
83 used for the separation of individual myofibres, no α 3-COLV was detected immediately after
84 isolation (Figure 1I). However, after 24h of culture, abundant, newly synthesized COLV
85 surrounded the MuSCs as visualized by optical sections of myofibre z-stacks (Figure 1I, 1J).

86

87 To assess the impact of the different collagens on MuSC behaviour, we incubated freshly
88 isolated MuSCs with COLV and COLVI. The ubiquitous collagen I (COLI) as well as the
89 solubilizing agent acetic acid (HOAc) were used as controls. Notably, only the COLV-
90 complemented medium induced a significant decrease in EdU uptake at 32h post-plating
91 (Figure 2A-B). Furthermore, an increase in the ratio of Pax7⁺ over Myogenin⁻ cells indicated
92 that just COLV exhibited an anti-myogenic activity (Figure 2C-D). Accordingly, MuSCs
93 cultured for 10 days to allow myoblast fusion showed a striking reduction in myotube
94 formation when treated with COLV, but not COLI or COLVI (Figure 2E-F). Remarkably,
95 COLV also rescued the precocious differentiation of *Rbpj*^{-/-} MuSCs⁴, indicating that it acts
96 downstream of Notch signalling (Figure 2G and S2A). Moreover, transcript analysis of these
97 cells showed that COLV strongly antagonized the expression of *Myogenin* even in the
98 absence of RBPJ (Figure S2B). Taken together, these results show that COLV in suspension
99 specifically induces a delay in cell cycle entry, differentiation, and fusion of MuSCs, and that
100 it acts epistatically to Notch signalling.

101

102 In a complementary approach, we tested the impact of COLV loss-of-function using short-
103 interfering RNA (siRNA) on isolated myofibres, where resident MuSCs enter the myogenic
104 program and form clusters composed of proliferating (Pax7⁺/MyoD⁺/MyoG⁻), differentiated
105 (Pax7⁻/MyoG⁺) and self-renewed (Pax7⁺/MyoD⁻) cells within 72h¹⁶. Targeting of either
106 *Col5a1* or *Col5a3* dramatically decreased the number of the self-renewing Pax7⁺/MyoD⁻ cells,
107 compared to scramble controls (Figure 2H and S2C). Of note, *siCol5a3* phenocopied
108 *siCol5a1*, strongly suggesting that the active triple helix is the α3-COLV isoform composed
109 of both α1 and α3 chains as an [α1(V)α2(V)α3(V)] heterotrimer. Taken together, these data
110 demonstrate that cell-autonomous production of COLV by MuSCs contributes to their niche
111 and promotes their self-renewal downstream of Notch signalling.

112

113 The observation that COLV could sustain primary MuSCs in a more stem-like, Pax7⁺ state *ex*
114 *vivo* is consistent with a putative role as regulator of the quiescent niche. To test this directly,
115 we analysed COLV-null MuSCs in compound *Tg:Pax7-CT2; Col5a1^{fllox}* mice^{4,17} (Figure 3A-
116 B). As the COL5A1 chain is present in all COLV isoforms, *Col5a1* deletion produces
117 complete COLV-null cells. Of interest, COLV-null MuSCs in resting muscle showed
118 upregulation of the activation and differentiation markers *Myod* and *Myog*, respectively, and
119 a concomitant reduction of the quiescence marker *Calcr*, as well as *Pax7* (Figure 3C).
120 Accordingly, mutant MuSCs in resting muscle were abnormally positive for MyoG protein
121 (Figure 3D). As loss of COLV function resulted in the loss of cellular quiescence, we
122 investigated if this cell state transition was accompanied by entry into S-phase, by exposing
123 the mice to uninterrupted BrdU for 6 days prior to sacrifice (Figure 3A). As shown in Figure
124 3E, a significantly increased number of cycling cells was detected in COLV mutants
125 compared to controls. Therefore, within a relatively short period of 2-4 weeks, inhibition of
126 *de novo* COLV production resulted in MuSCs spontaneously exiting from quiescence,
127 entering into the cell cycle, progressing to terminal differentiation. We next examined the
128 regeneration and self-renewal capacity of *Col5a1* null MuSCs in an acute, cardiotoxin-
129 induced injury of *Tibialis anterior* (TA) muscles (Figure 3F). Although overall regeneration
130 was comparable between mice following a relatively short period of Cre-mediated
131 recombination (Figure S3), we observed a significantly lower number of Pax7⁺ cells at day
132 18 post-injury in the *Col5a1* mutants compared to controls (Figure 3G). This observation
133 strongly suggested that the self-renewal of COLV-deficient MuSCs was impaired, in
134 agreement with the phenotype of *Col5a1* and *Col5a3* siRNA experiments (Figure 2H). Taken
135 together, our data lead us to conclude that MuSCs require continuous and cell-autonomous
136 COLV production, likely as an α3-COLV isoform to maintain their quiescent state.

137

138 Substrate rigidity and geometry have been demonstrated to control MuSC stemness,
139 differentiation and self-renewal¹⁸⁻²¹. We noted that COLV interacted with MuSCs only when
140 in solution, but not as a coating substrate in culture (data not shown), leading us to speculate
141 that in this scenario COLV acts as a signalling molecule rather than a biomechanical
142 modulator. To identify the cell surface receptor of collagen V on MuSCs, we used the
143 differentiation assay of primary MuSCs treated with COLV (see Figure 2E) coupled to
144 inhibitors of specific receptors previously shown to bind diverse collagen types, including
145 Integrin $\beta 1$ and the RTK receptor DDR^{22,23}. The DDR1 inhibitory small molecule 7rh, as well
146 as integrin inhibitors specifically directed against $\alpha 1\beta 1$, $\alpha 2\beta 1$ or the broad-spectrum integrin-
147 binding competitor RGDS peptide did not obscure the anti-myogenic activity of COLV
148 (Figure S4A). Since collagens have also been shown to bind G-protein coupled receptors in
149 some cases^{24,25}, we focused on the MuSC-expressed GPCR Calcitonin Receptor, a factor
150 critical for maintenance of MuSCs⁸. In addition to a strong induction of *Calcr* transcripts
151 observed in COLV-treated MuSCs (Figure S4B), CALCR protein was maintained in MuSCs
152 cultured for 72h in the presence of COLV, whereas it was undetectable in control cells,
153 suggesting a possible interaction between these two proteins (Figure 4A). To determine
154 whether CALCR can mediate COLV signalling, we isolated *Calcr* null MuSCs from
155 *Pax7^{CT2};Calcr^{lox}* mice (Figure 4B and S4C-D) and cultured them in the presence of COLV
156 for 10 days. Strikingly, in contrast to control cells, *Calcr^{-/-}* MuSCs did not respond to COLV
157 treatment, demonstrating that CALCR constitutes a crucial mediator of the COLV signal
158 (Figure 4C). To further test the role of CALCR in COLV induction, we generated CALCR-
159 overexpressing C2C12 cells by retroviral transduction, and compared them to mock-
160 transduced C2C12 cells which do not express the receptor⁸ (Figure 4D). Strikingly, the
161 response to COLV treatment was CALCR-dependent: mock cells did not respond to COLV,
162 whereas cells with CALCR showed decreased proliferation (Figures 4D). Similarly, primary
163 *Calcr^{-/-}* MuSCs were unresponsive to COLV, and proliferated (t32h, EdU⁺) and

164 differentiated (t72h, MyoG⁺) as controls (Figure 4E). Interestingly, these effects were
165 specific for COLV, but not COLI or COLVI. In summary, we show that CALCR is a critical
166 mediator of the effect of COLV for maintaining the quiescence and stemness properties of
167 MuSCs.

168

169 To date, it has been assumed that MuSC-CALCR is regulated by circulating peptide
170 hormones (calcitonin family members), pointing to an unusual model of systemic regulation
171 of MuSC quiescence in different muscle masses, although clear evidence for such a
172 mechanism are lacking. Following our functional association studies, we assessed if COLV
173 might serve as a local surrogate ligand for the CALCR receptor. Notably, on-cell ELISA
174 experiments showed that COLV selectively bound to the CALCR⁺, but not mock-transduced
175 C2C12 cells that lack this receptor (Figure 4F and 4G). To determine if this binding was
176 functional, we measured the intracellular levels of cAMP, a downstream reporter of CALCR
177 activation²⁶. Strikingly, COLV, but not COLI or COLVI, triggered cAMP upregulation only
178 in the *Calcr*-expressing cells, and at levels similar to the known CALCR ligand Elcatonin
179 (Figure 4H), with a half-maximal response (EC50) at 25 µg/ml (Figure 4I). Finally, a time
180 course study determined that cAMP increased markedly after 60 min and reached a plateau
181 after 180 minutes of exposure to COLV, indicating a rapid kinetics for activation response of
182 CALCR by COLV (Figure 4J). Of note, *in vitro* co-immunoprecipitation experiments and
183 Surface Plasmon Resonance (SPR) binding assays using the extracellular domain of CALCR,
184 did not detect an interaction with COLV (data not shown). Therefore, we propose that the
185 COLV/CALCR binding requires not solely the extracellular domain of CALCR, but
186 presumably a specific CALCR configuration found on the plasma membrane of cells,
187 possibly involving the extracellular loops of this GPCR or other co-factors. Taken together,
188 these data demonstrate that COLV physically and functionally interacts with CALCR thereby

189 identifying a cell-autonomous feedback loop for stem cell maintenance by reciprocal
190 interactions between MuSCs and their niche.

191

192 In this report we show that crosstalk between Notch and CalcR signalling, via the MuSC-
193 produced ECM protein collagen V (COLV), is critical for maintenance of MuSC equilibrium
194 in the niche. Given this remarkably specific interaction with COLV, but not COLI and
195 COLVI, we propose that COLV acts as a surrogate ligand for CALCR. Furthermore, we
196 demonstrate using functional studies that COLV requires CALCR to signal to MuSCs, and
197 that COLV specifically binds and activates this receptor. Taken together, our data identify a
198 specific collagen as a critical regulator of the muscle stem cell niche and also indicate that
199 MuSCs are maintained cell-autonomously by employing a Notch/COLV/CALCR signalling
200 pathway (Figure S4E). These findings reconcile the discordance between the critical role that
201 CALCR plays in stem cell maintenance, and the proposed control of the stem cell niche by its
202 systemically produced ligand. It would be of interest to extend the novel Notch/COLV/
203 CALCR signalling cascade described here to stem cells in other tissues and organisms. The
204 regulatory mechanism that we identify provides a framework to reconstruct a more complete
205 view of the stem cell niche, and to manipulate stem cell behaviour in a therapeutic context.

206

207 **Methods**

208 **Mouse strains**

209 Mouse lines used in this study have been described and kindly provided by the corresponding
210 laboratories: *Myf5^{Cre}* [1], *Pax7^{CreERT2}* [2], *R26^{stop-NICD-nGFP}* [3], *R26^{mTmG}* [4], *Rbpj^{flox/flox}* [5],
211 *Pax7^{CT2/+}*; *Calcr^{flox/flox}*, *R26^{YFP/YFP}* [6] and *Col5a1^{flox/flox}* [7]. *Tg:Pax7-CreERT2* and *Tg:Pax7-*
212 *nGFP* lines have been generated in the S.T. lab^{8,9}.

213

214

215 **Muscle injury, tamoxifen and BrdU administration**

216 For muscle injury, *Tg:Pax7-CreERT2;Col5a1^{flox};R26^{mTmG}* mice were anesthetized with 0.5%
217 Imalgene/2% Rompun and the *Tibialis anterior* (TA) muscle was injected with 50 μ l of
218 Cardiotoxin (10mM; Latoxan). *Tg:Pax7-CreERT2;Rbpj^{flox};R26^{mTmG}* and mice were injected
219 intraperitoneally with tamoxifen three times (250 to 300 μ l, 20mg/ml; Sigma T5648; diluted
220 in sunflower seed oil/5% ethanol). *Pax7^{CreERT2};Calcr^{flox};R26^{YFP}* were injected
221 intraperitoneally with tamoxifen twice (5mg/ 25g mouse) and sacrificed 2 weeks later.
222 *Pax7^{CreERT2};R26^{stop-NICD-ires-nGFP}* and *Tg:Pax7-CreERT2;Col5a1^{flox};R26^{mTmG}* were fed
223 tamoxifen containing diet for one and two weeks, respectively (Envigo, TD55125). Six days
224 prior sacrifice *Tg:Pax7-CreERT2;Col5a1^{flox};R26^{mTmG}* mice were given the thymidine
225 analogue 5-Bromo-2'-deoxyuridine (BrdU, 0.5mg/ml, #B5002; Sigma) in the drinking water
226 supplemented with sucrose (25mg/ml). Comparisons were done between age-matched
227 littermates using 8-12 week old mice. Animals were handled as per European Community
228 guidelines.

229

230 **Construction of luciferase reporters and luciferase assays**

231 For the generation of luciferase reporters, candidate enhancers of *Col5a1*, *Col5a3*, *Col6a1/2*
232 (shared enhancer) and *Hey1* were amplified by PCR from genomic DNA of C2C12 cells. The
233 enhancers were then cloned into the firefly-luciferase pGL3-Basic vector (Promega, E1751)
234 upstream of a minimal thymidine kinase promoter (minTK). The sequences of enhancers are
235 listed in Table S1. Transfected cells (Lipofectamine LTX, Life technologies, 15338030) were
236 lysed and luciferase signal was scored using the Dual-Luciferase Reporter Assay System
237 (Promega, E1910). For normalization, *Renilla* luciferase (pCMV-Renilla) was transfected at
238 1:20 ratio relative to firefly-luciferase constructs.

239

240

241 **RNA isolation and Quantitative RT-PCR**

242 Total RNA was extracted from MuSCs isolated by FACS using QIAGEN mini RNeasy kit
243 and reverse transcribed using SuperScript III (Invitrogen, 18080093) according to
244 manufacturers' instructions. RT-qPCR was performed using FastStart Universal SYBR
245 Green Master mix (Roche, 04913914001) and analysis was performed using the $2^{-\Delta\Delta CT}$
246 method¹⁰. Specific forward and reverse primers used in this study are listed in Table S2.

247

248 **Cell culture and Collagen incubation**

249 MuSCs isolated by FACS were plated at 3×10^3 cells/cm² on ibi-Treated μ -slides (Ibidi,
250 80826) pre-coated with 0.1% gelatin for 2h at 37°C. Cells were cultured in MuSC growth
251 medium (GM) containing Dulbecco's Modified Eagle's Medium (DMEM; Gibco)
252 supplemented with F12 (50:50; Gibco), 1% penicillin/streptomycin (PS; Gibco), 20% foetal
253 bovine serum (FBS; Gibco) and 2% Ultrosor (Pall; 15950-017) at 37°C, 3% O₂, 5% CO₂ for
254 the indicated time. Twelve hours after plating, collagens (COLI rat tail, BD Biosciences,
255 354236; COLV human placenta, Sigma, C3657; COLVI human placenta, AbD Serotec 2150-
256 0230) resuspended in HOAc acid at 1mg/ml, were added to the culture medium at a final
257 concentration of 50 μ g/ml and cells were fixed with 4% paraformaldehyde (PFA) for 10min.
258 To assess proliferation, cells were pulsed with the thymidine analogue 5-ethynyl-2'-
259 deoxyuridine (EdU), 1×10^{-6} M 2h prior to fixation (ThermoFisher Click-iT Plus EdU kit,
260 C10640). Inhibitors used: Obtustatin (Integrin $\alpha 1\beta 1$, Tocris, 4664, 100nM), TC-I 15 (Integrin
261 $\alpha 2\beta 1$ Tocris, 4527, 100 μ M), RGDS peptide (all integrins, Tocris, 3498, 100 μ M), 7rh¹¹
262 (DDR1, kind gift from Dr. Ke Ding, 20nM).

263

264 **Single myofibre isolation and siRNA transfection**

265 Single myofibres were isolated from EDL muscles following the previously described
266 protocol¹². Briefly, EDLs were dissected and incubated in 0.1% w/v collagenase (Sigma,

267 C0130)/DMEM for 1h in a 37°C shaking water bath at 40rpm. Following enzymatic
268 digestion, mechanical dissociation was performed to release individual myofibres that were
269 then transferred to serum-coated petri dishes. Single myofibres were transfected with siCol5a,
270 siCol5a3 (Dharmacon SMARTpool Col5a1 (12831) L-044167-01 and Col5a3 (53867) L-
271 048934-01-0005) or scramble siRNA (Dharmacon ON-TARGETplus Non-targeting siRNA
272 #2 D-001810-02-05) at a final concentration of 200nM, using Lipofectamine 2000
273 (ThermoFisher, 11668) in Opti-MEM (Gibco). Four hours after transfection, 6 volumes of
274 fresh MuSC growth medium was added and fibres were cultured for 72h at 37°C, 3%O₂.
275 Myofibres were fixed for 15min in 4% PFA/PBS.

276

277 **Immunostaining on cells, sections and myofibres**

278 Following fixation, cells and myofibers were washed three times with PBS, then
279 permeabilised and blocked at the same time in buffer containing 0.25% Triton X-100 (Sigma),
280 10% goat serum (GS; Gibco) for 30min at RT. For BrdU immunostaining, cells were
281 unmasked with DNaseI (1,000 U/ml, Roche, 04536282001) for 30 min at 37°C. Cells and
282 fibres were then incubated with primary antibodies (Table 3) for 4h at room temperature (RT).
283 Samples were washed with 1X PBS three times and incubated with Alexa-conjugated
284 secondary antibodies (Life Technologies, 1/1000) and Hoechst (Life Technologies, 1/5000)
285 for 45min at RT. EdU staining was chemically revealed using the Click-iT Plus kit according
286 to manufacturer's recommendations (Life Technologies, C10640). For collagen staining, the
287 myofibers and the muscle sections were incubated with 0.1% Triton X-100 for 30min at RT.
288 Myofibers and sections were then washed 3 x 10min and incubated with 10% GS in PBS for
289 30min. After one wash, samples were incubated with primary antibodies and secondary
290 antibodies as described in Table 3. Confocal images were acquired with a Leica SPE
291 microscope and Leica Application Suite or with Zeiss LSM 700 microscope and Zen Blue 2.0
292 software. 3D images were reconstructed from confocal Z-stacks using Imaris software. The

293 Section view function was used to inspect the MuSC environment by showing the cut in the
294 x-, y-, and z-axes.

295

296 **C2C12 cell manipulations**

297 Murine myoblast cell line C2C12 (provided by Yaffe D.¹³) was cultured in DMEM/ 20%
298 FBS/ 1% PS at 37°C, 5% CO₂. *Notch activation*: Notch activation was achieved by plating
299 cells on Dll1-coated dishes or by doxycycline inducible Notch constructs, as described
300 previously (Castel et al., 2013). *Calcr retrovirus preparation and transduction*: Calcitonin
301 receptor C1a-type (pMXs-Calcr-C1a-IRES-GFP) and mock control (pMXs-IRES-GFP)
302 retrovirus vectors were prepared as described previously^{6,14}. Briefly, 48h after transfection of
303 Platinum-E cells the supernatant was recovered and used to transduce C2C12. Two days later
304 stably labelled GFP⁺ C2C12 cells were isolated by FACS.

305

306 **Quantification of cAMP**

307 Transduced mock (IRES-GFP) and *Calcr* (CalcR-C1a-IRES-GFP) C2C12 cells were isolated
308 by FACS based on GFP and seeded on 0.1% gelatin-coated, white culture 96-well plates
309 (Falcon, 353296) at 3×10^3 cells/well. After overnight culture, the cells were incubated with
310 the complete induction medium containing DMEM/1%PS/500μM IBMX (isobutyl-1-
311 methylxanthine; Sigma, 17018)/100μM Ro 20-1724 ([4-(3-butoxy-4-methoxy-benzyl)
312 imidazolidone]); Sigma, B8279)/MgCl₂ 40mM, collagen, solvent HOAc or Elcatonin
313 (0.1U/ml; Mybiosource, MBS143228) for 3h. The amount of intracellular cAMP was
314 measured using cAMP-Glo Max Assay (Promega, V1681) following the manufacturer's
315 protocol. Luminescence was quantified with FLUOstar OPTIMA (BMG Labtech). EC50
316 value was determined with GraphPad Prism software using a sigmoid dose-response curve
317 (variable slope).

318

319 **On-cell Enzyme-Linked Immunosorbent Assay (ELISA)**

320 Transduced mock and *Calcr* C2C12 were seeded on a clear bottom 96-well plate (TPP,
321 92096) at 3×10^3 cells/well density. After overnight culture, cells were treated with 50 μ g/ml of
322 biotinylated collagens for 2h and fixed with 4%PFA/PBS for 15min. After 3x PBS washes,
323 cells were blocked with a solution containing 10% GS, 2% BSA, PBS for 1h at room
324 temperature, washed and incubated 1h/RT with goat anti-mouse biotin-HRP antibody
325 (Jackson, 1/1000e, 115-035-003). After 3x PBS washes, the HRP signal was developed by
326 addition of 3,3',5,5' tetramethylbenzidine (1-Step Ultra TMB-ELISA, Sigma, 34028). HRP
327 substrate and absorbance at 650nm was measured once every 30sec for 30min with FLUOstar
328 OPTIMA (BMG Labtech). The signal was normalized to the background signal (no
329 secondary antibody) and to the number of cells assessed by Janus green staining (Abcam,
330 ab111622).

331

332 **Muscle enzymatic dissociation and stem cell isolation**

333 Adult and foetal limb muscles were dissected, minced and incubated with a mix of Dispase II
334 (Roche, 04942078001) 3U/ml, Collagenase A (Roche, 11088793001) 100ug/ml and DNase I
335 (Roche, 11284932001) 10mg/ml in Hank's Balanced Salt Solution (HBSS, Gibco)
336 supplemented with 1% PS at 37°C at 60rpm in a shaking water bath for 2h. The muscle
337 suspension was successively filtered through 100 μ m and 70 μ m cell strainers (Milteny, 130-
338 098-463 and 130-098-462) and then span at 50g for 10min/4°C to remove large tissue
339 fragments. The supernatant was collected and washed twice by centrifugation at 600g for
340 15min. Prior to FACS, the final pellet was re-suspended in cold DMEM/1%PS supplemented
341 with 2% FBS and the cell suspension was filtered through a 40 μ m strainer. MuSCs were
342 sorted with Aria III (BD Biosciences) using either the GFP (*Tg:Pax7-nGFP*, *Tg:Pax-*
343 *CreERT2;Rbpj^{fllox};R26^{mTmG}*, *Tg:Pax7-CreERT2;Col5a1^{fllox};R26^{mTmG}*) or the YFP (*Pax7^{CT2}*;
344 *Calcr^{fllox};R26^{YFP}*) cell marker. Isolated, mononuclear cells were collected in

345 DMEM/1%PS/2%FBS. Enzymatic dissociated muscle was also plated directly without FACS
346 on Matrigel (Corning, 354248) coated dishes, 30min at 37°C, and fixed 12h later with
347 4%PFA/PBS. Cells were immunostained following the protocol described above in section
348 “Immunostaining on cells, sections and myofibres”.

349

350 **Muscle fixation and histological analysis**

351 Embryo forelimbs were fixed in 4% PFA/0.1% Triton for 2h, washed overnight with 1X PBS,
352 immersed in 20% sucrose/PBS overnight, embedded in OCT, frozen in liquid nitrogen and
353 sectioned transversely at 12-14µm. Isolated TA muscles were immediately frozen in liquid-
354 nitrogen cooled isopentane and sectioned transversely at 8µm. For Pax7 staining on adult TA,
355 sections were post-fixed with 4%PFA, 15min. After 3 washes with 1XPBS, antigen retrieval
356 was performed by incubating sections in boiling 10mM citrate buffer pH6 for 10min.
357 Sections were then blocked, permeabilised and incubated with primary and secondary
358 antibodies as described above in section “Immunostaining on cells, sections and myofibres”.

359

360 **Biotinylation of Collagens**

361 Commercial collagen proteins (COLI rat tail, BD Biosciences, 354236; COLV human
362 placenta, Sigma, C3657) were biotinylated using the Pierce EZ-Link Biotinylation Kit, with
363 slight modifications. Briefly, 20µl of 1M Hepes was added to 0.5ml of 1mg/ml collagen
364 dissolved in 0.5M HOAc. Then, 20µl of 100mM biotin reagent were added and incubated at
365 room temperature for 1.5h. Biotinylated collagens were next dialyzed in 25mM HEPES,
366 2.5M CaCl₂, 125mM NaCl, 0.005% Tween (Slide-A-Lyze MINI Dialysis Device,
367 ThermoFisher 88401) over-night at 4°C.

368

369

370

371 **Statistical analysis**

372 All experiments were carried out on a minimum of 3 mice (see Figure legends). No statistical
373 method was used to predetermine sample size, no animals were excluded from the analysis
374 and the experiments were not randomized. The investigators were not blinded to allocation
375 during experiments and outcome assessment. For comparison between two groups, two-tailed
376 Student's t test was performed to calculate p values and to determine statistically significant
377 differences (* p<0.05, ** p<0.01, *** p<0.001). All statistical analyses were performed with
378 Excel software and graphed using the GraphPad Prism software.

379

380 **References**

- 381 1 Watt, F. M. & Huck, W. T. Role of the extracellular matrix in regulating stem cell
382 fate. *Nature reviews. Molecular cell biology* **14**, 467-473, doi:10.1038/nrm3620
383 (2013).
- 384 2 Tanimura, S. *et al.* Hair follicle stem cells provide a functional niche for melanocyte
385 stem cells. *Cell stem cell* **8**, 177-187, doi:10.1016/j.stem.2010.11.029 (2011).
- 386 3 Chakkalakal, J. V., Jones, K. M., Basson, M. A. & Brack, A. S. The aged niche
387 disrupts muscle stem cell quiescence. *Nature* **490**, 355-360, doi:10.1038/nature11438
388 (2012).
- 389 4 Mourikis, P. *et al.* A critical requirement for notch signaling in maintenance of the
390 quiescent skeletal muscle stem cell state. *Stem Cells* **30**, 243-252,
391 doi:10.1002/stem.775 (2012).
- 392 5 Rozo, M., Li, L. & Fan, C. M. Targeting beta1-integrin signaling enhances
393 regeneration in aged and dystrophic muscle in mice. *Nat Med* **22**, 889-896,
394 doi:10.1038/nm.4116 (2016).
- 395 6 Zismanov, V. *et al.* Phosphorylation of eIF2alpha Is a Translational Control
396 Mechanism Regulating Muscle Stem Cell Quiescence and Self-Renewal. *Cell stem*
397 *cell* **18**, 79-90, doi:10.1016/j.stem.2015.09.020 (2016).
- 398 7 Cheung, T. H. & Rando, T. A. Molecular regulation of stem cell quiescence. *Nature*
399 *reviews. Molecular cell biology* **14**, 329-340, doi:10.1038/nrm3591 (2013).
- 400 8 Yamaguchi, M. *et al.* Calcitonin Receptor Signaling Inhibits Muscle Stem Cells from
401 Escaping the Quiescent State and the Niche. *Cell Rep* **13**, 302-314,
402 doi:10.1016/j.celrep.2015.08.083 (2015).

403 9 Creighton, M. P. *et al.* Histone H3K27ac separates active from poised enhancers and
404 predicts developmental state. *Proceedings of the National Academy of Sciences of the*
405 *United States of America* **107**, 21931-21936, doi:10.1073/pnas.1016071107 (2010).

406 10 Heintzman, N. D. *et al.* Histone modifications at human enhancers reflect global cell-
407 type-specific gene expression. *Nature* **459**, 108-112, doi:10.1038/nature07829 (2009).

408 11 Visel, A. *et al.* ChIP-seq accurately predicts tissue-specific activity of enhancers.
409 *Nature* **457**, 854-858, doi:10.1038/nature07730 (2009).

410 12 Castel, D. *et al.* Dynamic binding of RBPJ is determined by Notch signaling status.
411 *Genes Dev* **27**, 1059-1071, doi:10.1101/gad.211912.112 (2013).

412 13 Rocheteau, P., Gayraud-Morel, B., Siegl-Cachedenier, I., Blasco, M. A. & Tajbakhsh,
413 S. A subpopulation of adult skeletal muscle stem cells retains all template DNA
414 strands after cell division. *Cell* **148**, 112-125, doi:10.1016/j.cell.2011.11.049 (2012).

415 14 Vasyutina, E. *et al.* RBP-J (Rbpsi) is essential to maintain muscle progenitor cells
416 and to generate satellite cells. *Proceedings of the National Academy of Sciences of the*
417 *United States of America* **104**, 4443-4448, doi:10.1073/pnas.0610647104 [pii],
418 10.1073/pnas.0610647104 (2007).

419 15 Mourikis, P., Gopalakrishnan, S., Sambasivan, R. & Tajbakhsh, S. Cell-autonomous
420 Notch activity maintains the temporal specification potential of skeletal muscle stem
421 cells. *Development* **139**, 4536-4548, doi:10.1242/dev.084756 (2012).

422 16 Zammit, P. S. *et al.* Muscle satellite cells adopt divergent fates: a mechanism for self-
423 renewal? *J Cell Biol* **166**, 347-357, doi:10.1083/jcb.200312007 (2004).

424 17 Sun, M. *et al.* Targeted deletion of collagen V in tendons and ligaments results in a
425 classic Ehlers-Danlos syndrome joint phenotype. *Am J Pathol* **185**, 1436-1447,
426 doi:10.1016/j.ajpath.2015.01.031 (2015).

427 18 Urciuolo, A. *et al.* Collagen VI regulates satellite cell self-renewal and muscle
428 regeneration. *Nature communications* **4**, 1964, doi:10.1038/ncomms2964 (2013).

429 19 Lutolf, M. P., Gilbert, P. M. & Blau, H. M. Designing materials to direct stem-cell
430 fate. *Nature* **462**, 433-441, doi:10.1038/nature08602 (2009).

431 20 Gilbert, P. M. *et al.* Substrate elasticity regulates skeletal muscle stem cell self-
432 renewal in culture. *Science* **329**, 1078-1081, doi:10.1126/science.1191035 (2010).

433 21 Yennek, S., Burute, M., They, M. & Tajbakhsh, S. Cell adhesion geometry regulates
434 non-random DNA segregation and asymmetric cell fates in mouse skeletal muscle
435 stem cells. *Cell reports* **7**, 961-970, doi:10.1016/j.celrep.2014.04.016 (2014).

436 22 Leitinger, B. Transmembrane collagen receptors. *Annu Rev Cell Dev Biol* **27**, 265-290,
437 doi:10.1146/annurev-cellbio-092910-154013 (2011).

438 23 Vogel, W., Gish, G. D., Alves, F. & Pawson, T. The discoidin domain receptor
439 tyrosine kinases are activated by collagen. *Mol Cell* **1**, 13-23 (1997).

- 440 24 Paavola, K. J., Sidik, H., Zuchero, J. B., Eckart, M. & Talbot, W. S. Type IV collagen
441 is an activating ligand for the adhesion G protein-coupled receptor GPR126. *Sci*
442 *Signal* **7**, ra76, doi:10.1126/scisignal.2005347 (2014).
- 443 25 Luo, R. *et al.* G protein-coupled receptor 56 and collagen III, a receptor-ligand pair,
444 regulates cortical development and lamination. *Proc Natl Acad Sci U S A* **108**, 12925-
445 12930, doi:10.1073/pnas.1104821108 (2011).
- 446 26 Evans, B. N., Rosenblatt, M. I., Mnayer, L. O., Oliver, K. R. & Dickerson, I. M.
447 CGRP-RCP, a novel protein required for signal transduction at calcitonin gene-related
448 peptide and adrenomedullin receptors. *J Biol Chem* **275**, 31438-31443,
449 doi:10.1074/jbc.M005604200 (2000).

450

451 **References in Methods**

- 452 1 Haldar, M., Karan, G., Tvrdik, P. & Capecchi, M. R. Two cell lineages, myf5 and
453 myf5-independent, participate in mouse skeletal myogenesis. *Developmental cell* **14**,
454 437-445, doi:10.1016/j.devcel.2008.01.002 (2008).
- 455 2 Murphy, M. M., Lawson, J. A., Mathew, S. J., Hutcheson, D. A. & Kardon, G.
456 Satellite cells, connective tissue fibroblasts and their interactions are crucial for
457 muscle regeneration. *Development* **138**, 3625-3637, doi:10.1242/dev.064162 (2011).
- 458 3 Murtaugh, L. C., Stanger, B. Z., Kwan, K. M. & Melton, D. A. Notch signaling
459 controls multiple steps of pancreatic differentiation. *Proceedings of the National*
460 *Academy of Sciences of the United States of America* **100**, 14920-14925,
461 doi:10.1073/pnas.2436557100, 2436557100 [pii] (2003).
- 462 4 Muzumdar, M. D., Tasic, B., Miyamichi, K., Li, L. & Luo, L. A global double-
463 fluorescent Cre reporter mouse. *Genesis* **45**, 593-605, doi:10.1002/dvg.20335 (2007).
- 464 5 Han, H. *et al.* Inducible gene knockout of transcription factor recombination signal
465 binding protein-J reveals its essential role in T versus B lineage decision.
466 *International immunology* **14**, 637-645 (2002).
- 467 6 Yamaguchi, M. *et al.* Calcitonin Receptor Signaling Inhibits Muscle Stem Cells from
468 Escaping the Quiescent State and the Niche. *Cell Rep* **13**, 302-314,
469 doi:10.1016/j.celrep.2015.08.083 (2015).
- 470 7 Sun, M. *et al.* Collagen V is a dominant regulator of collagen fibrillogenesis:
471 dysfunctional regulation of structure and function in a corneal-stroma-specific
472 Col5a1-null mouse model. *J Cell Sci* **124**, 4096-4105, doi:10.1242/jcs.091363 (2011).
- 473 8 Sambasivan, R. *et al.* Distinct regulatory cascades govern extraocular and pharyngeal
474 arch muscle progenitor cell fates. *Developmental cell* **16**, 810-821,
475 doi:10.1016/j.devcel.2009.05.008 (2009).

- 476 9 Mourikis, P. *et al.* A critical requirement for notch signaling in maintenance of the
477 quiescent skeletal muscle stem cell state. *Stem Cells* **30**, 243-252,
478 doi:10.1002/stem.775 (2012).
- 479 10 Livak, K. J. & Schmittgen, T. D. Analysis of relative gene expression data using real-
480 time quantitative PCR and the 2(-Delta Delta C(T)) Method. *Methods* **25**, 402-408,
481 doi:10.1006/meth.2001.1262, S1046-2023(01)91262-9 [pii] (2001).
- 482 11 Gao, M. *et al.* Discovery and optimization of 3-(2-(Pyrazolo[1,5-a]pyrimidin-6-
483 yl)ethynyl)benzamides as novel selective and orally bioavailable discoidin domain
484 receptor 1 (DDR1) inhibitors. *J Med Chem* **56**, 3281-3295, doi:10.1021/jm301824k
485 (2013).
- 486 12 Shinin, V., Gayraud-Morel, B., Gomes, D. & Tajbakhsh, S. Asymmetric division and
487 cosegregation of template DNA strands in adult muscle satellite cells. *Nat Cell Biol* **8**,
488 677-687, doi:ncb1425 [pii], 10.1038/ncb1425 (2006).
- 489 13 Yaffe, D. & Saxel, O. Serial passaging and differentiation of myogenic cells isolated
490 from dystrophic mouse muscle. *Nature* **270**, 725-727 (1977).
- 491 14 Morita, S., Kojima, T. & Kitamura, T. Plat-E: an efficient and stable system for
492 transient packaging of retroviruses. *Gene therapy* **7**, 1063-1066,
493 doi:10.1038/sj.gt.3301206 (2000).

494

495 **Acknowledgments**

496 We would like to thank H. Stunnenberg for the generation of the ChiP-seq and RNA-seq data.
497 We are also grateful to D. Greenspan for kindly providing us the anti-Col5a3 antibody and
498 Col5a3 knock-out muscle samples, F. Aurade for the generation of CalcR expression
499 constructs, L. Machado for the generation of the microarray heatmaps and K. Ding for the
500 generous gift of the 7th DDR1 inhibitor. We also acknowledge the Flow Cytometry Platform
501 of the Technology Core-Center for Translational Science (CRT) at Institut Pasteur for
502 support in conducting this study. S.T. was funded by Institut Pasteur, Centre National pour la
503 Recherche Scientifique and the Agence Nationale de la Recherche (Laboratoire d'Excellence
504 Revive, Investissement d'Avenir; ANR-10-LABX- 73) and the European Research Council
505 (Advanced Research Grant 332893). M.B was funded by the Fondation pour la Recherche
506 Médicale (FRM).

507

508 **Author Contributions**

509 M.B.B., D.C., F.R., S.T. and P.M. proposed the concept and designed the experiments.
510 M.B.B. and P.M performed and analysed the experiments; S.F and D.E.B. provided mouse
511 models; M.B.B., S.T. and P.M. wrote the manuscript. All authors discussed, commented and
512 agreed with the manuscript.

Table 1 : Enhancer chromosomal location

Associated gene	Chromosome	Start	End	Size (bp)
Col5a1	Chr2	27717404	27718346	943
Col5a3	Chr9	20616518	20617495	978
Col6a1/2	Chr10	76111367	76112240	874
Hey1	Chr3	8717311	8718243	933

Table 2: RT-qPCR primers used in this study

Mouse RT-PCR primer	Sequence (5' > 3')
Col5a1_F	GCTACTCCTGTTCCCTGCTGC
Col5a1_R	TGAGGGCAAATTGTGAAAATC
Col5a1 flox_F	GACACCAATGGGATTGTCATGT
Col5a1 flox_R	GCTCGGTTGTCAGAGACGAA
Col5a2_F	AGAAGGGAGATGCTGGGTCT
Col5a2_R	GGGTTCCCTCTACCGCCTTTC
Col5a3_F	CCGGAGACTGGATCAGCTT
Col5a3_R	GCTTCCAGTACGTCCACAGG
Col6a1_F	TCGGTCACCACGATCAAGT
Col6a1_R	TACTTCGGGAAAGGCACCTA
Col6a2_F	TACCCAGGCATCTTCTCCAA
Col6a_R	AAGAGTCCCCCAATCAGGAG
Hey1_F	CACCTGAAAATGCTGCACAC
Hey1_R	ATGCTCAGATAACGGGCAAC
HeyL_F	GTCTTGCAGATGACCGTGGA
HeyL_R	CTCGGGCATCAAAGAACCCT
Calcr_F	TCATCATCCACCTGGTTGAG
Calcr_R	GCTCGTCCGTAAACACAGC
Myogenin_F	GTGAATGCAACTCCCACAGC
Myogenin_R	CGCGAGCAAATGATCTCCTG
Pax7_F	GACAAAGGGAACCGTCTGGAT
Pax7_R	TGTGAACGTGGTCCGACTG
Myod_F	CACTACAGTGGCGACTCAGATGCA
Myod_R	CCTGGACTCGCGCGCCGCTCACT
Gapdh_F	GGCAAAGTGGAGATTGTTGC
Gapdh_R	AATTTGCCGTGAGTGGAGTC
Tbp_F	ATCCCAAGCGATTTGCTG
Tbp_R	CCTGTGCACACCATTTTTC

Table 3: Antibodies used in this study

Antibody	Reference	Dilution
GFP chick polyclonal	Abcam, 13970	1/2000
Myogenin mouse monoclonal	DHSB, F5D	1/40
Myosin Heavy Chain mouse monoclonal	DHSB, MF20	1/40
MyoD mouse monoclonal	Dako, M3512	1/200
Calcitonin Receptor rabbit polyclonal	AbD Serotec, AHP635	1/100
Pax7 monoclonal mouse	DHSB	1/40
Mouse anti-BrdU	BD, 347580	1/100
Laminin rabbit polyclonal	Sigma, L9393	1/500
Laminin mouse monoclonal	Sigma, L8271	1/500
Col5a3 rabbit polyclonal	Gift from D.Greenspan	1/200
RBPJ rat polyclonal	Ascenion (1F1)	1/100

Baghdadi_Figure 1

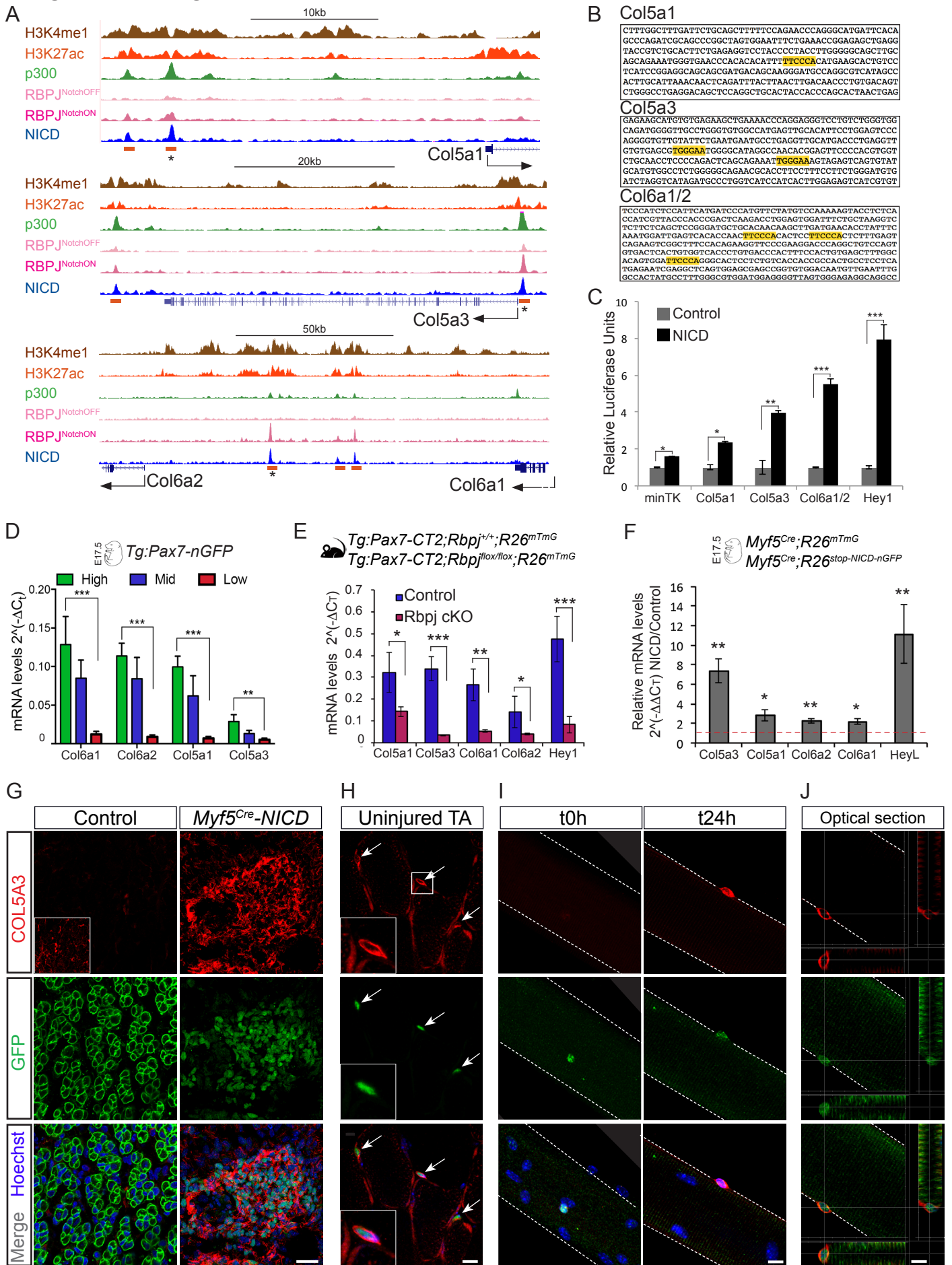


Figure 1. Transcription regulation of *Col5* and *Col6* genes by Notch signalling via NICD/RBPJ-bound regulatory elements.

(A) ChIP-seq tracks indicating NICD/RBPJ-occupied enhancers, associated to mouse *Collagen-5a1*, *-5a3*, *-6a1* and *-6a2* loci. H3K4me1, and H3K27ac, p300, RBPJ, and NICD are shown. Note absence RBPJ binding in DAPT-treated cells (RBPJ^{NotchOFF}). Orange rectangle indicates RBPJ binding position and asterisk the enhancers used for transcriptional activity assays for Figure 1C.

(B) Core sequences of the selected NICD/RBPJ-bound enhancers (asterisked orange rectangle in Figure 1A). The RBPJ consensus binding motif is highlighted in yellow.

(C) Transcriptional response of isolated enhancers to activation of Notch signalling in C2C12 cells. Firefly luciferase signal was measured in cells with doxycycline-inducible expressed hNotch1-GFP (NICD, black bars \pm SD, n=3) and GFP-control cells treated with DAPT (grey bars \pm SD, n=3) and were normalized to internal control (pCMV-*Renilla*). Data are expressed as Relative Luminescence Units (RLU).

(D) Transcript levels of collagens targeted by Notch in cells fractionated by FACS from E17.5 *Tg:Pax7-nGFP* fetuses: Pax7^{Hi} 20% of population (green), Pax7^{Mid} 40% (blue) and Pax7^{Lo} 20% (red), (n=3 fetuses/genotype).

(E) RT-qPCR analysis of collagen genes in *Rbpj* conditional KO (cKO) and control MuSCs. Cells were isolated by FACS at day 10 post-tamoxifen injections from resting TA muscles. Control: *Tg:Pax7-CT2; Rbpj*^{+/-}; *R26*^{mTmG/+} and *Rbpj* cKO: *Tg:Pax7-CT2; Rbpj*^{flox/-}; *R26*^{mTmG/+}. Decrease of *Heyl* is shown as internal control for inhibition of Notch signalling (n=3-4 mice/genotype).

(F) Induction of collagen genes in E17.5 control (*Myf5*^{Cre/+}; *R26*^{mTmG/+}) and *Myf5*^{Cre}-NICD (*Myf5*^{Cre/+}; *R26*^{stop-NICD-nGFP/+}), cells isolated by FACS assessed by RT-qPCR. *HeyL* is used as a reporter of Notch activity. All RT-qPCR data are normalized to *Gapdh* (n=3 mice/genotype). Error bars indicate SD, red line designates no change (ratio=1).

(G) Forelimb muscles of E17.5 *Myf5^{Cre}-NICD* fetuses show strong upregulation of COLVA3 compared to control. In control, muscle fibres are marked by membrane GFP (*R26^{mTmG}*); in *Myf5^{Cre}-NICD* the GFP is nuclear (*R26^{stop-NICD-nGFP}*). Lower COL5A3 expression in control limbs shown in inset captured at higher exposure time.

(H) Anti-GFP (MuSC) and anti-COLVA3 immunostaining on transverse sections of quiescent adult TA muscles overexpressing NICD (*Pax7^{CT2}-NICD*).

(I) Isolated single myofibers from *Pax7^{CT2}-NICD Extensor digitorum longus* (EDL) muscles fixed immediately after dissociation (t0h, left panel) or after 24h in culture (right panel) and stained for GFP and COLVA3.

(J) Vertical and horizontal optical sections of myofibers from *Pax7^{CT2}-NICD* mice after 24h in culture, as shown in (F), showing that COLV is surrounding the NICD-GFP MuSC.

*p<0.05, **p<0.01, ***p<0.001. Scale bar: 50µm for G, 10 µm for H-I. Scale bar in inset: 100 µm for G and 20 µm for H.

Baghdadi_Figure 2

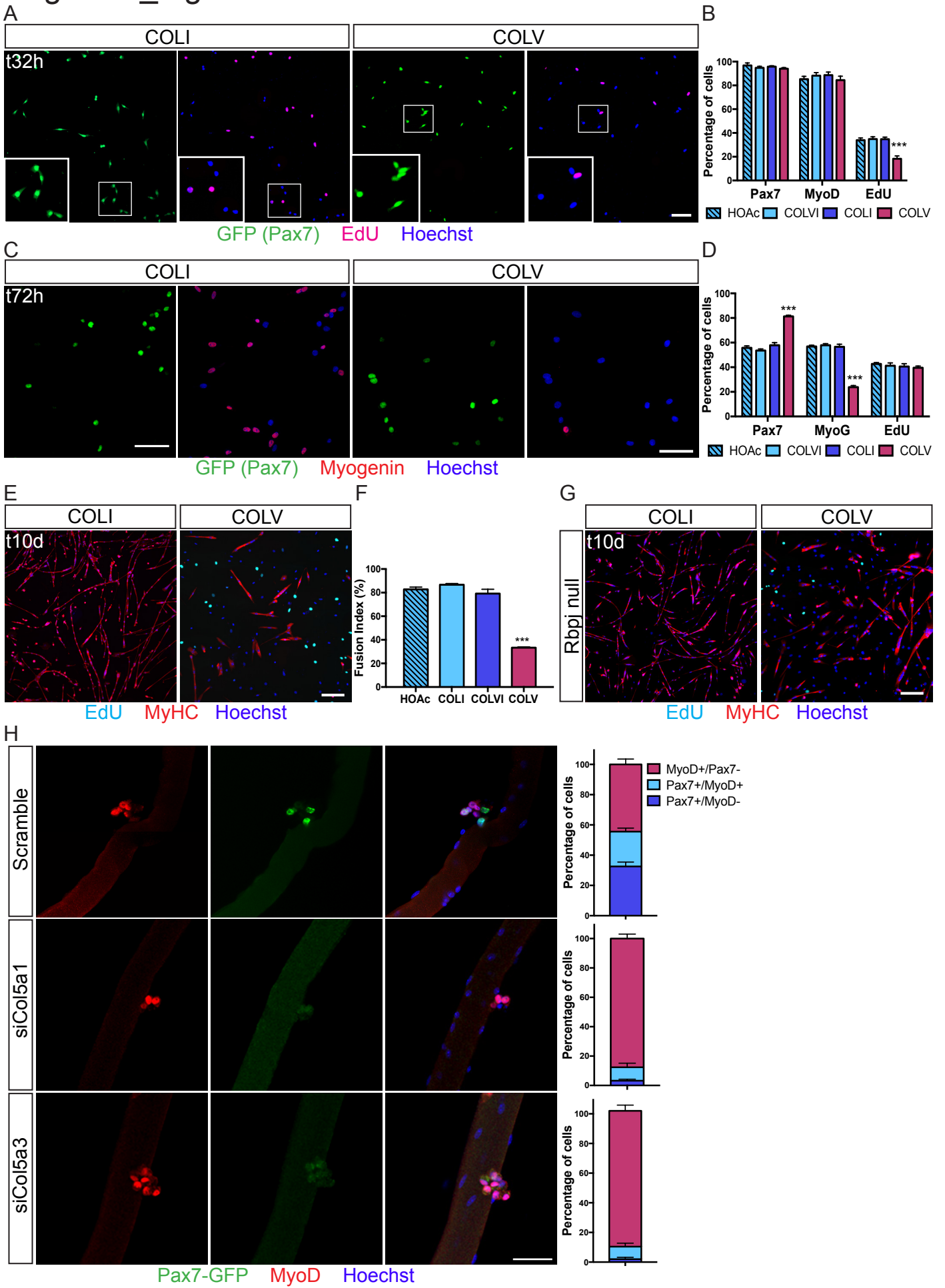


Figure 2. Collagen V delays proliferation and differentiation of MuSCs.

(A) GFP and EdU staining (2h chase) on *Tg:Pax7-nGFP* MuSCs isolated by FACS and incubated for 32h in the presence of 50µg/ml COLI or COLV in the culture medium.

(B) Quantification of total Pax7 (GFP), MyoD and EdU positive cells after 32h treatment with HOAc, COLVI, COLI or COLV: EdU: 18%, 34% and 35% for COLV, COLI and COLVI, respectively.

(C) GFP and Myogenin immunostaining on *Tg:Pax7-nGFP* MuSCs isolated by FACS and cultured for 72h in the presence of COLI or COLV.

(D) Quantification of total Pax7 (GFP), Myogenin and EdU positive cells after 72h treatment with HOAc or the indicated collagens: Pax7: 81%, 56% and 58%, MyoG: 23%, 56% and 58% for COLV, COLI and COLVI, respectively.

(E) Myosin Heavy Chain (MyHC) and EdU (2h chase) staining on *Tg:Pax7-nGFP* MuSCs isolated by FACS and cultured for 10 days in the presence of COLI or COLV.

(F) Fusion index of primary myoblasts after 10 days of culture with HOAc or the indicated collagens: 33% for COLV vs. 84% for COLI and 79% for COLVI.

(G) MyHC and EdU (2h chase) staining of *Rbpj* null *Tg:Pax7-CT2*; *Rbpj*^{fllox/fllox}; *R26*^{mTmG} MuSCs cultured for 10 days with suspended COLI or COLV.

Error bars indicate SD; n=4 mice, ≥250 cells counted, 2 wells/ condition. *p<0.05, **p<0.01, ***p<0.001.

(H) *siCol5a1* and *siCol5a3* transfection of *Tg:Pax7-nGFP* isolated single myofibers cultured for 72h and immunostained for GFP and MyoD. Quantification of Pax7⁺/MyoD⁻, Pax7⁺/MyoD⁺ and Pax7⁻/MyoD⁺ populations 72h after transfection. Scramble siRNA was used as negative control (n=3 mice, ≥15 fibres counted). Error bars indicate SD; ***p<0.001 in all conditions. Scale bar: 50µm.

Baghdadi_Figure 3

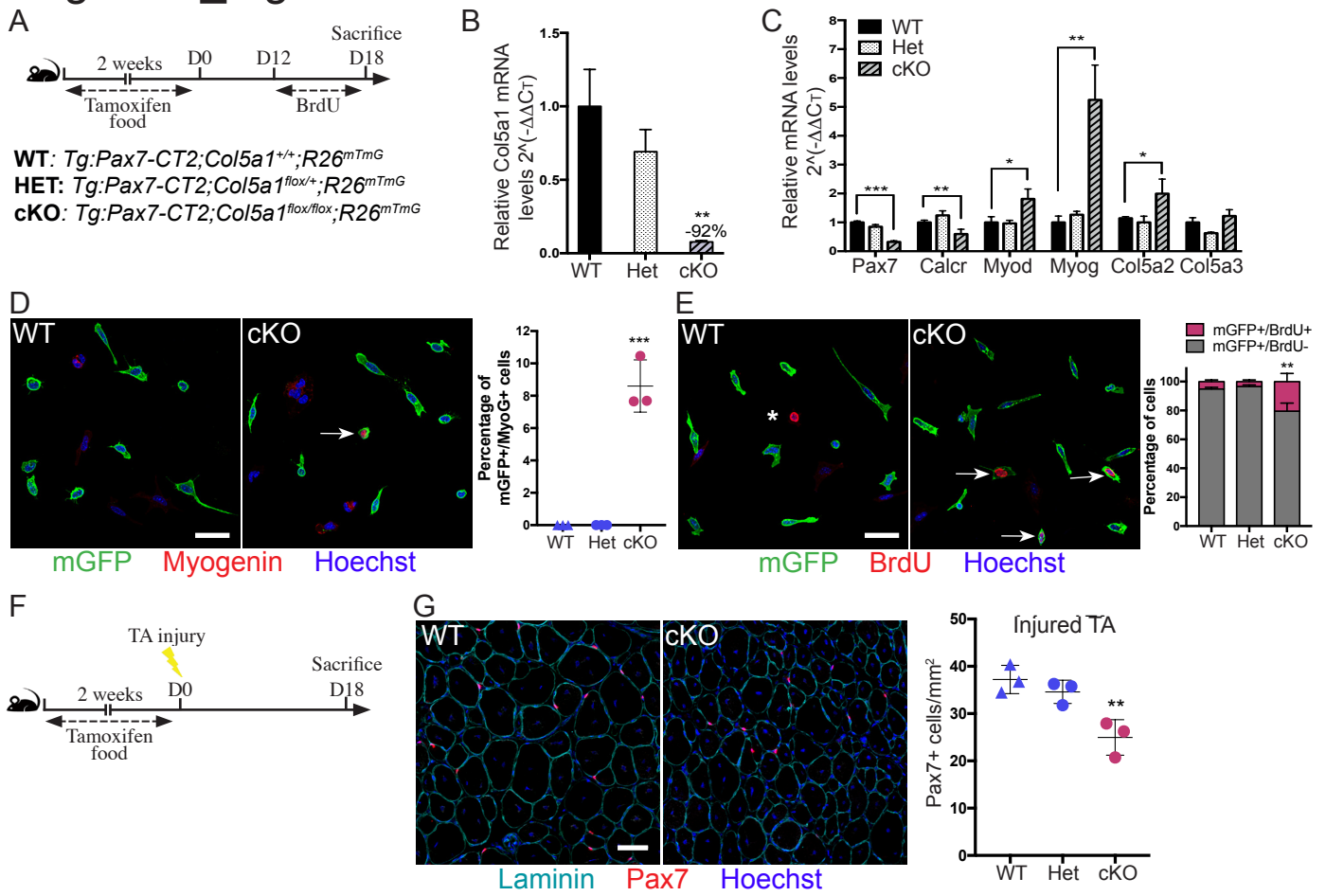


Figure 3. MuSC-produced COLV is required for self-renewal and maintenance of quiescence.

(A) Experimental scheme of tamoxifen and BrdU administration to wild type (WT), heterozygous (HET) and conditional knock-out (cKO) *Col5a1* mice. The end of tamoxifen treatment is designated as Day 0 (D0).

(B) RT-qPCR of *Col5a1* in wild type, heterozygous and cKO *Col5a1* cells isolated by FACS 18d post-tamoxifen (WT control mice set to 1; n=3 mice/genotype).

(C) RT-qPCR of quiescence (*Pax7*, *Calcr*) and differentiation (*Myod*, *Myog*) markers on *Col5a1* mutant and control MuSCs isolated by FACS from resting muscle. For putative redundancy, the collagen V chains $\alpha 2(V)$ and $\alpha 3(V)$ were quantified in addition to $\alpha 1(V)$ (n=3 mice/genotype).

(D) Representative images of membrane-GFP⁺ MuSCs from total muscle preparations plated for 12h and stained for Myogenin. Control WT: *Tg:Pax7-CT2*; *Col5a1*^{+/+}; *R26*^{mTmG/+} and *Col5a1* cKO: *Tg:Pax7-CT2*; *Col5a1*^{flx/flx}; *R26*^{mTmG/+}. Quantification of GFP⁺/Myogenin⁺ cells (n=3 mice/genotype, ≥ 200 cells counted).

(E) GFP⁺ MuSCs from total muscle preparations plated for 12h and stained for BrdU. Control WT: *Tg:Pax7-CT2*; *Col5a1*^{+/+}; *R26*^{mTmG/+} and *Col5a1* cKO: *Tg:Pax7-CT2*; *Col5a1*^{flx/flx}; *R26*^{mTmG/+}. Asterisk represents a non-recombined BrdU⁺ cell. Quantification of GFP⁺/BrdU⁺ cells (n=3 mice/genotype, ≥ 250 cells counted).

(F) TA muscle injury by cardiotoxin on mice fed with tamoxifen diet for two weeks. Regenerating TAs were collected on day 18 days post-injury.

(G) Immunostaining for Laminin and Pax7 on sections from day 18 post-cardiotoxin injury control and cKO TA muscles. Quantification of Pax7⁺ cells in *Col5a1* wild type, heterozygous and homozygous null mice (genotypes as described in 3A) (n=3 TA/genotype).

Error bars indicate SD, *p<0.05, **p<0.01, ***p<0.001. Scale bar: 50 μ m.

Baghdadi_Figure 4

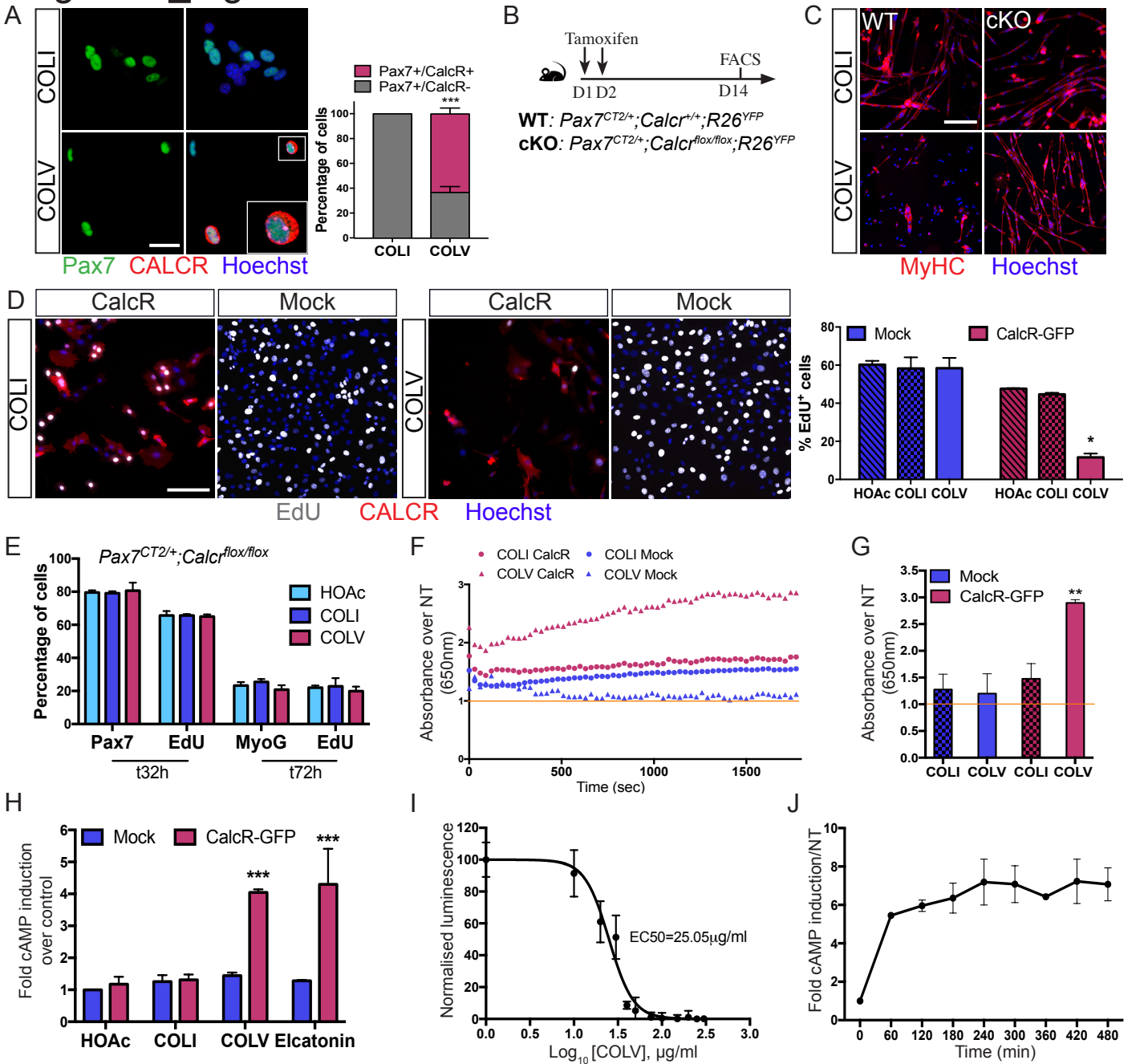


Figure 4. Collagen V physically and functionally interacts with the Calcitonin Receptor.

(A) Pax7 and CALCR immunostaining on *Tg:Pax7-nGFP* MuSCs isolated by FACS and cultured for 72h in the presence of COLI or COLV. Quantification of Pax7⁺, CALCR⁺ cells from *Tg:Pax7-nGFP* mice after 72h of COLI and COLV treatment (n=3 mice, ≥50 cells counted, 2 wells/condition).

(B) Experimental scheme of tamoxifen administration to WT: *Pax7^{CT2/+};Calcr^{+/+}* and cKO: *Pax7^{CT2/+};Calcr^{flox/flox}* mice.

(C) *Calcr*-deficient MuSC (*Pax7^{CT2/+}; Calcr^{flox/flox}; R26^{YFP/YFP}*) incubated 10 days with COLI or COLV and immunostained with MyHC to assess MuSCs differentiation (n=3 mice/genotype).

(D) EdU (2h chase) and CALCR staining of GFP⁺ C2C12 cells isolated by FACS and transduced with CalcR-GFP or Mock GFP retrovirus, then cultured for 24h with COLI (left) or COLV (right). Quantification of EdU positive cells of CalcR-C2C12 or Mock GFP cells treated for 24h COLV or control COLI and HOAc. Error bars indicate SEM from 3 experiments (≥250 cells counted, 2 wells/condition).

(E) Quantification of Pax7, Myogenin and EdU positive cells of CalcR-depleted MuSCs (*Pax7^{CT2/+}; Calcr^{flox/flox}; R26^{YFP/YFP}*) isolated by FACS and treated for 32h or 72h with control (COLI or HOAc) or COLV. Error bars indicate SD; n=3 mice/genotype, (≥250 cells counted, 2 wells/condition).

(F) Binding assay of COLV-CALCR by colorimetric on-cell ELISA (see Methods). Presence of bound biotinylated COLV specifically on CALCR-expressing C2C12 (red), but not on Mock cells (blue). Absorbance reflects the presence of COLV bound to CALCR, relative to non-treated (NT) cells (orange line).

(G) Measurements of absorbance after development of the HRP signal for 20min. Results are presented as a ratio of absorbance at 650nm over non-treated (NT) cells; n=4 independent measurements. Orange line designates no change (=1).

(H) cAMP measurements of CalcR-transduced C2C12 cells after 3h of COLI, HOAc or COLV treatment. The graph represents the fold cAMP induction over Mock cells treated with HOAc (=1). Error bars indicate SD from 4 independent assays. *** $p < 0.001$.

(I) Dose-response: fold cAMP concentration in CalcR-transduced C2C12 cells treated for 3h with increasing concentrations of collagen V. EC50 value=25.05 μ g/ml. All error bars indicate SD from 4 independent assays.

(J) Intracellular levels of cAMP in CalcR-C2C12 cells treated with COLV for up to 480min. Error bars indicate SD from 4 independent assays.

Scale bar: 50 μ m and 5 μ m in inlet.

Baghdadi_Figure S1

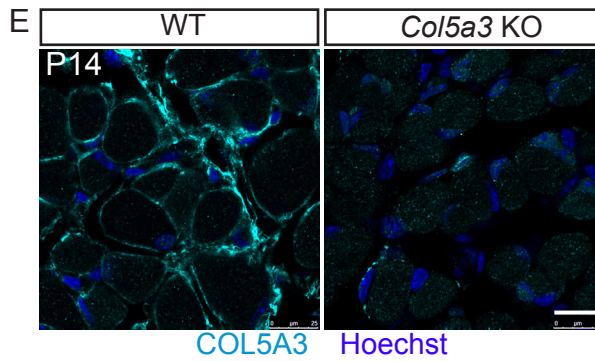
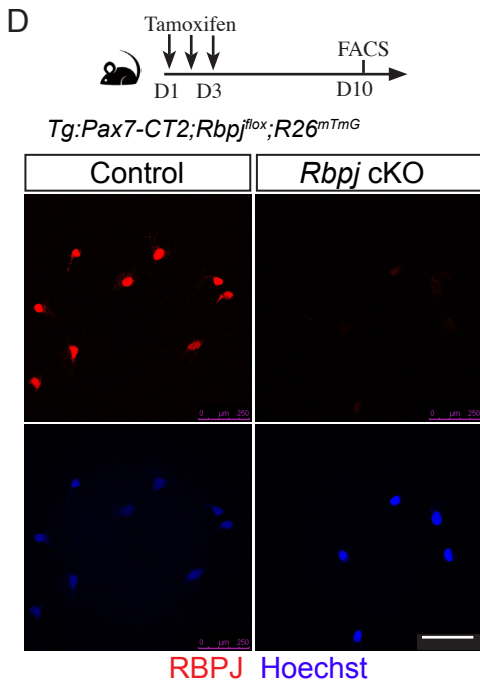
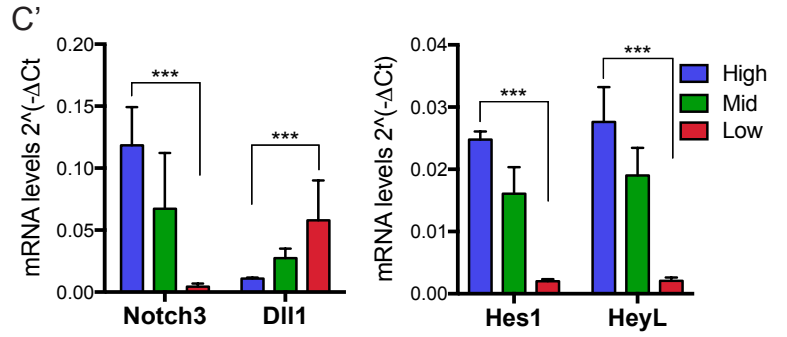
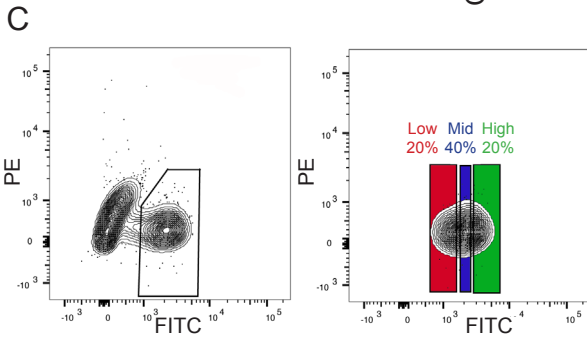
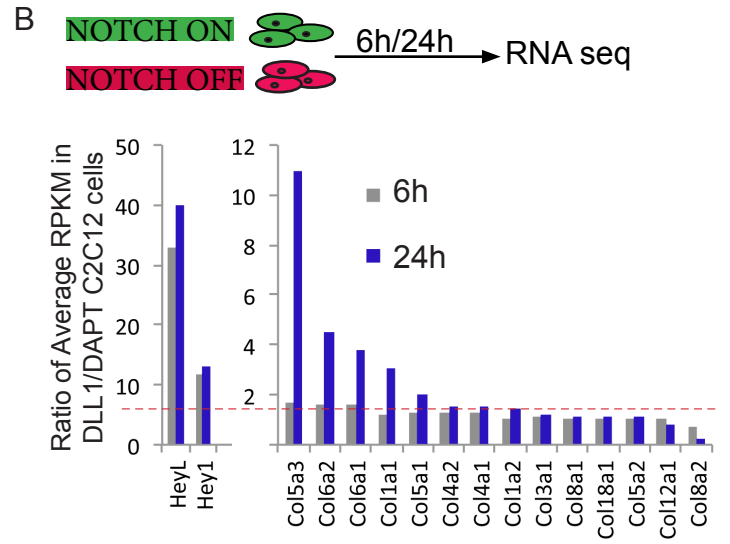
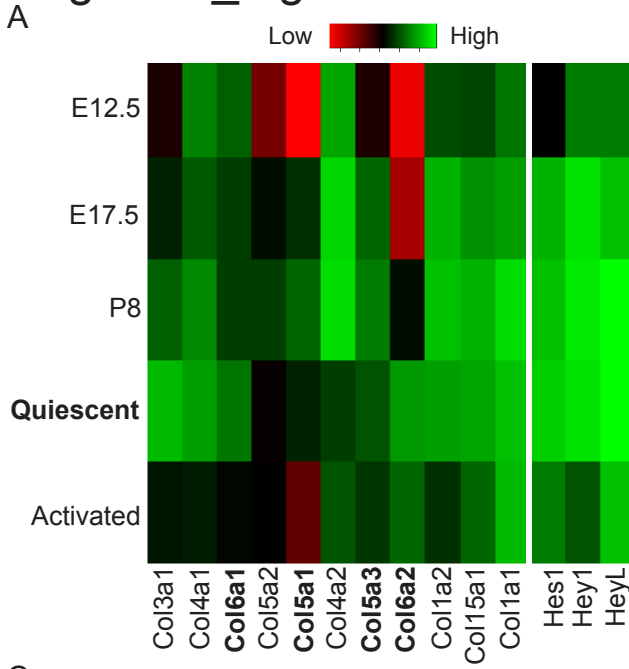


Figure S1: Notch signalling regulates *Col5* and *Col6* expression.

(A) Gene expression microarray data show that MuSCs express a specific subset of collagen types, which include the fibrillar COLI (*Col1a1* and *Col1a2*), COLIII (*Col3a1*, possibly as $[\alpha 1(\text{III})]_3$) and COLV (*Col5a1*, *Col5a2* and *Col5a3*) and the non-fibrillar COLIV (*Col4a1* and *Col4a2*), COLVI (*Col6a1* and *Col6a2*) and COLXV (*Col15a1*, possibly as $[\alpha 1(\text{XV})]_3$) (Figure 1B) ²⁷. The data are shown as a heatmap of normalized collagens transcripts expressed at different developmental time points (E12.5, E17.5, P08; *Tg-Pax7-nGFP*, GEO accession number GSE52192), quiescent and post-injury (t=60h post-BaCl₂ injury ²⁷).

(B) RNA-seq based expression measurements of collagen genes in myogenic C2C12 cells, with active (DLL1-treated) or inhibited (DAPT-treated) Notch signalling for 6 or 24 hours. Data are shown as DLL1/DAPT ratios of average RPKMs. Genes with low expression (RPKM <2) were eliminated. *HeyL* and *Hey1* transcripts indicate Notch pathway activation. Red line designates no change (ratio=1). Abbreviation: RPKM= Reads Per Kilobase of exon model per Million mapped reads.

(C) FACS plot showing the fractioning of GFP⁺ cells from E17.5 *Tg:Pax7-nGFP* fetuses into Pax7^{Hi} (20% of population), Pax7^{Mid} (40%), and Pax7^{Lo} (20%). Intensity of GFP signal reflects the activity of the Pax7 promoter (n=3 fetuses/genotype). (C') Transcript levels of GFP⁺ cells isolated by FACS demonstrate a tight correlation between lineage progression and Notch signalling activity.

(D) FACS isolated satellite cells from control (*Tg:Pax7-CT2; Rbpj^{+/-}; R26^{mTmG/+}*) and *Rbpj* null (*Tg:Pax7-CT2; Rbpj^{fllox/-}; R26^{mTmG/+}*) mice immunostained for RBPJ.

(E) Specificity of COLV3 antibody assessed by COLVa3 immunostaining of *Tibialis anterior* transverse section of WT and *Col5a3* KO P14 postnatal pups (n=3/genotype).

*p<0.05, **p<0.01, ***p<0.001. Scale bar: 25µm.

Baghdadi_Figure S2

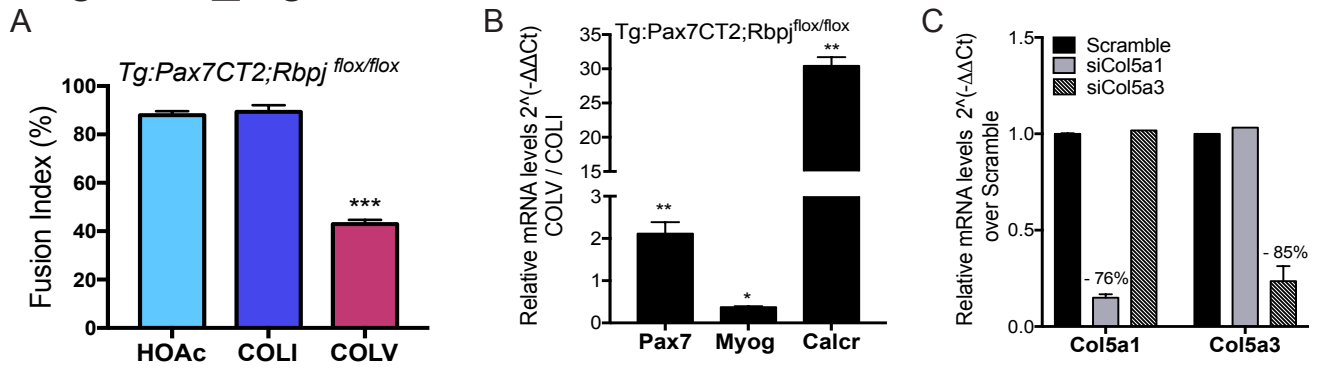


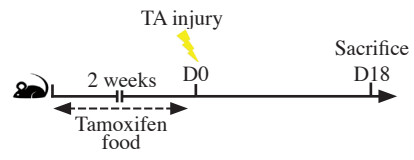
Figure S2: COLV treatment partially rescues premature differentiation of *Rbpj*-null MuSCs.

(A) Fusion index of recombined primary myoblasts from *Tg:Pax7-CreERT2; Rbpj^{fllox}; R26^{mTmG}* after 10 days of culture with the indicated collagens.

(B) RT-qPCR on *Rbpj* null MuSCs isolated by FACS and cultured for 72h in the presence of COLI or COLV. Results are normalized to *Tbp* and presented as ratio of COLV/COLI. Error bars indicate SD, n=4 mice.

(C) Transcript levels of the different *Col5* mRNA chains in C2C12 after transfection of either control scramble, siCol5a1 or siCol5a3 showing the specificity of each siRNA for its given targeted mRNA. Data are normalized to *Tbp* gene expression. Error bars indicate SD; n=3 experiments. *p<0.05, **p<0.01, ***p<0.001.

Baghdadi_Figure S3



Tg:Pax7-CT2;Col5a1^{flox};R26^{mTmG}

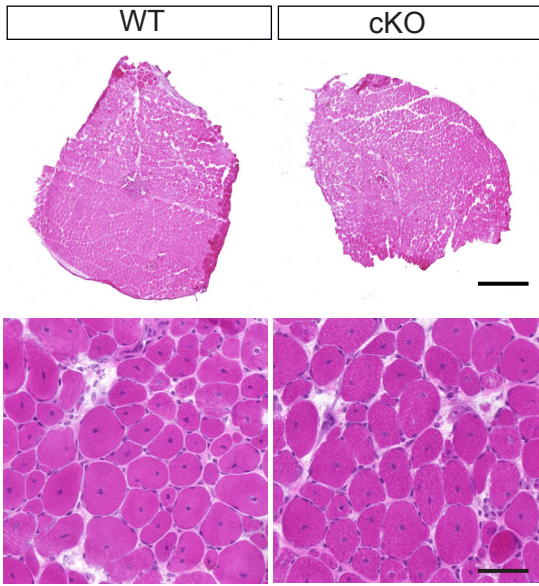


Figure S3: Muscle regeneration is normal in muscle with COLV-depleted MuSCs.

Hematoxylin and eosin staining of transverse sections of regenerating TA muscles 18 days after cardiotoxin injury (scheme shown at the top), of Col5a1 WT (*Tg:Pax7-CreERT2; Col5a1^{+/+}; R26^{mTmG}*) and cKO (*Tg:Pax7-CreERT2; Col5a1^{flox/flox}; R26^{mTmG}*) mice. Scale bar=750 μ m for top images and 100 μ m for bottom images.

Baghdadi_Figure S4

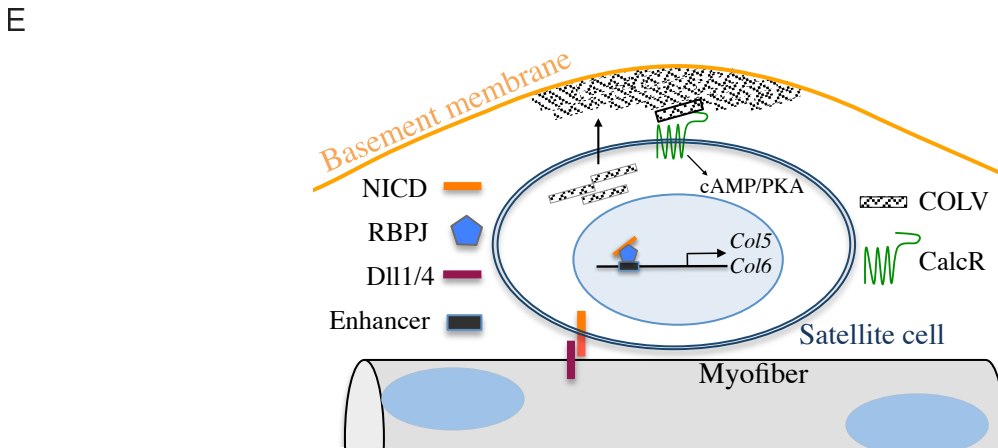
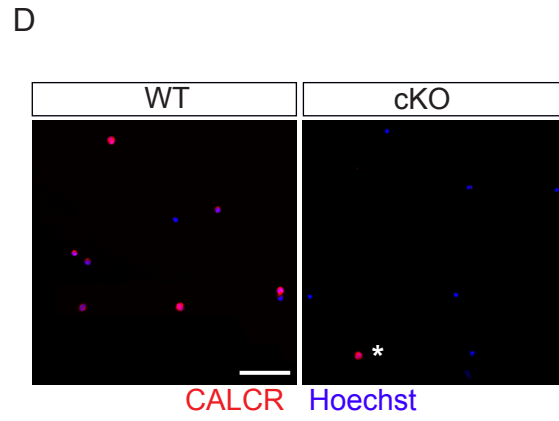
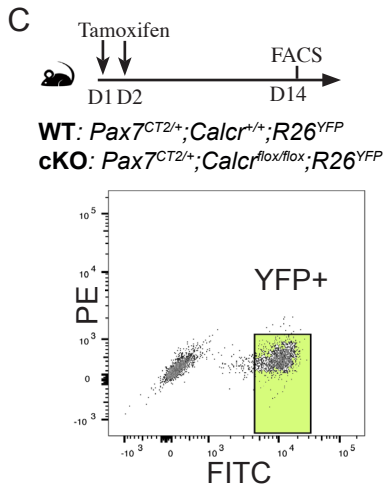
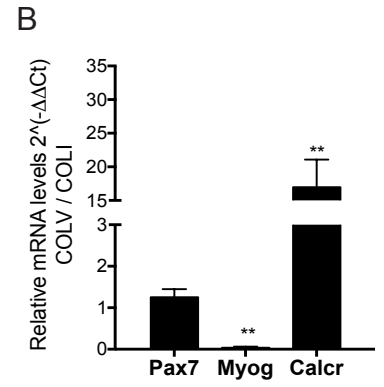
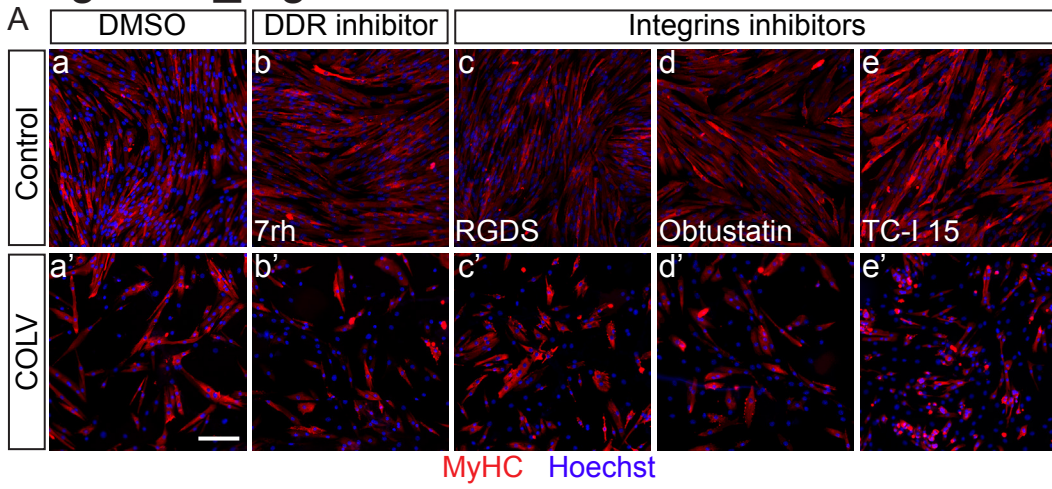


Figure S4: Screening for COLV receptor candidates identifies CALCR.

(A) Screening for the COLV receptor: MuSCs were incubated for 10 days with COLV and candidate receptors were targeted with respective inhibitor 7rh for DDR1 (b, b'), the broad-spectrum integrin-binding competitor RGDS peptide (c, c'), Obtustatin for integrin $\alpha 1\beta 1$ (d, d'), TC-I 15 for integrin $\alpha 2\beta 1$ (e, e'). DMSO solvent was used as a control for TC-I 15 and 7rh (a, a'). MuSCs differentiation was assessed by MyHC immunostaining (red).

(B) RT-qPCR on MuSCs isolated by FACS and cultured for 72h in the presence of COLI or COLV. Results are normalized to *Tbp* and presented as ratio of COLV/COLI. Error bars indicate SD, n=4 mice.

(C) Experimental scheme of tamoxifen administration to WT (*Calcr*^{+/+}) and cKo (*Calcr*^{flox/flox}) mice. FACS plot of MuSCs from *Pax7*^{CreERT2/+}; *Calcr*^{flox/flox}; *R26*^{YFP/YFP} and *Pax7*^{CreERT2/+}; *Calcr*^{+/+}; *R26*^{YFP/YFP} sorted based on the YFP intensity.

(D) *Pax7*^{CreERT2}; *Calcr*^{flox}; *R26*^{YFP} WT and cKO MuSCs isolated by FACS and fixed immediately after sorting and immunostained with CALCR to confirm the absence of CALCR protein from recombined cells. Asterisk shows a non-recombined, CALCR⁺ cell. Scale bar: 50 μ m.

(E) A Notch/COLV/CALCR signalling cascade actively maintains muscle stem cell quiescence. MuSCs are in direct contact with the plasma membrane of the myofibre (blue line) and an overlying basement membrane (orange line). Activation of the Notch receptor is achieved by ligand (likely Dll-1 or Dll4) present on the muscle fibre. Induction of *Col5a* and *Col6a* genes occurs via distal regulatory elements (blue box). Satellite cell produced COLV specifically binds and activates CALCR, expressed also by the MuSC, thus perpetuating a cell-autonomous feedback system.

Part II:

The Notch-induced microRNA-708 maintains quiescence and regulates migratory behavior of adult muscle stem cells

In preparation

1 **The Notch-induced microRNA-708 maintains quiescence and regulates**
2 **migratory behaviour of adult muscle stem cells**

3
4 Meryem B. Baghdadi^{1,2,3}, David Castel^{4,5}, Joao Firmino⁶, Philippos Mourikis⁷, Arne
5 Seitz⁶, Shahragim Tajbakhsh^{1,2*}.

6
7 *1: Stem Cells and Development, Department of Developmental & Stem Cell Biology,*
8 *Institut Pasteur, Paris 75015, France.*

9 *2: CNRS UMR 3738, Institut Pasteur, Paris 75015, France.*

10 *3: Sorbonne Universités, UPMC, University of Paris 06, IFD-ED 515, 4 Place*
11 *Jussieu, Paris 75252, France.*

12 *4: UMR8203 "Vectorologie et Thérapeutiques Anticancéreuses", CNRS, Gustave*
13 *Roussy, Univ. Paris- Sud, Université Paris-Saclay, 94805, Villejuif, France*

14 *5: Département de Cancérologie de l'Enfant et de l'Adolescent, Gustave Roussy,*
15 *Univ. Paris-Sud, Université Paris- Saclay, 94805, Villejuif, France*

16 *6: Bioimaging and Optics platform (BIOP), School of Life Sciences, Swiss Federal*
17 *Institute of Technology (EPFL), Lausanne, Switzerland.*

18 *7: INSERM IMRB U955-E10, UPEC, ENVA, EFS, Creteil 94000, France.*

19 ** Correspondence: shahragim.tajbakhsh@pasteur.fr*

20
21
22 **Abstract**
23

24 Adult skeletal muscle stem cells (MuSCs) reside on a myofibre niche and are
25 separated from interstitial cells by a basal lamina. They are responsible for tissue
26 homeostasis and repair following trauma, and have the key property of entering a
27 reversible quiescent state that allows them to maintain the stem cell pool over
28 extended periods. Several studies indicate that maintenance of quiescence in an active
29 process, yet the molecular mechanisms responsible for regulating this state remain
30 largely unknown. Recently, Notch signalling was identified to be the first crucial
31 regulator of MuSCs quiescence. Here we use ChIP sequencing for Notch signalling
32 and RNA sequencing in MuSCs and identify a Notch-induced quiescence-specific
33 microRNA, miR-708 to be involved in MuSC maintenance. Further *ex vivo* and *in*
34 *vivo* functional studies show that miR-708 regulates quiescence and self-renewal by
35 suppressing cell migration. We propose a two-step mechanism for niche residency
36 where cell cycle exit is followed by arrested migration through miR-708. These
37 findings provide a new axis for Notch signalling in regulating stem cell behaviour.

38
39

40 **Introduction**

41 The regenerative ability and plasticity of adult skeletal muscle is largely due to its
42 resident muscle stem (satellite) cells (MuSCs) located between the basal lamina and
43 the plasmalemma of the myofibers (Mauro, 1961) during homeostasis. In resting
44 muscle, MuSCs are quiescent (G₀ phase) and express the paired-box transcriptional
45 factor *Pax7* (Seale et al., 2000). Following injury, they re-enter the cell cycle,
46 proliferate to generate myoblasts that further differentiate and fuse to restore the
47 damaged fibre while a subpopulation of myogenic cells returns to quiescence for self-
48 renewal of the MuSC pool (Motohashi and Asakura, 2014).

49

50 The cell-cell communication pathway Notch is a crucial regulator of satellite cells as
51 the specific depletion of RBPJ, the DNA binding factor essential for mediating
52 canonical Notch signalling, induces spontaneous differentiation and a loss of MuSCs
53 during quiescence, and following injury (Bjornson et al., 2012; Mourikis et al.,
54 2012b). Notch receptors are expressed at the satellite cell surface and their putative
55 ligands, Delta-like ligand (DLL1, 4) and Jagged (JAG1, 2) are likely provided by the
56 myofibre upon which they reside. Binding of ligand to the receptor results in cleavage
57 of Notch (ADAM and γ -Secretase proteases), and release of the Notch intracellular
58 domain (NICD) to the nucleus where it binds RBPJ to activate immediate target
59 genes, notably the transcription factors *HeyL*, *Hes1* and *Hesr1/3* (Castel et al., 2013;
60 Jarriault et al., 1995; Kopan and Ilagan, 2009).

61

62 MicroRNAs (miRNAs), a family of small non-coding RNAs, regulate a broad range
63 of cellular processes involved in tissue determination, differentiation and maintenance
64 (Yao, 2016). The essential role of miRNAs in myogenesis has been demonstrated
65 where the conditional deletion of *Dicer* (a RNase III endonuclease required for
66 maturation of miRNAs) in the Pax7+ population results in a depletion of MuSCs and
67 a quasi-absence of repair upon injury (Cheung et al., 2012). Although numerous
68 miRNAs have been reported to regulate myoblast proliferation and differentiation
69 (Kirby et al., 2015), only miR-489 (Cheung et al., 2012) has been shown to regulate
70 MuSC quiescence and/or self-renewal. We performed a RNA deep sequencing
71 (Castel et al. manuscript in preparation) and identified a quiescence specific miRNA

72 that is regulated by Notch signalling, and that plays a critical role in satellite cell
73 maintenance in the quiescent niche *in vivo* by inhibition of cell migration.

74 **Results**

75

76 **A quiescence-specific microRNA is regulated by Notch signalling in MuSCs**

77 To define the expression of miRNAs expression during quiescence, activation and
78 differentiation, we performed a RNA-deep sequencing on freshly isolated MuSC
79 (Quiescent Satellite Cells, QSC), *in vitro* activated satellite cells for 60h (Activated
80 Satellite Cells, ASC) and differentiated cells cultured for 7 days (DIFF) (**Figure 1A**;
81 Castel et al., manuscript in preparation). We found an enrichment of specific sets of
82 miRNAs for each cell state, among those, miR-708 was exclusively expressed in
83 quiescent MuSCs (**Figure S1A**). Quantitative PCR (RT-qPCR) analysis showed miR-
84 708 expression to be significantly decreased *in vivo* in ASCs 5 days post-cardiotoxin
85 injury and in freshly isolated myofibers from EDL muscle (DIFF) compared to
86 freshly isolated MuSCs (QSC) (**Figure 1B**). In MuSCs, the miR-708-5p strand
87 constitutes the mature form of miR-708 while the passenger strand miR-708-3p is
88 degraded (**Figure 1A-C and S1A**). Therefore, miR-708-5p (Accession
89 MIMAT0004828) will be the focus of the remaining experiments in this study.
90 Interestingly, miR-708 is a highly conserved mirtron encoded in the quiescence-
91 specific gene *Odz4/Tenm4* (**Figure 1C**;
92 <http://people.csail.mit.edu/akiezun/microRNAviewer/>)(Yamaguchi et al., 2012). *Odz*
93 is the vertebrate homologue of the *Drosophila* pair-rule gene *odd Oz* (*Odz/Tenm*)
94 known to be a type II transmembrane protein; however, the function of the *Odz*
95 family remains unknown. Notably, *Odz4* expression is decreased in Notch-depleted
96 myogenic progenitors in embryos (*Pax3^{Cre/+}; Rbpj^{-/-}; Myod^{-/-}*) (Brohl et al., 2012)
97 suggesting a potential link with Notch signalling. To test this hypothesis, we used a
98 genome-wide ChIP-seq approach to identify direct targets of Notch signalling in adult
99 murine myoblasts (C2C12) in the context of inhibited (RBPJ^{NotchOFF}) or activated
100 (RBPJ^{NotchON}) Notch pathway (Castel et al., 2013). Intriguingly, we found two NICD
101 and RBPJ binding sites close to *Odz4*. The combination of histones modifications
102 H3K4me1, H3K27ac and the acetyltransferase p300 indicates that those sequences are
103 in *bona fide* enhancers (**Figure 1D**; data available at Gene Expression Omnibus,
104 Accession no. GSE37184). To test whether Notch signalling regulates the
105 transcription of *Odz4* and miR-708 *in vivo* we first conditionally ablated RBPJ in
106 *Pax7*-expressing cells driven by tamoxifen-inducible *Cre*-recombinase expression

107 (*Tg:Pax7-CT2; Rbpj^{flox/flox}; R26^{mTmG}* herein Rbpj null)(Mourikis et al., 2012b). RT-
108 qPCR performed on isolated GFP⁺ MuSCs showed a significant decrease in both
109 *Odz4* and miR-708 targets compared to control cells (**Figure 1E**). In a complementary
110 gain-of-function approach, we overexpressed NICD in embryonic myogenic
111 progenitors in which *Cre*-recombinase expression is under *Myf5* expression
112 (*Myf5^{Cre};R26^{stop-NICD-nGFP}*)(Mourikis et al., 2012a). RT-qPCR was performed on cells
113 isolated by FACS at E14.5, a developmental stage where the majority of myogenic
114 cells are still proliferating. Both *Odz4* and miR-708 are specifically upregulated in
115 response to Notch activation whereas miR-489, another quiescent miRNA (Cheung et
116 al., 2012), remained unchanged (**Figure 1F**). Importantly, transcriptional responses of
117 *Odz4* and miR-708 tightly follow Notch activity modulations in 8 days postnatal
118 *Tg:Pax7-nGFP* pups in which endogenous Notch activity gradually declines as cells
119 transit from an upstream Pax7^{Hi} to a committed Pax7^{Lo} state (Mourikis et al., 2012b;
120 Rocheteau et al., 2012) (**Figure S1B**). Taken together, these data demonstrate that
121 RBPJ/NICD signalling regulates the production of *Odz4* and by consequence miR-
122 708 in MuSCs *in vivo* by direct binding on distal transcriptional enhancers.

123

124 **miR-708 retains stemness and self-renewal capacities of MuSCs *ex vivo***

125 To assess whether the sustained expression of miR-708 could affect MuSC behaviour,
126 we overexpressed miR-708 in freshly isolated satellite cells from *Tg:Pax7-nGFP*
127 using transfection of Mimic-708 (**Figure S2A** for RT-qPCR validation). Proliferation
128 capacity based on the uptake of nucleotide analogue EdU (24h to 4days post-
129 transfection) showed that miR-708 overexpressing-myogenic cells exhibited a
130 decrease in proliferation at 24h and 48h compare to Scramble control (24h: 24% and
131 2% 48h: 69% and 61% for Scramble and Mimic-708, respectively; **Figure 2A, B**).
132 Primary myogenic cells in culture gradually stopped proliferating from 60-70h and
133 started to progressively express the differentiation marker *Myogenin*. To investigate
134 the role of miR-708 on MuSC differentiation, we scored for Myogenin (MyoG) at 72h
135 and 4 days after transfection of the mimic. Gain-of-function of miR-708 decreased the
136 number of MYOGENIN-expressing cells compared to control at both 72h and 4days
137 (72h: 37% and 4% 4d: 61% and 33% for Scramble and Mimic-708, respectively;
138 **Figure 2C**). Overall, these results show that miR-708 can retain MuSCs proliferation
139 and delay myogenic differentiation.

140 In a complementary loss-of-function assay, we depleted miR-708 using short-
141 interfering RNA (AntimiR-708) (**Figure S2C**) in an *ex vivo* system where resident
142 MuSCs on isolated myofibers exit quiescence, enter the myogenic program and form
143 clusters composed of proliferating (Pax7⁺/MyoD⁺/MyoG⁻), differentiated (Pax7⁻
144 /MyoG⁺) and self-renewed (Pax7⁺/MyoG⁻) cells within 72h (Zammit et al., 2004).
145 Single myofibres isolated from EDL muscle of *Tg:Pax7-nGFP* mice were transfected
146 with AntimiR-708 or Scramble control and cell clusters were analysed after 72h.
147 Targeting specifically miR-708-5p increased significantly the number of
148 differentiated cells per fibre (43% vs 79% for Scramble and AntimiR-708), and
149 reduced self-renewed events (21% vs 5% for Scramble and AntimiR-708) (**Figure**
150 **2D**). Thus, miR-708 inhibition results in a reduction in self-renewal, and increased
151 differentiation. We note that this did not result in a depletion in cell number
152 suggesting that some amplification of myogenic cells might have occurred in this
153 condition prior to differentiation.

154

155 **Antagonism of miR-708 *in vivo* induces spontaneous exit from quiescence and** 156 **premature differentiation of MuSCs**

157 To investigate the role of miR-708 function in maintenance of satellite cells *in vivo*,
158 we synthesized a miR-708 antagonist (AntagomiR-708) with an antisense sequence to
159 mature miR-708-5p, as well as control Scramble with the same modifications that
160 does not target any mouse gene or EST sequence (see Methods). To assess potential
161 secondary targets, we first assayed miR-708 expression in different cell types
162 extracted from skeletal muscles, namely endothelial cells, fibro-adipogenic
163 progenitors, resident and infiltrating macrophages. RT-qPCR analysis revealed that
164 among the different cell types tested, only MuSCs expressed miR-708 (data not
165 shown). We then performed lineage tracing of MuSCs using *Tg:Pax7-CT2; R26^{mTmG}*
166 mice fed two weeks with tamoxifen (95% efficiency of recombination, **Figure S3A**).
167 Control Scramble or AntagomiR-708 were then injected in the tail vein every day for
168 4 days, and resting muscles were analysed 10 days later (**Figure 3A**). RT-qPCR
169 analysis on mGFP⁺ cells isolated by FACS showed a significant reduction of miR-
170 708 and miR-489 levels, whereas miR-92 expression (activation enriched miRNA,
171 Figure 1A) was strongly upregulated (**Figure 3B**). These results suggest that MuSCs
172 treated with AntagomiR-708 spontaneously switch on the activation program in the

173 absence of muscle injury. To test this hypothesis, we analysed quiescence (*Pax7*,
174 *Odz4*), activation (*Myod*), and differentiation (*Myogenin*) genes expression in mGFP+
175 cells isolated by FACS. A significant decrease in the quiescence genes was noted,
176 whereas *Myod* and *Myogenin* expressions were strongly upregulated following
177 AntagomiR-708 treatment (**Figure 3C**). Consistent with these results,
178 immunostaining showed that 30% of mGFP+ cells lost Pax7 expression in mice that
179 received AntagomiR-708 (**Figure 3D**). The expression profile and the loss of Pax7
180 protein, indicate that reduced miR-708 levels in MuSCs leads to their spontaneous
181 exit from the quiescent state. Furthermore, when mGFP+ cells isolated by FACS from
182 AntagomiR-708 treated mice were cultured for 5 days they exhibited a striking
183 increase in myotube formation as indicated by a higher fusion index (24% for
184 Scramble vs. 51% for AntagomiR-708; **Figure 3E**). During homeostasis, MuSCs are
185 localized between the myofibre membrane and the basal lamina (Mauro, 1961).
186 Surprisingly, we observed abnormal localization of Pax7+ cells in the interstitial
187 space in the TA of AntagomiR-708 treated mice (2% for Scramble vs. 38% for
188 AntagomiR-708; **Figure 3F**) suggesting that those cells escaped the quiescent stem
189 cell niche.

190

191 We showed previously that alteration of Notch signalling induces MuSCs to
192 differentiate spontaneously without entering S-phase (Mourikis et al., 2012b). As loss
193 of miR-708 function promoted a loss of cellular quiescence and differentiation of
194 myogenic cells, we investigated whether this cell state transition was accompanied by
195 exit from G0 and entry into S-phase. To do so, mice were exposed to uninterrupted
196 BrdU administration through the drinking water for 5 days prior to sacrifice (**Figure**
197 **3A**). As shown in **figure 3E**, the loss of miR-708 induces an increase in BrdU uptake
198 quantified by the number of mGFP+/BrdU+ cells (2% for Scramble vs. 15% for
199 AntagomiR-708; **Figure 3G**) indicating that the knock-down of miR-708 induces
200 spontaneous exit from quiescence accompanied by proliferation.

201

202 To investigate in more detail the long-term impact of miR-708 inhibition *in vivo*, we
203 treated mice with tamoxifen and AntagomiR as described above, and analysed resting
204 muscle 28 days later (**Figure 3H**). Strikingly, the amount of mGFP+ cells isolated by
205 FACS was 50% lower than Scramble control (**Figure S3B and C**) and this result was

206 confirmed *in vivo* by the quantification of Pax7+ cells in sections of *Tibialis anterior*
207 (TA) muscle (30 Pax7+ cells/mm² for Scramble vs. 14 for AntagomiR-708; **Figure**
208 **3I**). We then investigated whether the loss of MuSCs was due to apoptosis or cell
209 fusion. Immunostaining with cleaved-caspase 3 did not reveal a significant change in
210 the number of apoptotic cells in AntagomiR-708 treated TA muscle compared to
211 control (data not shown). In contrast, we found numerous GFP+ fibres in resting
212 muscle indicating mGFP+ cells fused with pre-existing myofibers (**Figure 3J**) a
213 phenotype that is reminiscent of loss of function of *Rbpj* in MuSCs (Mourikis et al.,
214 2012b). Taken together, these results demonstrate that miR-708 is necessary for the
215 maintenance of MuSCs in the quiescent state and their localization in the niche.

216

217 We further analysed the behaviour of the 50% remaining satellite cells (Figure 3I) 28
218 days upon AntagomiR-708 treatment. Interestingly, RT-qPCR and culture
219 experiments did not show any perturbations in quiescence and differentiation
220 capacities (**Figure S3D**). Moreover, AntagomiR-708 treated mice depicted a delay in
221 regeneration at 14 days post-injury (dpi) as shown by hematoxylin/eosin histological
222 analysis (**Figure S3E**). However, this delay in regeneration was not overtly detectable
223 by 31dpi demonstrating the functionality of the remaining cells, that are likely
224 escapers, following the short period of AntagamiR-708 treatment (**Figure S3F**). We
225 propose that either the remaining cells were spared from the AntagomiR-708
226 treatment due to accessibilities issues, or that the short treatment did not have a lasting
227 effect and miR-708 levels were restored.

228

229 **miR-708 promotes myogenic differentiation by targeting MuSC motility and** 230 **migration capacities**

231 miR-708 has been shown to be downregulated in human prostate (Saini et al., 2012) ,
232 breast (Ryu et al., 2013), renal (Saini et al., 2011), ovarian (Lin et al., 2015) and
233 glioblastoma (Guo et al., 2013) cancer cells. Although the target genes were different,
234 those studies demonstrate a common feature of miR-708 in the suppression of
235 invasion and metastasis via inhibition of cell migration properties. To assess whether
236 miR-708 could affect satellite cell migration, we overexpressed miR-708 in activated
237 satellite cells, using a Mimic-708 transfection system, and monitored cell behaviour
238 *ex vivo* for 48h by live video microscopy (**Figure 4A**). In addition to the decrease in

239 the number of dividing cells mentioned above (Figure 2A), the distance and velocity
240 of myogenic treated with miR-708 strongly diminished compared to Scramble control
241 (Figure 4B-4C; see supplementary movies).

242

243 Active cell migration is a key property of satellite cells (Siegel et al., 2009) and it has
244 been shown that stimulation of migration improves myoblast dispersal following
245 transplantation, thereby resulting in enhanced engraftment efficiency (Bentzinger et
246 al., 2014). We examined the migration potential of miR-708-treated myogenic cells in
247 a transwell assay where satellite cells seeded on the upper part of the insert can
248 migrate in vertical direction through the membrane. Quantification of the number of
249 cells on the other side of the insert showed an impairment of migration in a miR-708-
250 overexpression context (52 cells/field for Scramble vs. 18 for AntagomiR-708;
251 Figure 4D). Taken together these results suggest that one of the functions of miR-708
252 is to inhibit migration and motility of satellite cells.

253

254 miRNAs bind to the 3'-untranslated region (3'UTR) of their target mRNAs inducing
255 their degradation or the inhibition of translation. Three target prediction algorithms
256 (TargetScan; miRanda; TargetRank) were used and the distribution of the number of
257 targets predicted for miR-708 is represented in the form of a Venn diagram (Figure
258 4E). Among the 24 genes that were predicted by the three algorithms (Figure S4A), 3
259 were differentially expressed in quiescent compared to activated satellite cells (Liu et
260 al., 2013) (Figure S4): Tensin-3 (*Tns3*), Dickkopf-3 (*Dkk3*) and Syndecan-1 (*Sdc1*).
261 To test whether the putative miR-708 target sequences could mediate translational
262 repression, we inserted the 3'UTR sequences of each of the predicted targets in a
263 luciferase reporter plasmid (Table 3). HEK293T cells were co-transfected with
264 constructs and with Mimic-708 or Scramble control. Notably, miR-708 repressed
265 luciferase activity of both *Dkk3* and *Tns3* but not *Sdc1* (Figure 4F).

266

267 Discussion

268 We identified miR-708 as a quiescence-specific mirtron in the *Odz4* gene, where this
269 miRNA acts as a downstream target of Notch signalling to maintain the quiescent
270 state and MuSCs within their niche. Validation of the transcriptional relevance was
271 done in genetically modified mice by *in vivo* gain and loss of function of Notch

272 activity. Direct validation of the two enhancers containing consensus RBPJ binding
273 sequences upstream of *Odz4* are currently ongoing and their functionality in a cell-
274 based luciferase assay in myogenic C2C12 cells under Notch-ON et Notch-OFF
275 conditions are being tested.

276

277 We show that miR-708 *in vivo* inhibition induces premature exit from quiescence in
278 MuSCs, proliferation and spontaneous fusion with the pre-existing fibre resulting in
279 the loss of about 50% of the satellite cell population. Given that the analysis was
280 performed on the total Pax7-nGFP population as in previous studies, we consider the
281 possibility that a subpopulation of MuSCs is not under miR-708 regulation; single cell
282 studies could address this point.

283

284 The *in silico* analysis of miR-708 potential target genes provided 3 candidates: *Dkk3*,
285 *Sdc1* and *Tns3*. We have validated *Dkk3* as a target gene. Dkks (Dkk1-4) represent a
286 family of evolutionary conserved secreted glycoproteins known to specifically inhibit
287 Wnt/ β -catenin signalling cascade. However, DKK3 appears to be a divergent member
288 of the Dkk family in DNA sequence, protein structure and function (Niehrs, 2006); as
289 it has no affinity for Wnt co-receptors LRP5/6 and Kremen, but instead it regulates
290 TGF- β (Transforming growth factor) signalling level (Romero et al., 2013) in
291 addition of the FGF-MAPK signalling (Lodygin et al., 2005; Pinho and Niehrs, 2007).
292 TGF- β /Smad has been shown to maintain satellite cell quiescence (Rathbone et al.,
293 2011) while FGF promotes exit of quiescence of satellite cells as well as myoblast
294 expansion and recruitment (Yablonka-Reuveni et al., 1999) (Chakkalakal et al.,
295 2012).

296

297 TNS3 is a member of focal adhesion (FA)-associated proteins that are important
298 regulators of cell adhesion and migration by association with multiple types of
299 adhesion structures such as FA or podosomes. Tensins have been shown to regulate
300 actin dynamics by modulation of Rho GTPase signalling pathways (Blangy, 2017).
301 Interestingly, miR-708 has been shown to negatively regulate the phosphorylation of
302 ERK (extracellular signal-regulated kinases) that further phosphorylates FA.
303 Therefore, we are currently investigating the possibility of a combined effect of
304 inhibition of TNS3 in addition to DKK3 for mediating miR-708 functional inhibition

305 of cell migration. To do so, analysis of TGF- β /Smad, FGF-MAPK and FA behaviour
306 under miR-708 gain/loss of function are on going.

307 We note that miR-708 overexpression resulted in a delay in satellite cell proliferation
308 however, analysis of miR-708 putative targets did not reveal any candidates that are
309 involved in cell cycle regulation. Thus, we propose that the inhibition of
310 migration/motility indirectly inhibits cell cycle progression. To uncouple proliferation
311 and migration properties, we aim to use the Fucci-green (Fluorescence ubiquitination-
312 based cell cycle indicator) mouse model to follow the cell cycle progress in isolated
313 MuSCs (Sakaue-Sawano et al., 2008). Taking advantage of the ubiquitin-mediated
314 proteolysis regulation of cell cycle, this approach will permit *ex vivo* analysis of
315 spatial and temporal patterns of cell-cycle dynamics, using Azami green to label
316 S/G2/M phases. We propose to overexpress miR-708 in freshly isolated quiescent
317 satellite cells and to assess whether migration precedes cell cycle entry. Moreover,
318 miR-708 expression in activated satellite cells from Fucci green mouse could inform
319 us on whether those cells transiently return to G₀-state, or if they will be blocked
320 within the cell cycle. These questions are currently under investigation
321 experimentally.

365 **Material and methods**

366

367 ***Mouse strains***

368 Mouse lines used in this study have been described and kindly provided by the
369 corresponding laboratories: *Myf5^{Cre}* (Haldar et al., 2008), *R26^{stop-NICD-nGFP}* (Murtaugh et
370 al., 2003), *R26^{mTmG}* (Muzumdar et al., 2007), *Rbpj^{flox/flox}* (Han et al., 2002), *Tg:Pax7-
371 CreERT2* and *Tg:Pax7-nGFP* lines have been generated in the S.T. lab and previously
372 described (Mourikis et al., 2012b; Sambasivan et al., 2009). Animals were handled
373 according to national and European community guide- lines, and protocols were
374 approved by the ethics committee at Institut Pasteur.

375

376 ***Muscle injury, tamoxifen and BrdU administration***

377 For muscle injury, mice were anesthetized with 0.5% Imalgene/2% Rompun and the
378 TA muscle was injected with 50 μ l of Cardiotoxin (10mM; Latoxan). *Tg:Pax7-
379 CreERT2; Rbpj^{flox}; R26^{mTmG}* and *Tg:Pax7-CreERT2; R26^{mTmG}* were fed with tamoxifen
380 containing diet for two or three weeks (Envigo, #TD55125). Five days prior sacrifice
381 *Tg:Pax-CreERT2; R26^{mTmG}* mice were given the thymidine analogue 5-Bromo-2'-
382 deoxyuridine (BrdU, 0.5mg/ml, #B5002; Sigma) in the drinking water supplemented
383 with sucrose (25mg/ml). Comparisons were done between age-matched littermates
384 using 8-12 week old mice.

385

386 ***Satellite cell dissociation and Fluorescence Activated Cell Sorting (FACS)***

387 Adult limb muscles were dissected, minced and digested in a solution containing
388 0.1% collagenase D (Roche #11088882001) and 0.25% trypsin (Invitrogen #15090)
389 diluted in Dulbecco's Modified Eagle's Medium (DMEM; Gibco) supplemented with
390 1% penicillin/streptomycin (PS; Gibco) and DNase I (10 mg/ml; Roche) for five
391 consecutive cycles of 30 min at 37°C with gentle agitation. Between each round, the
392 supernatant was filtered through 100 μ m then 70 μ m (Milteny, 130-098-463; 130-098-
393 462) and recovered in cold blocking foetal calf serum (FCS; Invitrogen). Supernatants
394 from each digestion were pooled and centrifuged a first time 10 min at 50g at 4°C to
395 remove large debris. The supernatant was collected and span twice 15 min at 600g.
396 Before FACS, the pellet was resuspended in DMEM/1% PS supplemented with 2%

397 FCS and filtered through 40µm. Cells were sorted using a FACS Aria III (BD
398 Biosciences) and collected in DMEM/1% PS/2% FCS.

399

400 ***RNA extraction and quantitative PCR (RT-qPCR)***

401 Micro-RNAs from cells or tissue were purified using (Qiagen miRNAeasy® Micro
402 Kit) and reverse transcribed in cDNA using miRCURY LNA® universal RT kit
403 (Exiqon; #203301): incubation 60 min at 42°C (5' polyadenylation of miRNA with
404 Poly(T) oligonucleotide primers) and 5 min at 95°C (heat inactivation of reverse
405 transcriptase). Expression of mature miRNAs was determined using ExiLent
406 SYBR® green master mix (Exiqon) and miRNA LNA™ PCR primers (Exiqon; hsa-
407 miR-708-5p, #204490; mmu-miR-489-3p, #205036; hsa-let-7e-3p, #205301). Two
408 snoRNA; RNU5G (Exiqon; #308014) and SNORD65 (Exiqon; #308016) were used
409 for normalization.

410 Total mRNA were isolated using (Qiagen RNAeasy® Micro Kit) and reverse
411 transcribed using SuperScriptIII® enzyme (Invitrogen, 18080093): 10 min at 25°C, 50
412 min at 42°C and 15 min at 70°C. The eventual remaining RNAs were degraded by
413 incubation 20 min at 37°C with RNase H endonuclease (Roche, #10786357001).
414 Expression of mature mRNAs was assessed with SYBR green master mix (Roche;
415 04913914001) and analysis were performed using the $2^{-\Delta\Delta CT}$ method (Livak and
416 Schmittgen, 2001). Specific forward and reverse primers used for RT-qPCR are listed
417 in Supplementary Table 1.

418

419 ***Satellite cell culture and transfection***

420 Satellite cells isolated by FACS, and total muscle preparations were seeded at 3×10^3
421 cells/cm² on Matrigel® (Corning, 354248) coated dishes for 30 min at 37°C. Cells
422 were cultured in a growth medium (GM) containing DMEM/F12 (50:50; Gibco), 1%
423 P/S, 20% FBS, 2% Ultrosor (Pall; 15950-017) and incubated at 37°C, 3% O₂, 5% CO₂
424 for the indicated time. Half of the medium was changed every 3 days. To assess
425 proliferation, cells were pulsed with the thymidin analogue 5-ethynyl-2'-deoxyuridine
426 (EdU), 1×10^{-6} M, 2h prior to fixation (ThermoFisher Click-iT Plus EdU kit, C10640).
427 Freshly isolated MuSCs from *Tg:Pax7-nGFP* were transfected in suspension
428 immediately after FACS with miRIDIAN microRNA mmu-miR-708-5p mimic
429 (Dharmacon, #C310987) and Control#1 (Dharmacon, #CN-001000) at 200nM final

430 concentration using Lipofectamine 2000 (ThermoFisher, #11668) in Opti-MEM
431 (Gibco). Four hours after transfection, 3 volumes of fresh growth medium was added
432 and cells were cultured for the indicated time. Cells were fixed with 4%
433 paraformaldehyde (PFA) in PBS 10 min at room temperature.

434

435 ***Single Myofibre isolation and Antimir transfection***

436 Single myofibres were isolated from EDL muscles following the previously described
437 protocol (Shinin et al., 2006). Briefly, EDLs were dissected and incubated in 0.1%
438 w/v collagenase (Sigma, #C0130)/DMEM for 1h in a 37°C shaking water bath at
439 40rpm. Following enzymatic digestion, mechanical dissociation was performed to
440 release individual myofibres that were then transferred to serum-coated petri dishes.
441 Single myofibres were transfected with miRCURY LNA™ mmu-miR-708-5p
442 inhibitor (Exiqon, #4101225) or Negative control A (Exiqon, #199096) at a final
443 concentration of 250nM, using Lipofectamine 2000 (ThermoFisher, 11668) in Opti-
444 MEM (Gibco). Four hours after transfection, 6 volumes of fresh MuSC growth
445 medium was added and fibres were cultured for 72h at 37°C, 3%O₂. Fibres were fixed
446 with 4%PFA/PBS 15 min at room temperature.

447

448 ***Immunostaining on cells, myofibers and sections***

449 Following fixation, cells and myofibers were washed three times with PBS, then
450 permeabilised and blocked at the same time in buffer containing 0.25% Triton X-100
451 (Sigma), 10% goat serum (GS; Gibco) for 30min at RT. For BrdU immunostaining,
452 cells were unmasked with DNaseI (1,000 U/ml, Roche, #04536282001) for 30 min at
453 37°C. Cells and fibres were then incubated with primary antibodies (Supplementary
454 Table 2) overnight at 4°C. Samples were washed with 1X PBS three times and
455 incubated with Alexa-conjugated secondary antibodies (Life Technologies, 1/1000)
456 and Hoechst (Life Technologies; 1/10000) for 45 min at RT. EdU staining was
457 chemically revealed using the Click-iT Plus kit according to manufacturer's
458 recommendations (Life Technologies, #C10640).

459 Isolated *Tibialis anterior* (TA) muscles were frozen in liquid-nitrogen cooled
460 isopentane and sectioned transversely at 8µm. Sections were post-fixed with 4%PFA
461 for 15min and washed 3times with PBS1X. For Pax7 staining, antigen retrieval was
462 performed by incubating sections in boiling 10mM citrate buffer pH6 in the 2100

463 Retriever device. Confocal images were acquired with Zeiss LSM 700 microscope and
464 Zen Blue 2.0 software.

465

466 *AntagomiR synthesis and administration*

467 AntagomiR and Scramble were designed as described before (Krutzfeldt et al., 2005).

468 PAGE-purified AntagomiR were synthesized with the following modifications

469 (Dharmacon): AntagomiR-708:

470 5'mC*mC*mCmAmGmCmUmmAmGmAmUmUmGmUmAmAmGmCmU*mC*m

471 U*mU*3'-Chl;

472 Scramble:

473 5'mU*mU*mUmCmUmAmAmUmCmAmAmGmGmGmUmCmUmGmUmG*mG*

474 mC*mU*3'-Chl. Where * represents phosphothiotate linkage at given position; m,

475 2'OMethyl-modified nucleotides; Chl, cholesterol linked through a hydroxyprolinol

476 linkage. AntagomiR molecules were resuspended in saline and injected every day for

477 4 days into tail veins at a dose of 8ug/g of mouse.

478

479 *Live Imaging*

480 Cells were transfected and seeded as indicated above. The plate was then incubated at

481 37°C, 5% CO₂, and 3% O₂ (Zeiss, Pecon). A Zeiss Observer.Z1 connected to an LCI

482 PlnN 10x/0.8 W objective and Hamamatsu Orca Flash 4 camera piloted with Zen

483 (Zeiss) was used. Cells were filmed and images were taken every 15 min for the time

484 indicated. Distance and velocity were obtained with Manual tracking of Fiji software.

485

486 *Transwell Assay*

487 The bottom part of a transwell membrane with 8µm pores size (Corning, #3428) was

488 coated with Matrigel 15min at 37°C. FACS isolated MuSCs from *Tg:Pax7-nGFP*

489 mouse were culture as described before for 24h prior to Mimic-708 or Scramble

490 transfection. Twenty-four hours post-transfection satellite cells were then trypsinized

491 (Gibco, #25200) 10 min at 37°C. Trypsin was washed away by the addition of

492 DMEM/10% FCS and cells were centrifuged 15min at 600g. Cell pellets were

493 resuspended in a low serum medium DMEM/2% FCS and seeded on the upper part of

494 the transwell. Cells were allowed to migrate in a vertical direction through the pores

495 of the membrane into the lower compartment, in which higher serum content was

496 present (GM). Six hours after seeding, the membrane was fixed 15min with Methanol
497 and non-migrated cells remaining on the topside of the filter are removed with a
498 cotton swab. The migrated cells are stained with Crystal Violet 0.5%/ 25% Methanol
499 for 1 to 5min (Sigma, #C0775) and washed 5 times in PBS1X.

500

501 ***Transfection and luciferase assay***

502 The full 3'UTR length of mouse Dkk3 and Sdc1 (<http://genome.ucsc.edu>) were
503 amplified using PCR. Partial Tns3 3'UTR containing miR-708 potential binding site
504 of interest was obtained from SourceBioscience (EST clone: IMAGp998D088514Q)
505 (Supplementary Table 3). 3'UTR were cloned in the pGL3-Control vector (Promega,
506 #E1741) downstream of the luciferase gene and co-transfected with Mimic-708 or
507 Scramble negative control in HEK293T like described above. A Renilla luciferase
508 plasmid (pCMV-Renilla, 1/200 ratio to firefly) was also co-transfected as transfection
509 control and empty pGL3 vector was use as a background negative control. The results
510 are expressed as firefly luciferase activity relative to Renilla luciferase activity.
511 Transfected HEK293T were cultured in DMEM/10%FCS, at 37°C, 5% CO₂, and 20%
512 O₂ for 48h and firefly and renilla luciferase activities were detected with Dual Glo[®]
513 luciferase assay system (Promega, #2920).

514

515 ***Statistical analysis***

516 For comparison between two groups, two-tailed Student's t test was performed to
517 calculate p values and to determine statistically significant differences (* p<0.05, **
518 p<0.01, *** p<0.001). In specific conditions, Mann-Whitney test has been used and
519 indicated in the figure legend. All statistical analyses were performed with Excel
520 software or GraphPad Prism software.

521

522 **Acknowledgement**

523 We would like to thank Clémire Cimper for the histology. Sébatien Mella for the
524 generation of the heatmap. Brendan Evano for designing the cloning strategy. Olivier
525 Burri for helping with movie processing. For the cytometry, we thank Sophie Novault
526 at the Flow Cytometry Platform of the Technology Core-Center for Translational
527 Science (CRT) at Institut Pasteur. ST acknowledges support from the Institut Pasteur,
528 Agence Nationale de la Recherche (Laboratoire d'Excellence Revive, Investissement

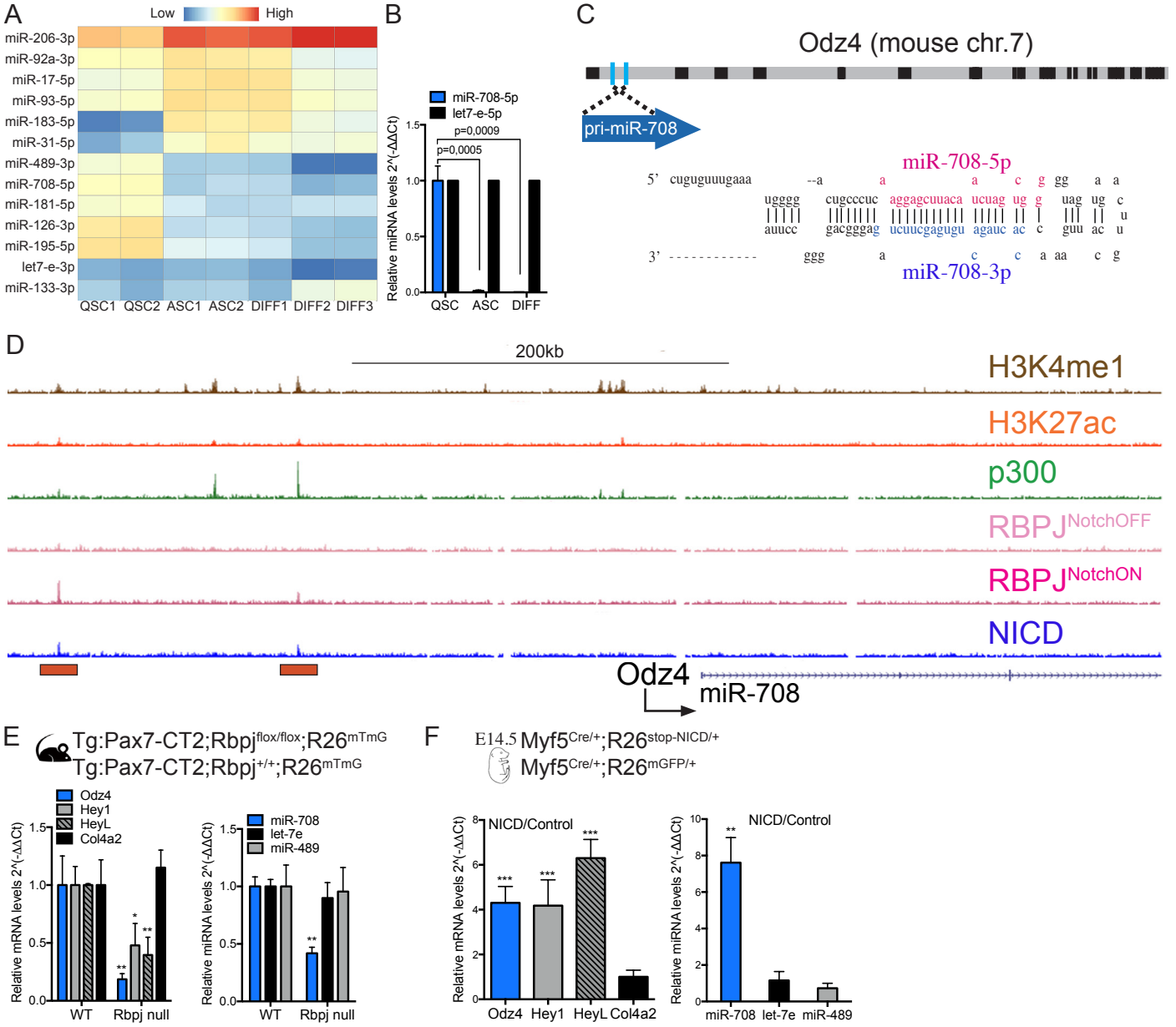
529 d'Avenir; ANR-10-LABX-73) and (ANR-06-BLAN-0039), the Association pour la
530 Recherche sur le Cancer, and the European Research Council (Advanced Research
531 Grant 332893). MBB was supported by a doctoral school fellowship and Fondation
532 pour la Recherche Médicale.

533

534 **Authors contributions**

535 S.T. and M.B.B proposed the concept and designed the experiments. M.B.B.
536 performed most of the experiments. D.C. performed the RNA-sequencing. M.B.B.
537 and S.T. wrote the paper.

Baghdadi_FIGURE 1



538 **Figure Legends**

539

540 **Figure 1. miR-708 is a Notch pathway target mirtron specifically expressed in**
541 **quiescent MuSCs.**

542 (A) Gene expression from RNA deep sequencing on freshly isolated MuSC
543 (Quiescent Satellite Cell, QSC, n=2), *in vitro* activated satellite cells for 60h
544 (Activated Satellite cells, ASC, n=2) and differentiated cells cultured for 7 days
545 (Differentiated cells, DIFF, n=3). miR-708, miR-489, miR-195, miR-126 are
546 quiescence-specific microRNAs. miR-183, miR-92, miR-17 and miR-93 are
547 activation-specific miRNAs.

548 (B) RT-qPCR validation of miR-708 expression on freshly isolated MuSC (QSC), *in*
549 *vivo* activated satellite cells 5 days post-injury (ASC) and freshly isolated myofibers
550 from EDL (DIFF) (n= 3 mice). *Let-7e* expression was found stable in every condition
551 (see Figure 1A) and is used as negative control.

552 (C) Schematic representation of mouse *Odz4* gene; black boxes represent exons. miR-
553 708 is encoded by the first intron of *Odz4*. Double stranded pri-miR-708 including
554 miR-708-5p (pink), the mature strand in MuSCs and the passenger strand, miR-708-
555 3p.

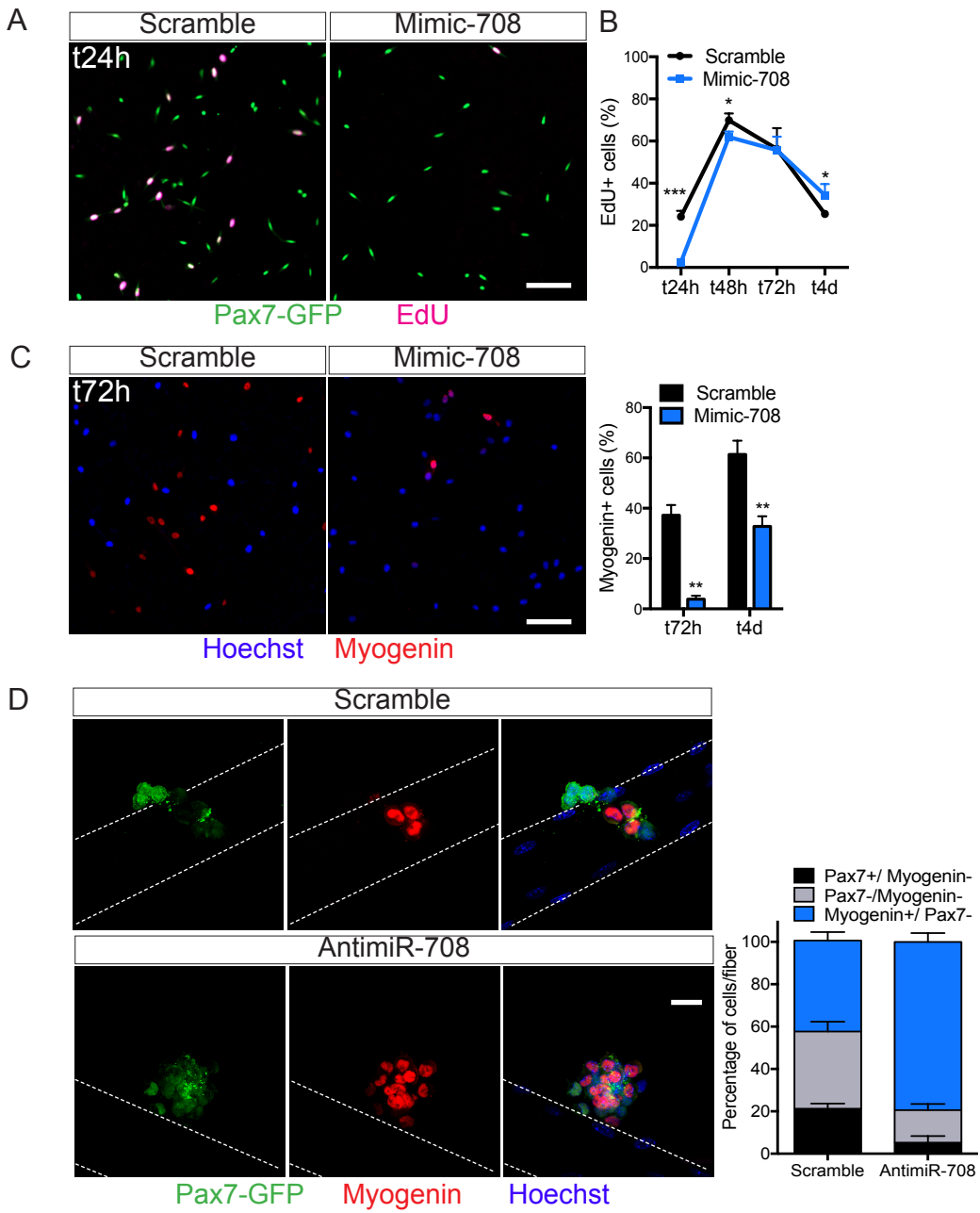
556 (D) ChIP-seq tracks showing NICD/RBPJ occupancy on enhancers associated to
557 mouse *Odz4* loci. H3K4me1, and H3K27ac, p300, RBPJ, and NICD are shown. Note
558 absence RBPJ binding in DAPT-treated cells (RBPJ^{NotchOFF}). Orange rectangle
559 indicates RBPJ binding positions.

560 (E) RT-qPCR analysis of *Odz4* (left) and miR-708 (right) genes in *Rbpj* conditional
561 KO (*Rbpj* null) and control (WT) MuSCs. Cells were isolated from resting muscles
562 by FACS 2 weeks post-tamoxifen treatment. WT: *Tg:Pax7-CT2; Rbpj^{+/+}; R26^{mTmG}* and
563 *Rbpj* null: *Tg:Pax7-CT2; Rbpj^{flox/flox}; R26^{mTmG}* (n=4 mice/genotype).

564 (F) Induction of *Odz4* (left) and miR-708 (right) genes in E14.5 control (*Myf5^{Cre/+}; R26^{mTmG/+}*)
565 and *Myf5Cre-NICD* (*Myf5^{Cre/+}; R26^{stop-NICD-nGFP/+}*) cells isolated by FACS
566 assessed by RT-qPCR. *Hey1/Heyl* are reporters of Notch activity, *Col4a2* and *let-7e*
567 are not Notch target genes.

568 Error bars indicate SD, *p<0.05, **p<0.01, ***p<0.001.

Baghdadi_FIGURE 2



569 **Figure 2. miR-708 retains MuSCs proliferation and differentiation while its**
570 **inhibition impairs self-renewal capacity *in vitro*.**

571 (A) EdU and GFP staining on isolated MuSCs from *Tg:Pax7-nGFP* mouse 24h after
572 Mimic-708 or Scramble control transfection.

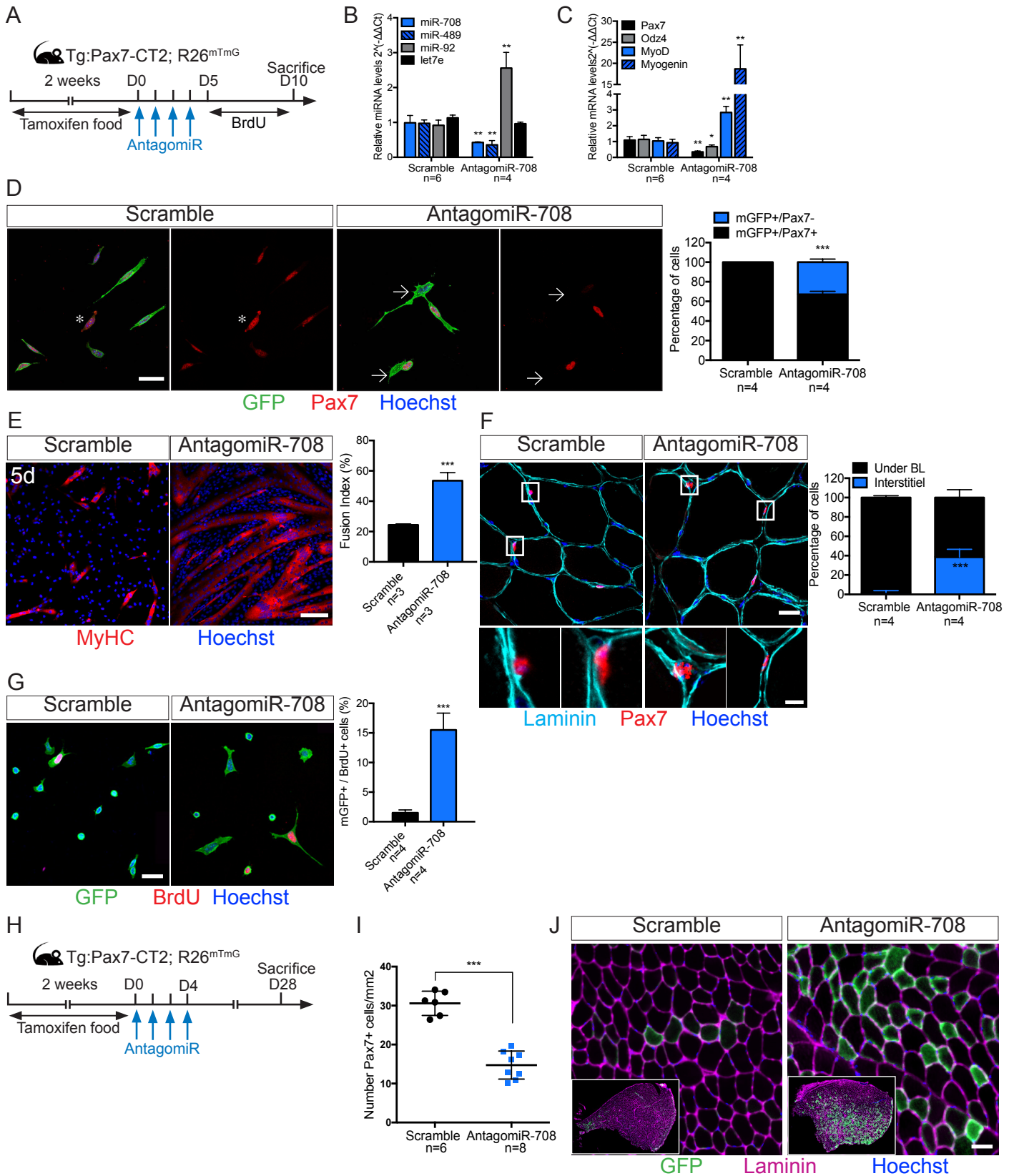
573 (B) Time course of proliferation by quantification of EdU 24h to 4days following
574 miR-708 overexpression (Mimic-708) or Scramble control.

575 (C) Myogenin and Hoechst staining on isolated MuSCs from *Tg:Pax7-nGFP* mouse
576 72h after Mimic-708 or control Scramble transfection. Quantification of Myogenin
577 positive cells at 72h and 4 days following Mimic-708 or Scramble transfection.

578 Error bars indicate SD; n=4 mice, ≥ 400 cells counted, 2 wells/ condition. *p<0.05,
579 **p<0.01, ***p<0.001. Scale bar: 50 μ m.

580 (D) miR-708 knock-down using AntimiR-708 transfection of *Tg:Pax7-nGFP* isolated
581 single myofibers from EDL cultured for 72h and immunostained for GFP and
582 Myogenin. Quantification of Pax7+/Myogenin $-$, Pax7+/Myogenin $+$ and
583 Myogenin+/Pax7 $-$ populations 72h after transfection. Scramble was used as negative
584 control (n=4 mice, ≥ 25 fibres counted). Error bars indicate SD; ***p<0.001 in all
585 conditions. Scale bar: 50 μ m.

Baghdadi_FIGURE 3



586 **Figure 3. miR-708 maintains the quiescent state in MuSCs.**

587 (A) Experimental scheme of tamoxifen, AntagomiR and BrdU administration to
588 *Tg:Pax7-CT2; R26^{mTmG}* mice. AntagomiR-708 and Scramble control were injected
589 every day for 4 days after the end of tamoxifen treatment (D0) and mice were
590 sacrificed 10 days post-AntagomiR treatment.

591 (B) miRNA expression assessed by RT-qPCR in control (Scramble) and miR-708
592 knock-down (AntagomiR-708) cells isolated by FACS 10days post-AntagomiR
593 treatment.

594 (C) mRNA expression assessed by RT-qPCR in control (Scramble) and miR-708
595 knock-down (AntagomiR-708) cells isolated by FACS 10days post-AntagomiR
596 treatment.

597 (D) Representative images of membrane-GFP+ MuSCs from total muscle
598 preparations from control (Scramble) and AntagomiR-708 treated mice plated for 12h
599 and stained for Pax7. Quantification of GFP+/Pax7+ and GFP+/Pax7- cells (≥ 250
600 cells counted, 2wells/condition). Scale bar: 25 μ m

601 (E) Myosin Heavy Chain (MyHC) staining on MuSCs from control (Scramble) and
602 AntagomiR-708 treated mice isolated by FACS and cultured for 5 days. Fusion index
603 of primary myoblasts after 5 days of culture (≥ 500 nuclei counted, 2wells/condition).
604 Scale bar: 50 μ m

605 (F) Immunostaining for Laminin and Pax7 on sections from non-injured TA muscles
606 of mice 10 days post Scramble and AntagomiR-708 treatment. Quantification of
607 Pax7+ cells under the basal lamina and in the interstitial space. Scale bar: 50 μ m and
608 10 μ m in inset.

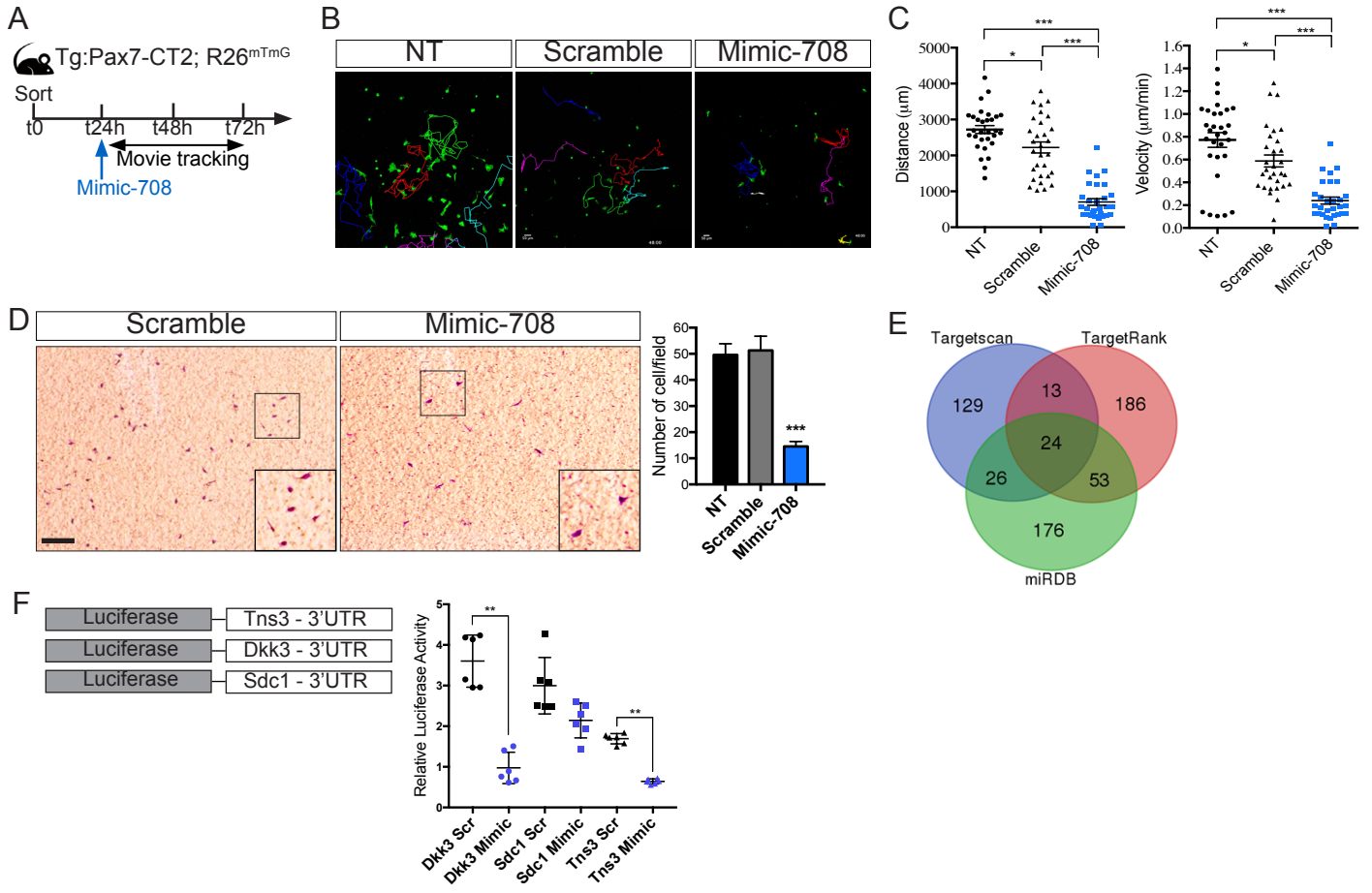
609 (G) membrane-GFP+ MuSCs from FACS isolated cells from control (Scramble) and
610 AntagomiR-708 treated mice, plated for 12h and stained for BrdU. Quantification of
611 mGFP+/BrdU+ cells (≥ 250 cells counted, 2wells/condition). Scale bar: 25 μ m

612 (H) Experimental scheme of tamoxifen, AntagomiR and BrdU administration to
613 *Tg:Pax7-CT2; R26^{mTmG}*. AntagomiR-708 and Scramble control were injected every
614 day for 4 days after the end of tamoxifen treatment (D0) and mice were sacrificed 28
615 days later.

616 (I) Quantification of Pax7+ cells/mm² on TA sections from quiescent muscle of
617 control (Scramble) and AntagomiR-708 treated mice.

618 (J) Immunostaining for Laminin and GFP on sections from TA muscles of mice 28
619 days post-Scramble and AntagomiR-708 treatment. The whole TA section is shown in
620 the inset. Scale bar: 100 μ m and 300 μ m in inset.
621 Error bars indicate SD, * p <0.05, ** p <0.01, *** p <0.001.

Baghdadi_FIGURE 4



622 **Figure 4. miR-708 regulate myogenic cell migration and motility**

623 (A) Experimental scheme of miR-708 overexpression on membrane-GFP purified
624 MuSC from *Tg:Pax7-CT2*; *R26^{mTmG}* mice treated 2 weeks with tamoxifen. 24h after
625 transfection, cells were filmed for 48h.

626 (B) Maximum projection of 48h-time-lapse experiment of mGFP cells overexpressing
627 miR-708 (Mimic-708) and controls (Scramble and Non-Transfected (NT)). Coloured
628 line depicts the trajectory of a cell for every condition.

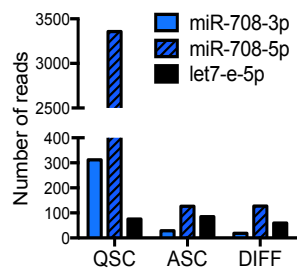
629 (C) Distance (left) and velocity (right) of miR-708 overexpressing cells (Mimic-708)
630 and controls (Scramble and Non-Transfected (NT)) were scored for 48h. (n=30 cells
631 tracked; Mann-Whitney test). See supplementary movies.

632 (D) Migration properties of miR-708-overexpressing satellite cells (Mimic-708) and
633 control measured by Transwell assay (cf Methods). MuSCs isolated by FACS from
634 *Tg:Pax7-nGFP* that migrated through the pores membrane were stained with Crystal
635 Violet and quantified. NT, Non-transfected control (n=4 mice, 2
636 membranes/condition, 3 fields counted/membrane). Scale bar: 100µm and 40µm in
637 inset. ***p<0.001

638 (E) Venn Diagram displays the putative targets of miR-708 as predicted by
639 TargetScan (purple), TargetRank (red) and MiRDB (green). Twenty-four targets were
640 commonly predicted by the three programs (see Figure S4).

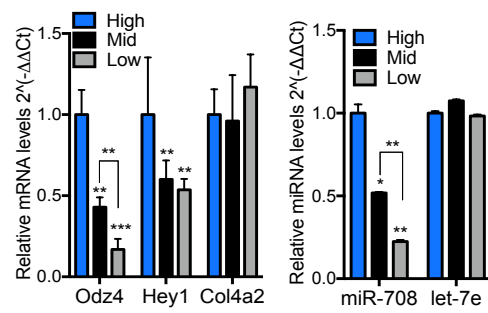
641 (F) Schematic constructs of *Tns3* (Tensin-3), *Dkk3* (Dickkopf-3) and *Sdc1*
642 (Syndecan-1) 3'UTR with the relative luciferase activity associated with each
643 construct in presence (Mimic-708) or absence (Scr: Scramble) of miR-708 (n=6
644 independent experiments, 2wells/conditions). Mann-Whitney statistical test, **p<0.01

A



B

P8 neonatal *Tg:Pax7-nGFP*



645 **SUPPLEMENTARY FIGURE LEGENDS:**

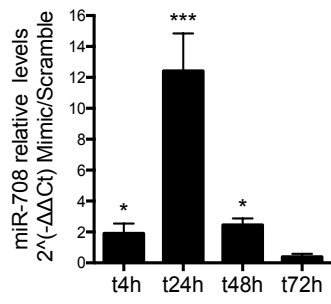
646

647 **Figure S1. Assessment of miR-708 expression in subpopulations of satellite cells.**

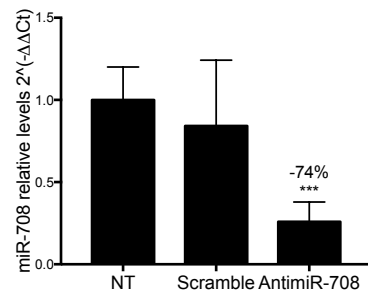
648 (A) micro-RNAs expression in number of reads using RNA deep sequencing on
649 freshly isolated MuSCs (Quiescent Satellite Cell, QSC, n=2), *in vitro* activated
650 satellite cells for 60h (Activated Satellite cells, ASC, n=2) and differentiated cells
651 cultured for 7 days (Differentiated cells, DIFF, n=3).

652 (B) Transcript levels of *Odz4* (left) and miR-708 (right) targeted by Notch in cells
653 fractionated by FACS from *Tg:Pax7-nGFP* 8 days old postnatal pups (P8) where
654 Notch activity gradually decreases from the more committed (high) to the most
655 differentiated population (low)(Mourikis et al., 2012b; Rocheteau et al., 2012):
656 Pax7High 20% of population (blue), Pax7Mid 40% (black) and Pax7Low 20% (grey),
657 (n=3 pups).

A



B



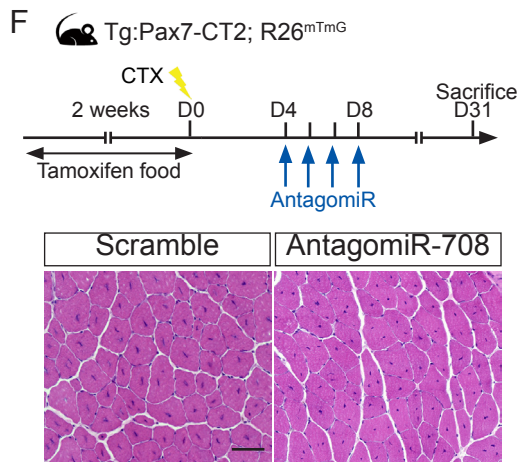
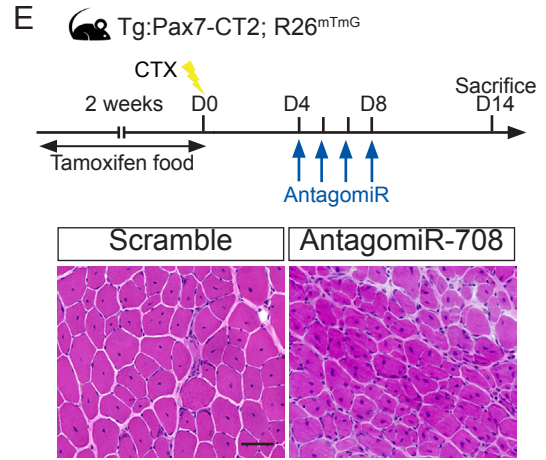
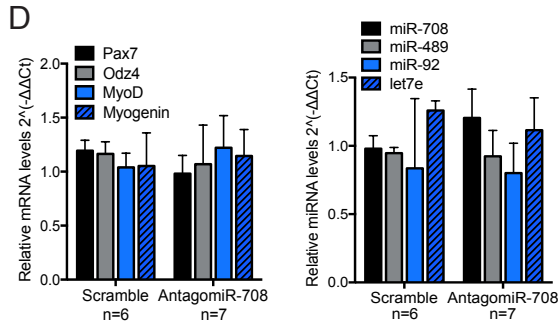
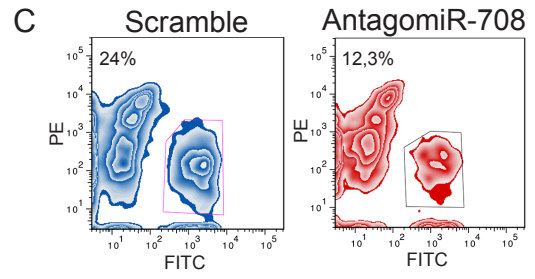
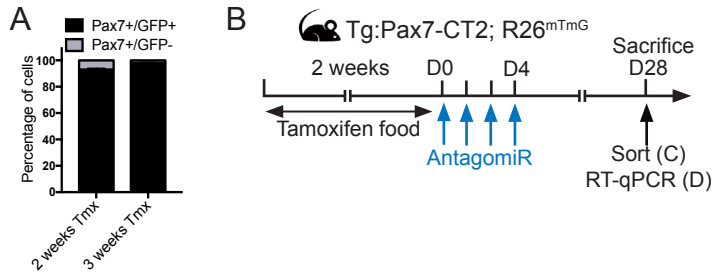
658 **Figure S2. *Ex vivo* gain and loss of function tool validation**

659 (A) RT-qPCR of miR-708 expression 4h, 24h, 48h and 72h after Mimic-708
660 transfection of MuSCs isolated from *Tg:Pax7-nGFP*.

661 (B) Transcript levels of miR-708 in MuSCs isolated from *Tg:Pax7-nGFP* 12h after
662 miR-708 inhibition using AntimiR-708 transfection.

663 Error bars indicate SD; n=3-4 mice. *p<0.05, **p<0.01, ***p<0.001.

Baghdadi_SUPP S3



664 **Figure S3. miR-708 *in vivo* inhibition induces spontaneous differentiation**

665 (A) Recombination efficiency of *Tg:Pax7-CT2; R26^{mTmG}* was assessed by
666 quantification of mGFP+/Pax7+ cells in total muscle preparation of mice fed 2 or 3
667 weeks with tamoxifen food. At 2 and 3 weeks after treatment, 95-97% of MuSC
668 (Pax7+) were recombined (mGFP+).

669 (B) Experimental scheme showing miR-708 *in vivo* knock-down. *Tg:Pax7-*
670 *CT2;R26^{mTmG}* mice were fed with tamoxifen for 2 weeks and injected 4 times with
671 AntagomiR or control Scramble. Satellite cells were purified by FACS from resting
672 muscle 28 days after AntagomiR/Scramble treatment.

673 (C) FACS profiles of mGFP positive cells from resting muscles of control (Scramble)
674 or AntagomiR-708 treated mice showing a decrease in MuSC number 28 days after
675 miR-708 *in vivo* inhibition.

676 (D) RT-qPCR of mGFP-positive cells isolated from resting muscle of Scramble or
677 AntagomiR-708 treated mice after 28 days. Expression of quiescence (*Pax7*, *Odz4*),
678 activation (*Myod*) and differentiation (*Myogenin*) genes is not affected (left);
679 quiescent miR-708, miR-489 and activated miR-92 expressions are also similar in
680 Scramble and AntagomiR-708 treated MuSCs (left).

681 (E) (F) miR-708 *in vivo* knock down induces a delay in muscle regeneration at 14
682 days (E) post injury, but this is no longer observed at 28 days post-injury (E).

683 Experimental scheme of miR-708 *in vivo* knock-down. *Tg:Pax7-CT2; R26^{mTmG}* mice
684 were fed with tamoxifen for 2 weeks. Four days following Cardiotoxin injury (CTX),
685 AntagomiR-708, or Scramble were injected every day for 4 days and injured muscles
686 were collected 14 days (E) or 28 days (F) post-injury. Hematoxylin and eosin staining
687 of transverse sections of regenerating TA muscles 14 days (D) or 28 days (E) post-
688 injury. Scale bar 100µm, n=4 mice/genotype.

Baghdadi_SUPP S4

A

Gene symbol	Gene name
Sdc1	syndecan 1
Tns3	tensin 3
Dkk3	dickkopf homolog 3 (Xenopus laevis)
Nnat	neuronatin
Foxj3	forkhead box J3
Slc44a5	solute carrier family 44, member 5
Mat2a	methionine adenosyltransferase II, alpha
Sp1	trans-acting transcription factor 1
Gpm6a	glycoprotein m6a
En2	engrailed 2
Rpp14	ribonuclease P 14 subunit
Slco3a1	solute carrier organic anion transporter family, member 3a1
Kif3c	kinesin family member 3C
Rap1b	RAS related protein 1b
Amph	amphiphysin
Iqsec2	IQ motif and Sec7 domain 2
Shprh	SNF2 histone linker PHD RING helicase
Amigo1	adhesion molecule with Ig like domain 1
4931406P16Rik	RIKEN cDNA 4931406P16 gene
Ssrp1	structure specific recognition protein 1
Luzp1	leucine zipper protein 1
Etf1	eukaryotic translation termination factor 1
Man2a1	mannosidase 2, alpha 1
Dcc	deleted in colorectal carcinoma

689 **Figure S4. Table listing the 24 putative target genes commonly predicted by**
690 **TargetScan, TargetRank and miRDB (See Figure 4E).** Genes of interest are in
691 bold; *Tns3*, *Dkk3* and *Sdc1* are strongly upregulated following satellite cell activation.

692 **Supplementary tables**

693 **Table 1**

Mouse RT-PCR primer	Sequence (5' > 3')
Odz4_F	GTGGGATGGAGGTTAGCTCG
Odz4_R	ATGGGTTCTACTGCCCAAGTG
Hey1_F	CACCTGAAAATGCTGCACAC
Hey1_R	ATGCTCAGATAACGGGCAAC
HeyL_F	GTCTTGCAGATGACCGTGGA
HeyL_R	CTCGGGCATCAAAGAACCCT
Myod_F	CACTACAGTGGCGACTCAGATGCA
Myod_R	CCTGGACTCGCGCGCCGCTCACT
Myogenin_F	GTGAATGCAACTCCCACAGC
Myogenin_R	CGCGAGCAAATGATCTCCTG
Pax7_F	GACAAAGGGAACCGTCTGGAT
Pax7_R	TATCTTGTGGCGGATGTGGTTA
Col4a2_F	GATACCCGGCGTAATCTCAA
Col4a2_R	ATGAGCACCTTGGAAATCCTG
Rpl13_R	GTGGTCCCTGCTGCTCTCAAG
Rpl13_F	CGATAGTGCATCTTGGCCTTTT
Tbp_F	ATCCCAAGCGATTTGCTG
Tbp_R	CCTGTGCACACCATTTTTCC

694

695 **Table 2**

Antibody	Reference	Dilution
GFP chick polyclonal	Abcam, 13970	1/2000
Myogenin mouse monoclonal	DHSB, F5D	1/40
Myosin Heavy Chain mouse monoclonal	DHSB, MF20	1/40
Pax7 monoclonal mouse	DHSB	1/40
Mouse anti-BrdU	BD, 347580	1/100
Laminin rabbit polyclonal	Sigma, L9393	1/500

696

697 **Table 3:** 3'-UTR of miR-708 predicted target genes. In bold and underlined: miR-708

698 seed sequence

Gene	3'UTR sequence
Dickkopf-3 (Dkk3)	GCCCAGACCCAGCTGAGTCACTGGTAGATGTGCAATAGAAATGGCTAATT TATTTTCCCAGGAGTGTCCCAAGTGTGGAATGGCCGCAGCTCCTTCCCAG TAGCTTTTCCTCTGGCTTGACAAGGTACAGTGCAGTACATTTCTTCCAGCC GCCCTGCTTCTCTGACTTGGGAAAGACAGGCATGGCGGGTAAGGGCAGCG GTGAGTCGTCCCTCGCTGTTGCTAGAAACGCTGTCTTGTTCCTCATGGATG GAAGATTTGTTTGAAGGGAGAGGATGGGAAGGGGTGAAGTCTGCTCATG ATGGATTTGGGGGATACAGGGAGGAGGATGCCTGCCTTGCAGACGTGGAC TTGGCAAATGTAACCTTTGCTTTTGTCTTGCGCCGCTCCCATGGGCTGAG GCAGTGGCTACACAAGAGCTATGCTGCTCTGTGGCCTCCCACATATTCATC CCTGTGTTT <u>AGCTCCT</u> ACCTCACTGTCAGCACAGCCCTTCATAGCCACGC CCCCTCTTGCTCACCACAGCCTAGGAGGGGACCAGAGGGGACTTCTCTCA GAGCCCCATGCTCTCTCTCAACCCCATACCAGCCTCTGTGCCAGCGACA GTCCTTCCAAATGGAGGGAGTCAAATCCTTTGGTTTTATTATTTCTCCTTC AAGGCACGCCTGCCACTAAGGTCAGGCTGACTTGCATGTCCCTCTAACGT TCGTAGCAGTGTGGTGGACACTGTCTTCCACCGACTGCTTCAATACCTCTG

	AAAGCCAGTGCTCGGAGTGCAGTTCGTGTAATTAATTTGCAGGAAGTAT ACTTGGCTAATTGTAGGGCTAGGATTGTGAATGAAATTTGCAAAGTCGCT TAGCAACAATGGAAAGCCTTTCTCAGTCACACCGAGAAGTCACAACCAAG CCAGGTTGTGTAGAGTACAGCTGTGACATACAGACAGAAGAAGGCTGGG CTGGATGTCAGGCCTCAGATGACGGTTTCAGGTGCCAGGAECTATTACCA TTCTGTATCTATCCAGAGTTATTAATAATTGAAAGTTGCACACATTTGTATA AGCATGCCTTTCTCCTGAGTTTTAAATTATATGTATACACAAACATGTGGC CCTCAAAGATCATGCACAAACCACTACTCTTTGCTAATTCTTGGACTTTTC TCTTTGATTTTCAATAAATAACAAATCCCCTTCATGCAAAAAAATTAACA ATCTGTAGTATAAAGAGACAAAAAATTCATAGAAAGCAGATTTTCCAGG CATCTGCAGTTTCCCTCTTTTAGAATCGGAATTCGTTGGAECTCTCATCCTT GTCTGGATGGGAATTAGCTTAAACAGAGAACTACTTCACCCTCTCCTGA AAGAACAATGGAATATATGAGTCTTCTCTTGGAGGCTCTTCCACTCAA ATGCAGTCTGGGGCTGTGCTAGCATTGATACTGTAACAAAACGGCTGAA GCAATGAACTTATATATTTAAAAAGTTAGGTTAATTGGGTTCCACTTTCA GGTTTCAGTCCTGATCCCATGGGGTTGAACTAAGGAGAGGCAGCACAGC GTGGCAAGGGAATGTGGTAGAGTCAAGCTGCTCCCTTCTGGCTAACAGG AGAGTGGGCAATGTGCAGTCTTGTGAGAATGCCAGGTCCTGGGGGAAG GGAGTGCCCTGGACATCACCTTAAAGGTGGAGACTTCTGCAGCTTTGGTTT TAGTTACTCTTCTGGGTGCTACAATCAAACGCCCAACAAGAAGCCACCTG AGGGATGAGGGTTTATTTTGGCTCCTGGTTCAAGCAGGGAGTCTTTCGTG GCAGGAGTGAAGGTTGCTTCCCTGCAGTGTGGAGGATCAGGAAGCAAAG AAAGAGCAATGCAAGACTCAGCTTTCTCTTTTCCCTGATTATTTATTCTG GAACCCCAACCCTTGGGGTGGTGGCCAGCCGAGTAAGAGTGAGTGTCTT TCCTTAGAACCTCTGAAAACCTTGGCCTCATAGAAATGTGCAGAGGTG TGTCACCTAAATTGTTCAAATCCATTCTGTTCCAAGACATGGGAGCGCTAT GTGCTAAGTCTTCCACATAAGAGCACCGAGTACCTCTTAAACGCCTGTAA ATCGCATCTGAAGATACCACAGTAAAGAGATGTAACATTTAGGAAAACA ATAAATGTAAGTGAAGTACC
Syndecan-1 (Sdc1)	TGGGGAAATAGTTCTTTCTCCCCCACAGCCCCTGCCACTCACTAGGCTCC CACTTGCCTCTTCTGTGAAAACTTCAAGCCCTGGCCTCCCCACCCTGGG TCATGTCTCTGCACCCAGGCCCTTCCAGCTGTTCTGCCCCGAGCGTCCC AGGGTGTGCTGGGAAGTATTCCCCTCCTTTGACTTCTGCCTAGAAGCTTG GGTCAAAGGGTTTCTTGCATCTGATCTTTCTACCACAACCACACCTGTCC TCCACTCTTCTGACTTGGTTTCTCCAAATGGGAGGAGACCCAGCTCTGGAC AGAAAGGGGACCCGACTGCTTTGGACCTAGATGGCCTATTGCGGCTGGAG GATCTGAGGACAGGAGAGGGGCTTCGGCTGACCAGCCATAGCACTTACC CATAGAGACCGCTAGGGTTGGCCGTGCTGTGGTGGGGGATGGAGGCCTGA GCTCCTTGGAAATCCACTTTTCAATGTGGGGAGGTCTACTTTAGACAATTG GTTTTGCACATATTTTCTCTAATTTCTCTGTTTCAGAGCCCCAGCAGACCTA TACTGGGGTAAGGCAAGTCTGTTGACTGGTGTCCCTCACCTCGTCTCCCT AATCTACATTCCAGGAGACCGAATCGGGGTTAATAAGACTTTTTTTGTGTTT TTGTTTTGTTTTAACCTAGAAGAACCAAACTGGACGCCAAAACGTAGG CTTAGTTGTGTGTTGTCTCTGAGTTTGTGCGCTCATGCGTACAACAGGGTA TGGACTATCTGTATGGTGTCCCATTTTTGGCGGCCCGTAAGTAGGCTGGCT AGTCCAGGATACTGTGGAATAGCCACCTCTTGACCAGTCATGCCTGTGTG CATGGACTCAGGGCCACGGCCTTGGCCTGGGCCACCGTGACATTGGAAGA GCCTGTGTGAGAACTTACTCGAAGTTCACAGTCTAGGAGTGGAGGGGAGG AGACTGTAGAGTTTTGGGGGAGGGTGGCAAGGGTGCCCAAGCGTCTCCC ACCTTTGGTACCATCTCTAGTCATCCTTCCCTCCCGGAAGTTGACAAGACAC ATCTTGAGTATGGCTGGCACTGGTTCCCTCATCAAGAACCAAGTTCACCTT CAGCTCCT GTGGCCCCGCCCCAGGCTGGAGTCAGAAATGTTTCCCAAAG AGTGAGTCTTTTGTCTTTGGCAAAACGCTACTTAATCCAATGGGTTCTGTA CAGTAGATTTTGCAGATGTAATAAACTTTAATATAAAGGAGTCCTATGAA CTCTACTGCTTCTGCTTCTTCTTCTGACTGGTGGTATAGATATAGCCAC CCTTTGCCCAAACCCTGGTAGCTCGGGGAAGCTTGGCTTAAGGCTGCACG CCTCCAATCCCCAAAGGGTAGGATCCTGGCTGGGTCCAGGGTTCTCTG ATTTATTTGGTTTTGTTGTGTTGTGTTGTGTTTTTCTTTTGGCTAAACTTCT TTGGAAGTTGGTAAGTTCAGCCAAGGTTTTACAGGCCCTGATGTCTGTCT TCTAAATGGTTTAAGTAATTGGGACTCTAGCACATCTTGACCTAGGGTAC

	<p>TAGAGCTAAGCTTGCTTTGCAGGGCAGACACCTGGGACAGCCTTCCTCCC TCATGTTTGCTGGGACACTGCTGAGCACCCCTTGCTTACTTAGCTCAGTGA TGTTCCAGCTCCTGGCTAGGCTGCTCAGCCACTCAGCTAGACAAAAGATC TGTGCCCTGTGTTTCATCCCAGAGCTTGTTGCCAGATCACATGGCTGGATG TGATGTGGGGTGGGGGTGGGGTCATATCTGAGACAGCCCTCAGCTGAGGG CTTGTGGGACAGTGTCCAAGCCTCAGGCTGGGCTCATTCATATAATTGCA ATAA</p>
Tensin-3 (Tns3)	<p>GTCTGTGTGTATACAGGTGGACCATTCCACTTTATGCTCATGTATGTCTGT GTGTATACAGGTGGACCATTCCACTTTTGCTCATGTATGTCTGTGTGTATA CAGGTGGACTATTCCACTTTTTAGCTCCTATTGATGCACCAAAAGCAAGT GCCTCATTCTGTGCCAAATGTTTGCCTTGGTCTTTAAGGACCTCCTTCGTG GACACTCTGATGTGCCTGTTAGAGGGAATGTGCCACCATTCCCTAGAGGC CCCATGTCTTCCACAGAGGCTTCTAGTGTTCAGTTACTCATATGCAGCTA AACTCCAGATGGGGGCAGGGGTGGGGCTGAAGTTGTGCTCTAAGAAGTAT CACATCCTATGATTATAAGTTTATATGCAGATGTGGCCCAGAGATCACAG CCCCGCACTCTTTTCCCTCCCGCTGGAGGGGGGTGGGGGTGGGGGGAGAGG GCCTAATTAGAAACTCAGCTGGGCTCTGCTGAAGCCCAGCTTTCGGTGA ATTGAATGCCACAAAGGTTGGCATGGAATGGCATCCAAGAAGCCACAAC GAATGTGCGTTTCAAACACTGACCGGGAGGGTATGATTCTTACTCCAGGAT ACAAGTCAGTCCAGGGTATCCAGGATCGACTGAGGGAACCCAGGGAGAC CGTCCACATGGTACAAACACTGGGGGCGGCCGGAACGAGGGAAGCGGGT TGACAACACAACGGACTACACACCGGGGCCACACGGACGAATACACAG T</p>

699

700 **REFERENCES**

- 701 Mourikis, P., Sambasivan, R., Castel, D., Rocheteau, P., Bizzarro, V., and Tajbakhsh,
702 S. (2012). A critical requirement for notch signaling in maintenance of the quiescent
703 skeletal muscle stem cell state. *Stem Cells* 30, 243-252.
- 704 Rocheteau, P., Gayraud-Morel, B., Siegl-Cachedenier, I., Blasco, M.A., and
705 Tajbakhsh, S. (2012). A subpopulation of adult skeletal muscle stem cells retains all
706 template DNA strands after cell division. *Cell* 148, 112-125.
- 707 Bentzinger, C.F., von Maltzahn, J., Dumont, N.A., Stark, D.A., Wang, Y.X., Nhan, K.,
708 Frenette, J., Cornelison, D.D., and Rudnicki, M.A. (2014). Wnt7a stimulates
709 myogenic stem cell motility and engraftment resulting in improved muscle
710 strength. *J Cell Biol* 205, 97-111.
- 711 Bjornson, C.R., Cheung, T.H., Liu, L., Tripathi, P.V., Steeper, K.M., and Rando, T.A.
712 (2012). Notch signaling is necessary to maintain quiescence in adult muscle stem
713 cells. *Stem Cells* 30, 232-242.
- 714 Blangy, A. (2017). Tensins are versatile regulators of Rho GTPase signalling and
715 cell adhesion. *Biology of the cell* 109, 115-126.
- 716 Brohl, D., Vasyutina, E., Czajkowski, M.T., Griger, J., Rassek, C., Rahn, H.P.,
717 Purfurst, B., Wende, H., and Birchmeier, C. (2012). Colonization of the satellite
718 cell niche by skeletal muscle progenitor cells depends on Notch signals. *Dev Cell*
719 23, 469-481.
- 720 Castel, D., Mourikis, P., Bartels, S.J., Brinkman, A.B., Tajbakhsh, S., and
721 Stunnenberg, H.G. (2013). Dynamic binding of RBPJ is determined by Notch
722 signaling status. *Genes Dev* 27, 1059-1071.
- 723 Chakkalakal, J.V., Jones, K.M., Basson, M.A., and Brack, A.S. (2012). The aged niche
724 disrupts muscle stem cell quiescence. *Nature* 490, 355-360.
- 725 Cheung, T.H., Quach, N.L., Charville, G.W., Liu, L., Park, L., Edalati, A., Yoo, B.,
726 Hoang, P., and Rando, T.A. (2012). Maintenance of muscle stem-cell quiescence
727 by microRNA-489. *Nature* 482, 524-528.
- 728 Guo, P., Lan, J., Ge, J., Nie, Q., Mao, Q., and Qiu, Y. (2013). miR-708 acts as a tumor
729 suppressor in human glioblastoma cells. *Oncology reports* 30, 870-876.
- 730 Haldar, M., Karan, G., Tvrdik, P., and Capecchi, M.R. (2008). Two cell lineages,
731 myf5 and myf5-independent, participate in mouse skeletal myogenesis. *Dev Cell*
732 14, 437-445.
- 733 Han, H., Tanigaki, K., Yamamoto, N., Kuroda, K., Yoshimoto, M., Nakahata, T.,
734 Ikuta, K., and Honjo, T. (2002). Inducible gene knockout of transcription factor
735 recombination signal binding protein-J reveals its essential role in T versus B
736 lineage decision. *Int Immunol* 14, 637-645.
- 737 Jarriault, S., Brou, C., Logeat, F., Schroeter, E.H., Kopan, R., and Israel, A. (1995).
738 Signalling downstream of activated mammalian Notch. *Nature* 377, 355-358.
- 739 Kopan, R., and Ilagan, M.X. (2009). The canonical Notch signaling pathway:
740 unfolding the activation mechanism. *Cell* 137, 216-233.
- 741 Krutzfeldt, J., Rajewsky, N., Braich, R., Rajeev, K.G., Tuschl, T., Manoharan, M., and
742 Stoffel, M. (2005). Silencing of microRNAs in vivo with 'antagomirs'. *Nature* 438,
743 685-689.
- 744 Lin, K.T., Yeh, Y.M., Chuang, C.M., Yang, S.Y., Chang, J.W., Sun, S.P., Wang, Y.S.,
745 Chao, K.C., and Wang, L.H. (2015). Glucocorticoids mediate induction of
746 microRNA-708 to suppress ovarian cancer metastasis through targeting Rap1B.
747 *Nature communications* 6, 5917.

748 Liu, L., Cheung, T.H., Charville, G.W., Hurgo, B.M., Leavitt, T., Shih, J., Brunet, A.,
749 and Rando, T.A. (2013). Chromatin modifications as determinants of muscle stem
750 cell quiescence and chronological aging. *Cell reports* 4, 189-204.
751 Livak, K.J., and Schmittgen, T.D. (2001). Analysis of relative gene expression data
752 using real-time quantitative PCR and the 2(-Delta Delta C(T)) Method. *Methods*
753 25, 402-408.
754 Lodygin, D., Epanchintsev, A., Menssen, A., Diebold, J., and Hermeking, H. (2005).
755 Functional epigenomics identifies genes frequently silenced in prostate cancer.
756 *Cancer research* 65, 4218-4227.
757 Mauro, A. (1961). Satellite cell of skeletal muscle fibers. *The Journal of*
758 *biophysical and biochemical cytology* 9, 493-495.
759 Motohashi, N., and Asakura, A. (2014). Muscle satellite cell heterogeneity and
760 self-renewal. *Frontiers in cell and developmental biology* 2, 1.
761 Mourikis, P., Gopalakrishnan, S., Sambasivan, R., and Tajbakhsh, S. (2012a). Cell-
762 autonomous Notch activity maintains the temporal specification potential of
763 skeletal muscle stem cells. *Development* 139, 4536-4548.
764 Mourikis, P., Sambasivan, R., Castel, D., Rocheteau, P., Bizzarro, V., and Tajbakhsh,
765 S. (2012b). A critical requirement for notch signaling in maintenance of the
766 quiescent skeletal muscle stem cell state. *Stem Cells* 30, 243-252.
767 Murtaugh, L.C., Stanger, B.Z., Kwan, K.M., and Melton, D.A. (2003). Notch
768 signaling controls multiple steps of pancreatic differentiation. *Proc Natl Acad Sci*
769 *U S A* 100, 14920-14925.
770 Muzumdar, M.D., Tasic, B., Miyamichi, K., Li, L., and Luo, L. (2007). A global
771 double-fluorescent Cre reporter mouse. *Genesis* 45, 593-605.
772 Niehrs, C. (2006). Function and biological roles of the Dickkopf family of Wnt
773 modulators. *Oncogene* 25, 7469-7481.
774 Pinho, S., and Niehrs, C. (2007). Dkk3 is required for TGF-beta signaling during
775 *Xenopus* mesoderm induction. *Differentiation; research in biological diversity*
776 75, 957-967.
777 Rathbone, C.R., Yamanouchi, K., Chen, X.K., Nevoret-Bell, C.J., Rhoads, R.P., and
778 Allen, R.E. (2011). Effects of transforming growth factor-beta (TGF-beta1) on
779 satellite cell activation and survival during oxidative stress. *Journal of muscle*
780 *research and cell motility* 32, 99-109.
781 Rocheteau, P., Gayraud-Morel, B., Siegl-Cachedenier, I., Blasco, M.A., and
782 Tajbakhsh, S. (2012). A subpopulation of adult skeletal muscle stem cells retains
783 all template DNA strands after cell division. *Cell* 148, 112-125.
784 Romero, D., Kawano, Y., Bengoa, N., Walker, M.M., Maltry, N., Niehrs, C., Waxman,
785 J., and Kypta, R. (2013). Downregulation of Dickkopf-3 disrupts prostate acinar
786 morphogenesis through TGF-beta/Smad signalling. *J Cell Sci* 126, 1858-1867.
787 Ryu, S., McDonnell, K., Choi, H., Gao, D., Hahn, M., Joshi, N., Park, S.M., Catena, R.,
788 Do, Y., Brazin, J., *et al.* (2013). Suppression of miRNA-708 by polycomb group
789 promotes metastases by calcium-induced cell migration. *Cancer cell* 23, 63-76.
790 Saini, S., Majid, S., Shahryari, V., Arora, S., Yamamura, S., Chang, I., Zaman, M.S.,
791 Deng, G., Tanaka, Y., and Dahiya, R. (2012). miRNA-708 control of CD44(+)
792 prostate cancer-initiating cells. *Cancer research* 72, 3618-3630.
793 Saini, S., Yamamura, S., Majid, S., Shahryari, V., Hirata, H., Tanaka, Y., and Dahiya,
794 R. (2011). MicroRNA-708 induces apoptosis and suppresses tumorigenicity in
795 renal cancer cells. *Cancer research* 71, 6208-6219.

796 Sakaue-Sawano, A., Kurokawa, H., Morimura, T., Hanyu, A., Hama, H., Osawa, H.,
797 Kashiwagi, S., Fukami, K., Miyata, T., Miyoshi, H., *et al.* (2008). Visualizing
798 spatiotemporal dynamics of multicellular cell-cycle progression. *Cell* 132, 487-
799 498.

800 Sambasivan, R., Gayraud-Morel, B., Dumas, G., Cimper, C., Paisant, S., Kelly, R.G.,
801 and Tajbakhsh, S. (2009). Distinct regulatory cascades govern extraocular and
802 pharyngeal arch muscle progenitor cell fates. *Dev Cell* 16, 810-821.

803 Seale, P., Sabourin, L.A., Girgis-Gabardo, A., Mansouri, A., Gruss, P., and Rudnicki,
804 M.A. (2000). Pax7 is required for the specification of myogenic satellite cells. *Cell*
805 102, 777-786.

806 Shinin, V., Gayraud-Morel, B., Gomes, D., and Tajbakhsh, S. (2006). Asymmetric
807 division and cosegregation of template DNA strands in adult muscle satellite
808 cells. *Nat Cell Biol* 8, 677-687.

809 Siegel, A.L., Atchison, K., Fisher, K.E., Davis, G.E., and Cornelison, D.D. (2009). 3D
810 timelapse analysis of muscle satellite cell motility. *Stem Cells* 27, 2527-2538.

811 Yablonka-Reuveni, Z., Seger, R., and Rivera, A.J. (1999). Fibroblast growth factor
812 promotes recruitment of skeletal muscle satellite cells in young and old rats. *The*
813 *journal of histochemistry and cytochemistry : official journal of the*
814 *Histochemistry Society* 47, 23-42.

815 Yamaguchi, M., Ogawa, R., Watanabe, Y., Uezumi, A., Miyagoe-Suzuki, Y.,
816 Tsujikawa, K., Yamamoto, H., Takeda, S., and Fukada, S. (2012). Calcitonin
817 receptor and *Odz4* are differently expressed in Pax7-positive cells during
818 skeletal muscle regeneration. *Journal of molecular histology* 43, 581-587.

819 Yao, S. (2016). MicroRNA biogenesis and their functions in regulating stem cell
820 potency and differentiation. *Biological procedures online* 18, 8.

821 Zammit, P.S., Golding, J.P., Nagata, Y., Hudon, V., Partridge, T.A., and Beauchamp,
822 J.R. (2004). Muscle satellite cells adopt divergent fates: a mechanism for self-
823 renewal? *J Cell Biol* 166, 347-357.

824

CONCLUSIONS AND PERSPECTIVES

1. Context of this thesis project

We and others have reported that Notch signalling is critical for the maintenance of MuSCs, as ablation of *Rbpj* results in the spontaneous differentiation and eventual depletion of the stem cell pool (Bjornson et al., 2012; Mourikis et al., 2012b). Nuclear NICD has been shown to antagonize myogenesis by the induction of transcriptional repressors (Hes/Hey family members) and the sequestration of Mastermind-like 1 that acts as a co-activator of the muscle differentiation factor Mef2c (Buas et al.; Shen et al., 2006). However, the function of Notch signalling in MuSCs appears to be broader and the role of Notch beyond the largely known targets Hes/Hey remains largely unknown. To uncover putative parallel pathways by which Notch signalling controls MuSCs, ChIP-seq screening was performed in myogenic cells for direct transcriptional targets of the major effector of all Notch receptors, RBPJ (Castel et al., 2013). Interestingly, an enrichment of RBPJ-bound enhancers was observed close to genes encoding ECM components and specifically different collagen types. In a first report, we describe a MuSC self-sustained signalling cascade, orchestrated by the Notch pathway and propagated by the ECM of the immediate stem cell niche.

In another study, the quiescent-specific micro-RNA, miR-708, was found to be a Notch pathway target gene, suggesting an additional role for Notch in the post-transcriptional regulation of quiescence.

Here, we unravelled two cell-autonomous mechanisms by which Notch can maintain quiescence: the regulation of specific ECM components and the inhibition of the migration via a specific micro-RNA. Both machineries converge to sustain adhesion and anchor MuSCs within their niche to sustain the stem cell pool.

However, the disruption of the downstream target of Notch signalling, *Col5a1* or miR-708 could not recapitulate all aspects of the *Rbpj* null phenotype observed in satellite cells suggesting that the lack of a clear mechanistic model for the effect of Notch signalling on myogenesis is mediated by multiple, compensatory pathways.

2. Notch signalling regulates ECM niche components

Satellite cells are intimately linked to, and regulated by their surrounding microenvironment. Isolation from their niche invariably leads to cell cycle entry and/or differentiation, thereby compromising their regenerative capacity (Montarras et al., 2005). Understanding the genetic circuits and active molecules that assemble the stem cell niche is of wide biological interest, and also fundamental for medical applications in the context of cell-based therapies. Expression studies in diverse tissues showed that stem cells express high levels of ECM molecules, favouring the idea of a cell-autonomous contribution to their niche (Ahmed and French-Constant, 2016; Kazanis et al., 2010; Kokovay et al., 2012). Indeed, quiescent cells tend to express higher levels of ECM-related molecules compared to their proliferating counterparts, suggesting that the ECM composition is a signature of quiescence and critical for niche stability. When cultured neural stem cells were forced to enter into quiescence, ECM proteins and receptors together with cell adhesion molecules were significantly upregulated (Martynoga et al., 2013). Similarly, in the epidermis, several ECM genes were found to be upregulated in the hair follicle bulge stem cells relative to other basal keratinocytes. These included the integrin $\alpha 8\beta 1$ ligand nephronectin that provides a niche for smooth muscle cells (Fujiwara et al., 2011). Notably, amongst the 17 ECM upregulated genes described in that study, six were collagens (*Col1a2*, *Col4a2*, *Col5a2*, *Col6a1*, *Col6a2*, and *Col18a1*).

In skeletal muscle, Collagen VI has drawn much attention as mutations in the *Col6a1*, *Col6a2* and *Col6a3* genes cause a certain class of muscle disorders, from the mildest Bethlem myopathy to the most severe Ullrich congenital muscular dystrophy (Allamand et al., 2011). Non-fibrillar COLVI forms a network of microfilaments in the basement membrane of the connective tissue that ensheaths each individual muscle fibre (Bonnemann, 2011) and it is important in maintaining muscle integrity. Moreover, careful analysis of germline *Col6a1*^{-/-} mice demonstrated that collagen VI indirectly regulates satellite cell self-renewal during muscle regeneration by decreasing muscle stiffness from 18 to 12kPa in injured muscle (Urciuolo et al., 2013). Consistently, the decrease of stiffness in resting muscle *Col6a1*^{-/-} from 12 to 7 kPa resulted in a slight increase in the number of proliferating and apoptotic Pax7⁺ cells, as well as the number of centrally nucleated fibres (over 6-fold more in EDL muscle)

(Urciuolo et al., 2013). These features are a signature of disturbed homeostasis of quiescent MuSCs and suggest that collagen VI could be participating in the quiescent niche.

The principal source of collagens in skeletal muscle is the interstitial fibroblasts (Zou et al., 2008), however, it is unclear what is the primary cellular source of collagen that acts on resting MuSCs, or proliferating myoblasts during regeneration. Interestingly, only the transplantation of WT fibroblasts in *Col6a1*^{-/-} muscles could restore muscle stiffness and thus rescuing satellite cell self-renewal defect in absence of COLVI (Urciuolo et al., 2013). In the satellite cells specific *Col5a1* mutant examined here (*Pax7*^{CreERT2/+}; *Col5a1*^{flox/flox}), the premature exit from quiescence and differentiation observed could not be rescued by the COLV produced by the muscle resident fibroblasts. This observation suggests that the COLV synthesized by MuSCs seem to be necessary for their maintenance by triggering the downstream CALCR/cAMP pathway.

One possibility to explain this phenotype would be the accessibility to the fibroblasts-produced COLV to the MuSCs; as mentioned previously, MuSCs are isolated under the basal lamina and are physically separated from the reticular lamina where fibroblasts and collagens are usually located. Another possibility is that the isoform types produced by fibroblasts and MuSCs respectively might not compensate fully. COLV is encountered in most tissues as an $\alpha1(V)_2\alpha2(V)$ isoform and the $\alpha3(V)$ -containing isoform appears to have more specialized functions as its tissue distribution is more restricted (Huang et al., 2011). Our siRNA experiments on single isolated muscle fibres showed that acute knock-down of either *Col5a1* or *Col5a3* had an effect of the same magnitude on MuSCs, suggesting that the effect resides in the $\alpha1(V)\alpha2(V)\alpha3(V)$, the only $\alpha3(V)$ -containing isoform. Moreover, in support of a putative involvement of this collagen isoform on cellular quiescence, the $\alpha1(V)\alpha2(V)\alpha3(V)$ heterotrimer can inhibit cell cycle progression of epithelial cells (mink lung Mv1Lu cells) and primary human keratinocytes (Parekh et al., 1998). Germline *Col5a3* knock-out mice are fertile and viable, but they have a decreased number of pancreatic islets and are glucose intolerant, insulin-resistant, and hyperglycemic (Huang et al., 2011). Their skeletal muscle is defective in glucose

uptake and mobilization of the glucose transporter GLUT4 to the plasma membrane in response to insulin, yet no MuSC phenotype has been reported (Huang et al., 2011). We analysed muscles of conditional *Col5a3* knockout mice at perinatal and adult stages, but could not detect an obvious phenotype in the establishment of satellite cells and behaviour during homeostasis and activation (muscle samples were kindly provided from the Greenspan lab). These results might reveal phenotypes that are compensatory during development in germline COL5A3 mutant mice. The analysis of *Pax7^{CreERT2/+}; Col5a3^{flx/flx}* mice would be an important *in vivo* experiment to assess whether *Col5a3* is necessary for the function of COLV in MuSCs; unfortunately the *Col5a3^{flx}* mouse model currently not available.

Here we identify Collagen V, as a major regulator of MuSC quiescence. Heterozygous mutation of *Col5a1* induces EDS, and although no information available on the status of MuSCs in EDS patients, our data in the mouse suggest that one copy of *Col5a1* is sufficient to sustain MuSCs. In the *Pax7^{CreERT2/+}; Col5a1^{flx/flx}* mouse model described here, all three COLV isoforms are affected, hence, the loss of quiescent MuSCs could be a result of a combinatorial effect.

During development, Notch signalling controls the assembly of the basal lamina around emerging satellite cells, and promotes the sustained adhesion between satellite cells and myofibers (Brohl et al., 2012). Thus, it would be interesting to assess the role of COLV in the stabilization of future satellite cells in the developing muscles and to define of the Notch/COLV/ CALCR axis that we defined in the adult is conserved in embryos.

Therefore, to understand the contribution of stem cell to the niche, it is essential to reconsider the role of collagens as signalling molecules rather than exclusively as structural components, and to explore other types of collagen-binding receptors.

3. Notch signalling positions MuSCs in their niche

To assess the specific role of miRNAs in adult myogenesis, we performed a RNA deep sequencing in quiescent, activated and differentiated satellite cells (David

Castel et al., manuscript in preparation). To date, only a few miRNAs have been proposed to regulate quiescence; among those, miR-489 expression was also found to be quiescent-specific in our RNA sequencing set of data. However, miR-31 expression could not be detected in quiescent cells but rather observed in activation and differentiation. miR-31 was proposed to sequester *Myf5* mRNA in mRNP granules to ensure their silencing. Upon activation, mRNP granules dissociate, releasing *Myf5* transcripts, followed by rapid translation to promote myogenesis (Crist et al., 2012). The discrepancies in results could be due to the cellular origin used in both studies: we used the *Tg:Pax7-nGFP* mouse to isolate all satellite cells and their progeny from all limb muscles. In contrast, Crist and colleagues isolated cells from *Pax3^{GFP/+}*; a mouse model carrying one knock-out allele of *Pax3* induced by the insertion of the GFP. In addition, *Pax3* expression is restricted to a subset of trunk and forelimb muscles (Relaix et al., 2005).

Similarly, miR-195/497 is specifically expressed in quiescence according to our RNA-seq. A recent microarray-based study highlights the role of miR-195/497 in the juvenile to adult transition MuSCs by targeting cell-cycle progression genes (Sato et al., 2014). However, Sato and colleagues isolated cells from the diaphragms of *Pax3^{GFP/+}*; *Myod^{Cre}*; *R26^{RFP/+}* mice, where cells originate from the lateral lip of embryonic dermomyotome. Thus, the role of miR195/497 in regulating cell cycle arrest remains to be verified in other somites-derived quiescent satellite cells. Taken together, these studies showed that the role of miRNAs in quiescence regulation remain largely unknown.

We found identified miR-708, a mirtron in *Odz4*, to be induced by Notch signalling in quiescent MuSCs and absent from activated cells. miR-708 has been found to inhibit migration properties maintaining the stem cell in its quiescent niche. Upon inhibition of miR-708 *in vivo*, satellite cells spontaneously exit quiescence, proliferate and fuse with the pre-existing fibre in the absence of induced muscle injury. However, about half of the satellite cells did not respond to miR-708 knock-down, and they remained properly located in their niche, expressing normal levels of quiescence and activation genes. Whether those cells were spared because of AntagomiR-708 accessibility issues, or because they are not under miR-708

regulation, is not clear. Single-cell analysis for miRNA expression, and miR-708 in particular, would be informative to address the questions.

The *in silico* analysis of potential miR-708 target genes identified 3 putative candidates: *Dkk3*, *Sdc1* and *Tns3*. Although, we validated *Dkk3* as a target gene, we cannot exclude the possibility that *Tns3* is also regulated by miR-708. Interestingly, it is likely that the role of *Dkk3* in regulating both TGF β /Smad pathway and FGF-MAPK signalling (Lodygin et al., 2005; Pinho and Niehrs, 2007) could converge toward one single goal: inhibition of migration. Similarly, *Tns3* is a member of focal adhesion (FA)-associated proteins that constitute important regulators of cell adhesion and migration by association with multiple types of adhesion structures such as FA or podosomes. Tensins have been shown to regulate actin dynamics by modulation of Rho GTPase signalling pathways (Blangy, 2017). As *Tns3*-3'UTR has not been tested yet, we cannot exclude the possibility of a combinatory inhibition of *Tns3* in addition to *Dkk3* by miR-708 to converge toward one common function: the global inhibition of cell migration.

Interestingly, miR-489 is also a mirtron located in the *Calcr* quiescence-specific gene. miR-489 has been shown to inhibit the oncogene *Dek* thereby regulating satellite cell activation (Cheung et al., 2012). In light of the role of these mirtrons in regulating quiescence, it would be of a interest to assess whether other miRNAs are “hidden” in additional quiescence specific genes, and if so, whether they potentially regulate quiescence as well.

Both COLV and miR-708 are Notch-induced genes and most likely act simultaneously to anchor the MuSC in its niche, protecting it from escaping quiescence. Such mechanisms show the requirement for active and cell-autonomous regulators for maintenance of stemness. It would be of a interest to assess how Notch signalling regulates the niche in stem cells in other tissues.

4. Potential regulation of Notch signalling by microRNAs

Notch signalling is downregulated within a few hours following activation ((Mourikis et al., 2012b), Mourikis P, personal communication), suggesting that Notch inhibition could potentially be triggered by miRNAs. To explore this hypothesis, we performed an *in silico* screen for all 3'UTRs of Notch pathway genes to assess potential regulation by miRNAs. Interestingly, we found that miR-17_92 family has highly conserved potential binding sites on several effectors of Notch signalling (Notch1, Adam, Rbpj and Maml1). The miR17_92 polycistronic cluster encodes for six individual miRNAs (miR-17, miR-18a, miR-19a, miR-20a, miR-19b-1 and miR-92a)(Concepcion et al., 2012). The organization and sequences of the miR17_92 cluster is highly conserved among vertebrates and has two paralogues in mammals: the miR-160b_25 and the miR-106a_363 cluster (Concepcion et al., 2012). Interestingly, in the RNA-seq screen described before, we found that miR-17_92 and miR-160b_25 clusters are specifically expressed during satellite cells activation (Castel D, manuscript in preparation), while miR-106a_363 cluster is not expressed in satellite cells. In addition, similarly to the rapid downregulation of Notch, miR-17_92 cluster is highly upregulated a few hours upon satellite cells activation (Mourikis P, personal communication). This observation reinforces our hypothesis that this specific cluster of miRNAs might target Notch for inhibition inducing cell activation. To study the specific involvement of miR-17_92 cluster in satellite cell behaviour, we have crossed a miR-17_92^{flox} (referred to as Mirc1^{flox} (Ventura et al., 2008), stock #008459) with a specific Cre-driver expressed in satellite cells (Pax7^{CreERT2}; (Murphy et al., 2011)). So far, we validated the specific deletion in satellite cells upon tamoxifen treatment, and experiments to examine the resulting phenotypes are ongoing.

ANNEX 1: Review

Regulation and phylogeny of muscle
regeneration

Developmental Biology, in press



Contents lists available at ScienceDirect

Developmental Biology

journal homepage: www.elsevier.com/locate/developmentalbiology

Review article

Regulation and phylogeny of skeletal muscle regeneration

Meryem B. Baghdadi^{a,b,c}, Shahrugim Tajbakhsh^{a,b,*}^a *Stem Cells and Development, CNRS URA 3738, Department of Developmental & Stem Cell Biology, Institut Pasteur, 25 rue du Dr. Roux, 75015 Paris, France*^b *CNRS UMR 3738, Institut Pasteur, Paris 75015, France*^c *Sorbonne Universités, UPMC, University of Paris 06, IFD-ED 515, 4 Place Jussieu, Paris 75252, France*

ARTICLE INFO

Keywords:

Skeletal muscle
Regeneration
Stem cells
Evolution
Quiescence
Injury

ABSTRACT

One of the most fascinating questions in regenerative biology is why some animals can regenerate injured structures while others cannot. Skeletal muscle has a remarkable capacity to regenerate even after repeated traumas, yet limited information is available on muscle repair mechanisms and how they have evolved. For decades, the main focus in the study of muscle regeneration was on muscle stem cells, however, their interaction with their progeny and stromal cells is only starting to emerge, and this is crucial for successful repair and re-establishment of homeostasis after injury. In addition, numerous murine injury models are used to investigate the regeneration process, and some can lead to discrepancies in observed phenotypes. This review addresses these issues and provides an overview of the some of the main regulatory cellular and molecular players involved in skeletal muscle repair.

1. Introduction

The ability to regenerate tissues and structures is a prevalent feature of metazoans although there is significant variability among species ranging from limited regeneration of a tissue (birds and mammals) to regeneration involving the entire organism (cnidarians, planarians, hydra). The intriguing evolutionary loss of regenerative capacity in more complex organisms highlights the importance of identifying the underlying mechanisms responsible for these diverse regenerative strategies. One of the most studied tissues that contributes to new appendage formation is skeletal muscle, thereby making it a major focus of regeneration studies during evolution. The emergence of new lineage-tracing tools in different animal models has permitted the identification of specific progenitor cell populations and their contribution to tissue repair.

Skeletal muscles allow voluntary movement and they play a key role in regulating metabolism and homeostasis in the organism. In mice and humans this tissue represents about 30–40% of the total body mass. This tissue provides an excellent tractable model to study regenerative myogenesis and the relative roles of stem and stromal cells following a single, or repeated rounds of injury. Although muscle regeneration relies mainly on its resident muscle stem (satellite) cells (MuSCs) to effect muscle repair, interactions with neighbouring stromal cells, by direct contact or via the release of soluble factors, is essential to restore proper function. Each step of the myogenic process is regulated by specific regulatory factors including extrinsic cues, yet

the nature and source of these signals remain unclear. This review will address these issues and discuss the different experimental models used to investigate the regenerative process.

2. Prenatal and postnatal skeletal muscle development

In amniotes, skeletal muscles in the limbs and trunk arise from somites through a series of successive waves that include embryonic and foetal phases of myoblast production (Biressi et al., 2007; Comai and Tajbakhsh, 2014). In response to key transcription factors, committed embryonic and foetal myoblasts align and fuse to generate small multinucleated myofibres during primary myogenesis in the embryo (from E11–E14.5), then myofibres containing hundreds of myonuclei during secondary myogenesis (from E14.5–to birth). During the early and late perinatal period that lasts about 4 weeks, continued myoblast fusion, or hyperplasia, is followed by muscle hypertrophy (Sambasivan and Tajbakhsh, 2007; Tajbakhsh, 2009; White et al., 2010). During adulthood, skeletal muscle is associated with little proliferative activity and generally returns to homeostasis about 1 month following injury.

Emerging MuSCs are found underneath a basement membrane from about 2 days before birth in mice and they continue to proliferate until mid-perinatal stages. The majority of quiescent MuSCs are established from about 2–4 weeks after birth (Tajbakhsh, 2009; White et al., 2010). During prenatal and postnatal myogenesis, stem cell self-renewal and commitment are governed by a gene regulatory

* Corresponding author at: Stem Cells and Development, CNRS URA 3738, Department of Developmental & Stem Cell Biology, Institut Pasteur, 25 rue du Dr. Roux, 75015 Paris, France.

<http://dx.doi.org/10.1016/j.ydbio.2017.07.026>

Received 13 June 2017; Received in revised form 30 July 2017; Accepted 31 July 2017
0012-1606/ © 2017 Elsevier Inc. All rights reserved.

network that includes the paired/homeodomain transcription factors Pax3 and Pax7, and basic helix-loop-helix (bHLH) myogenic regulatory factors (MRFs), Myf5, Mrf4, Myod and Myogenin. Pax3 plays a critical role in establishing MuSCs during embryonic development (except in cranial-derived muscles) and Pax7 during late foetal and perinatal growth. Indeed, Pax3: Pax7 double mutant mice exhibit severe hypoplasia due to a loss of stem and progenitor cells from mid embryonic stages, and these Pax genes appear to regulate apoptosis (Relaix et al., 2006, 2005; Sambasivan et al., 2009). During perinatal growth, Pax7 null mice are deficient in the number of MuSCs and fail to regenerate muscle after injury in adult mice (Lepper et al., 2009; Oustanina et al., 2004; Seale et al., 2000; von Maltzahn et al., 2013). The absolute requirement for MuSCs was shown by genetic elimination of satellite cells postnatally, which resulted in failed regeneration (Lepper et al., 2011; Murphy et al., 2011; Sambasivan et al., 2011).

The MRFs bind to consensus sites located in regulatory sequences of target genes to activate muscle-specific gene expression. Experiments using simple or double knockout mice have shown the temporal and functional roles of these different factors during myogenesis. Myf5, Mrf4 and Myod assign myogenic cell fate of muscle progenitor cells to give rise to myoblasts (Kassar-Duchossoy et al., 2004; Rudnicki et al., 1993; Tajbakhsh et al., 1996) whereas Myogenin plays a crucial role in myoblast differentiation prenatally (Hasty et al., 1993) but not postnatally as the conditional mutation of Myogenin in the adult has a relatively mild phenotype (Knapp et al., 2006; Meadows et al., 2008; Venuti et al., 1995). In the adult, Myod deficient mice that survive have increased precursor cell numbers accompanied by a delay in regeneration (Megeney et al., 1996; White et al., 2000); whereas Myf5 null mice showed a slight delay in repair (Gayraud-Morel et al., 2007). These studies suggested that Myf5, Mrf4 and Myod could in some cases have compensatory roles, but that robust regeneration requires all three MRFs. Interestingly, additional transcription factors have been shown to interact with MYOD to regulate myogenesis. For instance, ChIP-seq data demonstrated that KLF5 (Kruppel-like factor, member of a subfamily of zinc-finger transcription factors) (Hayashi et al., 2016) as well as RUNX1 (Umansky et al., 2015) binding to Myod-regulated enhancers is necessary to activate a set of myogenic differentiation genes. It is likely MRFs combined with other transcription factors fine-tune the myogenesis process and it would be important to explore further the set of co-activators/repressors required for each step of muscle repair.

3. Crucial regulators of muscle regeneration

Genetic compensatory mechanisms and MuSC heterogeneity highlight the complexity of the regulatory network governing each phase of prenatal and postnatal myogenesis. Notably, some regulators have been identified as essential for MuSCs behaviour and by consequence also for muscle regeneration. Pax7 is one critical postnatal regulator as its depletion (Pax7^{-/-}) results in a progressive loss of satellite cells during homeostasis and following injury (Gunther et al., 2013; Seale et al., 2000; von Maltzahn et al., 2013). This finding also typifies the relatively long lag in observed phenotypes during homeostasis following removal of a critical regulator, compared to proliferating myogenic cells.

The Notch signalling pathway is another crucial regulator of satellite cells as the specific depletion of RBPJ, the DNA binding factor essential for mediating canonical Notch signalling, induces a spontaneous differentiation and a loss of MuSCs during quiescence, and following injury (Bjornson et al., 2012; Mourikis et al., 2012). Notch receptors are expressed at the cell surface and its ligands, Delta-like ligand (Dll1, 4) and Jagged (JAG1, 2) are presumably provided by the myofibre. Binding of ligand to the receptor results in cleavage of Notch (ADAM and γ -Secretase proteases), and release of Notch IntraCellular Domain (NICD) to the nucleus where it binds RBPJ to activate immediate target genes, notably the transcription factors HeyL, Hes1

and Hesr1/3 (Castel et al., 2013; Jarriault et al., 1995; Kopan and Ilagan, 2009). Intriguingly, the double Hesr1 and Hesr3 knock-out triggers a progressive loss of MuSCs (< 20% in 20weeks) similar to RBPJ depletion (Fukada et al., 2011) whereas the absence of Notch3 receptor (Notch3^{-/-}) results in an increase in satellite cell number (+ 140% in 4months) (Kitamoto and Hanaoka, 2010). Surprisingly, over-expression of NICD in MuSCs induces a fate switch from myogenic to brown adipogenic lineage (Pax7^{CT2/+}; R26^{stop-NICD}), while it rescues the loss of satellite cells in adult Pax7-deficient mice (Pax7^{CT2/flox}; R26^{stop-NICD}) (Pasut et al., 2016). In addition, aged (Tg: MCK-Cre; R26^{stop-NICD}) and dystrophic mice (Tg: MCK-Cre; R26^{stop-NICD}; mdx) that experienced NICD specifically in myofibres improve muscle function and repair (Bi et al., 2016).

Several studies have shown that activation of the expression of a set of evolutionary conserved microRNAs (miRNAs) that function as post-transcriptional regulators, results in precise cellular responses in developmental, physiological, and pathological conditions (Williams et al., 2009). miRNAs are a class of endogenous, single-stranded, non-coding RNAs of about 20–23 nucleotides in length that bind to the 3' untranslated region (3'UTR) of their target mRNAs, resulting in either inhibition of protein translation or degradation of the targeted messenger RNA (mRNA) (Bartel, 2004). miRNAs are transcribed as double-stranded primary miRNA that is cleaved by Drosha (endonuclease) into a pre-miRNA. After nuclear export, Dicer (endonuclease) generates the mature miRNA that is incorporated into the RISC complex (Bartel, 2004; Finnegan and Pasquinelli, 2013; Pasquinelli, 2012). Profiling of whole *Tibialis anterior* (TA) muscle and MuSCs by small RNA-seq identified dynamic expression of specific miRNAs characterizing muscle regeneration (Aguilar et al., 2016) (Castel et al. submitted). The essential role of miRNAs in skeletal muscle regeneration has been demonstrated by conditional deletion of *Dicer* in Pax7+ cells resulting in their depletion (< 20%) and a quasi-absence of repair following injury (Cheung et al., 2012). Although numerous miRNAs have been reported to regulate myoblast proliferation and differentiation (Kirby et al., 2015), only one miRNA, miR-489 (Cheung et al., 2012) has been reported to regulate MuSC quiescence and/or self-renewal.

Long non-coding RNAs (lncRNAs) constitute a recently defined class of transcripts in several tissues with major roles in normal physiology as well as development, embryonic stem cell maintenance, and disease (Fatica and Bozzoni, 2014; Neguembor et al., 2014). lncRNAs are transcribed by RNA polymerase II and undergo splicing, capping and polyadenylation (Derrien et al., 2012). Similarly to miRNAs, RNA-seq revealed specific lncRNA signatures that dynamically evolve with muscle repair (Aguilar et al., 2016) and disease (Neguembor et al., 2014). Moreover, lncRNAs have been shown to be critical for myogenic differentiation by regulating *Myod* transcriptional activity (Yu et al., 2017), decay of specific differentiation miRNAs (Cesana et al., 2011) or by inhibition of translation (Gong et al., 2015). However, only a few functionally conserved lncRNAs have been identified, and in vivo gain/loss of function studies are largely lacking for this important class of regulators. Interestingly, LINC00961 was recently reported to generate a small polypeptide called SPAR that acts via the lysosome following starvation and amino-acid-mediated stimulation to suppress mTORC1 activity (Matsumoto et al., 2017; Tajbakhsh, 2017). This novel pathway modulates skeletal muscle regeneration following injury thereby linking lncRNA encoded polypeptide function to stress response following tissue damage.

A variety of intrinsic signals has been proposed to modulate muscle repair, but more recently extrinsic and biomechanical cues have emerged as equally crucial for MuSC regulation and regeneration. Skeletal muscle stiffness, defined by the elastic modulus of ≈ 12 kPa, is altered during aging, disease or following injury (Cosgrove et al., 2009). Similarly, in *Col6a1*^{-/-} mice that model Bethlem myopathy and Ullrich congenital muscular dystrophy, muscle regeneration is severely compromised after (triple) injury, and this is associated with decreased

muscle stiffness to ≈ 7 kPa (Urciuolo et al., 2013). Interestingly, engraftment of wild-type fibroblasts partially restores COLVI, muscle stiffness, and by consequence muscle repair. These observations were consistent with a previous study showing the increase of regenerative potential of satellite cells following culture on a substrate that recapitulates the rigidity of muscle tissue compared to plastic (≈ 10 kPa) (Gilbert et al., 2010). In addition, extracellular matrix (ECM) proteins are critical components of the MuSC microenvironment and they undergo gradual remodelling from foetal to adult stages, and during ageing (Chakkalal et al., 2012; Tierney et al., 2016). For example, fibronectin (Fn) is transiently expressed in activated satellite cells (5 dpi) (Bentzinger et al., 2013) and it decreases in aged mice (Lukjanenko et al., 2016). Interestingly, direct injection of Fn in injured aged mice showed improved muscle repair (Lukjanenko et al., 2016). Moreover, how MuSCs sense their microenvironment is also critical for effective function as shown by the restoration of $\beta 1$ -integrin in old and *mdx* mice leading to satellite cell expansion and muscle repair by enhancing MuSCs connectivity to the ECM (Roza et al., 2016). Notably, among the intrinsic/extrinsic factors investigated thus far, only a few were reported to dramatically diminish or deplete the satellite cell population thereby highlighting the robustness of muscle regeneration.

4. Choosing the appropriate regeneration model

The various phases of muscle repair have been well described (Laumonier and Menetrey, 2016). However, a plethora of acute and chronic injury models are used to investigate the regenerative process without a concerted discrimination among these models. Notably, the regeneration phenotype of the *Myf5* null mice varied in different injury models: both toxin (Cardiotoxin) and freeze injury induce a delay in regeneration, however, fibrosis and adipocyte infiltration was significantly increased only following the physical injury (Gayraud-Morel et al., 2007).

Furthermore, the sampling time after injury is also essential to fully score a regeneration phenotype: the extend of new muscle formation after different types of trauma (such as anaesthetic (Sadeh, 1988), denervation (Shavlakadze et al., 2010) or toxin injury (Collins et al., 2007)) is similar at 4 weeks in young (8 weeks) versus geriatric (30 months) individuals, whereas the delay in the onset of myogenesis observed at earlier time points (5–14 days post-injury) could be underestimated (Conboy et al., 2005). Furthermore, the endpoint of muscle regeneration, about 4 weeks after trauma, is generally based on histological criteria such as the presence of centrally nucleated fibres and self-renewed quiescent MuSCs. However, remodelling might continue to occur after this period; it is interesting to note that the number of satellite cells increases by 2–3 fold up to 3 months following a single round of injury (Hardy et al., 2016). Similarly, the injury induces an increase in the number of vessels/fibre that persists 6 months after trauma. Therefore quantifications of additional features are necessary to fully monitor the regeneration process. Here too it should be noted that the vast majority of studies on muscle regeneration are performed on the TA muscle. Given the genetic and phenotypic differences between muscles in different anatomical locations (Sambasivan et al., 2009), including the superior engraftment potential of extraocular derived satellite cells compared to those from the TA muscle (Stuelsatz et al., 2015), careful consideration needs to be given to other muscle groups.

The most commonly used acute injury models involve intramuscular injection of myotoxins (Cardiotoxin (CTX) and Notexin (NTX)), Barium chloride (BaCl_2), and mechanical injury (freeze, needle or crush injuries) (Gayraud-Morel et al., 2009; Hardy et al., 2016) (Fig. 1). Myotoxins diffuse readily within muscle and allow a homogenous myofibre regeneration throughout. However, the reproducibility of injury is limited by batch variability of toxin and satellite cell survival

following their administration (Gayraud-Morel et al., 2007; Hardy et al., 2016). Of note, NTX also has a neurotoxic effect by blocking acetylcholine release thereby altering the neuromuscular junction (NMJ) thus full muscle repair requires NMJ restoration as well. In addition, NTX injury induces calcium deposits and persistent macrophage infiltration detectable up to three months post-injury.

BaCl_2 does not suffer from batch variations and it induces uniform neofibre formation. However, a single injection often leaves non-injured zones within the tissue; thus, several injections of small volumes need to be performed. These chemical methods can provoke satellite cell loss up to 80%, and this can vary according to severity of injury.

By contrast, freeze-injury by direct contact of a liquid nitrogen pre-cooled metallic rod with the muscle is the most severe, provoking satellite cell loss of up to 90% depending on the number of freeze-thaw cycles administered. This cryolesion induces an acute necrosis giving rise to a “dead zone”, devoid of viable cells, and a distal spared zone that constitutes the cellular source for regeneration. This directional recovery is convenient in some cases to study directional migration and infiltration of the different populations within the tissue. In contrast to toxins or BaCl_2 treatment, freeze-injury also destroys vasculature.

Transient or permanent denervation can be performed generally by sectioning the sciatic nerve of the mouse leg (Fig. 1, double dashed lines). Denervation results in progressive degeneration characterized by an atrophy of the muscle and significant fibrosis. This model is suitable to study muscle fibre type specificity (fast vs slow) and the role of electrical stimulation of the muscle fibres by the nerve.

Notably, in some cases, a single round of injury is not sufficient to reveal a significant phenotype, whereas multiple rounds of injury can provoke dramatic phenotypes for both wild type and mutant muscles (Kitamoto and Hanaoka, 2010; Martinet et al., 2016; Urciuolo et al., 2013).

Models of chronic degeneration/regeneration are also available to study muscle repair in a pathological context. The most broadly used model is *Mdx*, an X-linked muscular dystrophy with nonsense mutation in exon 23 of dystrophin, a critical membrane protein connecting the extracellular matrix with cytoskeleton (Sicinski et al., 1989). Despite being deficient for dystrophin, *Mdx* mice do not suffer from the severe clinical symptoms found in human DMD patients (Chamberlain et al., 2007). Nevertheless, skeletal muscles in *Mdx* mice undergo repeated bouts of degeneration and regeneration thereby providing an excellent model to investigate stem and stromal cell dynamics and inflammation without external intervention. Intriguingly, satellite cells deficient for syndecan-3 (*Sdc3*^{-/-}), a cell-adhesion regulator, fail to replenish the pool of quiescent MuSCs upon injury (Pisconti et al., 2010); however, in the *Mdx* mouse, the loss of *Sdc3* increases the pool of proliferating myoblasts (*Myf5*⁺/*Pax7*⁺) resulting in enhanced muscle regeneration and function (Pisconti et al., 2016). *Mdx* mice also provide an important model to study MuSC heterogeneity in different muscle groups, where inaccessible muscles such as the extraocular, which are spared in human (Kaminski et al., 1992), can be investigated.

Skeletal muscle injuries resulting from direct trauma (contusions), partial tears, fatigue, following surgical procedures or myopathies are common and present a challenge in traumatology, as therapy and recuperation are not well supported. After trauma, the regeneration process involves the participation of diverse cell types that modulate their behaviours according to secreted and biomechanical cues. Although MuSC engraftment following transplantation has shown successful partial repair, their low survival and self-renewal capacities, and inability to diffuse in the tissue, remain a brake for cellular therapy. Interestingly, the combination of stem cells, growth factors and bioengineered scaffolds was shown to enhance the regenerative capacity of transplanted MuSCs, therefore opening new avenues of research (Rossi et al., 2011; Sadtler et al., 2016) (Fig. 1).

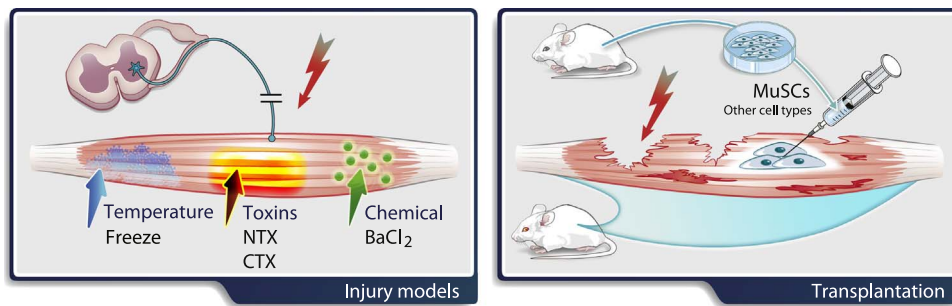


Fig. 1. Schematic representation of endogenous and transplanted cells during muscle regeneration. Left: CTX and NTX permeabilise or hydrolyse lipids on the myofibre membrane, respectively, resulting in myofibre degradation (Chang et al., 1972; Gutierrez and Ownby, 2003). Cardiotoxin (CTX, protein kinase C inhibitor) and Notexin (NTX, phospholipaseA2) are isolated from snake venom, and they trigger an increase in Ca^{2+} influx followed by fibre depolarization and consequently myofibre hypercontraction and necrosis. Chemical injury can be induced by using barium chloride (BaCl_2), a divalent alkaline earth metal that inhibits the Ca^{2+} efflux in the mitochondria in addition to stimulation of exocytosis by its barium ions. Right: Transplantation is generally performed using isolated Muscle Stem Cells (MuSCs). However, other cells types such as Fibro-Adipogenic Precursors (FAPs), Pw1 Interstitial Cells (PICs) and mesoangioblasts have been transplanted in different contexts.

5. Cellular regulators of muscle repair and their regenerative potential

Skeletal muscle regeneration follows three distinguishable and overlapping phases. The first phase of degeneration following severe injury is characterized by necrosis and significant inflammation. After clearance of cellular debris, new fibres form and transiently express embryonic and neonatal Myosin Heavy Chain (MyHC) from 3 to 14 dpi. The remodelling phase is characterized by hyperplasia and hypertrophy regulated in part by the IGF-1/Akt and TGF β /Smad pathways. IGF-1 affects the balance between protein synthesis and protein degradation thus inducing muscle hypertrophy, whereas TGF β negatively controls muscle growth (Schiaffino et al., 2013). Interestingly, recent studies demonstrated a new role for the TGF β /Smad pathway in satellite cell expansion (Paris et al., 2016) and differentiation (Rossi et al., 2016). During the final steps of muscle remodelling the vasculature and innervation patterns are restored and new MuSCs are set aside.

MuSCs are located between the basement membrane containing a basal lamina, and the plasmalemma of the muscle fibre (Mauro, 1961). MuSCs are quiescent (G_0 phase) during homeostasis (Rumman et al., 2015; Schultz et al., 1978). Following injury, they re-enter the cell cycle, proliferate to give rise to myoblasts that differentiate and fuse to restore the damaged fibre or generate myofibres *de novo* (Moss and Leblond, 1970; Reznik, 1969; Snow, 1977). During this process, a subpopulation of myogenic cells is set aside for self-renewal (Collins et al., 2005; Motohashi and Asakura, 2014; Relaix and Zammit, 2012). Once activated, MuSCs generate myoblast that differentiate, or self-renewal (Fig. 2) while undergoing symmetric (SCD) or asymmetric (ACD) cell divisions (Kuang et al., 2007; Rocheteau et al., 2012). How and when these decisions are regulated on a population level remains obscure.

Although satellite cells play a crucial role in restoring myofibres following injury, it is clear that other cells types impact on the regeneration process (Fig. 2). For example, fibro-adipogenic progenitors (FAPs) reside in the muscle interstitium, express the surface markers PDGFR α (platelet-derived growth factor receptor), Sca1 (stem cell antigen 1) and CD34, and are able to differentiate into fibroblasts and/or adipocytes (Joe et al., 2010; Uezumi et al., 2010). Following acute injury, FAPs activate and amplify, some are eliminated by apoptosis induced by pro-inflammatory cytokines such as IL4 (Joe et al., 2010). Coculture experiments demonstrated that FAPs represent a transient source of pro-differentiation factors for driving proliferating myoblast differentiation and fusion; and it has been shown that pharmacological inhibition of FAP proliferation and differentiation, or diphtheria toxin ablation of these cells results in impaired muscle regeneration (Fiore et al., 2016; Murphy et al., 2011). On the other hand, during chronic degeneration/regeneration, FAPs are the main

source of fibrosis, and in dystrophic mice, the combination of a pro- and anti-inflammatory secretome (Villalta et al., 2009) maintains FAPs survival and differentiation into matrix-producing cells similar to fibroblasts (Lemos et al., 2015). Thus, FAPs play a significant myogenic and trophic role in muscle physiology during regeneration.

Regeneration can also involve fusion of non-resident blood-derived cells to myofibres, however this occurs at too low a frequency to be considered as a viable therapeutic strategy (Ferrari et al., 1998). Pericytes are located peripheral to the endothelium of microvessels and are involved in blood vessel growth, remodelling, homeostasis, and permeability (Armulik et al., 2011). Pericytes in skeletal muscles are constituents of the satellite cell niche where they secrete molecules such as IGF1 (insulin growth factor-1) or ANGPT1 (angiopoetin-1) to modulate their behaviour but also postnatal myofibres growth and satellite cell entry in quiescence (Kostallari et al., 2015). After muscle injury, pericytes activate and give rise to a subset of vessel-associated progenitors called mesoangioblasts when isolated from the tissue. Originally isolated from the embryonic dorsal aorta, pericytes and mesoangioblasts of skeletal muscle were found to express similar markers (Dellavalle et al., 2011, 2007; Kostallari et al., 2015). Mesoangioblasts have a lower myogenic potential compared to MuSCs however, they expand, migrate and extravasate upon arterial delivery in dystrophic murine and canine models, resulting in increased engraftment efficiency and improved muscle function (Berry et al., 2007; Diaz-Manera et al., 2010; Sampaolesi et al., 2006).

In addition to these cell populations, mesenchymal cells that express the transcription factor Twist2 were recently reported to act as myogenic progenitors, however, with selective type IIb fibre-differentiation potential (Liu et al., 2017). PICs (Pw1+ Interstitial Cells) were also reported to engraft efficiently and contribute to myofibre regeneration following intramuscular injection (Mitchell et al., 2010). The imprinted stem response gene Pw1 is expressed in satellite cells, as well as a subset of interstitial cells, however, the relationship between PICs, FAPs, mesoangioblasts and Twist2+ cells remains unclear (Fig. 2). Mesenchymal "stem" cells (MSCs) have been isolated from virtually all tissues and organs, however, the lack of specific markers has made their characterisation challenging, particularly in light of a recent report showing that mesenchymal stromal cells from different tissues have different transcriptome profiles and differentiation potentials (Sacchetti et al., 2016). Given the advanced state of analysis interstitial cells in muscle, it would be important to establish their lineage relationships and myogenic potential, and define more clearly general features of MSCs. Recent technological advancements in single cell mass cytometry now permit investigations of cellular heterogeneity within specific cell populations (Spitzer and Nolan, 2016). This technique based on a combination of markers conjugated to metal isotopes led to the identification and classification of sub-populations of myogenic cells following muscle injury (Porphiglia et al.,

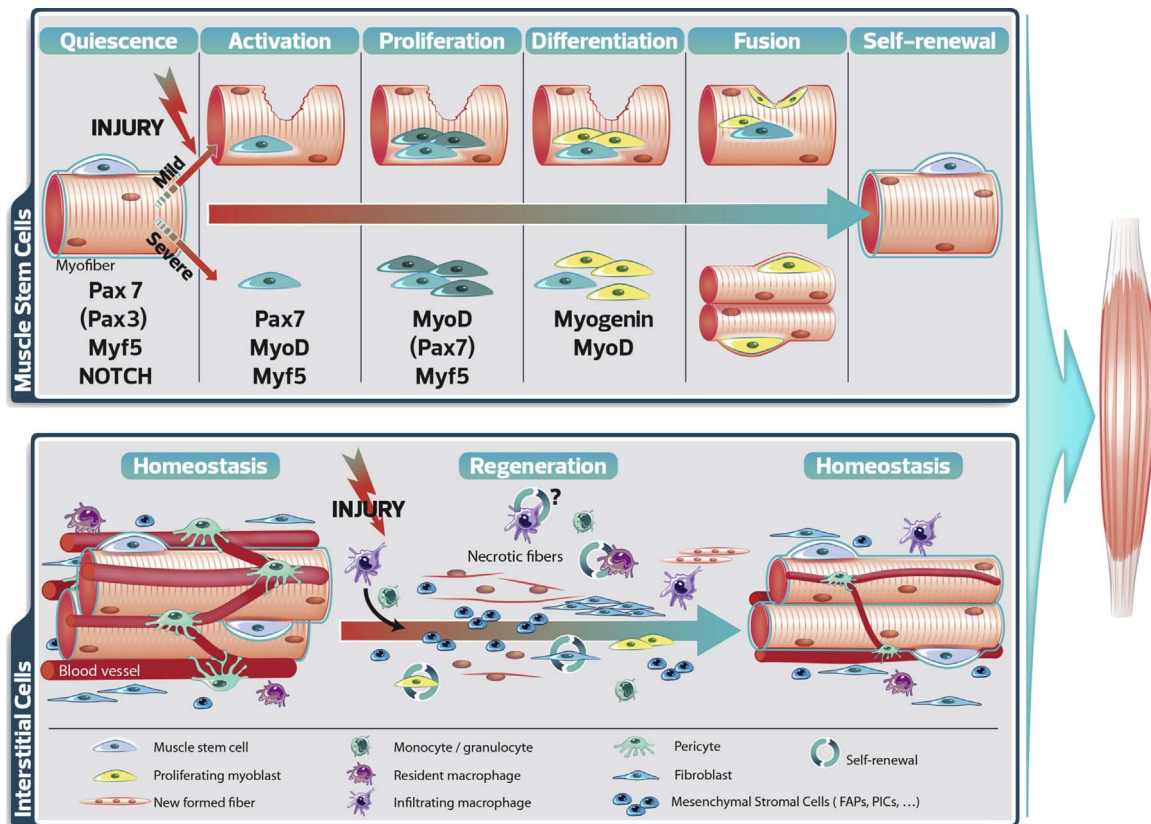


Fig. 2. Synoptic view of the different cell populations involved in muscle repair. Top: Following mild or severe injury, quiescent muscle stem cells (MuSCs) activate, differentiate and fuse to repair the damaged fibre. Mild injury induces fibre break and recruitment of surrounding satellite cells on the intact part of the fibre. In contrast, severe injury triggers complete myofibre destruction followed by satellite cell proliferation and differentiation on extracellular matrix remnants referred to as “ghost fibres” (Webster et al., 2016). Mild and severe injuries activate a tightly regulated myogenic process including interplay of key transcription factors. During homeostasis, satellite cells are quiescent and express *Pax7* (and *Pax3* in some muscles) and *Myf5*, and Notch signalling is highly active. Upon damage, they rapidly upregulate *Myod* and *Myf5*, and *Pax7* protein remains detectable. Following the amplification phase, myoblasts express the terminal differentiation gene *Myogenin* and exit the cell cycle. Differentiated myoblasts fuse to the pre-existing fibre (mild) or together to form new fibres (severe). During this process, some satellite cells self-renew to replenish the stem cell pool. Bottom: Although the generation of new fibres is dependent on MuSCs, other cell types such as macrophages, monocytes, mesenchymal stromal cells (including FAPs, mesoangioblasts and PICs), pericytes and fibroblasts are also critical for the regeneration process.

2017), and it can be used to assess the relative potential and role of myogenic as well as stromal cells at the single cell level.

As indicated above, muscle homeostasis and regeneration involve the interplay of numerous cell types. Inflammatory resident and infiltrating cells also play important roles. Neutrophils/monocytes are the first cells to be recruited following tissue damage, as they appear within 3 h following injury and they are no longer detectable after 3 days (Chazaud et al., 2003; Tidball and Villalta, 2010). Their action on the necrotic tissue relies on proteolysis, oxidation and phagocytosis. Muscle-specific inhibition of neutrophil/monocyte activation results in a delay in regeneration upon acute injury (Nguyen et al., 2005).

Macrophages play a critical role during the initial stages following tissue damage as they are required for phagocytosis and cytokine release. The first wave of macrophages (peak at 3 days) promotes myoblast proliferation via the secretion of pro-inflammatory molecules such as TNF α (Tumour Necrosis Factor α), INF α (Interferon α) or IL6 (Interleukin 6) (Lu et al., 2011). Subsequently, macrophages undergo a phenotypical and functional switch toward an anti-inflammatory fate characterized by the production of IL4 or IL10, for example (Arnold et al., 2007). As mentioned above, this anti-inflammatory response stimulates FAPs, mesoangioblasts, and also directly myoblasts to promote differentiation and fusion (Chazaud et al., 2003; Saclier et al., 2013). Importantly, muscle-resident macrophages are also involved in the immune response following injury (Brigitte et al., 2010; Juban and Chazaud, 2017) yet the cellular source of the homeostatic recovery of the resident macrophage population upon damage in adult mice is still lacking. Notably, two distinct embryonic

origins of macrophages have been reported: those arising from haematopoietic stem cells (HSCs), and resident macrophages that are found in all tissues and that are derived from the yolk sac (Gomez Perdiguero et al., 2015). Interestingly, upon acute lung injury, inflammatory macrophages undergo apoptosis while the resident cells persist (Janssen et al., 2011). However, resident macrophages could also arise from bone marrow-derived macrophages undergoing phenotypic conversion to become tissue-resident macrophages (Davies et al., 2013; Yona et al., 2013). It would be important to determine the relative roles and dynamics of yolk sac and HSC-derived macrophages in homeostasis and regeneration (Fig. 2).

Muscle vascularisation and angiogenesis provide structural, cellular and molecular support during homeostasis, regeneration and adaptation. The importance of microvessels in the composition of the stem cell niche is highlighted by the tight proximity (within 21 μ m) of \approx 90% of MuSCs with vessels (Christov et al., 2007). The number of MuSCs and capillaries, as well as the timing of angiogenesis and myogenesis, are orchestrated during regeneration suggesting a reciprocal interaction between these cell types (Luque et al., 1995). Co-culture experiments revealed that endothelial cells stimulate growth of satellite cells through the secretion of variety of growth factors including IGF-1 (insulin growth factor 1), VEGF (vascular endothelial growth factor), HGF (hepatocyte growth factor), PDGF-BB (platelet-derived growth factor) and FGF (fibroblast growth factor) (Christov et al., 2007). Furthermore, adenoviral overexpression of VEGF in vivo, combined with IGF treatment, resulted in increased satellite cell proliferation (Arsic et al., 2004). In a reciprocal manner, differentiating myoblasts,

	Type of wound	Cellular contribution	Reference
Pre-bilaterians Cnidarians Jellyfish	Scrapping off small part of swimming muscle	MDD	Lin, 2000
Bilaterians Arthropods Parhyale	Limb amputation	SLCs	Konstantinides, 2014
Cephalochordates Amphioxus	Tail amputation	SLCs	Somorjai, 2012
Fish Electric fish Zebrafish *	Tail amputation Puncture larvae ventral myotome	SLCs SLCs * MDD in EOM	Weber, 2012 Knappe, 2015 Saera-Vila, 2015
Vertebrates Amphibians Xenopus Axoltl Newt	Tadpole tail amputation Limb amputation Limb amputation	SLCs SLCs MDD adult SLCs in larvae	Chen, 2016 Sandoval-Guzman, 2014 Sandoval-Guzman, 2014 Tanaka, 2016
Amniotes Mammals Mouse Human	Toxins, chemicals, mechanical, Eccentric exercise	MuSCs MuSCs	Sambasivan, 2011 Whitehead, 1998

Fig. 3. Muscle regenerative ability of pre-bilaterians and bilaterians. MDD: Myofibre dedifferentiation, SLCs: Satellite-Like Cells, MuSCs: Muscle Stem Cells. * MDD contributes to zebrafish adult extraocular muscle (EOM) regeneration. Note that the newt regenerates muscle using MDD in the adult and SLCs in the larvae.

through VEGF, also stimulate angiogenesis (Chazaud et al., 2003; Christov et al., 2007; Rhoads et al., 2009). In addition, several other factors such as MCP-1 (monocyte chemotactic protein), ANGPT2, NGF (nerve growth factor) synthesized by endothelial cells at the early stages of regeneration can stimulate angiogenesis and thus muscle repair (see (Wagatsuma, 2007)). Finally, periendothelial cells (fibroblasts from the endomysium and smooth muscle cells) stabilise regenerated vessels and are capable of stimulating the self-renewal and re-entry in quiescence of a subset of myoblasts through the action of ANGPT1 (Abou-Khalil et al., 2009; Kostallari et al., 2015).

Adult satellite cells reside in a hypoxic microenvironment (Simon and Keith, 2008) and it has been shown that the lack of oxygen (anoxia) in post-mortem muscles, triggers satellite cells to enter a more quiescent state called dormancy (Latil et al., 2012; Rocheteau et al., 2012). Moreover, purified satellite cells cultured in hypoxia (3% O₂) showed higher engraftment and self-renewal capacities resulting in enhanced muscle repair (Liu et al., 2012). Consistently, the in vivo depletion of HIF1 α and HIF2 α (Hypoxia Inducible Factor), important transcription factors mediating the cellular response to low O₂ level, specifically in satellite cells (*Pax7^{CreERT2}; HIF^{flox}*) induces a delay in repair due to a self-renewal impairment and inhibition of Notch signalling (Yang et al., 2017).

It has been proposed that microvascular insufficiency could be responsible for the local inflammation and necrosis observed in both dystrophin-deficient mouse and human (Cazzato, 1968). Among the dystrophin-associated proteins is the nitric oxydase synthase (nNOS) that is associated with the sarcolemma, and produces diffusible NO to optimize blood flow by sympathetic vasoconstriction attenuation (Anderson, 2000; Kobayashi et al., 2008). In dystrophic animal models and human, the loss of NO abrogates this protective mechanism and the sustained vasoconstriction induces deleterious ischemia resulting in myofibre lysis (Kobayashi et al., 2008; Thomas et al., 1998). Thus, pharmacological restoration of NO downstream signalling to increase blood flow had been proposed, for example, by the use of phosphodiesterase 5A (PDE5A) inhibitors to increase the cGMP downstream effector of NO (Malik et al., 2012; Martin et al., 2012). In *Mdx* mice, PDE5A inhibition was reported to improve muscle ischemia, reduce muscle injury and fatigue (Kobayashi et al., 2008). Clinical trials with encouraging alleviation of microvascular ischemia and restoration of blood flow were reported in the majority of patients tested (Martin et al., 2012).

In summary, regenerative myogenesis involves the interplay of multiple cell types. The identification of subpopulations of mesenchymal stromal cells with different properties provides impetus to characterise in detail their respective roles in the regeneration process. It is not clear to what extent these stromal cell populations are present, and if they play similar roles in regeneration in other tissues, and in other organisms.

6. Strategies for muscle regeneration in different organisms

The process of regeneration is common in metazoans, from cnidarians such as *Hydra* to higher vertebrates, although their regenerative capacities vary widely. Some metazoans such as planarian or annelid worms can rebuild entire body parts when cut into segments, whereas vertebrates like salamanders can regenerate lens, retina, heart, CNS and can regrow fully functional appendages after amputation. In contrast, mammals fail to regenerate missing body portions, but they can repair injured skeletal muscles, peripheral nervous system or liver with reasonable efficiency (Carlson, 2005; Gurtner et al., 2008).

Interestingly, muscle regeneration constitutes a unique evolutionary conserved phenomenon among bilaterians, as it has been described in arthropods, planarian and annelid worms, ascidians, fish, amphibians (salamander, xenopus) and mammals (mouse, pig, bovine). However, the strategies and the cellular dynamics regulating muscle regeneration can be markedly distinct among species. To date, two main mechanisms have emerged for the origin of regenerated muscle: myofibre dedifferentiation, or the contribution of Satellite-Like Cells (SLCs), similar to satellite cells identified in other vertebrates (Fig. 3).

In *Xenopus*, the muscle repair process is studied by amputation of the tadpole tail which is composed mainly of striated muscle. Amputation induces the formation of a blastema, a mesenchymal structure composed of highly proliferative progenitors cells that will differentiate further and form a new functional limb (Straube and Tanaka, 2006). The regeneration of *Xenopus* muscle relies on the amplification of a Pax7+ myogenic cells in the blastema (Chen et al., 2006) rather than de-differentiation, as the fibres near the amputation site simply undergo cell death (Gargioli and Slack, 2004). Following ablation of the Pax7+ SLC population, the tail can still regenerate, but it contains little or no muscle (Chen et al., 2006).

The salamander, a urodele amphibian, can regenerate the limbs

multiple times, independently of its age (Straube and Tanaka, 2006). Using Cre-lox-based genetic fate mapping of muscle to compare limb repair in two salamander species, it was reported that in the newt (*Notophtalmus virisecens*), muscle regeneration relies mainly on fibres that de-differentiate into Pax7-negative proliferative mononucleated cells that further generate new myofibres (Sandoval-Guzman et al., 2014) whereas the larvae uses SLCs (Tanaka et al., 2016). In contrast, in the neotenic axolotl (*Ambystoma mexicanum*), myofibres do not contribute to muscle regeneration while grafting experiments showed the recruitment of Pax7-positive SLCs that proliferate in the blastema and regenerate new fibres (Sandoval-Guzman et al., 2014). These unexpected findings reveal that distinct muscle regeneration strategies appear to have evolved among these salamanders that are 100 million years apart (Steinfartz et al., 2007).

Similarly to mammals and amphibians, the presence of adult SLCs has been described in several fish species including salmon, carp, and electric fish (Weber et al., 2012). In zebrafish larvae, muscle injury by puncture wounds to the ventral myotome induces proliferation of SLCs, differentiation and fusion to repair damaged myofibres (Knapp et al., 2015). Of note, the Pax7 gene is duplicated in zebrafish (*Pax7a* and *Pax7b*), and they differ in expression pattern and function: *Pax7a*-cells participate in repair of the first wave of nascent fibres whereas *Pax7b*-cells generate larger fibres (Pipalia et al., 2016). The ablation of one population or the other results in deficits in repair suggesting lack of compensation (Pipalia et al., 2016). Similarly, it has been shown in the adult electric fish (*S. macrurus*) that muscle repair following tail amputation also involves Pax7-positive SLCs, but not myofibre dedifferentiation (Weber et al., 2012). Interestingly, according to the muscle type, the zebrafish is capable of exploiting both strategies: extraocular muscle injury using partial myectomy of the lateral rectus showed no SLC contribution to muscle regeneration, instead, residual myocytes undergo dedifferentiation (Saera-Vila et al., 2015).

Recently, other chordate models emerged to study the evolution of regenerative biology at the invertebrate-vertebrate transition. The basal chordate amphioxus shows a high regenerative potential and it is capable of regrowing both anterior and posterior structures during adult life, including neural tube, notochord, fin, and muscle after amputation (Somorjai et al., 2012). Interestingly, amphioxus possesses peripheral Pax3/7+ cells present in the embryo and located under the basal lamina in adult resting muscle. These cells amplify upon amputation migrate toward the periphery of degrading myofibres and fuse. These and other studies suggest that amphioxus is a tractable model for regenerative myogenesis, and it has extensive regenerative capacities beyond those of more complex vertebrates (Somorjai et al., 2012).

As another example, the crustacean *Parhyale hawaiiensis* develops a blastema structure after thoracic leg amputation followed by extensive growth of the limb and generation of a new musculature later after moulting (Konstantinides and Averof, 2014). Moreover, Pax3/7-expressing cells of mesodermal origin are tightly associated with mature *Parhyale* muscles and transplantation experiments of labelled SLCs in wild-type individuals have shown that muscle regeneration is based on SLCs as observed in vertebrates (Konstantinides and Averof, 2014).

In contrast, pre-bilaterian animals such as cnidarians possess muscles formed by epitheliomuscular cells that can be striated (*Medusa*) or not (*Hydra*) (Leclere and Rottinger, 2016). Although regeneration in cnidarians has been reported (Leclere and Rottinger, 2016), limited data is available on the cellular origin of muscle repair. After wounding, the striated muscle in jellyfish dedifferentiates into non-proliferating mononucleated cells that migrate toward the site of injury before undergoing differentiation (Lin et al., 2000).

The studies performed in diverse chordate species, arthropods and cnidarians suggest that the cellular basis of regeneration implicating Pax3/7-positive SLCs was present in the common ancestor of bilater-

ians (Fig. 3). The different strategies employed for muscle repair, even in evolutionary related species, highlights the highly conserved regulation of the regeneration process, and it points to satellite cells as an ancient evolutionary stem cell type present throughout bilaterian phylogeny (Fig. 3). However, the relative role of interstitial cells in regenerative myogenesis is less well understood in non-murine models. Furthermore, understanding the loss of regenerative capacity in human has been the topic of intense debate for decades thereby prompting more detailed investigations of animal models with superior regenerative capacity. One hypothesis proposes that suppression of dedifferentiation and cell cycle reentry were lost in mammals in favour of a tumour suppression program to prevent carcinogenesis. For example, the in vitro inhibition of two tumour suppressor proteins (ARF and Rb) in mouse primary muscle cells induce myotubes to reenter the cell cycle (Pajcini et al., 2010). Similarly, inhibition of the p53 tumour suppressor in newt primary myotubes triggers their fragmentation into mononucleated cells that reenter cell cycle (Wang et al., 2015). In addition, the knock-down of p16^{INK4}, another potent tumour suppressor that accumulates in aged individuals, leads to an extensive increase in regenerative potential of pancreatic islets (Krishnamurthy et al., 2006). However, whether those tumour suppressors are inhibited in the fish and amniotes requires investigations to support the cancer hypothesis. It would be interesting to explore the status of tumour suppressors using two structures that differ by their repair mechanism: such as the zebrafish extraocular muscle (dedifferentiation, (Saera-Vila et al., 2015)) versus the tail (SLCs).

7. Conclusion

Skeletal muscle has been used for decades to study regenerative medicine and stem cell biology, however, the field still lacks a standard injury and repair protocol allowing comparisons between laboratories. Although by 28 days post-injury the muscle is considered to be largely regenerated, the timing of regeneration can be different from one injury model to another: eg, new vessels are formed 2 dpi after chemical injuries while this event takes up to 12 days following freeze-injury (Hardy et al., 2016). Another area that requires detailed investigation is the study and characterisation of interstitial stromal cells. The identification of "mesenchymal stem cells" in tissues has generated some confusion as this population exhibits considerable heterogeneity. The identification of several stromal populations in skeletal muscle can be used as a starting point to isolate cells with potentially similar properties in other tissues with the aim to define stem-stromal interactions in niches of different tissues and organs. Finally, the inability to regenerate a whole appendage in mammals remains puzzling, although intriguingly, heart and digit tip regeneration have been reported to occur during early perinatal growth under certain conditions, but these capabilities are lost within days (Seifert et al., 2012). Detailed investigations on comparative evolutionary biology of organisms that have retained and lost regenerative capacity will allow us to identify the underlying mechanisms responsible for this fascinating phenomenon.

Acknowledgements

We acknowledge support from the Institut Pasteur, Agence Nationale de la Recherche (Laboratoire d'Excellence Revive, Investissement d'Avenir; ANR-10-LABX-73) and (ANR-06-BLAN-0039), the Association pour la Recherche sur le Cancer, and the European Research Council (Advanced Research Grant 332893). MBB was supported by a Doctoral School Fellowship and Fondation pour la Recherche Médicale. We thank Eglantine Heude for stimulating discussions on the topic of muscle regeneration phylogeny.

References

- Abou-Khalil, R., Le Grand, F., Pallafacchina, G., Valable, S., Authier, F.J., Rudnicki, M.A., Gherardi, R.K., Germain, S., Chretien, F., Sotiropoulos, A., Lafuste, P., Montarras, D., Chazaud, B., 2009. Autocrine and paracrine angiopoietin 1/Tie-2 signaling promotes muscle satellite cell self-renewal. *Cell Stem Cell* 5, 298–309.
- Agular, C.A., Pop, R., Shcherbina, A., Watts, A., Matheny, R.W., Jr., Cacchiarelli, D., Han, W.M., Shin, E., Nakhai, S.A., Jang, Y.C., Carrigan, C.T., Gifford, C.A., Kottke, M.A., Cesana, M., Lee, J., Urso, M.L., Meissner, A., 2016. Transcriptional and chromatin dynamics of muscle regeneration after severe trauma. *Stem Cell Rep.* 7, 983–997.
- Anderson, J.E., 2000. A role for nitric oxide in muscle repair: nitric oxide-mediated activation of muscle satellite cells. *Mol. Biol. Cell* 11, 1859–1874.
- Armulik, A., Genove, G., Betsholtz, C., 2011. Pericytes: developmental, physiological, and pathological perspectives, problems, and promises. *Dev. Cell* 21, 193–215.
- Arnold, L., Henry, A., Poron, F., Baba-Amer, Y., van Rooijen, N., Plonquet, A., Gherardi, R.K., Chazaud, B., 2007. Inflammatory monocytes recruited after skeletal muscle injury switch into anti-inflammatory macrophages to support myogenesis. *J. Exp. Med.* 204, 1057–1069.
- Arsic, N., Zaccagna, S., Zentilin, L., Ramirez-Correa, G., Pattarini, L., Salvi, A., Sinagra, G., Giacca, M., 2004. Vascular endothelial growth factor stimulates skeletal muscle regeneration in vivo. *Mol. Ther.* 10, 844–854.
- Bartel, D.P., 2004. MicroRNAs: genomics, biogenesis, mechanism, and function. *Cell* 116, 281–297.
- Bentzinger, C.F., Wang, Y.X., von Maltzahn, J., Soleimani, V.D., Yin, H., Rudnicki, M.A., 2013. Fibronectin regulates Wnt7a signaling and satellite cell expansion. *Cell Stem Cell* 12, 75–87.
- Berry, S.E., Liu, J., Chaney, E.J., Kaufman, S.J., 2007. Multipotential mesoangioblast stem cell therapy in the mdx/utrn^{-/-} mouse model for Duchenne muscular dystrophy. *Regen. Med.* 2, 275–288.
- Bi, P., Yue, F., Sato, Y., Wirbisky, S., Liu, W., Shan, T., Wen, Y., Zhou, D., Freeman, J., Kuang, S., 2016. Stage-specific effects of Notch activation during skeletal myogenesis. *eLife*, 5.
- Biressi, S., Molinaro, M., Cossu, G., 2007. Cellular heterogeneity during vertebrate skeletal muscle development. *Dev. Biol.* 308, 281–293.
- Bjornson, C.R., Cheung, T.H., Liu, L., Tripathi, P.V., Steeper, K.M., Rando, T.A., 2012. Notch signaling is necessary to maintain quiescence in adult muscle stem cells. *Stem Cells* 30, 232–242.
- Brigitte, M., Schilte, C., Plonquet, A., Baba-Amer, Y., Henri, A., Charlier, C., Tajbakhsh, S., Albert, M., Gherardi, R.K., Chretien, F., 2010. Muscle resident macrophages control the immune cell reaction in a mouse model of notexin-induced myoinjury. *Arthritis Rheum.* 62, 268–279.
- Carlson, B.M., 2005. Some principles of regeneration in mammalian systems. *Anat. Rec. Part B New Anat.* 287, 4–13.
- Castel, D., Mourikis, P., Bartels, S.J., Brinkman, A.B., Tajbakhsh, S., Stunnenberg, H.G., 2013. Dynamic binding of RBPJ is determined by Notch signaling status. *Genes Dev.* 27, 1059–1071.
- Cazzato, G., 1968. Considerations about a possible role played by connective tissue proliferation and vascular disturbances in the pathogenesis of progressive muscular dystrophy. *Eur. Neurol.* 1, 158–179.
- Cesana, M., Cacchiarelli, D., Legnini, I., Santini, T., Sthandier, O., Chinappi, M., Tramontano, A., Bozzoni, I., 2011. A long noncoding RNA controls muscle differentiation by functioning as a competing endogenous RNA. *Cell* 147, 358–369.
- Chakkalakal, J.V., Jones, K.M., Basson, M.A., Brack, A.S., 2012. The aged niche disrupts muscle stem cell quiescence. *Nature* 490, 355–360.
- Chamberlain, J.S., Metzger, J., Reyes, M., Townsend, D., Faulkner, J.A., 2007. Dystrophin-deficient mdx mice display a reduced life span and are susceptible to spontaneous rhabdomyosarcoma. *FASEB J.: Off. Publ. Fed. Am. Soc. Exp. Biol.* 21, 2195–2204.
- Chang, C.C., Chuang, S.T., Lee, C.Y., Wei, J.W., 1972. Role of cardiotoxin and phospholipase A in the blockade of nerve conduction and depolarization of skeletal muscle induced by cobra venom. *Br. J. Pharmacol.* 44, 752–764.
- Chazaud, B., Sonnet, C., Lafuste, P., Bassez, G., Rimaniol, A.C., Poron, F., Authier, F.J., Dreyfus, P.A., Gherardi, R.K., 2003. Satellite cells attract monocytes and use macrophages as a support to escape apoptosis and enhance muscle growth. *J. Cell Biol.* 163, 1133–1143.
- Chen, Y., Lin, G., Slack, J.M., 2006. Control of muscle regeneration in the *Xenopus* tadpole tail by Pax7. *Development* 133, 2303–2313.
- Cheung, T.H., Quach, N.L., Charville, G.W., Liu, L., Park, L., Edalati, A., Yoo, B., Hoang, P., Rando, T.A., 2012. Maintenance of muscle stem-cell quiescence by microRNA-489. *Nature* 482, 524–528.
- Christov, C., Chretien, F., Abou-Khalil, R., Bassez, G., Vallet, G., Authier, F.J., Bassaglia, Y., Shinin, V., Tajbakhsh, S., Chazaud, B., Gherardi, R.K., 2007. Muscle satellite cells and endothelial cells: close neighbors and privileged partners. *Mol. Biol. Cell* 18, 1397–1409.
- Collins, C.A., Olsen, I., Zammit, P.S., Heslop, L., Petrie, A., Partridge, T.A., Morgan, J.E., 2005. Stem cell function, self-renewal, and behavioral heterogeneity of cells from the adult muscle satellite cell niche. *Cell* 122, 289–301.
- Collins, C.A., Zammit, P.S., Ruiz, A.P., Morgan, J.E., Partridge, T.A., 2007. A population of myogenic stem cells that survives skeletal muscle aging. *Stem Cells* 25, 885–894.
- Comai, G., Tajbakhsh, S., 2014. Molecular and cellular regulation of skeletal myogenesis. *Curr. Top. Dev. Biol.* 110, 1–73.
- Conboy, L.M., Conboy, M.J., Wagers, A.J., Girma, E.R., Weissman, I.L., Rando, T.A., 2005. Rejuvenation of aged progenitor cells by exposure to a young systemic environment. *Nature* 433, 760–764.
- Cosgrove, B.D., Sacco, A., Gilbert, P.M., Blau, H.M., 2009. A home away from home: challenges and opportunities in engineering in vitro muscle satellite cell niches. *Differ. Res. Biol. Divers.* 78, 185–194.
- Davies, L.C., Jenkins, S.J., Allen, J.E., Taylor, P.R., 2013. Tissue-resident macrophages. *Nat. Immunol.* 14, 986–995.
- Dellavalle, A., Sampaoli, M., Tonlorenzi, R., Tagliacof, E., Sacchetti, B., Perani, L., Innocenzi, A., Galvez, B.G., Messina, G., Morosetti, R., Li, S., Belicchi, M., Peretti, G., Chamberlain, J.S., Wright, W.E., Torrente, Y., Ferrari, S., Bianco, P., Cossu, G., 2007. Pericytes of human skeletal muscle are myogenic precursors distinct from satellite cells. *Nat. Cell Biol.* 9, 255–267.
- Dellavalle, A., Maroli, G., Covarello, D., Azzoni, E., Innocenzi, A., Perani, L., Antonini, S., Sambasivan, R., Brunelli, S., Tajbakhsh, S., Cossu, G., 2011. Pericytes resident in postnatal skeletal muscle differentiate into muscle fibres and generate satellite cells. *Nat. Commun.* 2, 499.
- Derrien, T., Johnson, R., Bussotti, G., Tanzer, A., Djebali, S., Tilgner, H., Guernec, G., Martin, D., Merkel, A., Knowles, D.G., Lagarde, J., Veeravalli, L., Ruan, X., Ruan, Y., Lassmann, T., Carninci, P., Brown, J.B., Lipovich, L., Gonzalez, J.M., Thomas, M., Davis, C.A., Shiekhattar, R., Gingeras, T.R., Hubbard, T.J., Notredame, C., Harrow, J., Guigo, R., 2012. The GENCODE v7 catalog of human long noncoding RNAs: analysis of their gene structure, evolution, and expression. *Genome Res.* 22, 1775–1789.
- Diaz-Manera, J., Touvier, T., Dellavalle, A., Tonlorenzi, R., Tedesco, F.S., Messina, G., Meregalli, M., Navarro, C., Perani, L., Bonfanti, C., Illa, I., Torrente, Y., Cossu, G., 2010. Partial dysferlin reconstitution by adult murine mesoangioblasts is sufficient for full functional recovery in a murine model of dysferlinopathy. *Cell Death Dis.* 1, e61.
- Fatica, A., Bozzoni, I., 2014. Long non-coding RNAs: new players in cell differentiation and development. *Nat. Rev. Genet.* 15, 7–21.
- Ferrari, G., Cusella-De Angelis, G., Coletta, M., Paolucci, E., Stornaiuolo, A., Cossu, G., Mavilio, F., 1998. Muscle regeneration by bone marrow-derived myogenic progenitors. *Science* 279, 1528–1530.
- Finnegan, E.F., Pasquinelli, A.E., 2013. MicroRNA biogenesis: regulating the regulators. *Crit. Rev. Biochem. Mol. Biol.* 48, 51–68.
- Fiore, D., Judson, R.N., Low, M., Lee, S., Zhang, E., Hopkins, C., Xu, P., Lenzi, A., Rossi, F.M., Lemos, D.R., 2016. Pharmacological blockage of fibro/adipogenic progenitor expansion and suppression of regenerative fibrogenesis is associated with impaired skeletal muscle regeneration. *Stem Cell Res.* 17, 161–169.
- Fukada, S., Yamaguchi, M., Kokubo, H., Ogawa, R., Uezumi, A., Yoneda, T., Matev, M.M., Motohashi, N., Ito, T., Zolkiewska, A., Johnson, R.L., Saga, Y., Miyagoe-Suzuki, Y., Tsujikawa, K., Takeda, S., Yamamoto, H., 2011. Hesr1 and Hesr3 are essential to generate undifferentiated quiescent satellite cells and to maintain satellite cell numbers. *Development* 138, 4609–4619.
- Gargioli, C., Slack, J.M., 2004. Cell lineage tracing during *Xenopus* tail regeneration. *Development* 131, 2669–2679.
- Gayraud-Morel, B., Chretien, F., Flamant, P., Gomes, D., Zammit, P.S., Tajbakhsh, S., 2007. A role for the myogenic determination gene Myf5 in adult regenerative myogenesis. *Dev. Biol.* 312, 13–28.
- Gayraud-Morel, B., Chretien, F., Tajbakhsh, S., 2009. Skeletal muscle as a paradigm for regenerative biology and medicine. *Regen. Med.* 4, 293–319.
- Gilbert, P.M., Havenstrite, K.L., Magnusson, K.E., Sacco, A., Leonardi, N.A., Kraft, P., Nguyen, N.K., Thrun, S., Lutolf, M.P., Blau, H.M., 2010. Substrate elasticity regulates skeletal muscle stem cell self-renewal in culture. *Science* 329, 1078–1081.
- Gomez Perdiguer, E., Klapproth, K., Schulz, C., Busch, K., Azzoni, E., Crozet, L., Garner, H., Trouillet, C., de Bruijn, M.F., Geissmann, F., Rodewald, H.R., 2015. Tissue-resident macrophages originate from yolk-sac-derived erythro-myeloid progenitors. *Nature* 518, 547–551.
- Gong, C., Li, Z., Ramanujan, K., Clay, I., Zhang, Y., Lemire-Brachat, S., Glass, D.J., 2015. A long non-coding RNA, LncMyoD, regulates skeletal muscle differentiation by blocking IMP2-mediated mRNA translation. *Dev. Cell* 34, 181–191.
- Gunther, S., Kim, J., Kostin, S., Lepper, C., Fan, C.M., Braun, T., 2013. Myf5-positive satellite cells contribute to Pax7-dependent long-term maintenance of adult muscle stem cells. *Cell Stem Cell* 13, 590–601.
- Gurtner, G.C., Werner, S., Barrandon, Y., Longaker, M.T., 2008. Wound repair and regeneration. *Nature* 453, 314–321.
- Gutierrez, J.M., Ownby, C.L., 2003. Skeletal muscle degeneration induced by venom phospholipases A2: insights into the mechanisms of local and systemic myotoxicity. *Toxicol. Off. J. Int. Soc. Toxicol.* 42, 915–931.
- Hardy, D., Besnard, A., Latil, M., Jouvion, G., Briand, D., Thepenier, C., Pascal, Q., Guguin, A., Gayraud-Morel, B., Cavaillon, J.M., Tajbakhsh, S., Rocheteau, P., Chretien, F., 2016. Comparative study of injury models for studying muscle regeneration in mice. *PLoS One* 11, e0147198.
- Hasty, P., Bradley, A., Morris, J.H., Edmondson, D.G., Venuti, J.M., Olson, E.N., Klein, W.H., 1993. Muscle deficiency and neonatal death in mice with a targeted mutation in the myogenin gene. *Nature* 364, 501–506.
- Hayashi, S., Manabe, I., Suzuki, Y., Relaix, F., Oishi, Y., 2016. Klf5 regulates muscle differentiation by directly targeting muscle-specific genes in cooperation with MyoD in mice. *eLife* 5.
- Janssen, W.J., Barthel, L., Muldrow, A., Oberley-Deegan, R.E., Kearns, M.T., Jakubzik, C., Henson, P.M., 2011. Fas determines differential fates of resident and recruited macrophages during resolution of acute lung injury. *Am. J. Respir. Crit. Care Med.* 184, 547–560.
- Jarriault, S., Brou, C., Logeat, F., Schroeter, E.H., Kopan, R., Israel, A., 1995. Signalling downstream of activated mammalian Notch. *Nature* 377, 355–358.
- Joe, A.W., Yi, L., Natarajan, A., Le Grand, F., So, L., Wang, J., Rudnicki, M.A., Rossi, F.M., 2010. Muscle injury activates resident fibro/adipogenic progenitors that facilitate myogenesis. *Nat. Cell Biol.* 12, 153–163.

- Juban, G., Chazaud, B., 2017. Metabolic regulation of macrophages during tissue repair: insights from skeletal muscle regeneration. *FEBS Lett.*
- Kaminski, H.J., al-Hakim, M., Leigh, R.J., Katiqji, M.B., Ruff, R.L., 1992. Extraocular muscles are spared in advanced duchenne dystrophy. *Ann. Neurol.* 32, 586–588.
- Kassar-Duchossoy, L., Gayraud-Morel, B., Gomes, D., Rocancourt, D., Buckingham, M., Shinin, V., Tajbakhsh, S., 2004. Mrf4 determines skeletal muscle identity in Myf5: myod double-mutant mice. *Nature* 431, 466–471.
- Kirby, T.J., Chaillou, T., McCarthy, J.J., 2015. The role of microRNAs in skeletal muscle health and disease. *Front. Biosci. (Landmark Ed.)* 20, 37–77.
- Kitamoto, T., Hanaoka, K., 2010. Notch3 null mutation in mice causes muscle hyperplasia by repetitive muscle regeneration. *Stem Cells* 28, 2205–2216.
- Knapp, J.R., Davie, J.K., Myer, A., Meadows, E., Olson, E.N., Klein, W.H., 2006. Loss of myogenin in postnatal life leads to normal skeletal muscle but reduced body size. *Development* 133, 601–610.
- Knapp, S., Zammit, P.S., Knight, R.D., 2015. A population of Pax7-expressing muscle progenitor cells show differential responses to muscle injury dependent on developmental stage and injury extent. *Front. Aging Neurosci.* 7, 161.
- Kobayashi, Y.M., Rader, E.P., Crawford, R.W., Iyengar, N.K., Thedens, D.R., Faulkner, J.A., Parikh, S.V., Weiss, R.M., Chamberlain, J.S., Moore, S.A., Campbell, K.P., 2008. Sarcolemma-localized nNOS is required to maintain activity after mild exercise. *Nature* 456, 511–515.
- Konstantinides, N., Averof, M., 2014. A common cellular basis for muscle regeneration in arthropods and vertebrates. *Science* 343, 788–791.
- Kopan, R., Ilagan, M.X., 2009. The canonical Notch signaling pathway: unfolding the activation mechanism. *Cell* 137, 216–233.
- Kostallari, E., Baba-Amer, Y., Alonso-Martin, S., Ngho, P., Relaix, F., Lafuste, P., Gherardi, R.K., 2015. Pericytes in the myovascular niche promote post-natal myofiber growth and satellite cell quiescence. *Development* 142, 1242–1253.
- Krishnamurthy, J., Ramsey, M.R., Ligon, K.L., Torrice, C., Koh, A., Bonner-Weir, S., Sharpless, N.E., 2006. P16INK4a induces an age-dependent decline in islet regenerative potential. *Nature* 443, 453–457.
- Kuang, S., Kuroda, K., Le Grand, F., Rudnicki, M.A., 2007. Asymmetric self-renewal and commitment of satellite stem cells in muscle. *Cell* 129, 999–1010.
- Latil, M., Rocheteau, P., Chatre, L., Sanulli, S., Memet, S., Ricchetti, M., Tajbakhsh, S., Chretien, F., 2012. Skeletal muscle stem cells adopt a dormant cell state post mortem and retain regenerative capacity. *Nat. Commun.* 3, 903.
- Laumonier, T., Menetrey, J., 2016. Muscle injuries and strategies for improving their repair. *J. Exp. Orthop.* 3, 15.
- Leclere, L., Rottinger, E., 2016. Diversity of cnidarian muscles: function, anatomy, development and regeneration. *Front. Cell Dev. Biol.* 4, 157.
- Lemos, D.R., Babaeijandaghi, F., Low, M., Chang, C.K., Lee, S.T., Fiore, D., Zhang, R.H., Natarajan, A., Nedospasov, S.A., Rossi, F.M., 2015. Nilotinib reduces muscle fibrosis in chronic muscle injury by promoting TNF-mediated apoptosis of fibro/adipogenic progenitors. *Nat. Med.* 21, 786–794.
- Lepper, C., Conway, S.J., Fan, C.M., 2009. Adult satellite cells and embryonic muscle progenitors have distinct genetic requirements. *Nature* 460, 627–631.
- Lepper, C., Partridge, T.A., Fan, C.M., 2011. An absolute requirement for Pax7-positive satellite cells in acute injury-induced skeletal muscle regeneration. *Development* 138, 3639–3646.
- Lin, Y.C., Grigoriev, N.G., Spencer, A.N., 2000. Wound healing in jellyfish striated muscle involves rapid switching between two modes of cell motility and a change in the source of regulatory calcium. *Dev. Biol.* 225, 87–100.
- Liu, N., Garry, G.A., Li, S., Bezprozvannaya, S., Sanchez-Ortiz, E., Chen, B., Shelton, J.M., Jaichander, P., Bassel-Duby, R., Olson, E.N., 2017. A Twist2-dependent progenitor cell contributes to adult skeletal muscle. *Nat. Cell Biol.* 19, 202–213.
- Liu, W., Wen, Y., Bi, P., Lai, X., Liu, X.S., Liu, X., Kuang, S., 2012. Hypoxia promotes satellite cell self-renewal and enhances the efficiency of myoblast transplantation. *Development* 139, 2857–2865.
- Lu, H., Huang, D., Ransohoff, R.M., Zhou, L., 2011. Acute skeletal muscle injury: CCL2 expression by both monocytes and injured muscle is required for repair. *FASEB J.: Off. Publ. Fed. Am. Soc. Exp. Biol.* 25, 3344–3355.
- Lukjanenko, L., Jung, M.J., Hegde, N., Perruisseau-Carrier, C., Migliavacca, E., Roza, M., Karaz, S., Jacot, G., Schmidt, M., Li, L., Metairon, S., Raymond, F., Lee, U., Sizzano, F., Wilson, D.H., Dumont, N.A., Palini, A., Fassler, R., Steiner, P., Descombes, P., Rudnicki, M.A., Fan, C.M., von Maltzahn, J., Feige, J.N., Bentzinger, C.F., 2016. Loss of fibronectin from the aged stem cell niche affects the regenerative capacity of skeletal muscle in mice. *Nat. Med.* 22, 897–905.
- Luque, E., Pena, J., Martin, P., Jimena, I., Vaamonde, R., 1995. Capillary supply during development of individual regenerating muscle fibers. *Anat. Histol. Embryol.* 24, 87–89.
- Malik, V., Rodino-Klapac, L.R., Mendell, J.R., 2012. Emerging drugs for Duchenne muscular dystrophy. *Expert Opin. Emerg. Drugs* 17, 261–277.
- von Maltzahn, J., Jones, A.E., Parks, R.J., Rudnicki, M.A., 2013. Pax7 is critical for the normal function of satellite cells in adult skeletal muscle. *Proc. Natl. Acad. Sci. USA* 110, 16474–16479.
- Martin, E.A., Barresi, R., Byrne, B.J., Tsimmerinov, E.I., Scott, B.L., Walker, A.E., Gurudev, S.V., Anene, F., Elashoff, R.M., Thomas, G.D., Victor, R.G., 2012. Tadalafil alleviates muscle ischemia in patients with Becker muscular dystrophy. *Sci. Transl. Med.* 4, (162ra155).
- Martinet, C., Monnier, P., Louault, Y., Benard, M., Gabory, A., Dandolo, L., 2016. H19 controls reactivation of the imprinted gene network during muscle regeneration. *Development* 143, 962–971.
- Matsumoto, A., Pasut, A., Matsumoto, M., Yamashita, R., Fung, J., Monteleone, E., Saghatelian, A., Nakayama, K.I., Clohessy, J.G., Pandolfi, P.P., 2017. mTORC1 and muscle regeneration are regulated by the LINC00961-encoded SPAR polypeptide. *Nature* 541, 228–232.
- Mauro, A., 1961. Satellite cell of skeletal muscle fibers. *J. Biophys. Biochem. Cytol.* 9, 493–495.
- Meadows, E., Cho, J.H., Flynn, J.M., Klein, W.H., 2008. Myogenin regulates a distinct genetic program in adult muscle stem cells. *Dev. Biol.* 322, 406–414.
- Megeney, L.A., Kablar, B., Garrett, K., Anderson, J.E., Rudnicki, M.A., 1996. MyoD is required for myogenic stem cell function in adult skeletal muscle. *Genes Dev.* 10, 1173–1183.
- Mitchell, K.J., Pannerec, A., Cadot, B., Parlakian, A., Besson, V., Gomes, E.R., Marazzi, G., Sassoon, D.A., 2010. Identification and characterization of a non-satellite cell muscle resident progenitor during postnatal development. *Nat. Cell Biol.* 12, 257–266.
- Moss, F.P., Leblond, C.P., 1970. Nature of dividing nuclei in skeletal muscle of growing rats. *J. Cell Biol.* 44, 459–462.
- Motohashi, N., Asakura, A., 2014. Muscle satellite cell heterogeneity and self-renewal. *Front. Cell Dev. Biol.* 2, 1.
- Mourikis, P., Sambasivan, R., Castel, D., Rocheteau, P., Bizzarro, V., Tajbakhsh, S., 2012. A critical requirement for notch signaling in maintenance of the quiescent skeletal muscle stem cell state. *Stem Cells* 30, 243–252.
- Murphy, M.M., Lawson, J.A., Mathew, S.J., Hutcheson, D.A., Kardon, G., 2011. Satellite cells, connective tissue fibroblasts and their interactions are crucial for muscle regeneration. *Development* 138, 3625–3637.
- Neguembor, M.V., Jothi, M., Gabellini, D., 2014. Long noncoding RNAs, emerging players in muscle differentiation and disease. *Skelet. Muscle* 4, 8.
- Nguyen, H.X., Lusic, A.J., Tidball, J.G., 2005. Null mutation of myeloperoxidase in mice prevents mechanical activation of neutrophil lysis of muscle cell membranes in vitro and in vivo. *J. Physiol.* 565, 403–413.
- Oustanina, S., Hause, G., Braun, T., 2004. Pax7 directs postnatal renewal and propagation of myogenic satellite cells but not their specification. *EMBO J.* 23, 3430–3439.
- Pajcini, K.V., Corbel, S.Y., Sage, J., Pomerantz, J.H., Blau, H.M., 2010. Transient inactivation of Rb and ARF yields regenerative cells from postmitotic mammalian muscle. *Cell Stem Cell* 7, 198–213.
- Paris, N.D., Soroka, A., Klose, A., Liu, W., Chakkalakal, J.V., 2016. Smad4 restricts differentiation to promote expansion of satellite cell derived progenitors during skeletal muscle regeneration. *eLife* 5.
- Pasquini, A.E., 2012. MicroRNAs and their targets: recognition, regulation and an emerging reciprocal relationship. *Nat. Rev. Genet.* 13, 271–282.
- Pasut, A., Chang, N.C., Gurriaran-Rodriguez, U., Faulkes, S., Yin, H., Lacaria, M., Ming, H., Rudnicki, M.A., 2016. Notch signaling rescues loss of satellite cells lacking Pax7 and promotes brown adipogenic differentiation. *Cell Rep.* 16, 333–343.
- Pipalia, T.G., Koth, J., Roy, S.D., Hammond, C.L., Kawakami, K., Hughes, S.M., 2016. Cellular dynamics of regeneration reveals role of two distinct Pax7 stem cell populations in larval zebrafish muscle repair. *Dis. Models Mech.* 9, 671–684.
- Pisconti, A., Cornelison, D.D., Olguin, H.C., Antwine, T.L., Olwin, B.B., 2010. Syndecan-3 and notch cooperate in regulating adult myogenesis. *J. Cell Biol.* 190, 427–441.
- Pisconti, A., Banks, G.B., Babaeijandaghi, F., Betta, N.D., Rossi, F.M., Chamberlain, J.S., Olwin, B.B., 2016. Loss of niche-satellite cell interactions in syndecan-3 null mice alters muscle progenitor cell homeostasis improving muscle regeneration. *Skelet. Muscle* 6, 34.
- Porpiglia, E., Samusik, N., Van, Ho, A.T., Cosgrove, B.D., Mai, T., Davis, K.L., Jager, A., Nolan, G.P., Bendall, S.C., Fantl, W.J., Blau, H.M., 2017. High-resolution myogenic lineage mapping by single-cell mass cytometry. *Nat. Cell Biol.* 19, 558–567.
- Relaix, F., Zammit, P.S., 2012. Satellite cells are essential for skeletal muscle regeneration: the cell on the edge returns centre stage. *Development* 139, 2845–2856.
- Relaix, F., Rocancourt, D., Mansouri, A., Buckingham, M., 2005. A Pax3/Pax7-dependent population of skeletal muscle progenitor cells. *Nature* 435, 948–953.
- Relaix, F., Montarras, D., Zafrani, S., Gayraud-Morel, B., Rocancourt, D., Tajbakhsh, S., Mansouri, A., Cumano, A., Buckingham, M., 2006. Pax3 and Pax7 have distinct and overlapping functions in adult muscle progenitor cells. *J. Cell Biol.* 172, 91–102.
- Reznik, M., 1969. Thymidine-3H uptake by satellite cells of regenerating skeletal muscle. *J. Cell Biol.* 40, 568–571.
- Rhoads, R.P., Johnson, R.M., Rathbone, C.R., Liu, X., Temm-Grove, C., Sheehan, S.M., Hoying, J.B., Allen, R.E., 2009. Satellite cell-mediated angiogenesis in vitro coincides with a functional hypoxia-inducible factor pathway. *Am. J. Physiol. Cell Physiol.* 296, C1321–C1328.
- Rocheteau, P., Gayraud-Morel, B., Siegl-Cachedenier, I., Blasco, M.A., Tajbakhsh, S., 2012. A subpopulation of adult skeletal muscle stem cells retains all template DNA strands after cell division. *Cell* 148, 112–125.
- Rossi, C.A., Flaibani, M., Blaauw, B., Pozzobon, M., Figallo, E., Reggiani, C., Vitiello, L., Elvassore, N., De Coppi, P., 2011. In vivo tissue engineering of functional skeletal muscle by freshly isolated satellite cells embedded in a photopolymerizable hydrogel. *FASEB J.: Off. Publ. Fed. Am. Soc. Exp. Biol.* 25, 2296–2304.
- Rossi, G., Antonini, S., Bonfanti, C., Monteverde, S., Vezzali, C., Tajbakhsh, S., Cossu, G., Messina, G., 2016. Nfix regulates temporal progression of muscle regeneration through modulation of myostatin expression. *Cell Rep.* 14, 2238–2249.
- Roza, M., Li, L., Fan, C.M., 2016. Targeting beta1-integrin signaling enhances regeneration in aged and dystrophic muscle in mice. *Nat. Med.* 22, 889–896.
- Rudnicki, M.A., Schnegelsberg, P.N., Stead, R.H., Braun, T., Arnold, H.H., Jaenisch, R., 1993. MyoD or Myf-5 is required for the formation of skeletal muscle. *Cell* 75, 1351–1359.
- Rumman, M., Dhawan, J., Kassem, M., 2015. Concise review: quiescence in adult stem cells: biological significance and relevance to tissue regeneration. *Stem Cells* 33, 2903–2912.
- Sacchetti, B., Funari, A., Remoli, C., Giannicola, G., Kogler, G., Liedtke, S., Cossu, G., Serafini, M., Sampaoli, M., Tagliacof, E., Tenedini, E., Saggio, I., Robey, P.G.,

- Riminucci, M., Bianco, P., 2016. No identical "mesenchymal stem cells" at different times and sites: human committed progenitors of distinct origin and differentiation potential are incorporated as adventitial cells in microvessels. *Stem Cell Rep.* 6, 897–913.
- Saclier, M., Yacoub-Youssef, H., Mackey, A.L., Arnold, L., Ardjoune, H., Magnan, M., Saillhan, F., Chelly, J., Pavlath, G.K., Mounier, R., Kjaer, M., Chazaud, B., 2013. Differentially activated macrophages orchestrate myogenic precursor cell fate during human skeletal muscle regeneration. *Stem Cells* 31, 384–396.
- Sadeh, M., 1988. Effects of aging on skeletal muscle regeneration. *J. Neurol. Sci.* 87, 67–74.
- Sadtler, K., Estrellas, K., Allen, B.W., Wolf, M.T., Fan, H., Tam, A.J., Patel, C.H., Luber, B.S., Wang, H., Wagner, K.R., Powell, J.D., Housseau, F., Pardoll, D.M., Elisseeff, J.H., 2016. Developing a pro-regenerative biomaterial scaffold microenvironment requires T helper 2 cells. *Science* 352, 366–370.
- Saera-Vila, A., Kasprick, D.S., Junttila, T.L., Grzegorski, S.J., Louie, K.W., Chiari, E.F., Kish, P.E., Kahana, A., 2015. Myocyte dedifferentiation drives extraocular muscle regeneration in adult zebrafish. *Investig. Ophthalmol. Vis. Sci.* 56, 4977–4993.
- Sambasivan, R., Tajbakhsh, S., 2007. Skeletal muscle stem cell birth and properties. *Semin. Cell Dev. Biol.* 18, 870–882.
- Sambasivan, R., Gayraud-Morel, B., Dumas, G., Cimper, C., Paisant, S., Kelly, R.G., Tajbakhsh, S., 2009. Distinct regulatory cascades govern extraocular and pharyngeal arch muscle progenitor cell fates. *Dev. Cell* 16, 810–821.
- Sambasivan, R., Yao, R., Kissenpfennig, A., Van Wittenberghe, L., Paldi, A., Gayraud-Morel, B., Guenou, H., Malissen, B., Tajbakhsh, S., Galy, A., 2011. Pax7-expressing satellite cells are indispensable for adult skeletal muscle regeneration. *Development* 138, 3647–3656.
- Sampaolesi, M., Blot, S., D'Antona, G., Granger, N., Tonlorenzi, R., Innocenzi, A., Mognol, P., Thibaud, J.L., Galvez, B.G., Barthelemy, I., Perani, L.M., Mantero, S., Guttinger, M., Pansarasa, O., Rinaldi, C., Cusella De Angelis, M.G., Torrente, Y., Bordignon, C., Bottinelli, R., Cossu, G., 2006. Mesoangioblast stem cells ameliorate muscle function in dystrophic dogs. *Nature* 444, 574–579.
- Sandoval-Guzman, T., Wang, H., Khattak, S., Schuez, M., Roensch, K., Nacu, E., Tazaki, A., Joven, A., Tanaka, E.M., Simon, A., 2014. Fundamental differences in dedifferentiation and stem cell recruitment during skeletal muscle regeneration in two salamander species. *Cell Stem Cell* 14, 174–187.
- Schiaffino, S., Dyar, K.A., Cicilioti, S., Blaauw, B., Sandri, M., 2013. Mechanisms regulating skeletal muscle growth and atrophy. *FEBS J.* 280, 4294–4314.
- Schultz, E., Gibson, M.C., Champion, T., 1978. Satellite cells are mitotically quiescent in mature mouse muscle: an EM and radioautographic study. *J. Exp. Zool.* 206, 451–456.
- Seale, P., Sabourin, L.A., Girgis-Gabardo, A., Mansouri, A., Gruss, P., Rudnicki, M.A., 2000. Pax7 is required for the specification of myogenic satellite cells. *Cell* 102, 777–786.
- Seifert, A.W., Monaghan, J.R., Smith, M.D., Pasch, B., Stier, A.C., Michonneau, F., Maden, M., 2012. The influence of fundamental traits on mechanisms controlling appendage regeneration. *Biol. Rev. Camb. Philos. Soc.* 87, 330–345.
- Shavlakadze, T., McGeachie, J., Grounds, M.D., 2010. Delayed but excellent myogenic stem cell response of regenerating geriatric skeletal muscles in mice. *Biogerontology* 11, 363–376.
- Sicinski, P., Geng, Y., Ryder-Cook, A.S., Barnard, E.A., Darlison, M.G., Barnard, P.J., 1989. The molecular basis of muscular dystrophy in the mdx mouse: a point mutation. *Science* 244, 1578–1580.
- Simon, M.C., Keith, B., 2008. The role of oxygen availability in embryonic development and stem cell function. *Nat. Rev. Mol. Cell Biol.* 9, 285–296.
- Snow, M.H., 1977. Myogenic cell formation in regenerating rat skeletal muscle injured by mincing. II. Autoradiogr. Study *Anat. Rec.* 188, 201–217.
- Somorjai, I.M., Somorjai, R.L., Garcia-Fernandez, J., Escrava, H., 2012. Vertebrate-like regeneration in the invertebrate chordate amphioxus. *Proc. Natl. Acad. Sci. USA* 109, 517–522.
- Spitzer, M.H., Nolan, G.P., 2016. Mass cytometry: single. Cells, Many. Features *Cell* 165, 780–791.
- Steinfartz, S., Weitere, M., Tautz, D., 2007. Tracing the first step to speciation: ecological and genetic differentiation of a salamander population in a small forest. *Mol. Ecol.* 16, 4550–4561.
- Straube, W.L., Tanaka, E.M., 2006. Reversibility of the differentiated state: regeneration in amphibians. *Artif. Organs* 30, 743–755.
- Stuelsatz, P., Shearer, A., Li, Y., Muir, L.A., Ieronimakis, N., Shen, Q.W., Kirillova, I., Yablonka-Reuveni, Z., 2015. Extraocular muscle satellite cells are high performance myo-engines retaining efficient regenerative capacity in dystrophin deficiency. *Dev. Biol.* 397, 31–44.
- Tajbakhsh, S., 2009. Skeletal muscle stem cells in developmental versus regenerative myogenesis. *J. Intern. Med.* 266, 372–389.
- Tajbakhsh, S., 2017. lncRNA-encoded polypeptide SPAR(s) with mTORC1 to regulate skeletal muscle regeneration. *Cell Stem Cell* 20, 428–430.
- Tajbakhsh, S., Rocancourt, D., Buckingham, M., 1996. Muscle progenitor cells failing to respond to positional cues adopt non-myogenic fates in myf-5 null mice. *Nature* 384, 266–270.
- Tanaka, H.V., Ng, N.C., Yang Yu, Z., Casco-Robles, M.M., Maruo, F., Tsonis, P.A., Chiba, C., 2016. A developmentally regulated switch from stem cells to dedifferentiation for limb muscle regeneration in newts. *Nat. Commun.* 7, 11069.
- Thomas, G.D., Sander, M., Lau, K.S., Huang, P.L., Stull, J.T., Victor, R.G., 1998. Impaired metabolic modulation of alpha-adrenergic vasoconstriction in dystrophin-deficient skeletal muscle. *Proc. Natl. Acad. Sci. USA* 95, 15090–15095.
- Tidball, J.G., Villalta, S.A., 2010. Regulatory interactions between muscle and the immune system during muscle regeneration. *Am. J. Physiol. Regul. Integr. Comp. Physiol.* 298, R1173–R1187.
- Tierney, M.T., Gromova, A., Sesillo, F.B., Sala, D., Spence, C., Orend, G., Sacco, A., 2016. Autonomous extracellular matrix remodeling controls a progressive adaptation in muscle stem cell regenerative capacity during development. *Cell Rep.* 14, 1940–1952.
- Uezumi, A., Fukada, S., Yamamoto, N., Takeda, S., Tsuchida, K., 2010. Mesenchymal progenitors distinct from satellite cells contribute to ectopic fat cell formation in skeletal muscle. *Nat. Cell Biol.* 12, 143–152.
- Umansky, K.B., Gruenbaum-Cohen, Y., Tsoory, M., Feldmesser, E., Goldenberg, D., Brenner, O., Groner, Y., 2015. Runx1 transcription factor is required for myoblast proliferation during muscle regeneration. *PLoS Genet.* 11, e1005457.
- Urciuoli, A., Quarta, M., Morbidoni, V., Gattazzo, F., Molon, S., Grumati, P., Montemurro, F., Tedesco, F.S., Blaauw, B., Cossu, G., Vozzi, G., Rando, T.A., Bonaldo, P., 2013. Collagen VI regulates satellite cell self-renewal and muscle regeneration. *Nat. Commun.* 4, 1964.
- Venuti, J.M., Morris, J.H., Vivian, J.L., Olson, E.N., Klein, W.H., 1995. Myogenin is required for late but not early aspects of myogenesis during mouse development. *J. Cell Biol.* 128, 563–576.
- Villalta, S.A., Nguyen, H.X., Deng, B., Gotoh, T., Tidball, J.G., 2009. Shifts in macrophage phenotypes and macrophage competition for arginine metabolism affect the severity of muscle pathology in muscular dystrophy. *Hum. Mol. Genet.* 18, 482–496.
- Wagatsuma, A., 2007. Endogenous expression of angiogenesis-related factors in response to muscle injury. *Mol. Cell. Biochem.* 298, 151–159.
- Wang, H., Loof, S., Borg, P., Nader, G.A., Blau, H.M., Simon, A., 2015. Turning terminally differentiated skeletal muscle cells into regenerative progenitors. *Nat. Commun.* 6, 7916.
- Weber, C.M., Martindale, M.Q., Tapscott, S.J., Unguez, G.A., 2012. Activation of Pax7-positive cells in a non-contractile tissue contributes to regeneration of myogenic tissues in the electric fish *S. macrurus*. *PLoS One* 7, e36819.
- Webster, M.T., Manor, U., Lippincott-Schwartz, J., Fan, C.M., 2016. Intravital imaging reveals ghost fibers as architectural units guiding myogenic progenitors during regeneration. *Cell Stem Cell* 18, 243–252.
- White, J.D., Scaffidi, A., Davies, M., McGeachie, J., Rudnicki, M.A., Grounds, M.D., 2000. Myotube formation is delayed but not prevented in MyoD-deficient skeletal muscle: studies in regenerating whole muscle grafts of adult mice. *J. Histochem. Cytochem.: Off. J. Histochem. Soc.* 48, 1531–1544.
- White, R.B., Bierinx, A.S., Gnocchi, V.F., Zammit, P.S., 2010. Dynamics of muscle fibre growth during postnatal mouse development. *BMC Dev. Biol.* 10, 21.
- Williams, A.H., Liu, N., van Rooij, E., Olson, E.N., 2009. MicroRNA control of muscle development and disease. *Curr. Opin. Cell Biol.* 21, 461–469.
- Yang, X., Yang, S., Wang, C., Kuang, S., 2017. The hypoxia-inducible factors HIF1alpha and HIF2alpha are dispensable for embryonic muscle development but essential for postnatal muscle regeneration. *J. Biol. Chem.* 292, 5981–5991.
- Yona, S., Kim, K.W., Wolf, Y., Mildner, A., Varol, D., Breker, M., Strauss-Ayali, D., Viukov, S., Guilliams, M., Misharin, A., Hume, D.A., Perlman, H., Malissen, B., Zelder, E., Jung, S., 2013. Fate mapping reveals origins and dynamics of monocytes and tissue macrophages under homeostasis. *Immunity* 38, 79–91.
- Yu, X., Zhang, Y., Li, T., Ma, Z., Jia, H., Chen, Q., Zhao, Y., Zhai, L., Zhong, R., Li, C., Zou, X., Meng, J., Chen, A.K., Puri, P.L., Chen, M., Zhu, D., 2017. Long non-coding RNA Linc-RAM enhances myogenic differentiation by interacting with MyoD. *Nat. Commun.* 8, 14016.

ANNEX 2: Resource paper

Comparison of multiple transcriptomes using a new analytical pipeline *Sherpa* exposes unified and divergent features of quiescent and activated skeletal muscle stem cells

Submitted

1
2
3
4
5
6
7
8
9
10
11
12
13
14
15
16
17
18
19
20
21
22
23
24
25
26
27
28
29
30

Comparison of multiple transcriptomes using a new analytical pipeline *Sherpa* exposes unified and divergent features of quiescent and activated skeletal muscle stem cells

Natalia Pietrosemoli^{1,*}, Sébastien Mella^{2,3,*}, Siham Yennek^{2,3,#,*}, Meryem B. Baghdadi^{2,3,*}, Hiroshi Sakai^{2,3,*}, Ramkumar Sambasivan^{4,*}, Francesca Pala^{2,3}, Daniella Di Grimaldo^{2,5}, and Shahragim Tajbakhsh^{2,3,§}

1: Bioinformatics and Biostatistics Hub, C3BI, USR 3756 IP CNRS, Institut Pasteur, Paris 75015, France.

2: Stem Cells and Development, Department of Developmental & Stem Cell Biology, Institut Pasteur, Paris 75015, France.

3: CNRS UMR 3738, Institut Pasteur, Paris 75015, France.

4: Institute for Stem Cell Biology and Regenerative Medicine, GKVK PO, Bellary Road, Bengaluru 560065, India

5: Dipartimento di Medicina Clinica e Chirurgia, Università degli Studi di Napoli "Federico II", Via S. Pansini 5, 80131, Napoli, Italy

§ Correspondence: shahragim.tajbakhsh@pasteur.fr

** equal contribution*

31 **Abstract**

32 Skeletal muscle stem cells are quiescent in adult mice and can undergo multiple rounds of
33 proliferation and self-renewal following muscle injury. As transcriptomics technologies became
34 available, several labs profiled transcripts of myogenic cells during developmental and adult
35 myogenesis. Here we focused on the quiescent cell state and generated new transcriptome profiles
36 that include subfractionation of adult MuSC populations and artificially induced prenatal quiescent
37 state using constitutive Notch signaling, to identify a series of core signatures for quiescent and
38 proliferating adult myogenic cells. In an attempt to compare with available data we were confronted
39 with several issues including diversity of datasets and biological conditions. To address these issues,
40 we established an analytical pipeline called *Sherpa* for standardizing available data. *Sherpa* facilitates
41 analysis and comparisons, has general features that can be adapted to other transcriptomic data sets,
42 and it can be used to analyse transcriptome data generated from other conditions and tissues. Our
43 analysis shows that although many *bona fide* quiescent markers have been identified to date, several
44 classes of transcripts present in the literature as quiescent are due to procedural artifacts inherent in
45 isolating cells from solid tissues. These include stress activated genes such as *Jun* and *Fos* that were
46 empirically shown to be absent in quiescent cells if they were fixed prior to extraction of the cells, then
47 processed for analysis. Therefore, these findings provide impetus to define and distinguish transcripts
48 associated with true *in vivo* quiescence from those that are first responding genes associated with
49 disruption of the stem cell niche.

50

51

52 **Introduction**

53 Most adult stem cell populations identified to date are in a quiescent state [1]. Following tissue
54 damage or disruption of the stem cell niche, skeletal muscle stem (satellite) cells (MuSCs) transit
55 through different cell states from reversible cell cycle exit to a postmitotic multinucleate state in
56 myofibres. In mouse skeletal muscle, the transcription factor Pax7 marks MuSCs during quiescence
57 and proliferation, and it has been used to identify and isolate myogenic populations from skeletal
58 muscle [2, 3]. Myogenic cells have also been isolated by FACS using a variety of surface markers,
59 including $\alpha 7$ -integrin, VCAM and CD34 [4] Although these cells have been extensively studied by
60 transcriptome, and to a more limited extend by proteome profiling, different methods have been used

61 to isolate and profile myogenic cells thereby making comparisons between laboratories laborious and
62 challenging. To address this issue, it is necessary to generate comprehensive catalogs of gene
63 expression data of myogenic cells across distinct states and in different conditions.

64

65 Soon after their introduction two decades ago, high-throughput microarray studies started to be
66 compiled into common repositories that provide to the community access to the data. Several gene
67 expression repositories for specific diseases, such as the Cancer Genome Atlas (TCGA) [5], the
68 Parkinson's disease expression database ParkDB [6], or for specific tissues, such the Allen Human
69 and Mouse Brain Atlases [7][8] among many, have been crucial in allowing scientists the comparison
70 of datasets, the application of novel methods to existing datasets, and thus a more global view of
71 these biological systems.

72

73 In this work, we generated transcriptome data sets of MuSCs in different conditions and aimed to
74 perform comparisons with published data sets. Due to the diversity of platforms and formats of
75 published datasets, this was not readily achievable. For this reason, we developed an interactive tool
76 called *Sherpa* (SHiny ExploRation tool for transcriPtomc Analysis) to provide comprehensive access
77 to the individual datasets analysed in a homogeneous manner. This webserver allows users to: i)
78 identify differentially expressed genes of the individual datasets, ii) identify the enriched gene sets of
79 the individual datasets, and iii) effectively compare the chosen datasets. *Sherpa* is adaptable and
80 serves as a repository for the integration and analysis of future transcriptomic data. It has a generic
81 design that makes it adaptable to the analysis of other transcriptome data sets generated in a variety
82 of conditions and tissues.

83

84 Using *Sherpa*, we analyse gene expression profiles (GEPs) of activated and quiescent states of
85 mouse MuSCs derived from three high-throughput experimental setups and six publicly available
86 microarray datasets to define a consensus molecular signature of the quiescent state. This large
87 compendium of expression data offers the first comparison and integration of nine independent
88 studies of the quiescent state of mouse satellite cells. In addition, we have adapted a protocol for the
89 fixation and capture of mRNA directly from the tissue without the alteration in gene expression that
90 could arise during the isolation procedure, which typically takes several hours with solid tissues.

91 Strikingly, several genes, including members of the *Jun* and *Fos* family were found to be present in
92 isolated MuSCs using conventional isolation procedures, but they were absent *in vivo*. These findings,
93 and the unique atlas that we report, will undoubtedly improve our current understanding of the
94 molecular mechanisms governing the quiescent state and contribute to the identification of critical
95 regulatory genes involved in different cell states.

96

97

98 **Methods**

99 **Individual dataset transcriptomic analysis**

100 The analysis comprised a total of nine datasets, three novel microarray datasets and six publicly
101 available datasets [9][10][11][12][13][14], choosing only samples with overall similar conditions. All
102 datasets were analysed independently following the same generalized pipeline based on ad-hoc R
103 implemented scripts (Fig. 2).

104

105 ***Gene expression profiles***

106 The microarray data compared activated satellite cells (ASCs) and quiescent satellite cells (QSCs)
107 from different experiments. Table 1 describes the public datasets that were taken into account for the
108 analysis with the GEO data sources, references and sample distribution. The new mouse microarray
109 datasets include the following comparisons: young adult Quiescent(adult) / Activated(postnatal day 8),
110 and Quiescent [high/low] / D3Activated [high/low], and Foetal_NICD [E17.5/E14.5]. Table 1 details the
111 sample distribution.

112

113 ***Animals, injuries and cell sorting***

114 Animals were handled according to national and European Community guidelines, and an ethics
115 committee of the Institut Pasteur (CTEA) in France. For isolation of quiescent MuSCs, *Tg: Pax7-nGFP*
116 mice (6-12 weeks) [2] were anesthetized prior to injury. *Tibialis anterior* (TA) muscles were injured with
117 notexin (10µl – 10µM; Latoxan). Cells were then isolated by Fluorescence Activated Cell Sorting
118 (FACS) using BD FACS ARIA III, MoFlo Astrios and Legacy sorters. Pax7^{Hi} and Pax7^{Lo} cells
119 correspond to the 10% of cells with the highest and the lowest expression of nGFP, respectively, as
120 defined previously [3].

121 For isolation of activated MuSCs, TA muscles (day 3 post-injury (D3) and non-injured) were collected
122 and subjected to 4-5 rounds of digestion in a solution of 0.08% Collagenase D (Roche) and 0.1%
123 Trypsin (Invitrogen) diluted in DMEM-1% P/S (Invitrogen) supplemented with DNase I at 10µg/ml
124 (Roche) [2][3]. Cells were then isolated by FACS based on Pax7-nGFP intensity, using BD FACS
125 ARIA III (BD Biosciences) and MoFlo Astrios (Beckman Coulter) sorters. Pax7^{Hi} and Pax7^{Lo} cells
126 correspond to the 10% of cells with the highest and the lowest expression of nGFP, respectively, as
127 defined previously [3].

128 Skeletal muscle progenitors were obtained also from the forelimbs of E14.5 and E17.5 fetuses of
129 *Myf5^{CreCAP/+};R26R^{stop-NICD-nGFP}* [15] compound mice. Tissues were dissociated in DMEM (GIBCO,
130 31966), 0.1% Collagenase D (Roche, 1088866), 0.25% trypsin (GIBCO, 15090-046), DNase 10 µg/ml
131 (Roche, 11284932001) for three consecutive cycles of 15 min at 37°C in a water bath under gentle
132 agitation. For each round, supernatant containing dissociated cells was filtered through 70µm cell
133 strainer and trypsin was inhibited with calf serum. Pooled supernatants from each round of digestion
134 were centrifuged at 1600rpm for 15 min at 4°C and pellet was re-suspended in cold DMEM/1%
135 PS/2%FBS and filtered through 40µm cell strainer. Cells were then isolated by FACS using BD FACS
136 ARIA III. Total mRNAs were isolated using (Qiagen RNeasy® Micro Kit) according to the
137 manufacturer's recommendations.

138 In other experiments, skeletal muscles from the limbs, body wall and diaphragm were collected from
139 pups at postnatal day 8 (P8, mitotically active satellite cells) and 4-5 weeks old mice (quiescent
140 satellite cells) of *Pax7^{nGFP/+}* knock-in line [16]. GFP positive cells were then isolated from these
141 muscles by FACS.

142

143 ***Microarray sample preparation***

144 Total RNA isolation of Pax7^{Hi} and Pax7^{Lo} cells was performed using RNeasy Micro Plus Kits (Qiagen).
145 5 ng of total RNA was reverse transcribed and amplified following the manufacturer's protocols
146 (Ovation Pico WTA System v2 (Nugen Technologies, Inc. #3302-12); Applause WTA Amp-Plus
147 System (Nugen Technologies, Inc. #5510-24)), fragmented and biotin labeled using the Encore Biotin
148 Module (Nugen Technologies, Inc. #4200-12). Gene expression was determined by hybridization of
149 the labeled template to Genechip microarrays Mouse Gene 1.0 ST (Affymetrix). Hybridization cocktail
150 and post-hybridization processing was performed according to the "Target Preparation for Affymetrix

151 GeneChip Eukaryotic Array Analysis” protocol found in the appendix of the Nugen protocol of the
152 fragmentation kit. Arrays were hybridized for 18 hours and washed using fluidics protocol FS450 0007
153 on a GeneChip Fluidic Station 450 (Affymetrix) and scanned with an Affymetrix Genechip Scanner
154 3000, generating CEL les for each array. Three biological replicates were run for each condition.

155

156 **Western blot analysis**

157 Total protein extracts from satellite cells isolated by FACS were run on a 4-12% Bis-Tris Gel NuPAGE
158 (Invitrogen) and transferred on Amersham Hybond-P transfer membrane (Ge Healthcare). The
159 membrane was then blocked with 5% nonfat dry milk in TBS, probed with anti-JunD (329) (1:1000, sc-
160 74 Santa Cruz Biotechnology Inc.), anti-JunB (N-17) (1:1000, sc-46 Santa Cruz Biotechnology Inc.) or
161 anti-c-Jun (H-79) (1:1000, sc-1694 Santa Cruz Biotechnology Inc.) overnight, washed and incubated
162 with HRP-conjugated donkey anti-rabbit IgG secondary antibody (1:3000), and detected by
163 chemiluminescence (Pierce ECL2 western blotting substrate, Thermo Scientific) using the Typhoon
164 imaging system. After extensive washing, the membrane was incubated with anti-Histone H3 antibody
165 (ab1691, 1:10000; abcam) as loading control. All Western blots were run in triplicate and bands were
166 quantitated in 1 representative gel. Quantification was done using ImageJ software.

167

168 **Isolation of fixed mouse muscle stem cells and real-time PCR**

169 For empirical analysis of genes by RT-qPCR (e.g. *Jun* and *Fos*), skeletal muscles were fixed
170 immediately in 0.5% for 1 h in paraformaldehyde (PFA) using a protocol based on the notion that
171 transcripts are stabilized by PFA fixation [17](P. Mourikis and F. Relaix, personal communication).
172 Briefly, PFA fixed and unfixed skeletal muscles were minced as described [4], fixed samples were
173 incubated with collagenase at double the normal concentration and mRNA was isolated following
174 FACS based on size, granularity and GFP levels using a FACS Aria II (BD Bioscience). Total RNA
175 was extracted from fixed cells with RecoverAll™ Total Nucleic Acid Isolation Kit Ambion,
176 ThermoFisher), according to manufacturer instructions. cDNA was prepared by random-primed
177 reverse transcription (Super-Script II, Invitrogen, 18064-014), and real-time PCR was done using
178 SYBR Green Universal Mix (Roche, 13608700) StepOne-Plus, Perkin-Elmer (Applied Biosystems).
179 Specific primers for each gene were designed, using the Primer3Plus online software, to work under
180 the same cycling conditions. For each reaction, standard curves for reference genes were constructed

181 based on six 4-fold serial dilutions of cDNA. All samples were run in triplicate. The relative amounts of
182 gene expression were calculated with RPL13 expression as an internal standard (calibrator). The
183 following primers were used:

184 Atf3 (Fw:TTGTTTCGACACTTGGCAGC, Rv:TAAACACCTCTGCCATCGGA);
185 BMP6(Fw:TCACCACCCACAGATTGCTA, Rv:ACTGTGTGGTGGGGAGTTTT);
186 Btg1(Fv:GCGGTGTCCTTCATCTCCAA, Rv:GTAACCTGATCCCTTGCACG);
187 Btg2(Fw:ACCTTGCTGATGATGGGGTC, Rv:GGGTTTCCTCTCCAGTCTCC);
188 Nr4a1(Fw:GAGGCTGCTTGGGTTTTGAA, Rv:AAAGCGCCAAGTACATCTGC);
189 CalcitoninR(Fw:ATGAGGTGCAAGTCACCCTG, Rv:ACTAACTACGCGGTTGGTGG);
190 Pax7(Fw:GACAAAGGGAACCGTCTGGAT, Rv:TGTGAACGTGGTCCGACTG),
191 c-Jun (Fw:CCTTCTACGACGATGCCCTC, Rv:GGTTCAAGGTCATGCTCTGTTT),
192 MyoD (Fw:CACTACAGTGGCGACTCAGATGCA, Rv:CCTGGACTCGCGCGCCGCCTCACT);
193 c-Fos(Fw:CGGGTTTCAACGCCGACTA, Rv:TTGGCACTAGAGACGGACAGA);
194 Jun B (Fw:TCACGACGACTCTTACGCAG, Rv:CCTTGAGACCCCGATAGGGA);
195 Jun D (Fw:GAAACGCCCTTCTATGGCGA, Rv:CAGCGCGTCTTTCTTCAGC);
196 RPL13(Fw:GTGGTCCCTGCTGCTCTCAAG, Rv:CGATAGTGCATCTTGGCCTTTT).

197

198 **Normalisation, quality control and filtering**

199 GEPs were processed using standard quality control tools to obtain normalised, probeset-level
200 expression data. For all raw datasets derived from affymetrix chips, Robust Multi-Array Average
201 expression measure (rma) was used as normalization method using the *affy* and the *oligo* R packages
202 [18][19]. All analyses were preferentially conducted at the probeset level. Probesets were annotated to
203 gene symbol and gene ENTREZ using chip-specific annotations. For gene level results, the probeset
204 with the highest expression variability was selected to represent the corresponding gene. Quality
205 controls were performed on raw data using Relative Log Expression (RLE) and Normalised Unscaled
206 Standard Errors (NUSE) plots from the *affyPLM* R package [20]. Sample distribution was examined
207 using hierarchical clustering of the Euclidean distance and Principal Component Analysis from the
208 *stats* [21] and *FactoMineR* R packages [22] (See Additional file 1: Fig. S1 for the resulting plots for
209 dataset Quiescent [high/low] / D3Activated [high/low]). The resulting plots of the remaining datasets

210 are not shown but they show similar trends, which can be explored through the interactive webserver
211 Sherpa.

212

213 ***Differential gene level analysis***

214 Statistically differentially expressed genes (DEGs) were identified between the ASC and the QSC
215 groups using the linear model method implemented in the *Limma* R package [23]. The basic statistic
216 was the moderated t-statistic with a Benjamini and Hochberg's multiple testing correction to control the
217 false discovery rate (FDR) [24].

218

219 ***Individual and multiple gene-set analyses***

220 Each dataset was tested for gene set enrichment independently. The gene set analysis was based on
221 three gene set collections from the mouse version of the Molecular Signatures Database MSigDB v6.0
222 [25][26]: 1) Hallmark gene sets (H), which summarize and represent specific well-defined biological
223 states or processes displaying a coordinate gene expression, 2) KEGG canonical pathways (C2
224 CP:KEGG), derived from the Kyoto Encyclopedia of Genes and Genomes [27] and 3) Reactome
225 canonical pathways (C2 CP:Reactome) from the curated and peer reviewed pathway database [28].
226 To test for the enrichment of these gene sets, we used the competitive gene set test CAMERA from
227 the *Limma* R package [23], which takes into account the inter-gene correlation [29]. For multi-set
228 analysis, the ensemble of the gene level and gene-set level results from the individual datasets was
229 examined to produce a consensus gene signature and a consensus list of gene sets that describe the
230 quiescent state of MuSCs.

231

232 ***Gene level analysis***

233 The combinatorial landscape of datasets was explored using the *SuperExactTest* [30] and the *UpSetR*
234 [31] R packages to visualize and test the intersection of the datasets. Additionally, the Jaccard index
235 [32] of similarity was calculated to assess the extent of similarity between DEGs of each pair of
236 datasets. A significance ranking was calculated for each individual dataset to determine its presence
237 or absence in the final dataset ensemble, which was used for determining the gene signature. Once
238 the dataset ensemble was defined, the overlapping differentially up and down-regulated genes (DEGs,
239 as defined by the adjusted p-value ≤ 0.05) were used to build the quiescent signature.

240 **Gene set level analysis**

241 Two approaches were used to assess the agreement of enriched gene sets across the ensemble of
242 datasets. First, an over representation analysis (ORA) [33] by a one-sided Fisher's exact test
243 implemented in R script with a Benjamini and Hochberg's multiple testing correction of the p-value.
244 This ORA was performed using the DEGs from the quiescent signature was performed using the
245 Hallmark, Kegg and Reactome gene sets. Then, the individual results from the functional scoring
246 method (FSC) [33] CAMERA [29] were compared to identify gene sets common to all the datasets in
247 the ensemble and the directionality of the enrichment (of over or under expressed genes).

248

249 **Web application: Sherpa**

250 We developed an interactive web application for the exploration, analysis and visualization of the
251 individual datasets and their combination (<http://sherpa.pasteur.fr>). This application allows the user to
252 effectively and efficiently analyse the individual datasets one by one (individual dataset analysis) or as
253 an ensemble of datasets (multi-set analysis) and was developed with the *Shiny* R package [34].

254

255

256 **Results**

257 This study consists of an individual dataset analysis followed by a multi-set analysis (Fig. 1). First,
258 each raw dataset was normalised, filtered and subjected to the same quality controls and checks.
259 Gene level differential analysis and gene set analysis were then performed (Fig. 2). Finally, a multi-set
260 analysis assembled a platform-independent list of genes specific to the quiescence state. When
261 analysing multiple microarray GEPs, however, several issues needed to be addressed regarding the
262 experimental set-up, the microarray platforms and the laboratory conditions [35]. First, the individual
263 studies, even if related, had different aims, experimental designs and cell populations of interests (e.g.
264 developmental stage, and gender of mice). Second, the different microarray platforms contained
265 different probes and probesets with specific locations and alternative splicing that might produce
266 different expression results [36]. Finally, sample preparation, protocols and dates of extractions might
267 have influenced array hybridization and introduced bias [37]. This experimental heterogeneity required
268 critical data processing to ensure statistically meaningful assumptions to drive biological interpretation
269 and compile gene signatures. Table 1 summarizes the main biological and experimental variations in

270 this study, as well as the technical differences present in the datasets.

271

272 Three new sets of microarrays of quiescent versus activated satellite cell are reported here (see Table
273 1). The first one is part of a developmental and postnatal series that was reported previously [15]
274 (E12.5 vs. E17.5), and here P8 (postnatal day 8, *in vivo* proliferating) and 4-5 week old (quiescent)
275 mice were compared. The second one is based on previously reported differences in quiescent and
276 proliferating cell states in subpopulations of MuSCs (*Quiescent*: dormant, top 10% GFP+ cells vs.
277 primed, bottom 10% GFP+ cells isolated from *Tg:Pax7-nGFP* mice; *Proliferating*: 3 days post-injury
278 [3]). The third dataset is based on previous observations that the *Notch* intracellular domain (NICD)
279 when expressed constitutively (*Myf5^{Cre}: R26^{stop-NICD}*) in prenatal muscle progenitors leads to cell-
280 autonomous expansion of the myogenic progenitor population (Pax7+/Myod-) and the absence of
281 differentiation, followed by premature quiescence at late foetal stages (E175) [15]. Here, E17.5
282 (quiescent) and E14.5 (proliferating) prenatal progenitors were compared. Except for our datasets
283 *Quiescent(adult)/Activated(P8)* and *Foetal_NICD[E17.5/E14.5]*, all the studies were conducted on
284 adult mice (male and female) with ages ranging from 8 weeks to 6 months.

285

286 While all datasets shared similar cell states (quiescent (QSC) and activated (ASC) satellite cells), the
287 experimental procedures varied between studies. Activation of cells, for instance, was achieved in
288 different ways: i) *in vitro*, by culturing freshly isolated MuSCs in culture for several days, ii) *in vivo*, by
289 extracting ASCs from an injured muscle. Furthermore, for *in vivo* activation, several techniques were
290 used to induce the injuries: BaCl₂, or the snake venoms cardiotoxin or notexin. Cell extraction
291 protocols also varied among the different studies: i) using transgenic mice expressing a reporter gene
292 that marks satellite cells (several alleles) and ii) using a combination of antibodies targeting surface
293 cell antigens specific to satellite cells (several combinations, see Table 1). Finally, the nine datasets
294 examined in this study date from 2007 to 2016. During this period, microarray technologies evolved
295 and the different chips available may introduce yet another source of variation among the compared
296 datasets. This experimental heterogeneity required critical data processing to ensure statistically
297 meaningful assumptions driving biological interpretations and gene signatures.

298

299

300 **The number of differentially expressed genes varies significantly among different datasets**

301 A total of 32 samples from ASCs and 34 samples from QSCs from the nine datasets were analysed.
302 After the quality control, one sample from the GSE38870 dataset was considered to be an outlier and
303 was not included in the final analysis.

304
305 The number of significantly up and down regulated genes (DEGs) resulting from the differential
306 expression analysis of the quiescent with respect to the activated states were noted (Additional file
307 2:Table S1). DEGs were identified as having $|\logFC| \geq 1$ and a false discovery rate $FDR \leq 0.05$.
308 The statistical analysis was performed at the probeset level, and only those probesets matching to
309 genes are reported. On average, the datasets exhibited 1548 up-regulated genes with a standard
310 deviation of 1173 genes. The down-regulated genes were 2122, with a standard deviation of 1658
311 genes. The lowest number of DEGs was the reported in the *Foetal_NICD[E17.5/E14.5]* dataset (39
312 up, 136 down), while the highest number of DEGs belongs to the GSE70376 dataset (4367 up, 6346
313 down). Additionally, an analysis of the distribution of the logFC across the datasets revealed that there
314 were significant differences among the ranges and shapes of such distributions for each dataset
315 (Additional file 3: Fig. S2).

316
317 **Gene-set level analysis reveals common underlying biological processes across the datasets**

318 Despite the great difference among the number of DEGs for the different sets, clear trends among the
319 significantly enriched pathways were found (Fig. 3A). The heatmap shows each dataset as a column
320 and each gene set tested for enrichment as a row. The gene set collection shown corresponds to the
321 Hallmark gene set collection from MSigDB [38]. Over-represented gene sets are shown in red, while
322 under-represented gene sets are shown in blue. Out of the 11 datasets, GSE38870 stood as an outlier
323 for both over and under-represented gene sets. For the rest of the 10 datasets, most of them showed
324 an enrichment of the quiescent state for the TNFA_SIGNALING_VIA_NFKB pathway (9 datasets),
325 while 8 datasets are enriched in UV_RESPONSE_DN, IL6_JAK_STAT3_SIGNALING,
326 APICAL_SURFACE and KRAS-SIGNALING_DN pathways. Similarly, the 10 datasets share the same
327 trends of under-represented pathways MYC_TARGETS_V1, E2F_TARGETS, G2M_CHECKPOINT,
328 and OXYDATIVE_PHOSPORylation, which are expected to be absent in the quiescent state. Fig.
329 3B shows a network representation of the top 3 most common over (TNFA_SIGNALING_VIA_NFKB,

330 UV_RESPONSE_DN, IL6_JAK_STAT3_SIGNALING) and under-represented gene sets
331 (MYC_TARGETS_V1, E2F_TARGETS, G2M_CHECKPOINT), together with those gene sets which
332 share common genes with them. The size of each node is proportional to the number of genes in the
333 gene set, and the thickness of the edges is proportional to the number of genes shared among the
334 connected gene sets. Gene sets having less than 10% of their genes in common are not shown. Two
335 subnetworks corresponding to 8 under and 15 over-represented gene sets can be clearly
336 distinguished. In Fig. 3B, we see that different gene sets have a varying number of genes in common,
337 if the gene overlap is large, those gene sets (and their corresponding biological functions) will likely be
338 also affected (i.e. activated or repressed). For the 3 most common under represented gene sets, for
339 example, we see that gene set MYC_TARGETS_V1 shares most of its genes with gene sets
340 E2F_TARGETS and G2M_CHECKPOINT, thus, this suggests that three functions represented by
341 these gene sets have an interplay of genes that displays them as all under represented. The size of
342 the gene sets will also affect this interplay, e.g. over-represented gene set UV_RESPONSE_DN is a
343 relatively small gene set, hence its sharing of genes with other gene sets, especially larger ones such
344 as KRAS_SIGNALING_DN and BILE_ACID_METABOLISM, is less functionally relevant.

345

346 **Determining a quiescent transcriptional signature among all datasets**

347 Our strategy to determine a consensus quiescent signature from the datasets was to compare the
348 genes found to be differentially expressed within each dataset, in order to identify genes commonly up
349 or down regulated in the quiescent state. Although the aforementioned technical and experimental
350 heterogeneity could introduce noise in this analysis, such variation was distinguishable from the more
351 stable, underlying common quiescent signature. Given that the distribution and ranges of the logFCs
352 varied so drastically between datasets (Fig. S2), a single FC threshold could not be chosen to be used
353 for all datasets. Thus, for the combinatorial analysis approach, having the goal of maximizing the
354 number of differentially expressed genes common to all the datasets considered, only the adjusted p-
355 value was used as threshold to define DEGs. Even in this low constrained set-up, combining all the
356 datasets together resulted in very few overlapping genes found: 12 up (*Arntl*, *Atf3*, *Atp1a2*, *Cdh13*,
357 *Dnajb1*, *Enpp2*, *Ier2*, *Jun*, *Nfkbiz*, *Rgs4*, *Usp2*, *Zfp36*) and 1 down (*Igfbp2*). Alternatively, if certain
358 datasets were excluded from the analysis, the number of DEGs increased (Fig. 4a).

359

360 **Combinatorial assessment of datasets according to significance and similarity criteria**

361 To find the best combination of datasets defining a consistent and sufficiently large quiescent
362 signature, we ranked them according to their significance. First, the dataset should have a minimum
363 number of DEGs. Our *Foetal_NICD[E17.5/E14.5]* dataset, for instance, had only 250 DEGs (Table
364 S1), and using it in the analysis resulted in a dramatically low number of overlapping DEGs. Indeed,
365 Fig. 4a shows that when this dataset was included, regardless of the number of combined datasets,
366 the extent of the overlap was always very low. A second criterion was the presence of genes known to
367 be differentially expressed between quiescent and activated states from previous studies. In this case,
368 datasets GSE38870 and GSE81096 had to be excluded, since they lacked *CalcR Bmp6, notch1* and
369 *Chrdl2, Klf9, Lama3, Pax7, Bmp6* genes, respectively. Besides these two criteria, others can be used
370 to assess the significance of the datasets. Choosing the datasets according to the activation or
371 extraction method of the cells, for example, would result in a more stringent ensemble of datasets.

372

373 Dataset similarity was assessed using the Jaccard Index (JI) and a matrix of the JIs for the up and
374 down regulated genes was generated (Figs. 4b, c, respectively). In both matrices, the closest pairs of
375 datasets were GSE47177 at 60 hours and GSE47177 at 84 hours (JI = 0.46 and 0.44 for the up and
376 down regulated genes, respectively), followed by the second pair of closest sets Quiescent [high] /
377 D3Activated [high] and Quiescent [low] / D3Activated [low] (JI = 0.39 and 0.33, for up and down
378 regulated genes, respectively). The fact that the first two closest datasets belong to the same study
379 highlights the effect of technical biases. The hierarchical clustering of the Euclidean distance of the
380 Jaccard indexes shows that for up and down regulated genes, the datasets
381 *Foetal_NICD[E17.5/E14.5]*, GSE38870 and GSE81096 had a tendency to not group with the rest of
382 the datasets.

383

384 Taking into account the dataset significance (based on number of DEGs and presence of some
385 reported quiescent markers) and the low extent of overlap between *Foetal_NICD[E17.5/E14.5]*,
386 GSE38870 and GSE81096 datasets with respect to the remaining datasets, these three datasets were
387 excluded from the multi-dataset analyses. The final ensemble comprised the eight remaining datasets
388 which had 207 and 542 genes commonly up and down regulated, respectively. To further characterise
389 these commonly regulated genes, we performed an over-representation analysis (ORA) of the gene

390 sets. An enrichment was detected for the 207 commonly up-regulated genes in seven different
391 Hallmark gene-sets (Fig. 5a). Some genes were shared among different pathways (e.g. *Atf3* and *IL6*
392 were found in six different gene-sets), while others were found in one gene-set only (e.g. *Tgfb3*,
393 *Spsb1*). These results are consistent with the individual gene set enrichment analysis (see Fig. 3)
394 emphasizing that these genes reflect the global traits associated with the quiescent state. Notice that
395 only a fraction of these 207 genes is found in known existing gene sets (57/207), leaving about three
396 quarters of the commonly up regulated genes not associated with any existing gene set. This is not
397 unexpected given that a quiescent signature is still to be determined and thus current gene-sets lack
398 such annotations. To facilitate the analysis of transcriptomes as described here, we have developed
399 an online interactive tool called *Sherpa* (Fig. 6). *Sherpa* allows users to perform analyses on individual
400 and on multiple datasets. Each individual dataset analysis involves the identification of differentially
401 expressed genes, comparison of the expression of selected genes in the quiescent and activated
402 states using heatmaps, exploration of the distribution of the samples according to their variability
403 through Principal Component Analysis, and cluster analysis. The multiple dataset analysis allows the
404 comparison of selected datasets according to the commonly differentially expressed genes. All these
405 analyses are interactive, as they allow the user to select the thresholds of fold change (logFC) and
406 false discovery rate (adj. P-value).

407
408 To assign a global function to the commonly regulated genes, we annotated them using GOSlim
409 terms, which summarize broad terms based on Gene Ontology terms [39]. To identify categories of
410 genes, heatmaps of the logFC in the different datasets for a subset of the 207 UP genes belonging to
411 extracellular matrix, nucleic acid binding activity (+/- cell cycle proliferation) and signal transduction
412 activity were generated (Fig. 5b). Unexpectedly, genes associated with cell cycle proliferation were up-
413 regulated in the quiescent cell analyses, such as *c-Fos*, *c-Jun*. To verify the expression level of these
414 genes in quiescent cells, we used a protocol to isolate MuSCs in which a short fixation (PFA)
415 treatment was performed prior to harvesting the cells to arrest *de novo* transcription during the
416 isolation protocol (see Methods). Then, expression level quantification for certain genes both at the
417 mRNA (RT-qPCR) and the protein (western blot) levels was conducted at different time points after
418 isolation. Notably, quantification of *c-Jun*, *Jun B* and *Jun D* show clearly that at time 0 (+PFA), these
419 genes are not detected in quiescent cells, neither at the mRNA level (right panel), nor at the protein

420 level (left panel) (Fig 7a). As expected, these genes were upregulated using conventional protocols
421 that take several hours to isolated MuSCs by FACS, followed by a rapid downregulation (Fig. 7a, b),
422 before being upregulated again as MuSCs engage in the cell cycle (data not shown).

423

424 **Discussion**

425 The last decades have witnessed many efforts to analyse microarray data to provide relevant gene
426 signatures. In cancer biology, for example, gene markers were sought either for prognosis, i.e. lists of
427 genes able to predict clinical outcome [40] or for molecular subtyping, i.e. list of genes able to classify
428 different subtypes of a disease [41][42]. However, even if markers performed well, gene signatures
429 derived from studies on the same treatments and diseases often resulted in gene lists with little
430 overlap [43]. In other cases, the signatures proved to be unstable, having other gene lists on the same
431 dataset with the same predictive power [44]. These observations suggest that such signatures may
432 include causally related genes, i.e. downstream of the phenotype causing genes and that these gene
433 lists may share the same biological pathways [45].

434

435 Gene Set Enrichment Analysis (GSEA) has become an efficient complementary approach for
436 analysing *omic* data in general and GEPs in particular [46][45][47]. It shifts the expression analysis
437 from a *gene* space to a *gene-set* space, where genes are organized into gene sets according to a
438 common feature, such as a functional annotation (e.g. a Gene Ontology term) or a specific metabolic
439 pathway (e.g. a KEGG pathway). In this way, it incorporates previously existent biological knowledge
440 to drive and increase interpretation, while offering greater robustness and sensitivity than gene level
441 strategies [45][48][49].

442

443 The transcriptome analysis and pipeline, as well as the *Sherpa* interface that we describe here, allow
444 multiscale comparisons across divergent datasets that are heterogeneous in platform and biological
445 condition. Notably, examination of 11 datasets, including 3 novel transcriptomes from our work point to
446 a variety of gene sets that appear in different GO categories. Some markers such as *CalcR*,
447 *Teneurin4* (*Tenm4*), and stress pathways were identified previously [50][51][11]. However, we also
448 report that virtually all datasets contained genes that would be expected to be present during
449 activation or cell cycle entry, such as members of the *Fos* and *Jun* family [52]. Using a novel isolation

450 protocol (P. Mourikis, F. Rélaix, personal communication) based on the notion that tissues that are
451 fixed prior to processing result in stabilized mRNA [17], we validated the expression of *CalcrR* and
452 *Bmp6* as true quiescent markers. In contrast, we show that *Fos* and *Jun* transcripts, and *Jun* family
453 proteins are not present at significant levels *in vivo*, but are robustly induced within 5 hours, the
454 average processing time taken for isolation by FACS of MuSCs. We propose that these and other
455 stress response genes mitigate the quiescent to activation transition that accompany the initial steps
456 of exit from G0.

457

458 Given these unexpected findings, it would be important to compare transcriptomes of MuSCs from a
459 fixed/*in vivo* state with those that were described here to delineate homeostatic vs. immediate early
460 response genes. Beyond the present findings, we propose that all transcriptome data obtained from
461 cells isolated from solid tissues, which require extensive enzymatic digestion and processing before
462 isolation of RNA, need to be re-evaluated to distinguish those genes that are expressed during the
463 isolation procedure.

464

465 In addition to making this compendium of GEPs available to the community, we provide a
466 standardized pipeline that sets the basis for a multi-set analysis for an effective and systematic
467 comparison of individual datasets. Analysing multiple datasets provides generalized information
468 across different studies [36][53]. The cancer field was a pioneer in combining several works [54] [55]
469 and other fields, such as neurodegenerative diseases [56][57] and regulatory genomics have
470 successfully adopted this strategy [58]. The multidimensional approach presented here offers i)
471 increased power, due to the higher sample size and ii) increased robustness, by highlighting variations
472 in individual studies results [35][59]. Such variations are a consequence of the high level of noise and
473 artefacts, and are typically associated with microarray data [60].

474

475

476

477

478

479

480 **Acknowledgments**

481 We would like to thank K. Soni and U. Borello for their assistance during this work, and P. Mourikis
482 and F. Relaix for communicating unpublished results and sharing protocols. We also acknowledge the
483 Flow Cytometry Platform of the Technology Core-Center for Translational Science (CRT) at Institut
484 Pasteur for support in conducting this study and the microarray platform at Institut Cochin. S.T. was
485 funded by Institut Pasteur, Centre National pour la Recherche Scientific and the Agence Nationale de
486 la Recherche (Laboratoire d'Excellence Revive, Investissement d'Avenir; ANR-10-LABX- 73) and the
487 European Research Council (Advanced Research Grant 332893). None of the authors have any
488 competing interests in the manuscript.

489

490

491

492

493

494

495

496

497

498

499

500

501

502

503

504

505

506

507

508

509 Figure and Table Legends

Ref/Code	Quiescent [high/low] 3D Activated [high/low]	Quiescent Activated	Foetal R26 ^{NICD} [E17.5/E14.5]	GSE47177 Liu et al [9]	GSE3483 Fukada et al [10]	GSE15155 Pallafacchina et al [11]	GSE38870 Farina et al. [12]	GSE70376 García-Prat et al. [13]	GSE81096 Lukjanenko et al. [14]
Num. of samples	3 QSC_Pax 7 low, 3 ASC_Pax 7 low, 3 QSC_Pax 7 high, 3 ASC_Pax 7 high	3 QSC, 3 P8_ASC	3 eq_QSC, 3 eq_ASC	3 QSC, 3 ASC 60h, 3 ASC 84h	3 QSC, 3 ASC	3 QSC, 3 ASC	3 QSC, 3 ASC	4 QSC, 4 ASC	6 QSC, 5 ASC
Date	2013	2007	2015	2013	2007	2010	2012	2015	2016
Anatomy	Tibialis anterior	Limb, bodywall, diaphragm	Hindlimb	Hindlimb	Hindlimb	Diaphragm, pectorales, abdominal muscles	Tibialis anterior	Tibialis anterior	Tibialis anterior, gastro-necmius, quadriceps
Sex	M		M,F	M	F	M,F	F	M	M
Age	6-8 w	P8, 4-5 w	E14.5, E17.5	8 w	8-12 w	6 w	3-6 m	Young: 3 m, old: 20-24 m	Young: 9-15 w, old: 20-24 m
Strain	C57BL/6	B6.129		C57BL/6 (Jackson)	C57BL/7 (nihon clea)		C57BL/6 x DBA2 (??)	C57BL/6	C57BL/6 (Janvier)
Reporter	Tg:Pax7-nGFP (10% high, 10% low)	Pax7 ^{nGFP/+}	Myf5 ^{Cre+} ; R26 ^{stop-NICDgfp/+}	Pax7 ^{CreER/+} R26 ^{eYFP/+}		Pax3 ^{GFP/+} (high GFP)			
Activation	Notexin	P8 = "Activated"	E14.5 = "Activated"	BaCl ₂	QSCs in culture for 4 d	Pax3 ^{GFP/+} , Pax3 ^{GFP/+} :mdx :mdx Adult; Adult mdx; 1 w old; 3 d in culture	Injury: BaCl ₂ (50µL 1.2%)	Cardiotoxin	Cardiotoxin
QSCs Purif.	Reporter	Reporter	Reporter	FACS: Pax7 ^{CreER/+} ; R26 ^{eYFP/+}	FACS: CD45-/SM/C-2.6+	Reporter	FACS: Syndecan-3	FACS: integrin-alpha7+ /Lin-/CD31-/CD45-/CD11b-/Sca1-	CD34+/ integrin-alpha7+/Lin-
Timing	quiescent & 3 d post-injury		See age	36h (1.5d), 60h (2.5 d), 84h (3.5d) post-injury	4 d in culture	3 d in culture	12h or 48h post-injury	72h (3d)	72h (3d)
Platform	Affymetrix Mouse Gene 1.0ST	Affymetrix 430_2.0	Affymetrix Mouse Gene 1.0ST, Affymetrix Mouse Gene 2.0ST	Affymetrix Mouse Gene 1.0ST	Affymetrix 430A	Affymetrix 430_2.0	Affymetrix 430_2.0	Agilent 028005 SurePrint G3Mouse 8x60k Microarray	Illumina MouseRef-8 v2.0

510
511
512
513
514
515
516
517
518
519
520
521
522
523
524
525
526
527
528
529
530
531
532
533
534
535
536
537
538
539
540

Table 1. Summary of analysed transcriptomic datasets of activated and quiescent states of mouse muscle stem (satellite) cells. Three high-throughput experimental setups and six publically available microarray datasets comparing activated satellite cells (ASCs) and quiescent satellite cells (QSCs) are shown in the rows. The biological, experimental and technical details of each experiment are shown in the different columns of the Table. (h=hours, d=days, w=weeks, m=months).

Fig. 1. General framework of the analysis: an individual dataset analysis followed by a multi-set analysis. The individual dataset analysis consisted of: i) the analysis of gene expression profiles (GEPs) of each dataset, including normalisation, filtering and quality control check of each raw dataset, and the differential analysis to identify dataset-specific differentially expressed genes (DEGs); ii) the Gene set analysis (GSA) performed in the gene-set space. The GSA consisted in identifying enriched pathways from three gene sets of the MSigDB collection[26] (Hallmark gene sets, CP:KEGG gene sets and CP: Reactome gene sets); iii) a multi-set analysis to assemble a study-independent gene signature, i.e. a list of genes specific to the quiescence state.

Fig. 2. Workflow of the standardized individual dataset analysis. The analysis of the nine datasets was performed in a consistent manner for each dataset using ad-hoc R scripts. It included a first step of data preparation followed by a second step of data analysis. GEPs were processed using standard quality control tools to obtain normalised, probeset-level expression data. For raw datasets derived from affymetrix chips, Robust Multi-Array Average expression measure (rma) was used as normalization method. All analyses were conducted at probeset level. Probesets were annotated to gene symbol and gene ENTREZ using chip-specific annotations. Quality controls were performed on raw data using RLE and NUSE plots. The distribution of the QSC and ASC samples according to their GEPs was explored using hierarchical clustering of the Euclidean distance and Principal Component Analysis (Additional file 1: Figure S1). Statistically differentially expressed genes (DEGs) were identified between the ASC and the QSC groups using the linear model implemented by the Limma R package [10]. Gene set analysis was based on three gene set collections from the mouse version of the Molecular Signatures Database MSigDB v6.0 [12][13]: 1) Hallmark, which summarizes and represents specific well-defined biological states or processes displaying a coordinate gene expression, 2) KEGG canonical pathways, derived from the Kyoto Encyclopedia of Genes and

541 Genomes [14] and 3) Reactome canonical pathways from the curated and peer reviewed pathway
542 database [15]. To test for the enrichment of these gene sets, the competitive gene set test CAMERA
543 [16] was used.

544

545 **Fig. 3 Enriched gene sets across individual datasets.** Over-represented gene sets are shown in
546 red; under-represented gene sets are shown in blue. a) Gene set enrichment profiles using the
547 Hallmark gene set collection from MSigDB[25], each row corresponds to a gene-set, and each column
548 corresponds to a dataset. b) Network representation of 3 most common over and under-represented
549 gene-sets along with gene-sets sharing genes with them. Nodes represent gene-sets with a node size
550 proportional to the gene-set size. Edges indicate that genes are shared among the gene-sets.
551 Thickness of the edge is proportional to the number of shared genes.

552

553 **Fig. 4. Different combinatorial landscapes result in different degrees of stringency for the list of**
554 **genes defining the quiescent state of MuSCs.** a) Barplot indicating the number of overlapping
555 differentially expressed genes (DEGs) for each best combination of intersections, from degree 2 to 11.
556 The dots underneath the barplot indicate the datasets included in the intersections. The total number
557 of up (UP) and down (DOWN) DEGs for each dataset are indicated in light grey and dark grey,
558 respectively. b) and c) are colored matrices showing the Jaccard index between each pair of datasets,
559 for UP DEGs and DOWN DEGs, respectively. Dendrograms show the hierarchical clustering using the
560 Jaccard index as euclidean distance.

561

562 **Fig. 5. Gene expression of differentially expressed genes (DEGs) in MuSCs.** a) Binary heatmap
563 of the over representation analysis. Each column represents one enriched (over-represented) gene-
564 set, and each row corresponds to a gene. Red cells indicate the presence of the corresponding gene
565 in a given gene set. b) Network representation of 39 GOSlim terms used to characterize the commonly
566 regulated genes in MuSCs. Nodes represent gene-sets with a node size proportional to the gene-set
567 size. Edges indicate that genes are shared among the gene-sets. Thickness of the edge is
568 proportional to the number of shared genes. Also shown are the heatmaps of logFC for genes
569 belonging to extracellular matrix, nucleic acid binding and cell cycle and proliferation, nucleic acid
570 binding and signal transduction activity, respectively. Each row corresponds to a gene and each

571 column corresponds to a dataset. Dendrograms show hierarchical clustering using the euclidean
572 distance.

573

574 **Fig. 6. Snapshot of the interactive web application for transcriptomic data exploration and**
575 **comparison.** *Sherpa* (<http://sherpa.pasteur.fr>) allows users to perform individual dataset and multiple
576 dataset analysis. In the individual dataset analysis (shown), the user chooses the dataset for which the
577 analysis is to be performed. Then, it is possible to identify differentially expressed genes (e.g. Volcano
578 plot), compare the expression of selected genes in the quiescent and activated state (e.g heatmap, as
579 shown in Figure), the distribution of the samples according to their variability (Principal Component
580 Analysis). All these analyses are interactive, as they allow the user to set the thresholds of fold change
581 (logFC) and false discovery rate (adj. P-value).

582

583 **Fig. 7. Direct comparison of fixed and unfixed MuSCs identify *Fos* and *Jun* as immediate**
584 **response genes not present the in vivo state.** a) *c-Jun*, *Jun B* and *Jun D* protein levels from MuSCs
585 at 0, 5, 10, 15h after isolation (with and without PFA treatment) were measured by Western blotting
586 and band intensities were quantified by densitometric analysis with the ImageLab software (right).
587 Basal levels of *c-Jun*, *Jun B* and *Jun D* mRNA from MuSCs at 0, 5, 10, 15h after isolation (with and
588 without PFA treatment) were measured by real-time PCR (left). b) Fold change of mRNA (log₁₀)
589 between 0h+PFA and 5h (with and without PFA treatment).

590

591

592 **Supplementary Table and Figure Legends**

593 **Fig. S1. Quality controls and data sample distribution for Quiescent [high/low] / D3Activated**
594 **[high/low] dataset.** a) Relative Log Expression (RLE) and b) Normalised Unscaled Standard Errors
595 (NUSE) plots for the D3P7 dataset show that as expected for good quality data, RLE median values
596 are centered around 0.0 while the median standard error should be 1 for most genes in the NUSE
597 plots. Sample distribution is distributed according to status (D3H: activated, high; D3L: activated, low;
598 QH: quiescent, high; QL: quiescent, low) using c) Principal Component Analysis and d) hierarchical
599 clustering of the Euclidean distance .

600

601 **Fig. S2. Violin plots of the logFC distribution for each individual dataset.** Density plots of the
602 logFC ($|\logFC| < 1$ in red; $|\logFC| > 1$ in blue).

603

604 **Table S1. Identified differentially expressed genes in the quiescent satellite cell condition for**
605 **the 9 datasets**

606

607 **Additional Material**

608 File name: Additional_file1_FigureS1.pdf

609 File format: .pdf

610 Title of data: Quality controls and data sample distribution for Quiescent [high/low] / D3Activated
611 [high/low] dataset.

612 Description of data: a) Relative Log Expression (RLE) and b) Normalised Unscaled Standard Errors

613 (NUSE) plots for the D3P7 dataset show that as expected for good quality data, RLE median values

614 are centered around 0.0 while the median standard error should be 1 for most genes in the NUSE

615 plots. Sample distribution is distributed according to status (D3H: activated, high; D3L: activated, low;

616 QH: quiescent, high; QL: quiescent, low) using Principal Component Analysis (c) and hierarchical

617 clustering of the Euclidean distance (d).

618

619 File name: Additional_file2_TableS2.xlsx

620 File format: .xlsx

621 Title of data: Identified differentially expressed genes in the QSCs condition for the 9 datasets

622 Description of data: Differentially expressed genes in the QSCs condition for the 9 datasets using

623 $\logFC = 1$ and $FDR = 0.05$.

624

625 File name: Additional_file3_FigureS2.pdf

626 File format: .pdf

627 Title of data: Violin plots of the logFC distribution for each individual dataset

628 Description of data: Density plots of the logFC ($|\logFC| < 1$ in red; $|\logFC| > 1$ in blue).

629

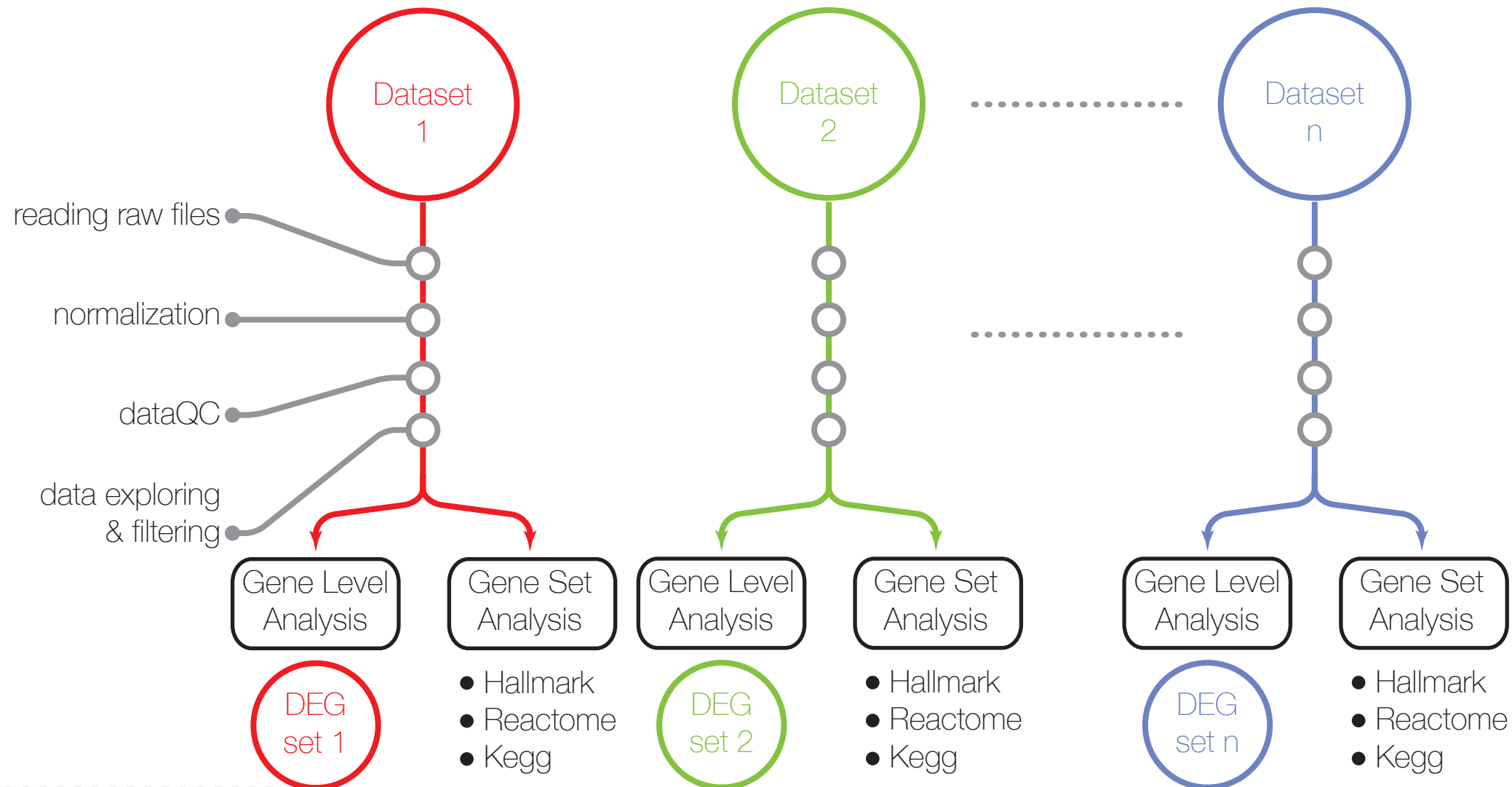
630 **Bibliography**

- 631 [1] Li L, Clevers H. Coexistence of quiescent and active adult stem cells in mammals.
632 *Science* 2010; 327: 542–545.
- 633 [2] Sambasivan R, Gayraud-Morel B, Dumas G, et al. Distinct regulatory cascades govern
634 extraocular and pharyngeal arch muscle progenitor cell fates. *Dev Cell* 2009; 16: 810–821.
- 635 [3] Rocheteau P, Gayraud-Morel B, Siegl-Cachedenier I, et al. A subpopulation of adult
636 skeletal muscle stem cells retains all template DNA strands after cell division. *Cell* 2012; 148:
637 112–125.
- 638 [4] Gayraud-Morel B, Pala F, Sakai H, et al. Isolation of Muscle Stem Cells from Mouse
639 Skeletal Muscle. *Methods Mol Biol Clifton NJ* 2017; 1556: 23–39.
- 640 [5] Network TCGAR, Weinstein JN, Collisson EA, et al. The Cancer Genome Atlas Pan-
641 Cancer analysis project. *Nat Genet* 2013; 45: 1113–1120.
- 642 [6] Taccioli C, Maselli V, Tegnér J, et al. ParkDB: a Parkinson’s disease gene expression
643 database. *Database*; 2011. Epub ahead of print 1 January 2011. DOI:
644 10.1093/database/bar007.
- 645 [7] Hawrylycz MJ, Lein ES, Guillozet-Bongaarts AL, et al. An anatomically
646 comprehensive atlas of the adult human brain transcriptome. *Nature* 2012; 489: 391–399.
- 647 [8] Lein ES, Hawrylycz MJ, Ao N, et al. Genome-wide atlas of gene expression in the
648 adult mouse brain. *Nature* 2007; 445: 168–176.
- 649 [9] Liu L, Cheung TH, Charville GW, et al. Chromatin Modifications as Determinants of
650 Muscle Stem Cell Quiescence and Chronological Aging. *Cell Rep* 2013; 4: 189–204.
- 651 [10] Fukada S, Uezumi A, Ikemoto M, et al. Molecular Signature of Quiescent Satellite
652 Cells in Adult Skeletal Muscle. *STEM CELLS* 2007; 25: 2448–2459.
- 653 [11] Pallafacchina G, François S, Regnault B, et al. An adult tissue-specific stem cell in its
654 niche: a gene profiling analysis of in vivo quiescent and activated muscle satellite cells. *Stem*
655 *Cell Res* 2010; 4: 77–91.
- 656 [12] Farina NH, Hausburg M, Betta ND, et al. A role for RNA post-transcriptional
657 regulation in satellite cell activation. *Skelet Muscle* 2012; 2: 21.
- 658 [13] García-Prat L, Martínez-Vicente M, Perdiguero E, et al. Autophagy maintains
659 stemness by preventing senescence. *Nature* 2016; 529: 37–42.
- 660 [14] Lukjanenko L, Jung MJ, Hegde N, et al. Loss of fibronectin from the aged stem cell
661 niche affects the regenerative capacity of skeletal muscle in mice. *Nat Med* 2016; 22: 897–
662 905.
- 663 [15] Mourikis P, Gopalakrishnan S, Sambasivan R, et al. Cell-autonomous Notch activity
664 maintains the temporal specification potential of skeletal muscle stem cells. *Dev Camb Engl*
665 2012; 139: 4536–4548.
- 666 [16] Sambasivan R, Comai G, Le Roux I, et al. Embryonic founders of adult muscle stem
667 cells are primed by the determination gene Mrf4. *Dev Biol* 2013; 381: 241–255.
- 668 [17] Houzelstein D, Tajbakhsh S. Increased in situ hybridization sensitivity using non-
669 radioactive probes after staining for β -galactosidase activity. *Tech Tips Online* 1998; 3: 147–
670 149.
- 671 [18] Gautier L, Cope L, Bolstad BM, et al. affy—analysis of Affymetrix GeneChip data at
672 the probe level. *Bioinformatics* 2004; 20: 307–315.
- 673 [19] Carvalho BS, Irizarry RA. A framework for oligonucleotide microarray preprocessing.
674 *Bioinformatics* 2010; 26: 2363–2367.
- 675 [20] Bolstad BM. *Low-level Analysis of High-density Oligonucleotide Array Data:
676 Background, Normalization and Summarization*. University of California, 2004.
- 677 [21] R Core Team. *R: A Language and Environment for Statistical Computing*. Vienna,
678 Austria: R Foundation for Statistical Computing <https://www.R-project.org/> (2017).

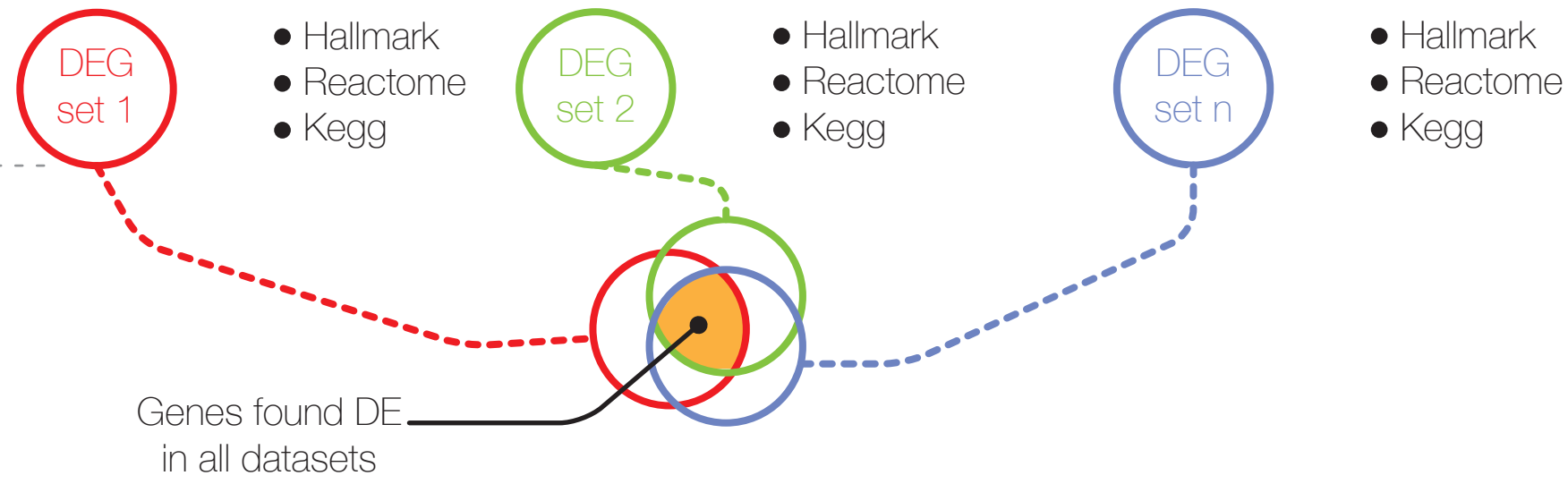
- 679 [22] FactoMineR: An R Package for Multivariate Analysis | Lê | Journal of Statistical
680 Software <https://www.jstatsoft.org/article/view/v025i01> (accessed 1 June 2017).
- 681 [23] Ritchie ME, Phipson B, Wu D, et al. limma powers differential expression analyses
682 for RNA-sequencing and microarray studies. *Nucleic Acids Res* 2015; 43: e47.
- 683 [24] Benjamini Y, Hochberg Y. Controlling the False Discovery Rate: A Practical and
684 Powerful Approach to Multiple Testing. *J R Stat Soc Ser B Methodol* 1995; 57: 289–300.
- 685 [25] Subramanian A, Tamayo P, Mootha VK, et al. Gene set enrichment analysis: A
686 knowledge-based approach for interpreting genome-wide expression profiles. *Proc Natl Acad
687 Sci* 2005; 102: 15545–15550.
- 688 [26] WEHI Bioinformatics - mouse and human orthologs of the
689 MSigDB <http://bioinf.wehi.edu.au/software/MSigDB/> (accessed 20 April 2017).
- 690 [27] KEGG: Kyoto Encyclopedia of Genes and Genomes <http://www.genome.jp/kegg/>
691 (accessed 20 April 2017).
- 692 [28] Reactome Pathway Database <http://www.reactome.org/> (accessed 20 April 2017).
- 693 [29] Wu D, Smyth GK. Camera: a competitive gene set test accounting for inter-gene
694 correlation. *Nucleic Acids Res* 2012; 40: e133.
- 695 [30] Wang M, Zhao Y, Zhang B. Efficient Test and Visualization of Multi-Set
696 Intersections. *Sci Rep* 2015; 5: 16923.
- 697 [31] Lex A, Gehlenborg N, Strobel H, et al. UpSet: Visualization of Intersecting Sets.
698 *IEEE Trans Vis Comput Graph* 2014; 20: 1983–1992.
- 699 [32] Jaccard P. Étude comparative de la distribution florale dans une portion des Alpes et
700 des Jura. *Bull Société Vaudoise Sci Nat* 1901; 37: 547–579.
- 701 [33] Khatri P, Sirota M, Butte AJ. Ten Years of Pathway Analysis: Current Approaches
702 and Outstanding Challenges. *PLOS Comput Biol* 2012; 8: e1002375.
- 703 [34] Winston Chang and Joe Cheng and JJ Allaire and Yihui Xie and Jonathan McPherson.
704 *shiny: Web Application Framework for R* <https://CRAN.R-project.org/package=shiny> (2017).
- 705 [35] Campain A, Yang YH. Comparison study of microarray meta-analysis methods. *BMC
706 Bioinformatics* 2010; 11: 408.
- 707 [36] Ramasamy A, Mondry A, Holmes CC, et al. Key Issues in Conducting a Meta-
708 Analysis of Gene Expression Microarray Datasets. *PLoS Med*; 5. Epub ahead of print
709 September 2008. DOI: 10.1371/journal.pmed.0050184.
- 710 [37] Irizarry RA, Warren D, Spencer F, et al. Multiple-laboratory comparison of
711 microarray platforms. *Nat Methods* 2005; 2: 345–350.
- 712 [38] Liberzon A, Birger C, Thorvaldsdóttir H, et al. The Molecular Signatures Database
713 (MSigDB) hallmark gene set collection. *Cell Syst* 2015; 1: 417–425.
- 714 [39] Ashburner M, Ball CA, Blake JA, et al. Gene Ontology: tool for the unification of
715 biology. *Nat Genet* 2000; 25: 25–29.
- 716 [40] Paquet ER, Cui J, Davidson D, et al. A 12-gene signature to distinguish colon cancer
717 patients with better clinical outcome following treatment with 5-fluorouracil or FOLFIRI. *J
718 Pathol Clin Res* 2015; 1: 160–172.
- 719 [41] Wang J, Mi J-Q, Debernardi A, et al. A six gene expression signature defines
720 aggressive subtypes and predicts outcome in childhood and adult acute lymphoblastic
721 leukemia. *Oncotarget* 2015; 6: 16527–16542.
- 722 [42] Three-Gene Model to Robustly Identify Breast Cancer Molecular Subtypes | JNCI:
723 Journal of the National Cancer Institute | Oxford
724 Academic <https://academic.oup.com/jnci/article-lookup/doi/10.1093/jnci/djr545> (accessed 5
725 June 2017).
- 726 [43] Fan C, Oh DS, Wessels L, et al. Concordance among gene-expression-based
727 predictors for breast cancer. *N Engl J Med* 2006; 355: 560–569.
- 728 [44] Michiels S, Koscielny S, Hill C. Prediction of cancer outcome with microarrays: a

729 multiple random validation strategy. *The Lancet* 2005; 365: 488–492.
730 [45] Abraham G, Kowalczyk A, Loi S, et al. Prediction of breast cancer prognosis using
731 gene set statistics provides signature stability and biological context. *BMC Bioinformatics*
732 2010; 11: 277.
733 [46] Mootha VK, Lindgren CM, Eriksson K-F, et al. PGC-1alpha-responsive genes
734 involved in oxidative phosphorylation are coordinately downregulated in human diabetes. *Nat*
735 *Genet* 2003; 34: 267–273.
736 [47] Varn FS, Ung MH, Lou SK, et al. Integrative analysis of survival-associated gene sets
737 in breast cancer. *BMC Med Genomics*; 8. Epub ahead of print 12 March 2015. DOI:
738 10.1186/s12920-015-0086-0.
739 [48] Goeman JJ, Bühlmann P. Analyzing gene expression data in terms of gene sets:
740 methodological issues. *Bioinformatics* 2007; 23: 980–987.
741 [49] Luo W, Friedman MS, Shedden K, et al. GAGE: generally applicable gene set
742 enrichment for pathway analysis. *BMC Bioinformatics* 2009; 10: 161.
743 [50] Yamaguchi M, Watanabe Y, Ohtani T, et al. Calcitonin Receptor Signaling Inhibits
744 Muscle Stem Cells from Escaping the Quiescent State and the Niche. *Cell Rep* 2015; 13: 302–
745 314.
746 [51] Ishii K, Suzuki N, Mabuchi Y, et al. Muscle Satellite Cell Protein Teneurin-4
747 Regulates Differentiation During Muscle Regeneration. *STEM CELLS* 2015; 33: 3017–3027.
748 [52] Lamph WW, Wamsley P, Sassone-Corsi P, et al. Induction of proto-oncogene
749 JUN/AP-1 by serum and TPA. *Nature* 1988; 334: 629–631.
750 [53] Irizarry RA, Warren D, Spencer F, et al. Multiple-laboratory comparison of
751 microarray platforms. *Nat Methods* 2005; 2: 345–350.
752 [54] Rhodes DR, Barrette TR, Rubin MA, et al. Meta-analysis of microarrays: interstudy
753 validation of gene expression profiles reveals pathway dysregulation in prostate cancer.
754 *Cancer Res* 2002; 62: 4427–4433.
755 [55] Grützmann R, Boriss H, Ammerpohl O, et al. Meta-analysis of microarray data on
756 pancreatic cancer defines a set of commonly dysregulated genes. *Oncogene* 2005; 24: 5079–
757 5088.
758 [56] Cruz-Montegudo M, Borges F, Paz-y-Miño C, et al. Efficient and biologically
759 relevant consensus strategy for Parkinson’s disease gene prioritization. *BMC Med Genomics*;
760 9. Epub ahead of print 9 March 2016. DOI: 10.1186/s12920-016-0173-x.
761 [57] Oerton E, Bender A. Concordance analysis of microarray studies identifies
762 representative gene expression changes in Parkinson’s disease: a comparison of 33 human and
763 animal studies. *BMC Neurol*; 17. Epub ahead of print 23 March 2017. DOI: 10.1186/s12883-
764 017-0838-x.
765 [58] Consortium TEP. An integrated encyclopedia of DNA elements in the human genome.
766 *Nature* 2012; 489: 57–74.
767 [59] Russ J, Futschik ME. Comparison and consolidation of microarray data sets of human
768 tissue expression. *BMC Genomics* 2010; 11: 305.
769 [60] Kitchen RR, Sabine VS, Simen AA, et al. Relative impact of key sources of
770 systematic noise in Affymetrix and Illumina gene-expression microarray experiments. *BMC*
771 *Genomics* 2011; 12: 589.
772
773
774
775

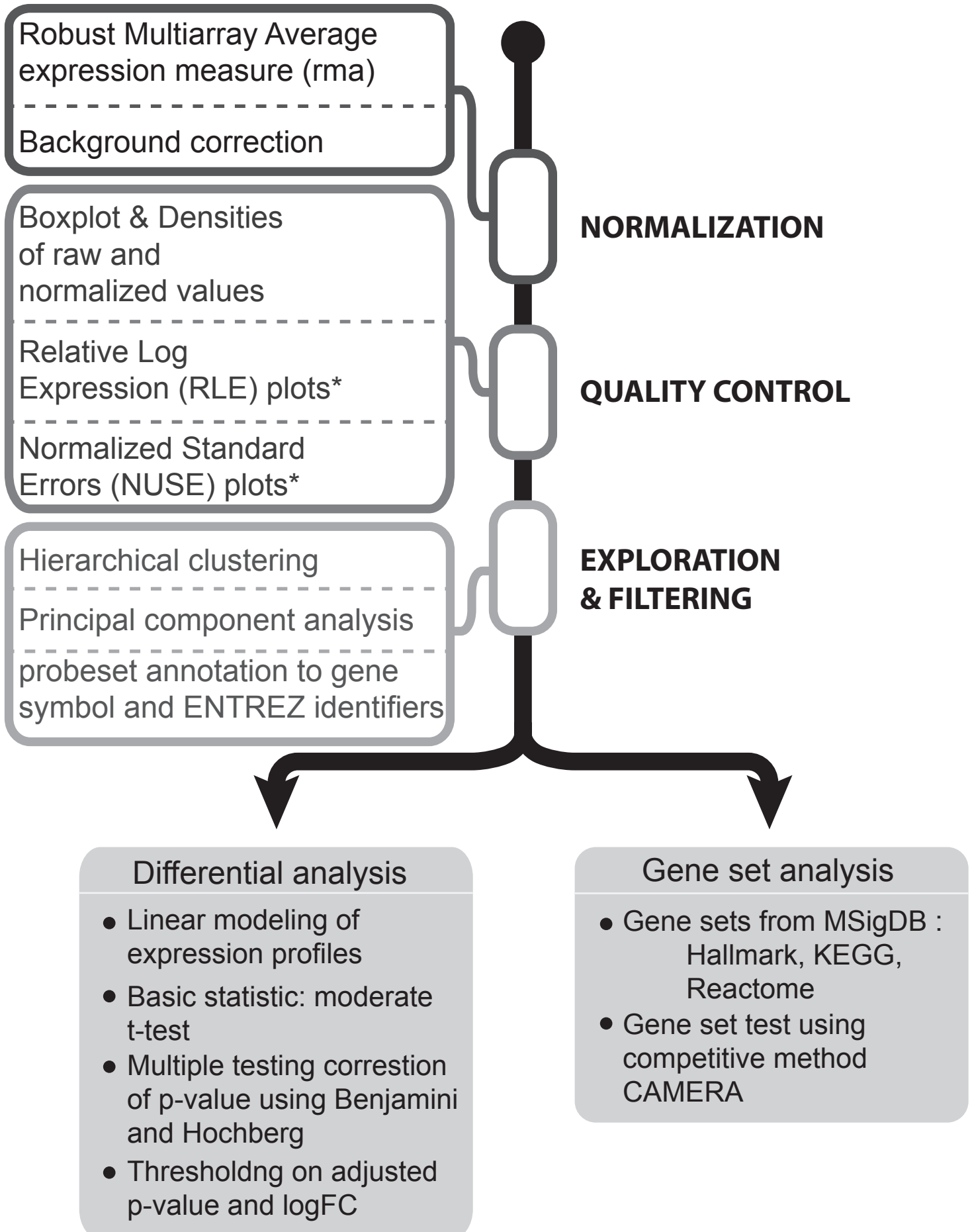
INDIVIDUAL SET ANALYSIS



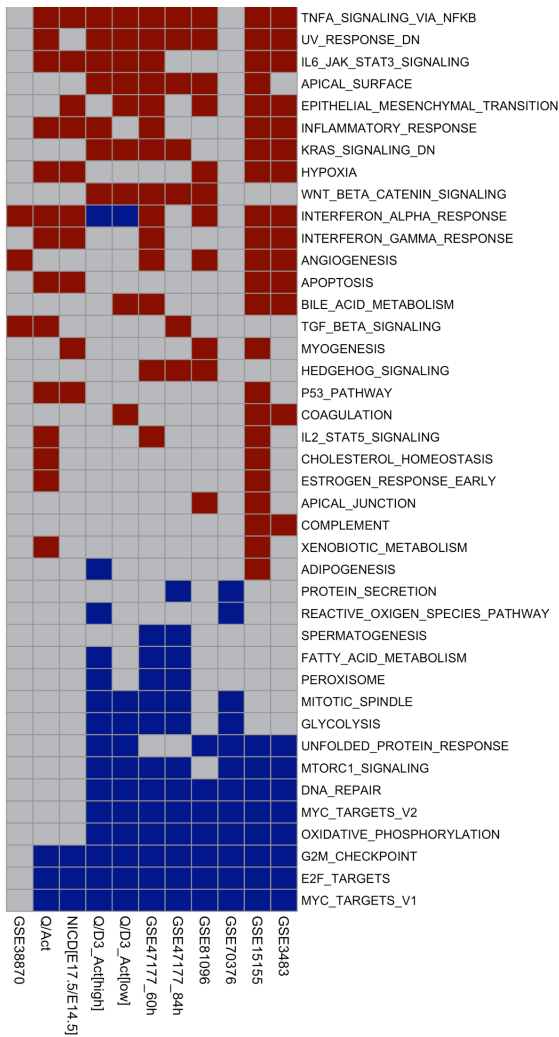
MULTI-SET ANALYSIS



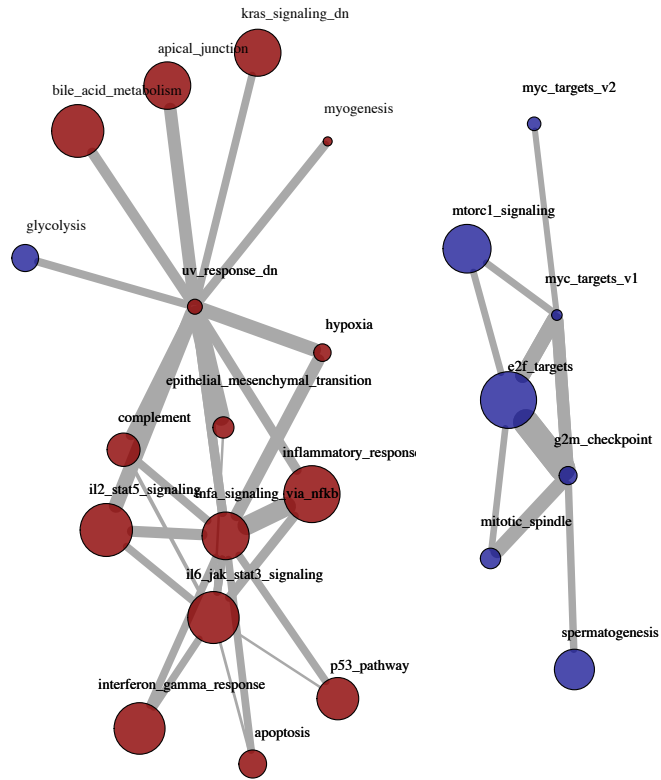
Raw data



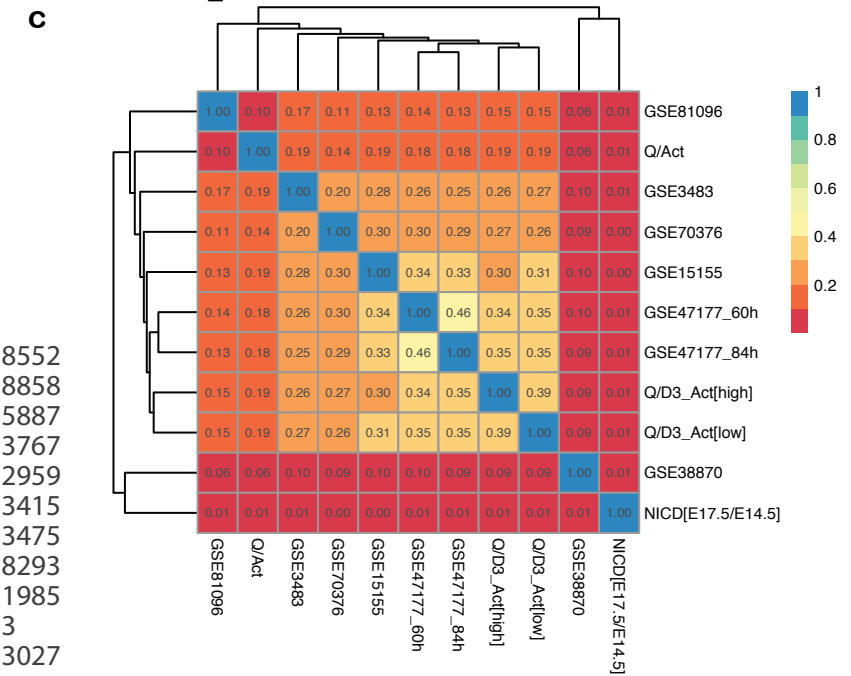
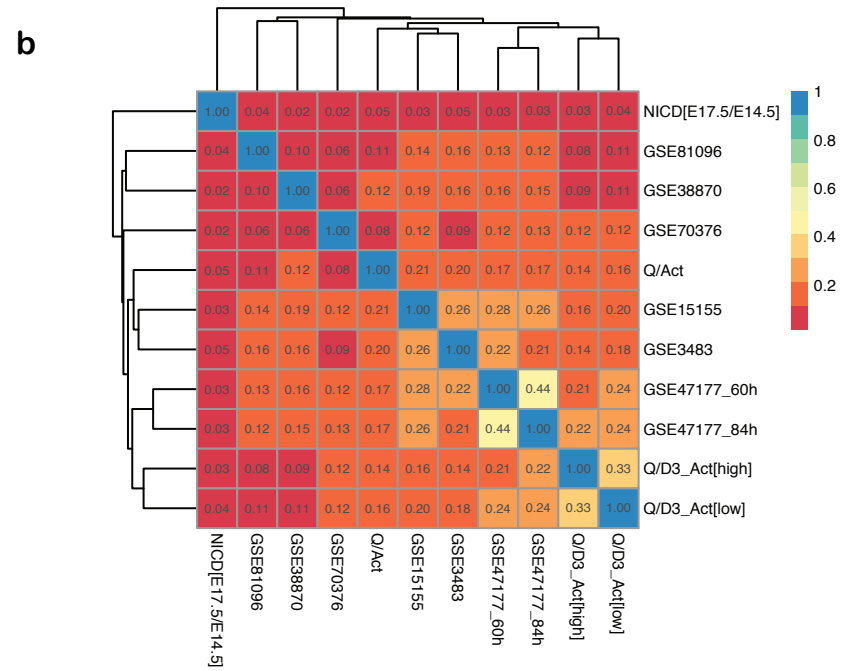
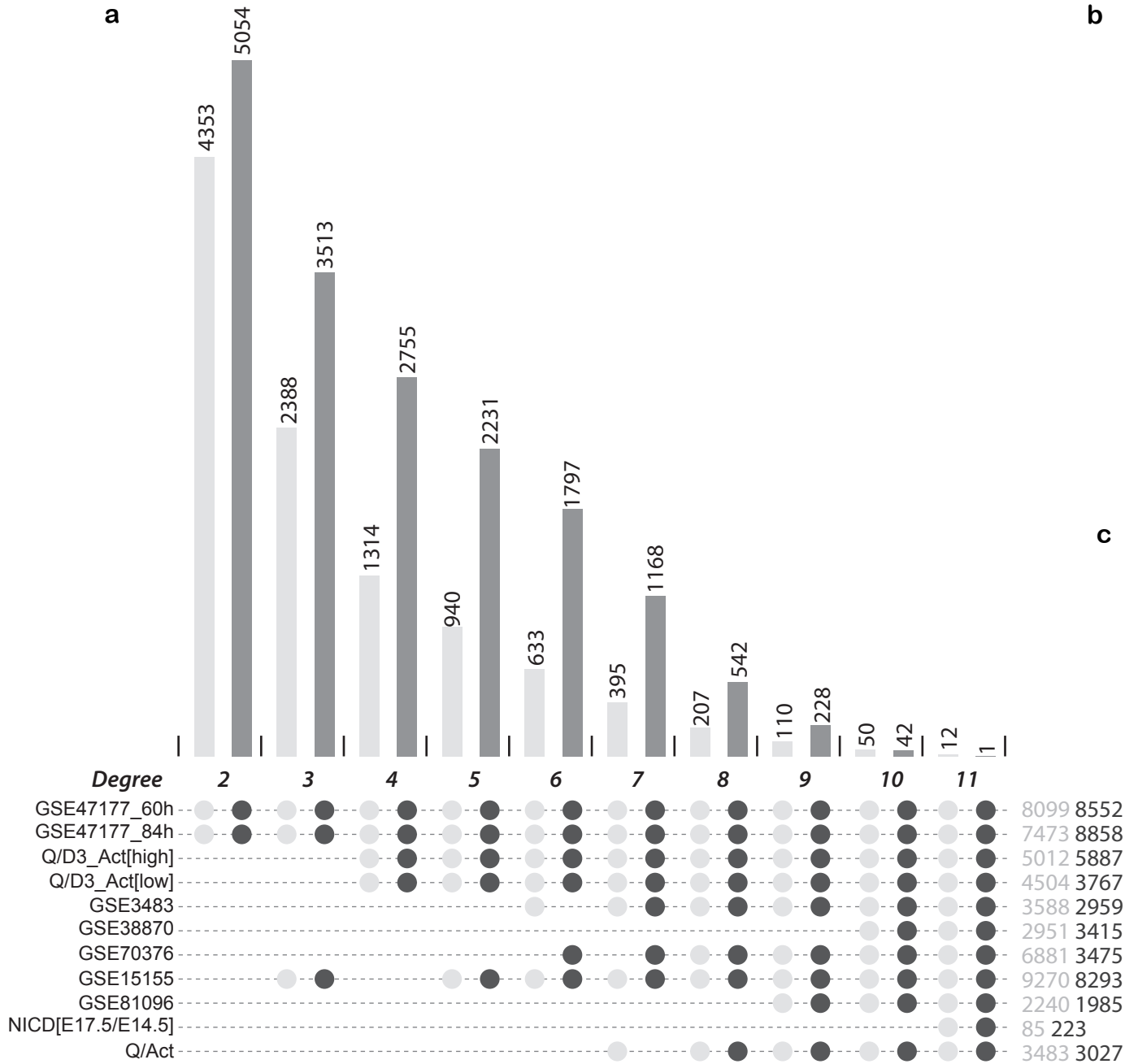
a



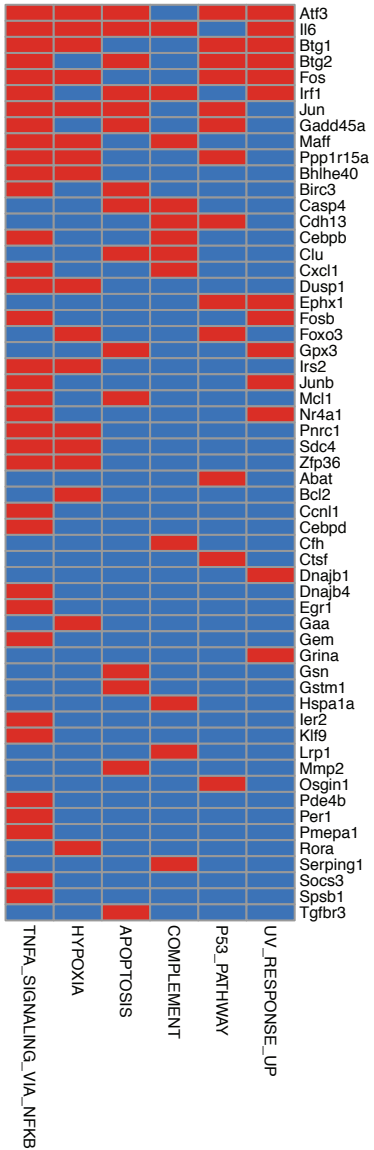
b



Dataset	Description
Q / Act	Quiescent / Activated
Q [high/low] /D3_Act [high/low]	Quiescent [high/low] /D3Activated [high/low]
NICD [E17.5/E14.5]	Fetal_NICD [E17.5/E14.5]
GSE3483	GSE3483 Fukada et al.
GSE15155	GSE15155 Pallafacchina et al.
GSE38870	GSE38870 Farina et al.
GSE47177	GSE47177 Liu et al.
GSE70376	GSE70376 Garcia-Prat et al.
GSE81096	GSE81096 Lukjanenko et al.

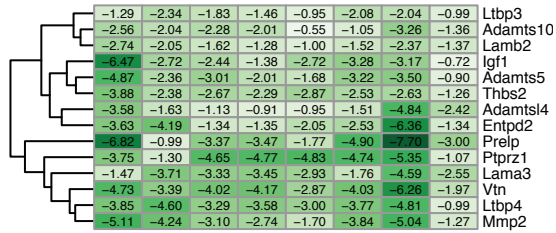


a

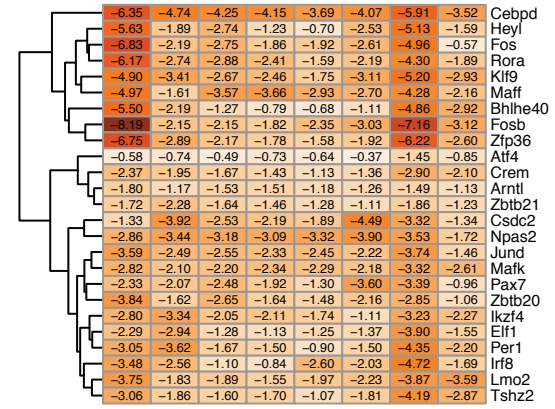
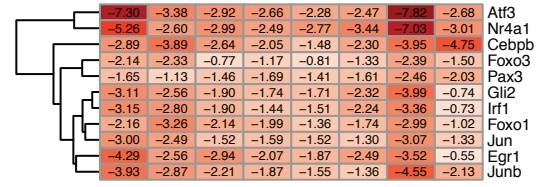


b

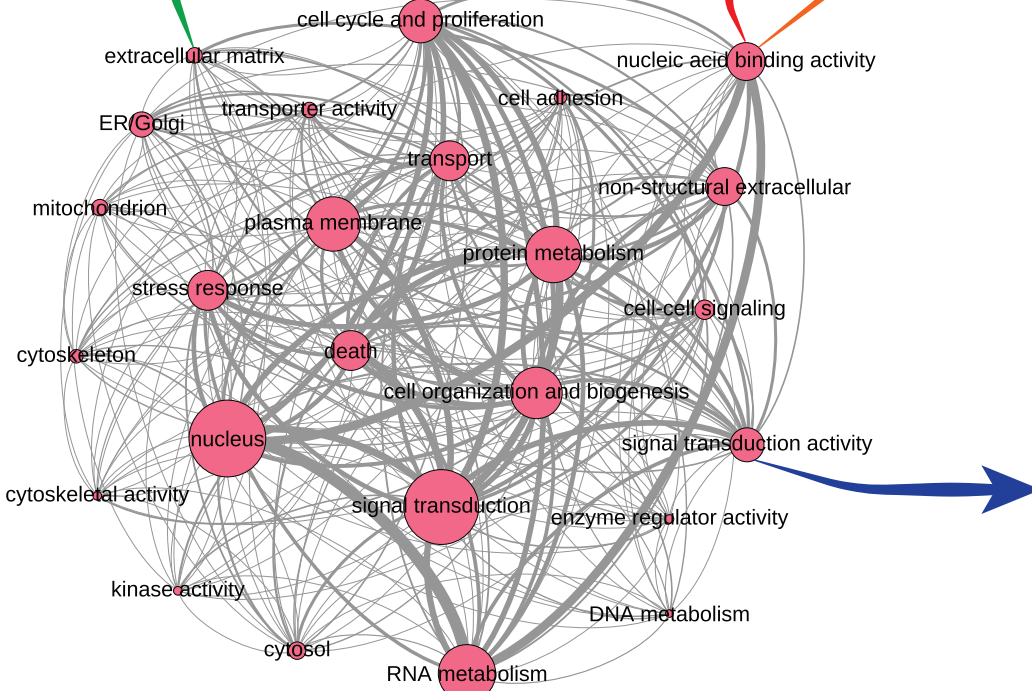
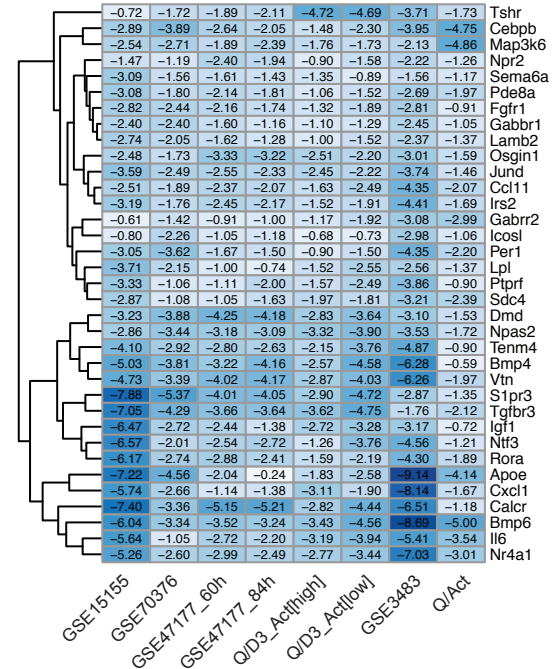
extracellular matrix



nucleic acid binding



signal transduction

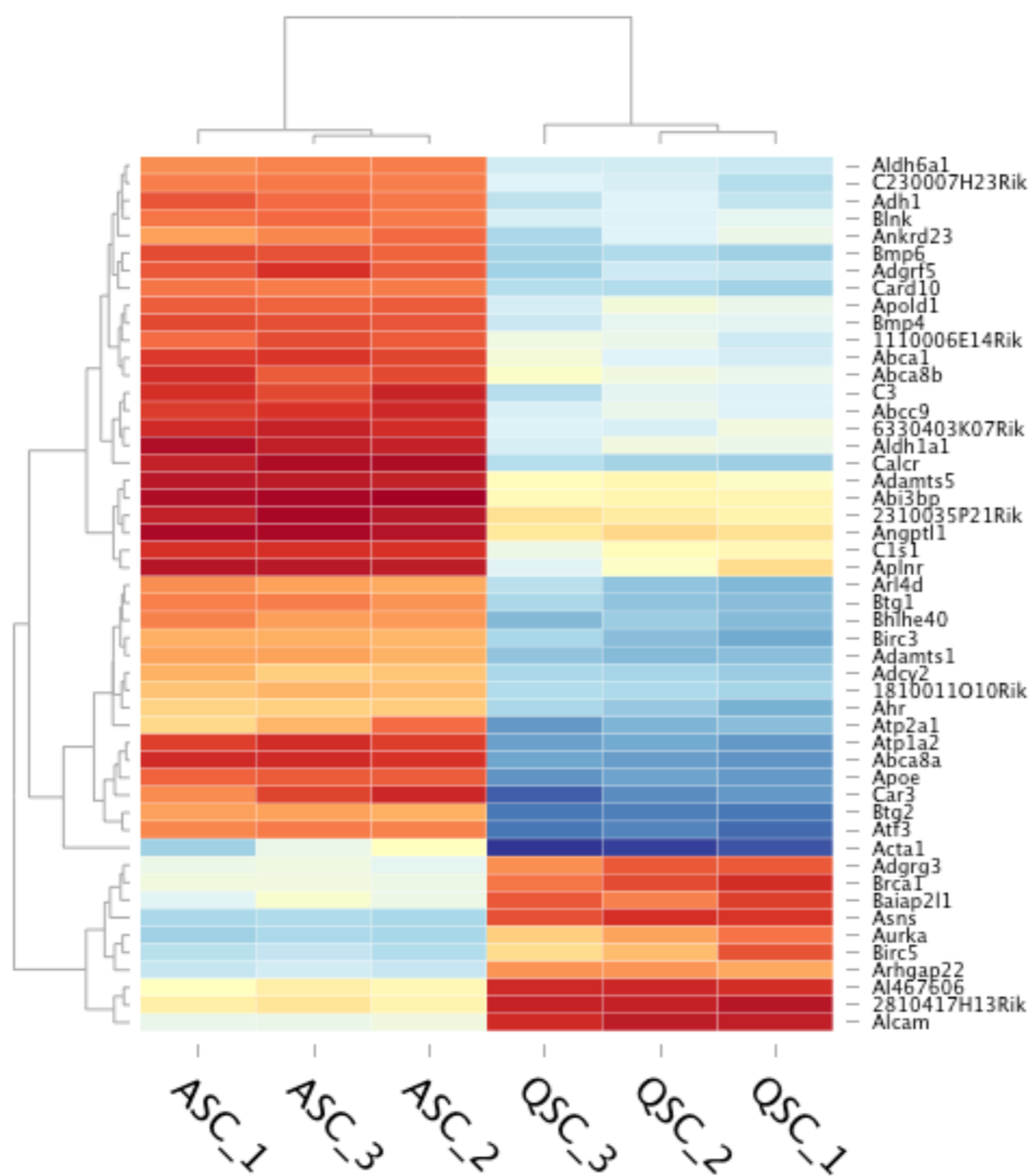


INDIVIDUAL ANALYSIS



Home Individual Analysis Multiple analysis Upload

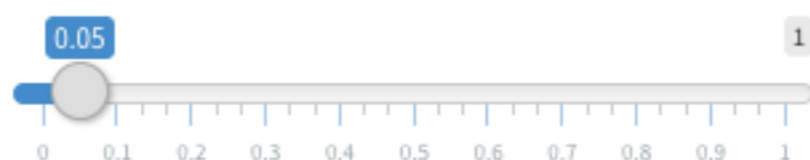
Heatmap



logFC



Adj. P-value



DATASETS

- Buckingham
- Garcia-Prat
- Lukjanenko
- Rando60H
- Rando84H
- SYD3H
- SYD3L
- Takeda
- Farina
- RK
- MBHS

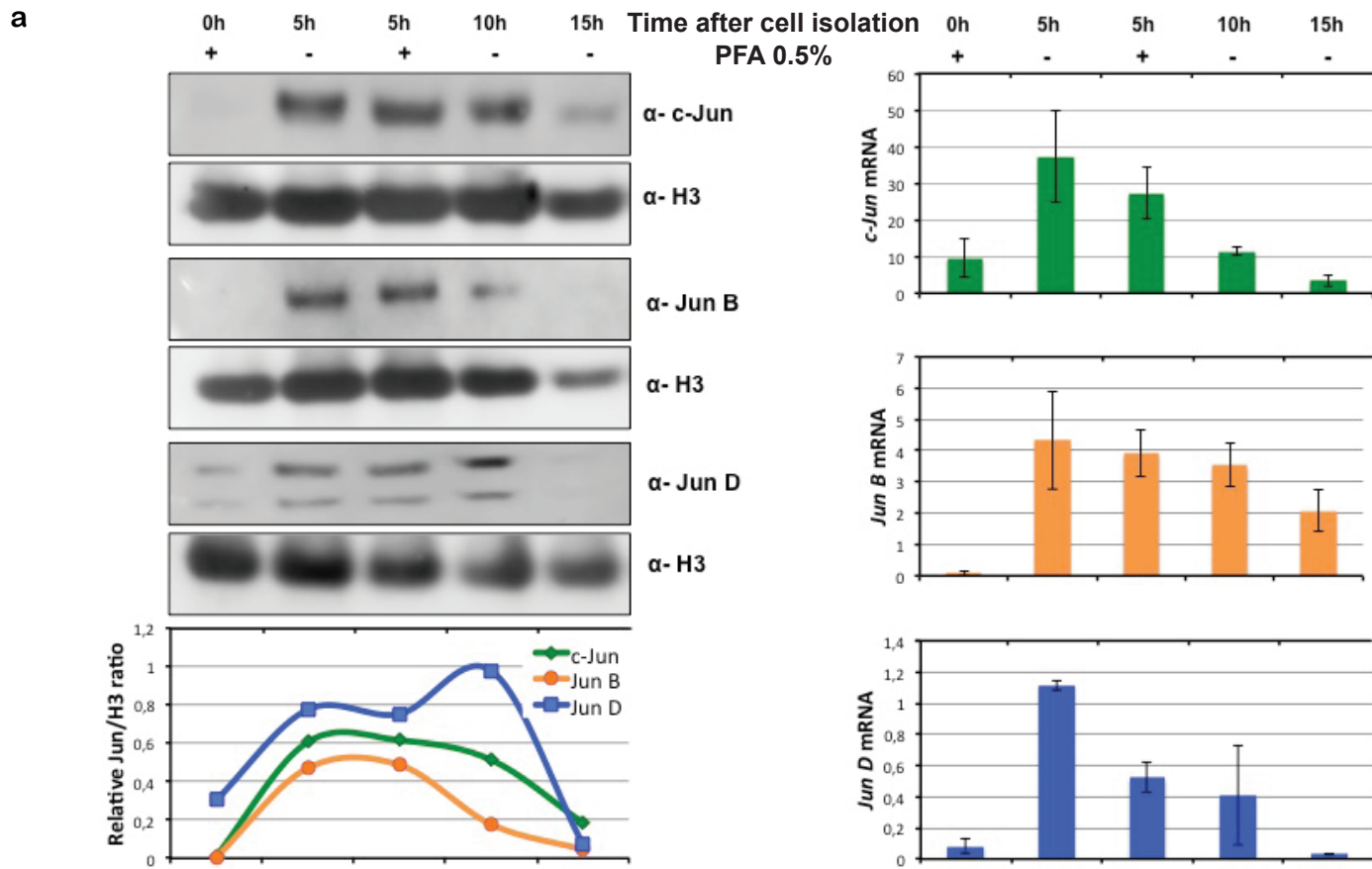
Dataset characterization

Table

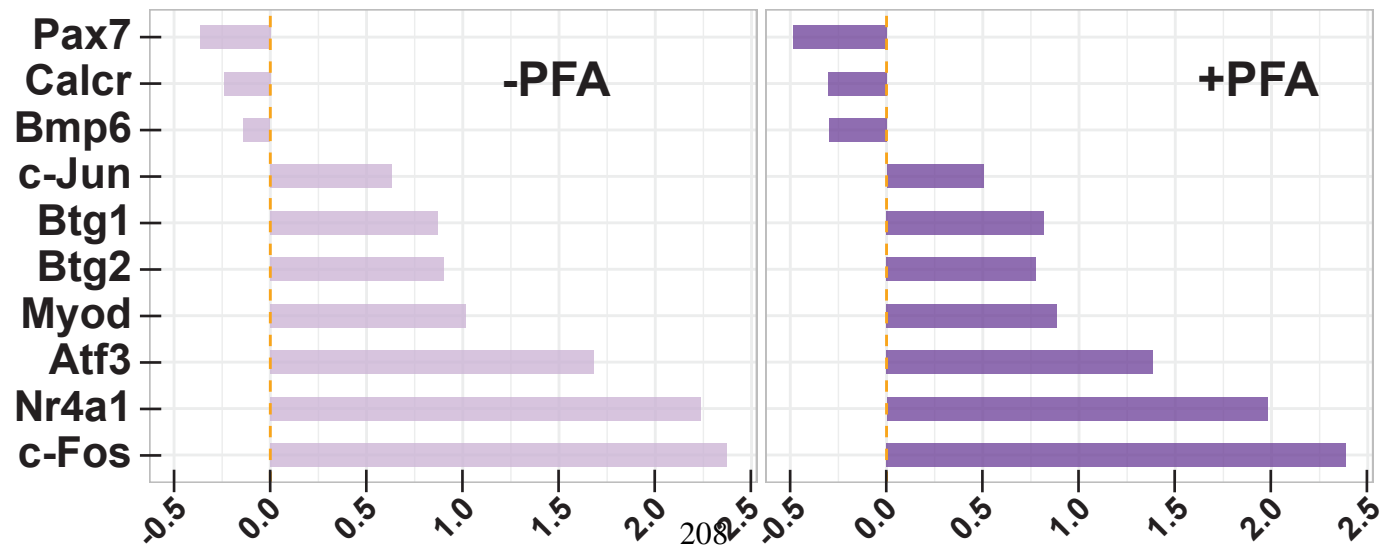
Volcano plot

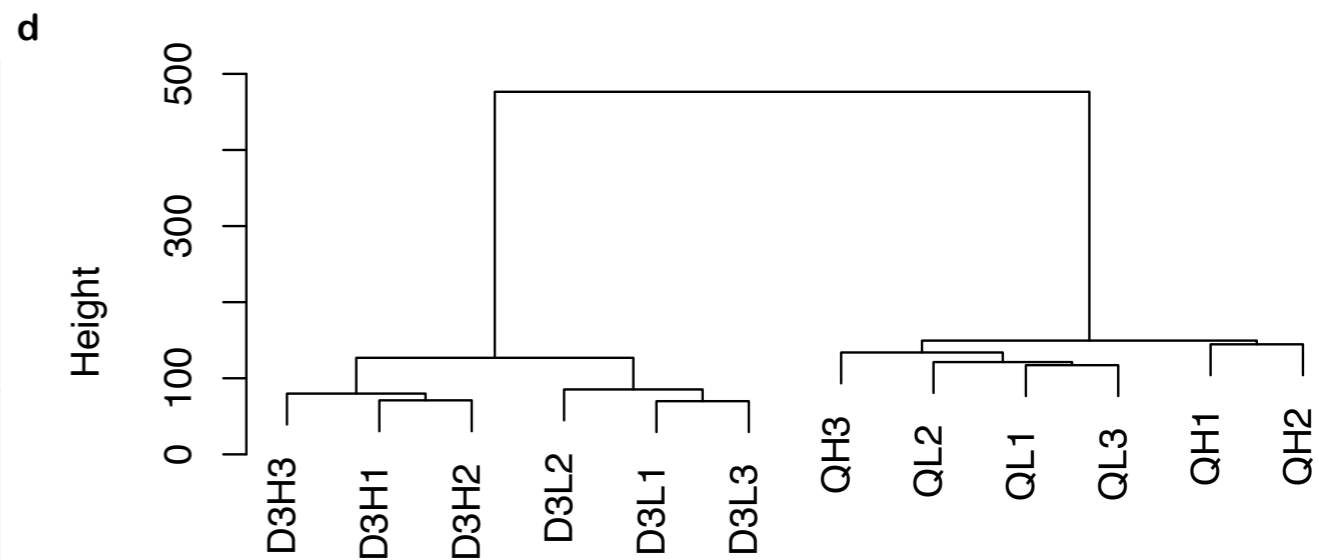
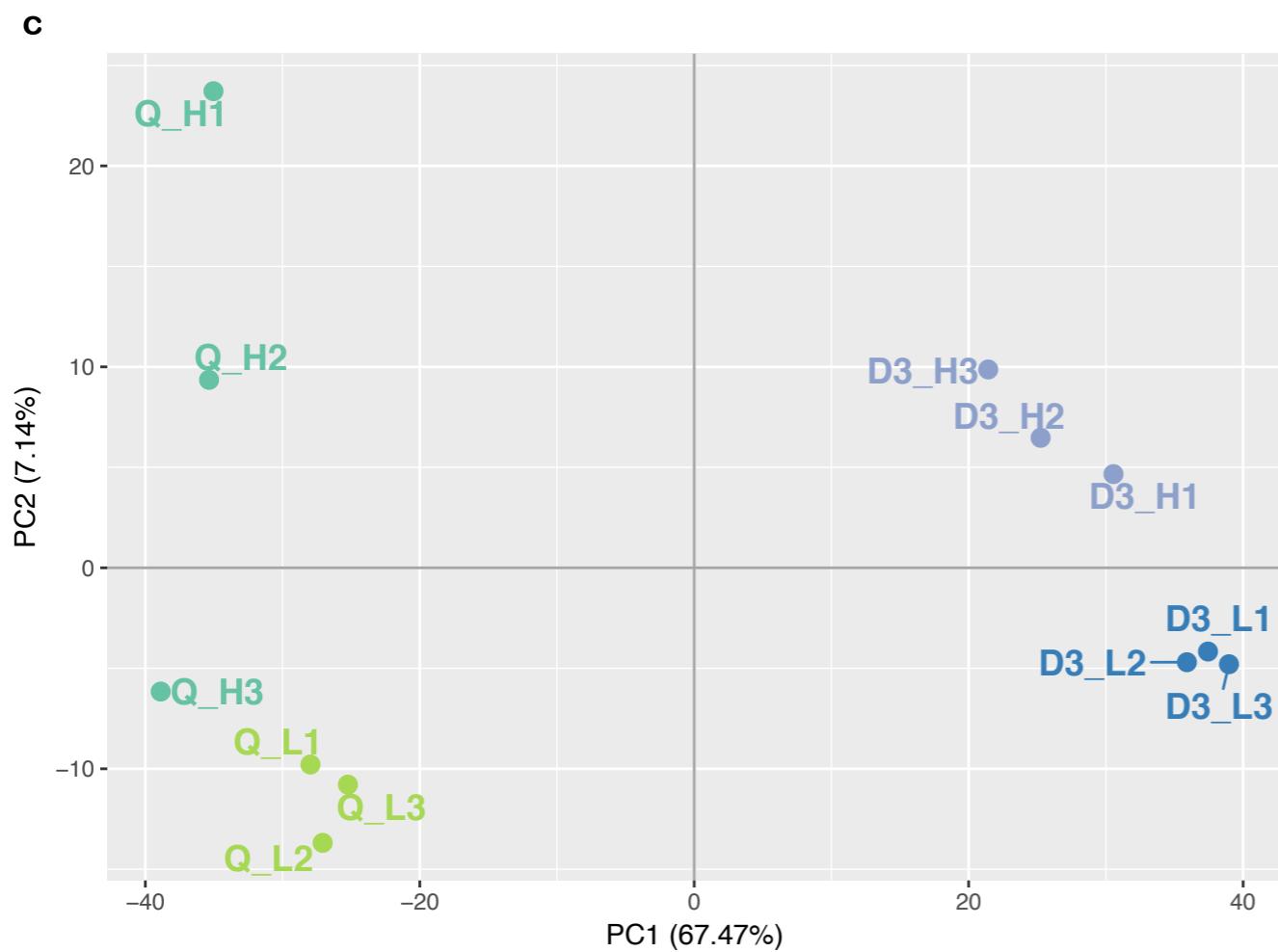
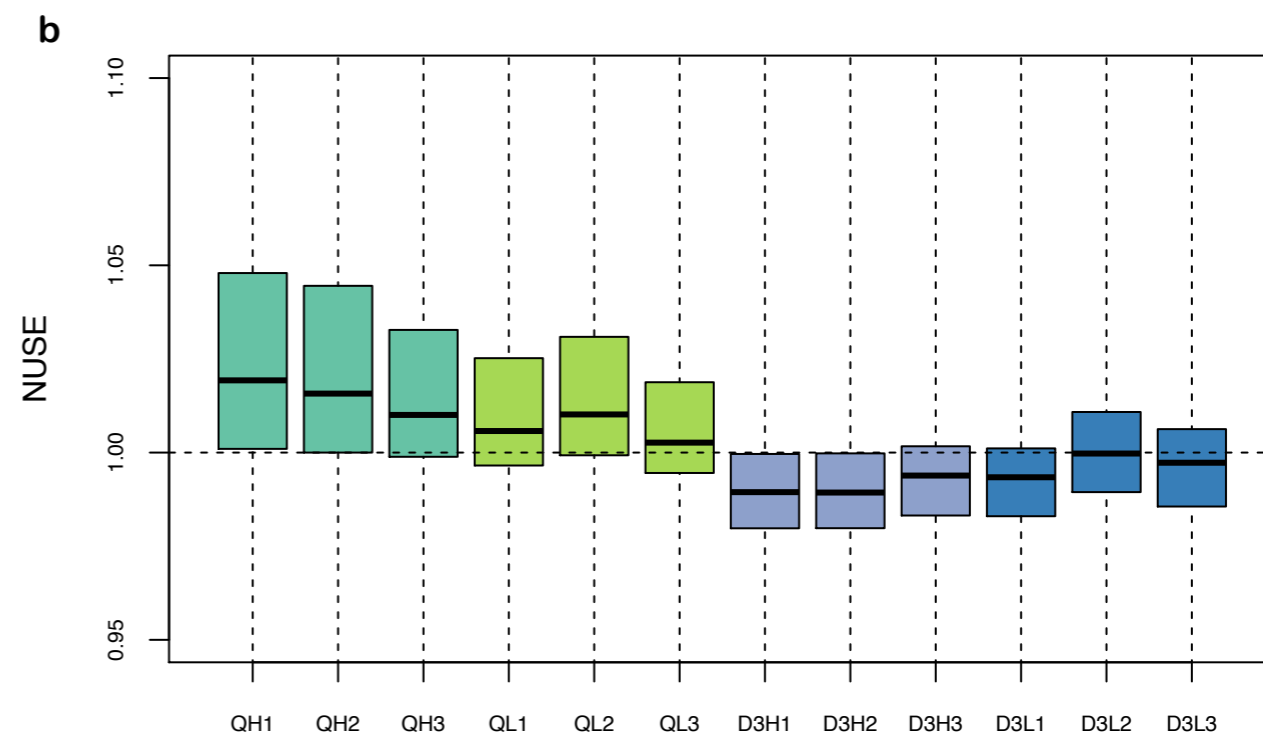
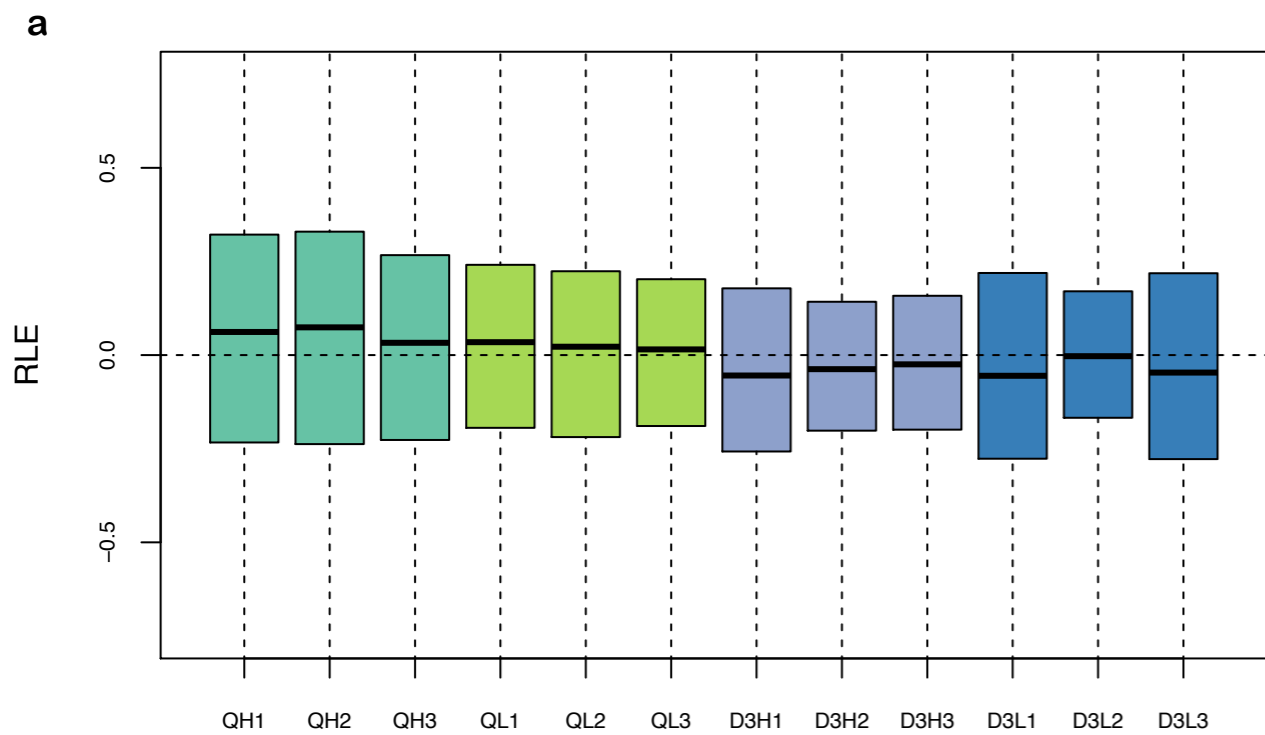
Heat map

PCA



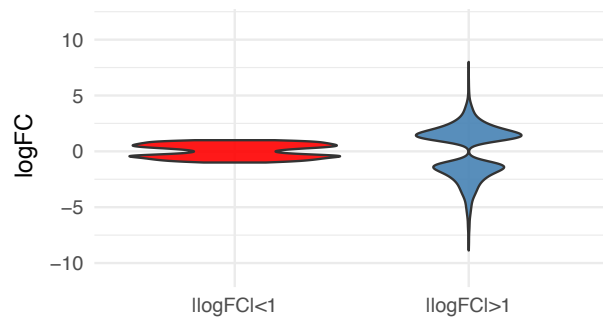
b Fold change between Time 0h+PFA and Time 5h +/-PFA (log10)



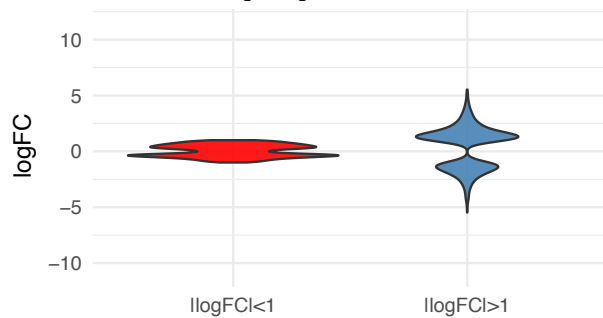


Dataset	Up-regulated genes	Down-regulated genes
Quiescent / Activated	1111	1244
Quiescent [high/low] /D3Activated[high/low]	820 (h) / 997 (l)	2585 (h) / 2344 (l)
Foetal_NICD [E17.5/E14.5]	39	136
GSE3483 Fukada et al.	1967	2311
GSE15155 Pallafacchina et al.	2588	3074
GSE38870 Farina et al.	1959	1092
GSE47177 Liu et al.	1461 (60h) /1110 (84h)	1938 (60h) /1726 (84h)
GSE70376 García-Prat et al.	4367	6346
GSE81096 Lukjanenko et al.	610	545

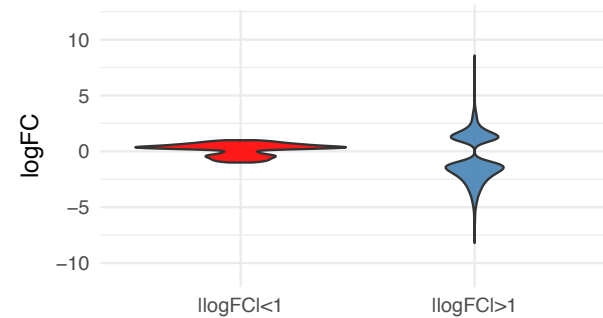
GSE15155 Pallafacchina et al.



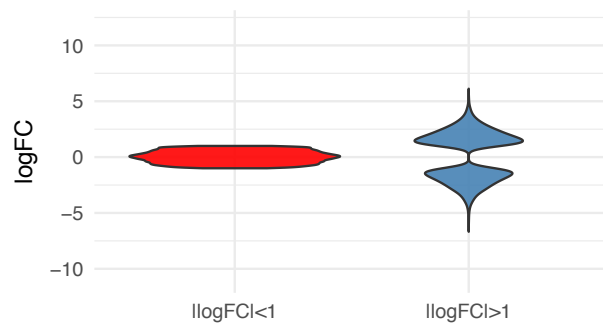
GSE47177 [84h] Liu et al.



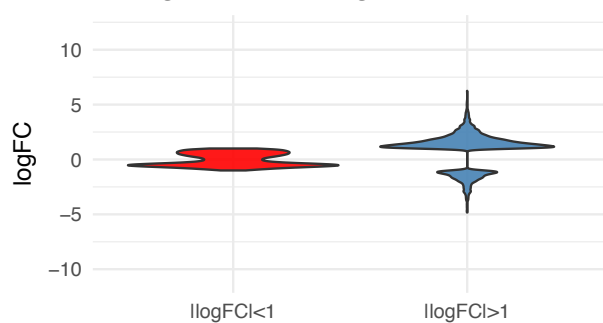
GSE38870 Farina et al.



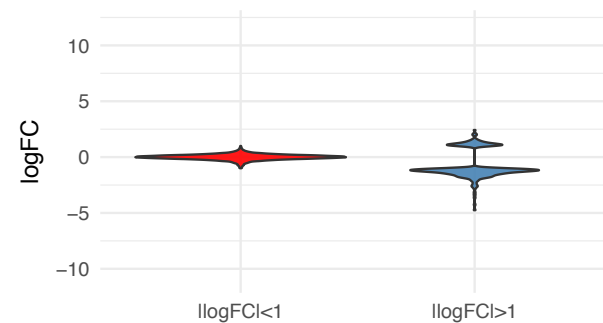
GSE70376 García-Prat et al.



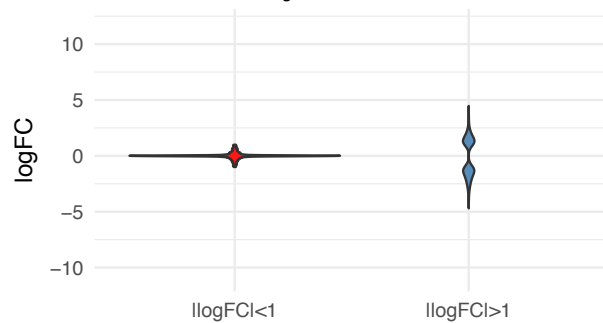
Q [high] / D3_Act [high]



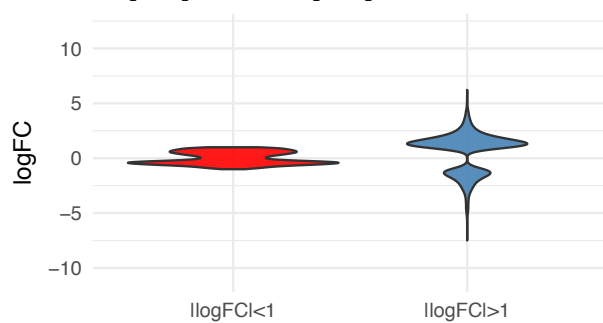
Foetal_NICD [E17.5/E14.5]



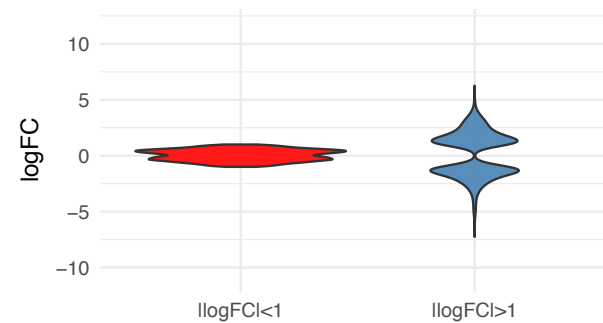
GSE81096 Lukjanenko et al.



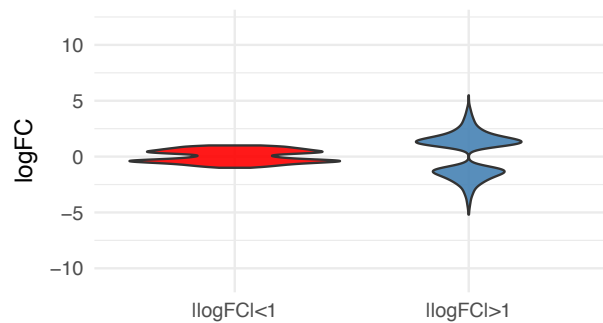
Q [low] / D3_Act [low]



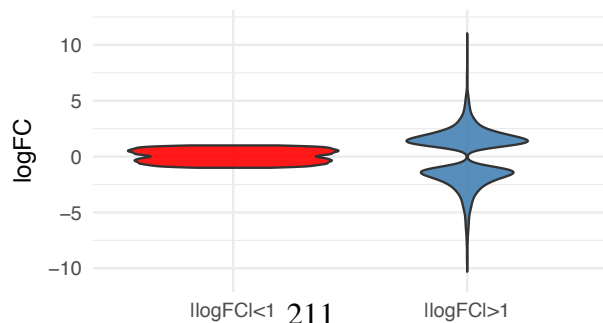
Q / Act



GSE47177 [60h] Liu et al.



GSE3483 Fukada et al.



ANNEX 3:

Small-RNA sequencing identifies dynamic
microRNA deregulation during muscle lineage
progression

Submitted

Small-RNA sequencing identifies dynamic microRNA deregulation during muscle lineage progression

David Castel^{1#}, Meryem Baghdadi^{1,2,3}, Sébastien Mella^{1,2}, Barbara Gayraud-Morel^{1,2}, Christophe Antoniewski^{4,5} & Shahragim Tajbakhsh^{1,2*}

¹ *Stem Cells and Development, Department of Developmental & Stem Cell Biology, Institut Pasteur, Paris 75015, France*

² *CNRS UMR 3738, Institut Pasteur, Paris 75015, France.*

³ *Sorbonne Universités, UPMC, University of Paris 06, IFD-ED 515, 4 Place Jussieu, Paris 75252, France.*

⁴ *Sorbonne Universités, Université Pierre et Marie Curie (UPMC), CNRS, Institut de Biologie Paris Seine (IBPS), Developmental Biology Department, Paris, France.*

⁵ *Sorbonne Universités, Université Pierre et Marie Curie (UPMC), CNRS, Institut de Biologie Paris Seine (IBPS), ARTbio Bioinformatics Analysis Facility, Paris, France*

present address: *Département de Cancérologie de l'Enfant et de l'Adolescent & UMR8203 "Vectorologie et Thérapeutiques Anticancéreuses", CNRS, Gustave Roussy, Univ. Paris-Sud, Université Paris-Saclay, 94805, Villejuif, France*

* Correspondence: shahragim.tajbakhsh@pasteur.fr

Keywords: Muscle Satellite cells / microRNA / Quiescence /lineage progression/ small-RNA sequencing

Abstract

Skeletal muscle satellite cells are quiescent adult resident stem cells that can activate, proliferate and differentiate to generate myofibres following injury. They harbour a robust proliferation potential and self-renewing capacity enabling lifelong damage-induced muscle regeneration. Although several classes of microRNAs have been shown to regulate adult myogenesis, a systematic examination of stage-specific microRNAs during lineage progression from the quiescent state is lacking. Here we provide a genome-wide assessment of the expression of small RNAs during the quiescence/activation transition and differentiation by RNA-sequencing. We show that the majority of small RNAs present in quiescent, activated and differentiated muscle cells belong to the microRNA class. Furthermore, by comparing expression between these distinct cell states, we report a massive and dynamic regulation of microRNAs, both in numbers and amplitude, that highlights their pivotal role in the regulation of quiescence, activation and differentiation. We also identify a number of microRNAs with reliable and specific expression in quiescence. Unexpectedly, the majority of class-switching miRNAs are associated with the quiescence/activation transition suggesting a poised program that is actively repressed. These data constitute a key resource for functional analyses of miRNAs in skeletal myogenesis, and more broadly, in the regulation of stem cell self-renewal and tissue homeostasis.

Introduction

Adult skeletal muscles can regenerate robustly to confront mild and severe lesions induced by exercise or trauma. This extraordinary regenerative capacity occurs largely through the mobilization of resident muscle satellite (stem) cells (MuSCs). These cells are quiescent in resting muscle and can activate, proliferate and differentiate to form new muscle fibres¹. During lineage progression, a subset of proliferating MuSCs self-renew in their niche by reversibly exiting the cell cycle. Therefore, skeletal myogenesis is a tractable model to study the regulation of quiescence, self-renewal and differentiation.

Micro-RNAs (miRNAs) are ~22-nucleotide long non-coding RNAs that participate in post-transcriptional regulation of gene expression through mRNAs decay or translational repression². Stem-loop structured pre-miRNAs are excised from primary miRNAs and exported to the cytoplasm. Further excision of the loop of pre-miRNA by *Dicer* gives rise to miRNA/miRNA* duplexes. Single-strand miRNAs are then loaded within the RNA-Induced Silencing Complex and guide RISC to complementary sequences in 3'UTR of target mRNAs^{3,4}. The miRNA pathway has been shown to play a major role in cell specification and differentiation in many organisms, and also more broadly in organism development, tissue homeostasis. Germ line loss of *Dicer* is lethal at gastrulation, demonstrating an absolute requirement of miRNAs for mouse development⁵. Other studies have demonstrated the specific requirement of miRNAs in ES cells and tissue specific stem cells^{6,7}.

A set of miRNAs is associated with differentiation of skeletal muscle cell lines⁸⁻¹⁰. These so-called myomirs, are induced by Myod and Myog, and can promote muscle differentiation *in vitro*. Conditional deletion of *Dicer* in *Myod*-expressing cells from embryos (*Myod*^{Cre}; *Dicer*^{flox}) results in muscle hypoplasia and perinatal lethality¹¹ supporting an essential role of miRNAs in muscle development. This role was further dissected during muscle formation and homeostasis in experiments using *Dicer* conditional KO alleles in conjunction with a *Pax7-Cre*^{ERT2} driver mouse, where MuSCs exiting from quiescence exhausted, thus resulting in failed regeneration after muscle injury¹². The initial finding that some miRNAs were expressed in a tissue-specific fashion was confirmed in a study showing that miR-1, miR-122a and miR-

124a expression is restricted to striated muscle, liver and brain, respectively¹³, whereas 30 miRNAs are enriched or specifically expressed in skeletal muscle¹⁴. Interestingly, myomirs either appear to have uniform expression throughout the muscle (miR-1 and miR-133a)^{15,16}, or are enriched in slow-twitch, type I muscles (miR-206, miR-208b and miR-499)^{17,18}. In addition, several candidate miRNAs that regulate the quiescence-activation transition in MuSCs were identified, most notably miR-27b¹⁹, miR-489¹², miR-31²⁰ and miR-195/497²¹.

As previous quantitative and differential data obtained using RT-qPCR or miRNA-microarrays were limited to the quantification of known molecules, we performed an unbiased analysis of small-RNA profiles from stem to differentiated cells in adult myogenesis. Our data provide a key resource for functional studies of the involvement of small-RNAs - including miRNAs, in skeletal muscle, and more broadly in the regulation of stem cell self-renewal and tissue homeostasis.

Results

Small RNA profiling during lineage progression of muscle satellite cells

To identify small RNAs expressed during muscle lineage progression, we sequenced small-RNAs from total RNA of quiescent (freshly isolated), activated (60 h in culture) and differentiated (7 days in culture) myogenic cells. Quiescent satellite cells were isolated by fluorescence-activated cell sorting (FACS) from adult transgenic *Tg:Pax7-nGFP* mouse limb muscles and subsequently lysed for RNA extraction or *in vitro* culture (Figure 1A). Immunological staining confirmed that freshly isolated cells expressed Pax7 whereas Myod expression was undetectable (Figure 1B). Sixty hours after plating in proliferation medium, myoblasts expressed Myod and retained Pax7 expression, whereas Pax7 expression was largely lost after 7 days in culture when the majority of the cells were differentiated.

After RNA extraction, small RNAs were size selected on gel (15-35 nucleotides), cloned and sequenced on an Illumina GAIIx platform. For each time point, 2 to 3 biological replicates yielded on average 3.8 million reads [2.3-4.4] that were mapped to Mm9 genome (Figure 1C). Further alignment of reads to tRNA and mRNA

sequences revealed a low level of contamination from degraded tRNA sequences (0.6 to 3%), whereas mRNA sequences were barely detectable, thereby confirming the quality of the samples. As expected, alignment against mature miRNA sequences (miRBase Release 19) highlighted the fact that the vast majority of sequences corresponded to miRNAs (93% [86-97%]) and marginally to intronic sequences (3% [0.6-6%]). Other classes of small RNAs and in particular piRNAs were not detected in our samples. We subsequently focused on the expression profiles of miRNAs.

miRNAs are widely expressed throughout the muscle lineage

By examining in more detail the miRNA expression data, we observed that out of the 1,281 miRNA sequences used as reference for alignment at the time of the analysis (miRbase r19), 412 (32%) mature miRNAs with an average of more than 10 reads were detected in one biological condition, demonstrating a wide miRNA repertoire expressed in the adult muscle lineage (Figure 1D). Furthermore, a very large expression range was observed among these miRNAs, with more than 100 miRNAs showing more than 1000 reads in one condition (Figure 1E). The distribution of the number of expressed miRNAs according to their expression level was closely comparable for each of the quiescent, activated and differentiated biological states, suggesting an overall similar miRNA abundance during myogenic commitment. However, examination of the relative abundance of the few miRNAs highly expressed during quiescence in the other two conditions pointed to dramatic changes in expression of distinct miRNAs (Figure S1). This observation underscored the importance of robust normalization of the datasets to avoid skewing of the expression profiles as a result of the high expression of a limited number of miRNAs.

miRNAs expression profiles show dynamic regulation during lineage progression

Following normalization, hierarchical clustering regrouped the samples according to each biological condition (Pearson correlation coefficient $R^2 > 0.92$ among replicates) demonstrating the robustness of the datasets (Figure S2). We confirmed the increase in expression of myomirs (*i.e.* miR-1, miR-133, miR-206 and miR-378) during myogenic commitment (Figure S3A-E), as well as the expression of quiescence associated miR-195 and miR-489 previously reported (Figure S3F-G)^{8,10,12,21}. However, we did not recapitulate the expression profiles of miR-27b and miR-31 that

were reported to be upregulated in Pax3-positive quiescent MuSCs isolated from abdominal and diaphragm muscles (Figure S3H-I)^{19,20}. Our data are in agreement with expression profiles previously published for these miRNAs using RT-qPCR of quiescent and activated MuSCs from limb muscles¹².

We then conducted a differential analysis between quiescent MuSCs, activated and differentiated myogenic cells. Out of the 412 miRNAs that were expressed, we identified 249 differentially expressed miRNAs in the 3-pairwise comparisons (corrected p -value<0.001): 209 between quiescent and activated, 126 between quiescent and differentiated, and 110 between activated and differentiated muscle cells (Figure 2A-C). Thus, micro-RNAs appear to be involved in the regulation of each of the tested cell states. Importantly, we observed that the majority of differential miRNA expression patterns were related to the transition from quiescence to activation (Figure S4).

We then regrouped the differentially expressed miRNAs according to their expression profiles using K-means clustering which reveals 4 classes (Figure 2D). The first consisted of 59 miRNAs whose expression was found to be associated with quiescence. The second and third clusters comprised miRNAs either expressed during activation, or conversely silenced in this cell state; they represented 70 and 64 miRNAs, respectively. Finally, the last cluster was composed of miRNAs showing an increase in expression during commitment and differentiation, among which were the myomir class. Overall, the most important transition was between quiescence and activation, where more than half of the differentially expressed miRNAs identified were specific to these states. This finding highlights the concerted role that miRNAs play during the regulation in this transition.

Dynamic regulation of miRNAs during regenerative myogenesis in vivo

To validate the expression of differentially regulated miRNAs during commitment in vitro, we isolated myogenic cells from (i) resting *Tibialis anterior* (TA) muscle, (ii) 3 days post-notexin injury of TA muscle, and (iii) dissociated Extensor Digitorum Longus (EDL) muscle fibres with stripped satellite cells. To compare the miRNA expression profiles by RT-qPCR across distinct cell states during myogenic commitment, we chose to normalize for the number of cells. Of 6 differentially

expressed miRNAs identified by sequencing, 5 showed both the expected trend and magnitude of dynamic expression. For the remaining miRNA (miR-26b), the trend was similar but a less pronounced magnitude was observed. If considering that the behaviour of miRNAs that are co-clustered with several that we tested show similar trends, this provides validation of a larger set of miRNAs. Additionally, we compared our sequencing dataset to the published profiling of miRNA during *in-vivo* activation obtained by RT-qPCR¹². When focusing on the 228 miRNAs that were detected by both methods, we observed an overall concordance of data (Figure S5A). A number of miRNAs absent from the RT-qPCR dataset were however detected, completing the miRNA profiling in the Quiescence/Activation transition. Also, several miRNAs amplified by PCR were unambiguously absent from the sequencing dataset. Taken together, these observations validated our *in vitro* model of MuSC lineage progression and the quiescence/activation transition.

A subset of miRNAs is disproportionately upregulated in quiescent MuSCs

Quiescent MuSCs have a reduced cytoplasmic to nuclear ratio, reduced metabolism, and lower levels of total mRNA and protein compared to activated and differentiated cells^{22,23}. Previous reports stated that miRNAs were globally downregulated in human muscle stem cells²⁴. We thus compared the miRNA and total RNA content in quiescent and activated MuSCs and found that the miRNA/total RNA ratio did not change significantly. Moreover, given the per-cell normalization we used in our RT-qPCR assay, our analysis leads us to propose that tens of miRNAs have higher levels of expression in quiescent MuSCs compared to activated and differentiating myoblasts. Taken together, these findings suggest that the miRNAs over-expressed during quiescence are potent regulators in exerting their effect in satellite cells.

Comparative analysis of expressed miRs and Quiescence vs. Activated transcriptomes

Having identified a set of miRNAs specifically expressed during quiescence, we set out to assess their influence globally on the transcriptome. To that end, we retrieved high-confidence miRNA targets from Targetscan 7 database (<http://www.targetscan.org>) with either more than 2 conserved or more than 3 non-conserved target sites, and a Cumulative weighted context++ score < -0.2 ²⁵. First, we selected mRNA targeted by the 59 miRNAs expressed in quiescence and obtained a

list of 8,013 transcripts. We compared their expression level to non-targeted mRNA in a published dataset of quiescent vs. activated MuSCs²⁶, but did not find any difference with the non-targeted transcripts (Figure S6). We then decided to focus on mRNA transcripts that were targeted only by quiescent-specific miRNAs, thus excluding mRNAs also targeted by activation- and differentiation-miRNAs. We obtained a reduced list of 186 putative targets. Interestingly, these transcripts were upregulated during activation of muscle cells, concomitantly with downregulation of quiescent-specific miRNAs (Figure 4).

Discussion

In the framework of the present work, we provide the first open platform for analysis of small RNAs expressed during lineage progression of adult muscle stem cells. In this adult tissue stem cell paradigm, we did not observe the expression of piwi-RNAs that were reported to be expressed in germ cells²⁷. However, some reads mapped to intronic regions that could constitute endo-siRNAs. Our data show that small RNAs expressed in the muscle lineage overwhelmingly correspond to microRNAs. Several reports have shed light on the regulation of miRNAs in muscle, but they detected only a limited number of small RNAs using RT-qPCR¹² or miRNA microarrays²¹. The only miR-seq dataset reported did not include an isolated quiescent MuSC sample, impeding the study of miRNA regulation in the transition states from quiescent to activated muscle stem cells²⁸. Our comparisons with that report²⁸ pointed to some discrepancies (e.g. absence of increase in miR-206 level during MuSC activation, or absence of deregulation in miR-489 expression during early injury). However, our dataset was globally concordant with an RT-qPCR based analysis¹².

We observed massive deregulation of miRNAs during the quiescence-activation transition in mouse MuSCs. This was unexpected given low level of regulatory activity and small cytoplasmic content of quiescent muscle stem cells. Instead, the relatively high number of miRNAs enriched during quiescence lead us to propose that the cellular quiescence represents a poised state that is actively repressed by class-specific miRNAs. We showed experimentally that many miRNAs have a higher expression in quiescent satellite cells compared to activated cells underscoring the notion that the regulation of the quiescent state in MuSCs is an actively maintained

process involving in part a large repertoire of miRNAs. Accordingly, the identification of miR-195/497 and miR-489 as regulators of the quiescence/activation transitions, and Notch signaling as a key mediator of the retention of MuSCs in their niche reinforces this notion^{12,21,29,30}.

Our observations in the mouse are in clear contradiction with a report stating that miRNAs were all downregulated in human quiescent MuSCs which lead to the proposal that quiescent cells represent minimal regulatory activity²⁴. These discrepancies could be linked to a low number of miRNAs detected in the human study, that impeded the normalization and robustness of the data, or they might be related to *bona fide* species differences. Interestingly, Pax7-positive quiescent cells showed miR-27b expression, but absence of miR-31 expression, thus pointing to potential differences in miRNA regulation between Pax3- and Pax7 expressing cells from trunk and limb, respectively^{19,20}.

In this study, we identified novel miRNA candidates as potential regulators of cell state-specific transitions during myogenic lineage progression, and were interested to identify their influence on mRNA levels. We could not observe this repression on the several thousand mRNAs putatively targeted by quiescence miRNAs. But when focusing on mRNAs only targeted by these quiescent miRNA, we observed a clear trend towards a downregulation of these transcripts. These observations point to a collective control by miRNAs on the expression of specific mRNAs during these cell transitions. Nevertheless, future work will be required in gain or loss of function experiments to uncover the molecular function of these differentially expressed miRNAs, and to identify their relevant targets in the context of induction and maintenance of quiescence, beyond the pivotal role of miR-489 and miR-195/497 already noted in Pax7-positive cells. In addition, identifying the signaling pathways upstream of these miRNAs will allow us to shed light on this tightly regulated biological process.

In summary, our findings that a relatively significant variety of miRNAs are dedicated to negotiate the quiescence to activation states of muscle stem cells suggests that quiescence is actively repressed by this class of regulators, but in a poised state.

These results can impact on our views of genetic and epigenetic regulation of quiescence and how this critical cell state is regulated in homeostasis and trauma.

Methods

Mice and flow cytometry of MuSC

Quiescent muscle stem cells were collected from adult *Tg:Pax7-nGFP* mice as described previously³¹. Six-weeks old male mice were sacrificed by cervical dislocation, and their limb muscle were dissected, minced and digested in collagenase 0.1% and trypsin 0.25% at 37°C under gentle agitation. Cells were collected in serum-containing medium and subjected to FACS sorting based on positive GFP-fluorescence and negative Propidium Iodide fluorescence (10µg/ml; Sigma-Aldrich). *In-vivo* activated satellite cells were collected by FACS from regenerating injured muscle. The *Tibialis anterior* (TA) muscle of 6-week-old *Tg:Pax7-nGFP* mice was injured by intramuscular injection of the snake venom notexin under anesthesia (0.5% Imalgene/2% Rompun) as described³². Four days after injury, regenerating TA muscles were dissected, dissociated and cells were isolated as aforementioned. The differentiated samples used for the validations of the sequencing data were obtained by dissociation of single fibers of *Extensor digitorum longus* muscle from adult 6-week-old *Tg:Pax7-nGFP* mice as described³³, with slight increase of both Collagenase D concentration (0.5% final) and incubation time (1 hour at 37°C), in order to strip off satellite cells. This removal of MuSCs was assessed by microscopy after immunostaining for Pax7. All experiments with animals were performed under conditions established by the European Community and approved by the local Ethic Committee at Institut Pasteur, and the French Ministry.

Antibodies and immunostainings

Cells were fixed in 4% paraformaldehyde (EMS) for 5 minutes at room temperature, permeabilised for 5 min in 0.05% Triton-X100 (Sigma-Aldrich) and blocked in 10% normal goat-serum. Cells were stained for Pax7 (1/20, DSHB), Rabbit anti-Myod (1/200, Santa Cruz) and Rabbit anti-Myogenin (1/200, Santa Cruz) and secondary Fab'2 antibodies raised in goat coupled to Alexa-488 and Alexa-546 (1/500,

Invitrogen). Nuclei were counterstained using Hoechst, and after mounting cells were imaged using an upright fluorescent microscope (Zeiss).

Satellite Cell Culture and differentiation

Freshly isolated satellite cells were seeded at 3,000 cells/cm² in 1:1 DMEM:MCDB (Gibco and Sigma-Aldrich, respectively) containing 20% serum FBS (Gibco) and 1% Ultrosor G (Pall) on Matrigel coated flasks (BD Biosciences) and cultured in an incubator under physiological oxygen pressure (37°C, 6.5% CO₂, 3% O₂). Sixty hours after plating, medium was replaced to remove Ultrosor G, and cells were cultured for a total of 7 days to reach early differentiation.

Total RNA extraction and small RNAs deep sequencing

For RNA collection, quiescent cells were directly sorted into Trizol-LS reagent (Invitrogen), and *in-vitro* cultured cells (activated at 60 hours and differentiated at 7 days) collected in Qiazol reagent (Qiagen). Total RNA was subsequently purified using the miRNeasy Mini Kit following the manufacturer instructions (Qiagen). Ten micrograms of total RNA obtained from several animals for the quiescent samples, were used for each biological replicate prepared for deep sequencing (*i.e.* 2 replicates for the quiescent and differentiated samples, and 3 replicates for the *in vitro* activated sample). For RT-qPCR validations all samples were extracted using the same methods (Trizol LS after FACS for quiescent and *in-vivo* activated MuSC; Qiazol for isolated single fibres).

Quantitative RT-PCR

For validations, reverse transcription was performed on RNA amount corresponding to fixed absolute number of cells for quiescent and activated SC (*i.e.* 25,000 cells per RT) in order to be compared. For differentiated muscle fibres, the amount of RNA used in the reverse transcription and following PCR was comparable to the activated cells. Reverse transcription of miRNAs was performed on total RNA using the miRCURY LNA Universal RT-PCR system following the manufacturer's instructions (Exiqon). Quantitative PCR was performed using SYBR Green based mix (Exiqon) and LNA™ PCR primer set (Exiqon) targeting mmu-miR-127-3p (Ref.204048), mmu-miR-379 (Ref.204296), mmu-mir26a (Ref.204724), mmu-mir-195 (Ref.204186),

mmu-miR-183 (Ref.204652), mmu-mir-17 (Ref.204108), U6 snRNA (Ref.203907) and RNU5G (Ref.203908). Analysis was performed using the $2^{-\Delta\text{CT}}$ method³⁴.

Size fractionation of RNAs

For each biological replicate, 10 µg of total RNA (in 10 µl) were mixed with 10 µl of 2X TBE-Urea Sample Buffer (Invitrogen) and loaded in a well of a 15% polyacrylamide TBE-urea gel (Biorad). After migration, the gel was soaked in a SYBR gold (Invitrogen) solution, and imaged on a Dark Reader transilluminator. The 18-35 nucleotide region was cut using a scalpel for each sample, and the RNA eluted in 300 µl of 0.3 M NaCl solution under rotation for 4 hours at room temperature. The eluate was transferred together with gel debris onto a Spin X cellulose acetate filter (VWR) and centrifuged for 2 minutes at 12,000 xg. Small RNAs were finally precipitated by addition of 1 µl of glycogen (Invitrogen) and 750 µl of room temperature 100% ethanol followed by an incubation at -80°C for 30 min, and centrifugation for 25 minutes at 14,000 rpm and +4°C. The pellet was washed with 750 µl 75% Ethanol, dried and resuspended in 5 µl ultrapure water with 0.5 µl of RNaseOUT (Invitrogen).

Library preparation for small RNA-seq

Small RNAs purified on gel were mixed to 1 µl of 10 µM pre-adenylated 3' Illumina linker V1.5 (5'-rAppATCTCGTATGCCGTCTTCTGCTTG/3ddC/-3'), denatured for 2 min at 70°C, and further mixed with 1 µl of 10X T4 RNA-Ligase Truncated Reaction buffer, 0.8 µl 100 mM MgCl₂, 0.5 µl RNaseOut and 1.5 µl of T4 RNA Ligase 2 truncated (New England Biolabs). Ligation was performed at 22°C for 1 h. Then, 0.5µl of 5'-RNA adapter (5'-r(GUU CAG AGU UCU ACA GUC CGA CGA UC) -3'), 1 µl of 10 mM ATP and 1µl T4 RNA ligase (Ambion) were added, and ligation was performed at 20°C for 6 h. Adaptor ligated RNA in a volume of 4µl were then mixed with 1 µl of 20µM Solexa RT primer (5'- CAA GCA GAA GAC GGC ATA CGA -3') and denatured at 70°C and cooled on ice. Reverse transcription was then performed after addition of 2µl 5X first strand buffer (Invitrogen), 0.5µl of 12.5 mM dNTP mix, 1µl of 100 mM DTT, 0.5µl_ RNase OUT and 1 µl SuperScript III Reverse Transcriptase (Invitrogen) at 50°C for 1 h, followed by 10 min at 70°C. The obtained cDNA was PCR amplified by addition of 27 µl Ultra-pure water, 10µl 5X Phusion-HF buffer, 1µl of 25µM Forward Primer (5'- AAT GAT ACG GCG ACC ACC GAC AGG TTC AGA

GTT CTA CAG TCC GA -3'), 1µl of 25 µM reverse Primer(5'- CAA GCA GAA GAC GGC ATA CGA -3'), 0.5µl of 25 mM dNTP mix, and 0.5µl Phusion DNA Polymerase (Finnzymes) using 12 cycles 98°C 10 sec / 60°C 30 sec / 72°C 15 sec. The library was finally purified on a 5% TBE PAGE gel, by cutting the region corresponding to the 92-106bp (the ligated linkers corresponding to a 73bp band visible on the gel). The gel was crushed by centrifugation and eluted in 1X Elution buffer (Illumina) by rotation for 2 hours at RT. The eluate was cleared using a Spin-X column and precipitated after addition of 1 µl of glycogen, 10 µl of 3M NaOAc and 325 µl of -20°C 100% ethanol, followed by centrifugation for 20 min at 14,000 rpm. After washing, the pellet was resuspended in 1ml dH₂O. Finally, the sample was diluted to 10 nM and submitted to sequencing on a Solexa GA-IIX at the core sequencing facility.

Bioinformatic analysis and statistics

Analysis of the microRNAs expression was performed from fastq raw files using the Galaxy Mississippi tool suite (<https://mississippi.snv.jussieu.fr>) provided by ARTbio bioinformatics analysis facility (Sorbonne Universités, UPMC Univ. Paris 06, CNRS FR3631 Institut de Biologie Paris Seine, Paris, France). Briefly, after trimming of adapters, reads were mapped on *Mus musculus* mature miRNA sequences from miRbase 19 using sRbowtie. Normalization of miRNAs counts and differential analysis was further performed using DESeq2 using replicate samples. MicroRNAs with a corrected p-value < 0.001 (Benjamini-Hochberg method) were considered as differentially expressed. Annotation of reads were performed by sequential alignment of reads on collections of annotated RNA sequences including ribosomal, mitochondrial RNA, exonic and intronic mRNA, piRNA and miRNAs as previously described³⁵. For the mRNA/miRNA correlation analyses, data from Targetscan 7 database were filtered using in-house scripts using stringency in the number of sites and Total context++ score²⁵. For correlation with mRNA expression level, the publicly available dataset GSE47177 was obtained from the Gene Expression Omnibus (www.ncbi.nlm.nih.gov/geo). Comparisons of expression level between the groups of transcripts at the different time post (quiescent, 60h and 84 hours post injury) were performed using a Kruskal-Wallis test. Then, post-hoc comparisons were performed to assess significance in pairwise comparisons with a threshold of 0.05. All statistical tests were performed in R.

Data Availability

The small RNA-seq data generated and analysed during the current study have been deposited in the ArrayExpress database at EMBL-EBI (www.ebi.ac.uk/arrayexpress) under accession number E-MTAB-5955 [<https://www.ebi.ac.uk/arrayexpress/experiments/E-MTAB-5955>].

Acknowledgments

We acknowledge the Flow Cytometry Platform of the Technology Core-Center for Translational Science (CRT) and the Transcriptome and EpiGenome Platform of the Center for Innovation & Technological Research at Institut Pasteur for support in conducting this study. S.T. was funded by Institut Pasteur, Centre National pour la Recherche Scientifique and the Agence Nationale de la Recherche (Laboratoire d'Excellence Revive, Investissement d'Avenir; ANR-10-LABX- 73), the European Research Council (Advanced Research Grant 332893) and the French Muscular Dystrophy Association (AFM-Téléthon). M.B was funded by the Fondation pour la Recherche Médicale (FRM).

Author Contributions Statement

Conceptualization, D.C. and S.T.; Methodology, D.C., S.M., C.A. and S.T.; Investigation, D.C., M.B., S.M., B.G.M., C.A. and S.T; Writing, D.C. and S.T.; Funding Acquisition, S.T.

Conflicts of Interest Statement

The author declare that they have no competing financial interests.

References

1. Collins, C. A. *et al.* Stem Cell Function, Self-Renewal, and Behavioral Heterogeneity of Cells from the Adult Muscle Satellite Cell Niche. *Cell* **122**, 289–301 (2005).
2. Bartel, D. P. MicroRNAs: genomics, biogenesis, mechanism, and function. *Cell* **116**, 281–297 (2004).
3. Elbashir, S. M. *et al.* Duplexes of 21-nucleotide RNAs mediate RNA interference in cultured mammalian cells. *Nature* **411**, 494–498 (2001).
4. Elbashir, S. M., Martinez, J., Patkaniowska, A., Lendeckel, W. & Tuschl, T. Functional anatomy of siRNAs for mediating efficient RNAi in *Drosophila melanogaster* embryo lysate. *EMBO J.* **20**, 6877–6888 (2001).
5. Bernstein, E. *et al.* Dicer is essential for mouse development. *Nat. Genet.* **35**, 215–217 (2003).
6. Kanellopoulou, C. *et al.* Dicer-deficient mouse embryonic stem cells are defective in differentiation and centromeric silencing. *Genes Dev.* **19**, 489–501 (2005).
7. Teta, M. *et al.* Inducible deletion of epidermal Dicer and Drosha reveals multiple functions for miRNAs in postnatal skin. *Dev. Camb. Engl.* **139**, 1405–1416 (2012).
8. Chen, J.-F. *et al.* The role of microRNA-1 and microRNA-133 in skeletal muscle proliferation and differentiation. *Nat. Genet.* **38**, 228–233 (2006).
9. Rao, P. K., Kumar, R. M., Farkhondeh, M., Baskerville, S. & Lodish, H. F. Myogenic factors that regulate expression of muscle-specific microRNAs. *Proc. Natl. Acad. Sci. U. S. A.* **103**, 8721–8726 (2006).
10. Gagan, J., Dey, B. K., Layer, R., Yan, Z. & Dutta, A. MicroRNA-378 targets the myogenic repressor MyoR during myoblast differentiation. *J. Biol. Chem.* **286**, 19431–19438 (2011).
11. O'Rourke, J. R. *et al.* Essential role for Dicer during skeletal muscle development. *Dev. Biol.* **311**, 359–368 (2007).
12. Cheung, T. H. *et al.* Maintenance of muscle stem-cell quiescence by microRNA-489. *Nature* **482**, 524–528 (2012).
13. Lagos-Quintana, M. *et al.* Identification of tissue-specific microRNAs from mouse. *Curr. Biol. CB* **12**, 735–739 (2002).
14. Sempere, L. F., Cole, C. N., McPeck, M. A. & Peterson, K. J. The phylogenetic distribution of metazoan microRNAs: insights into evolutionary complexity and constraint. *J. Exp. Zool. B Mol. Dev. Evol.* **306**, 575–588 (2006).
15. McCarthy, J. J. & Esser, K. A. MicroRNA-1 and microRNA-133a expression are decreased during skeletal muscle hypertrophy. *J. Appl. Physiol. Bethesda Md 1985* **102**, 306–313 (2007).
16. van Rooij, E. *et al.* A family of microRNAs encoded by myosin genes governs myosin expression and muscle performance. *Dev. Cell* **17**, 662–673 (2009).
17. Liu, Y. *et al.* Identification of differences in microRNA transcriptomes between porcine oxidative and glycolytic skeletal muscles. *BMC Mol. Biol.* **14**, 7 (2013).
18. Muroya, S. *et al.* Profiling of differentially expressed microRNA and the bioinformatic target gene analyses in bovine fast- and slow-type muscles by massively parallel sequencing. *J. Anim. Sci.* **91**, 90–103 (2013).
19. Crist, C. G. *et al.* Muscle stem cell behavior is modified by microRNA-27 regulation of Pax3 expression. *Proc. Natl. Acad. Sci. U. S. A.* **106**, 13383–13387 (2009).

20. Crist, C. G., Montarras, D. & Buckingham, M. Muscle Satellite Cells Are Primed for Myogenesis but Maintain Quiescence with Sequestration of Myf5 mRNA Targeted by microRNA-31 in mRNP Granules. *Cell Stem Cell* **11**, 118–126 (2012).
21. Sato, T., Yamamoto, T. & Sehara-Fujisawa, A. miR-195/497 induce postnatal quiescence of skeletal muscle stem cells. *Nat. Commun.* **5**, 4597 (2014).
22. Rocheteau, P., Gayraud-Morel, B., Siegl-Cachedenier, I., Blasco, M. A. & Tajbakhsh, S. A subpopulation of adult skeletal muscle stem cells retains all template DNA strands after cell division. *Cell* **148**, 112–125 (2012).
23. Rodgers, J. T. *et al.* mTORC1 controls the adaptive transition of quiescent stem cells from G0 to G(Alert). *Nature* **510**, 393–396 (2014).
24. Koning, M., Werker, P. M. N., van Luyn, M. J. A., Krenning, G. & Harmsen, M. C. A global downregulation of microRNAs occurs in human quiescent satellite cells during myogenesis. *Differ. Res. Biol. Divers.* **84**, 314–321 (2012).
25. Agarwal, V., Bell, G. W., Nam, J.-W. & Bartel, D. P. Predicting effective microRNA target sites in mammalian mRNAs. *eLife* **4**, (2015).
26. Liu, L. *et al.* Chromatin modifications as determinants of muscle stem cell quiescence and chronological aging. *Cell Rep.* **4**, 189–204 (2013).
27. Aravin, A. *et al.* A novel class of small RNAs bind to MILI protein in mouse testes. *Nature* **442**, 203–207 (2006).
28. Aguilar, C. A. *et al.* Transcriptional and Chromatin Dynamics of Muscle Regeneration after Severe Trauma. *Stem Cell Rep.* **7**, 983 (2016).
29. Bjornson, C. R. R. *et al.* Notch signaling is necessary to maintain quiescence in adult muscle stem cells. *Stem Cells Dayt. Ohio* **30**, 232–242 (2012).
30. Mourikis, P. *et al.* A Critical Requirement for Notch Signaling in Maintenance of the Quiescent Skeletal Muscle Stem Cell State. *STEM CELLS* **30**, 243–252 (2012).
31. Gayraud-Morel, B., Pala, F., Sakai, H. & Tajbakhsh, S. Isolation of Muscle Stem Cells from Mouse Skeletal Muscle. *Methods Mol. Biol. Clifton NJ* **1556**, 23–39 (2017).
32. Gayraud-Morel, B. *et al.* A role for the myogenic determination gene Myf5 in adult regenerative myogenesis. *Dev. Biol.* **312**, 13–28 (2007).
33. Gayraud-Morel, B. *et al.* Myf5 haploinsufficiency reveals distinct cell fate potentials for adult skeletal muscle stem cells. *J. Cell Sci.* **125**, 1738–1749 (2012).
34. Livak, K. J. & Schmittgen, T. D. Analysis of relative gene expression data using real-time quantitative PCR and the 2(-Delta Delta C(T)) Method. *Methods San Diego Calif* **25**, 402–408 (2001).
35. Jouneau, A. *et al.* Naive and primed murine pluripotent stem cells have distinct miRNA expression profiles. *RNA* **18**, 253–264 (2012).

Figure Legends

Figure 1. Unbiased identification of stage specific small RNAs during lineage progression from muscle stem cells.

(A) Quiescent MuSCs were isolated after digestion of resting limb muscles and diaphragm from adult *Tg:Pax7-nGFP* mice by FACS using GFP fluorescence. An aliquot was cultured *in vitro* for 60 h or 7 days, and the remainder was lysed directly for RNA extraction. After size selecting 15-35 nucleotides small RNAs on a polyacrylamide gel, sequencing libraries were prepared and analysed.

(B) Schematic representation of lineage progression in adult skeletal muscle. Quiescent, activated and differentiated samples are represented. Immunofluorescence images confirmed the cellular identity of the 3 populations (i) quiescent MuSC: Pax7(+), MyoD(-) ; Activated MuSC/myoblasts: Pax7(+), MyoD(+) ; Differentiated muscle cells: Pax7(-) Myog(+). Note the presence of rare self-renewing “reserve cells” expressing Pax7 in the differentiated sample.

(C) Sequenced small RNA corresponded overwhelmingly to miRNAs in all 3 samples, and showed low contamination by degraded tRNA. Despite the inclusion of the 25-32 nt size range in the analysis, no piRNAs sequences were detected, whereas reads mapping to intronic regions were identified in particular in the quiescent samples (>5% reads).

(D) 412 and 231 miRNAs were detected in at least one sample type more than 10 or 100 times, respectively.

(E) Frequency histogram displaying the miRNAs distribution according to their expression levels in all 3 samples highlight their large dynamic range in expression.

Figure 2. Identification of differentially expressed miRNAs during myogenic lineage progression.

(A) Scatter plot of miRNA expression level in Quiescent vs. Activated,

(B) Quiescent vs. Differentiated and

(C) Activated vs. Differentiated myogenic cells. Results are presented as the median of log transformed normalized counts for each miRNA. Out of 412 miRNAs detected, 249 showed a modulation that reached statistical significance in the 3 pairwise comparisons. (corrected p -value ≤ 0.001). Statistically significant up- or down-regulated miRNAs were colored in yellow and blue, respectively.

(D) Heatmap presenting 4 classes of differentially expressed miRNAs identified by Kmeans clustering. MicroRNAs are involved in the regulation of all processes – quiescence, activation and self-renewal and differentiation, and a large number of miRNAs with expression specific of one particular state were identified. High expression is coloured in yellow, whereas low expression is blue as in previous panels.

Figure 3. Validation of miRNA regulation on *in vivo* activated MuSCs

Histogram presenting parallel expression measured by small-RNAseq following *in vitro* culture, vs. *in vivo* activated MuSCs and isolated single muscle fibres.

(A-F) The trend in expression was confirmed for 6 out of 6 tested miRNAs, and only miR-26a did not show the same amplitude of deregulation on *in vivo* activated samples.

(G-J) identical results were obtained for activation specific miRNAs, thus validating the miRNA-sequencing data using an *in vitro* activation paradigm. Normalization based on cell number allowed to confirm the higher expression level of many miRNAs during quiescence.

Figure 4. Comparative analysis of differentially expressed miRNAs and Quiescent vs. Activated MuSCs transcriptomes

A subset of 183 mRNAs predicted as specific targets of the 59 miRNAs expressed in quiescent MuSC was selected from Targetscan database (blue). Their expression was compared to all other mRNAs (red) during lineage progression from quiescence to activation at 60 and 84 hours post-injury. The mRNAs targeted by quiescent miRNAs display lower expression compared to other mRNAs in quiescent MuSCs, but not in activated MuSCs (at 60 and 84 hours post-injury). When focusing on the expression level of these 183 quiescent-miRNAs targets during lineage progression, we observed global upregulation, concomitantly with the loss of expression of quiescent miRNAs) that reached statistical significance at 84 hours post injury.

Asterisk: comparison that reach statistical significance in a Kruskal-Wallis test followed by post-hoc comparisons with a 0.05 threshold.

Supplemental Figure Legends

Figure S1. Comparison of expression of the seven most abundant miRNAs in quiescence during lineage progression.

Pie-charts display the percentage of reads of the mostly expressed miRNAs in differentiated cells in all 3 biological conditions. A wide variety of miRNAs are expressed in quiescent cells, whereas some miRNAs such as mir-21 (middle) or miR-1 and miR-206 account for increasing part of the detected miRNAs (around 60% of reads in differentiated samples). This points to wide modulation of miRNA expression in the muscle lineage and also raised the necessity of robust normalization of the data.

Figure S2. Assessment of overall similarities and dissimilarities between biological samples.

An unsupervised hierarchical clustering of biological samples was performed using the euclidian distance metrics based on rlog-transformed miRNAs expression counts. The heatmap displays the similarities between samples with dark blue color, together with a dendrogram. All samples regrouped according to the 3 each biological condition (quiescent, activated or differentiated) confirming the similitude of biological replicates. The activated and differentiated samples also appeared more closely related than the quiescent cells.

Figure S3. Expression profile of miRNAs previously identified in the muscle lineage.

Histogram of normalized miRNAs counts measured in quiescent, activated & differentiated MuSCs.

(A-E) Canonical myomiRs, i.e. miR-206, miR-378, miR-1 and miR-133, previously identified as upregulated during activation and differentiation show a robust induction in the small RNA-seq dataset.

(F,G) miR-489 and miR-195, previously associated with MuSCs quiescence are specifically expressed in quiescent samples.

(H, I) miR-31 and miR-27b expression profiles were discordant with the Pax-3 expressing MuSCs showing a down-regulation, or a high expression in quiescent cells, respectively.

Figure S4. Comparison of differentially expressed miRNAs between the different cellular states.

Many miRNAs identified as regulated during lineage progression concern the comparisons with the quiescent condition. Conversely, most miRNAs that are deregulated between activated and differentiated myoblasts are also deregulated between quiescent & activated MuSCs or quiescent MuSCs & differentiated myoblasts.

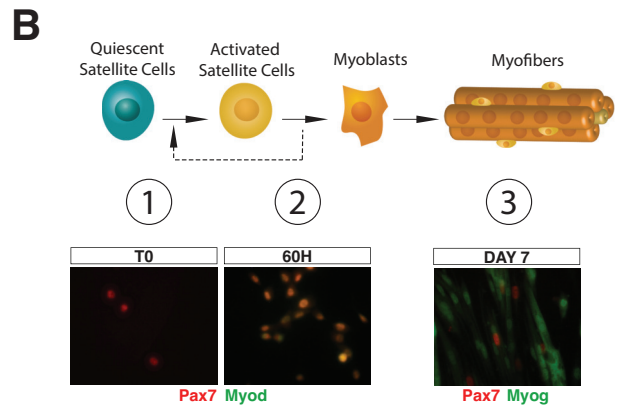
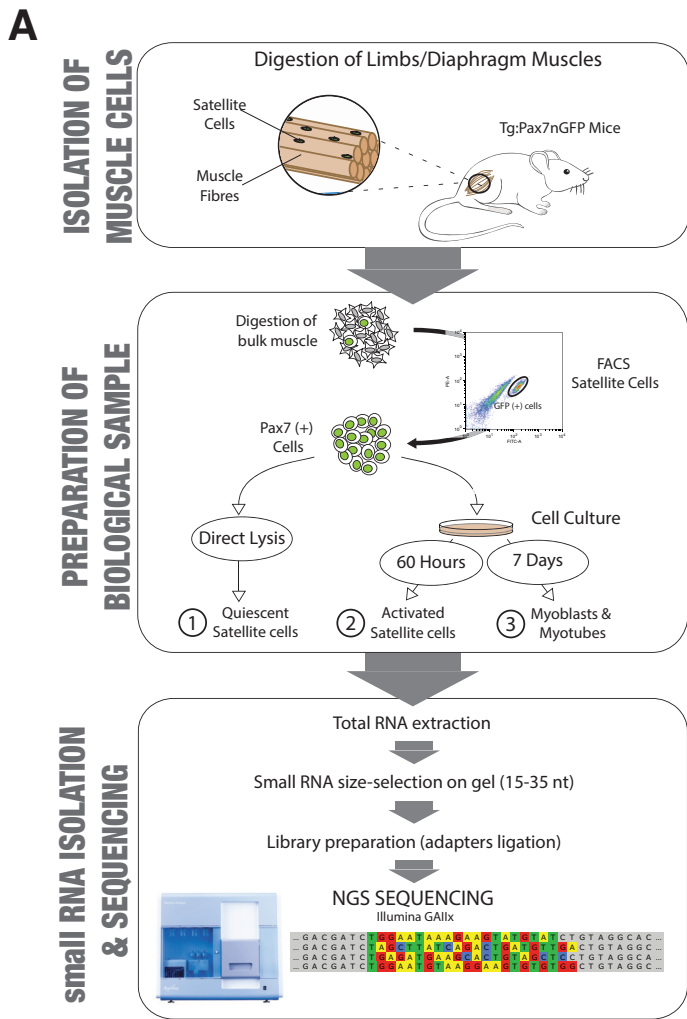
Figure S5. Comparison of data from the miR-seq study and from RT-qPCR profiling previously published by Cheung *and coll.*¹²

A) The log-transformed ratios of [Activated/Quiescent] expression level were plotted to examine the concordance of data between the present dataset and those reported previously¹². Data were filtered for the 228 miRNAs detected by both methods, to highlight the identical trend in expression observed in the two datasets.

B) The same data as in panel A but unfiltered are presented. Circles were colored from white to black according to the average expression level in the miRseq dataset. A subset of miRNAs distributing on the X-axis (white circles) were not detected in the sequencing dataset as opposed to the PCR experiment constituting potential false-positive. Conversely, an important subset of miRNAs were not detected in the RT-qPCR experiment, were detected in the sequencing dataset and distribute on the Y-axis.

Figure S6. Comparative analysis of differentially expressed miRNAs and quiescence vs. activated transcriptomes

High-confidence miRNA targets with either ≥ 2 conserved or ≥ 3 non-conserved target sites, and a Cumulative weighted context++ score < -0.2 were trimmed from Targetscan 7 database. All transcripts targeted by the 59 quiescence-specific miRNAs were selected (n= 8,013). Violin plots display the expression level of targeted mRNAs (blue) vs. non-targeted mRNAs (red) in quiescent or *in vivo* activated MuSCs at 60 and 84 hours post-injury. No difference in the expression levels was observed between the two groups.

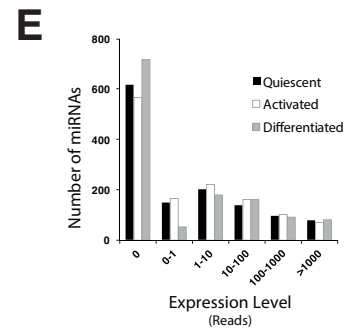


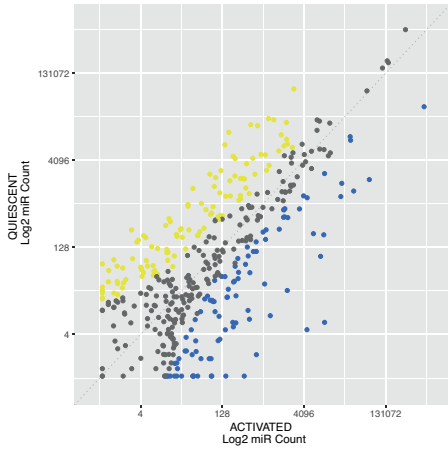
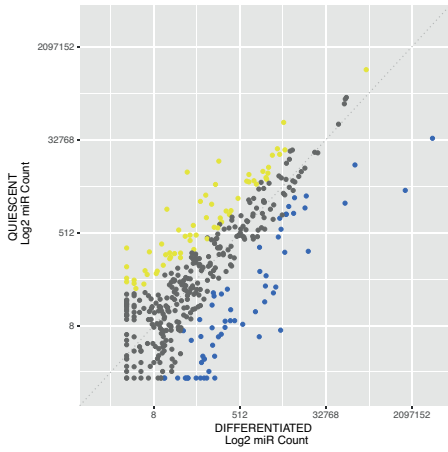
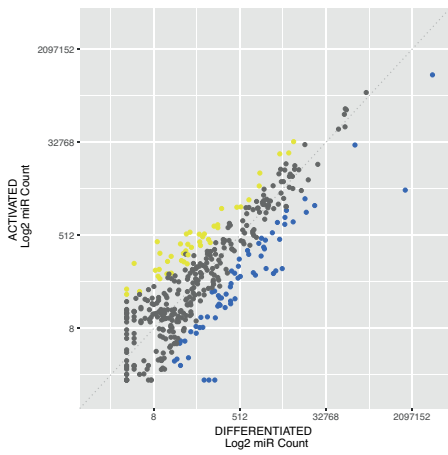
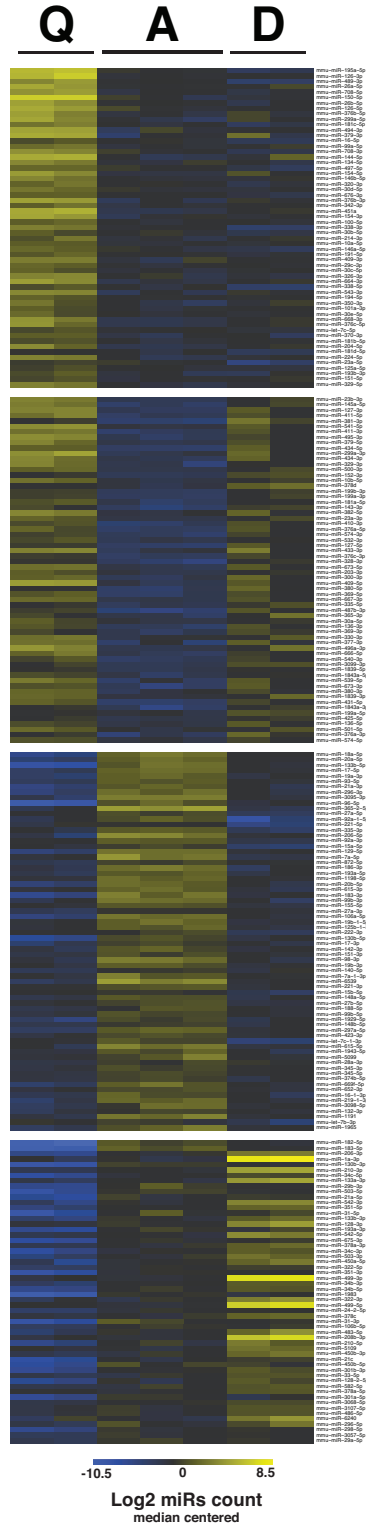
C

Type	Sample	# Mapped Reads	Reads Mapping		
			tRNA (%)	introns (%)	miRNAs (%)
Quiescent	Q1	2 354 632	3.0	4.8	88.0
	Q2	3 572 407	2.2	6.1	86.4
Activated	A1	3 975 094	1.3	2.6	93.0
	A2	4 087 062	0.8	2.1	93.6
	A3	3 689 254	0.6	2.4	94.2
Differentiated	D1	4 580 456	1.4	0.6	97.4
	D2	4 437 330	1.5	0.8	96.8

D

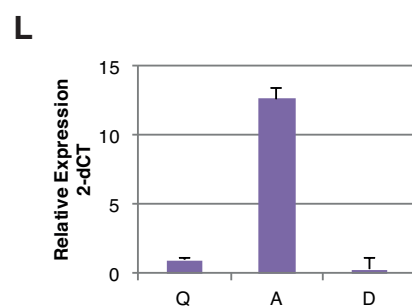
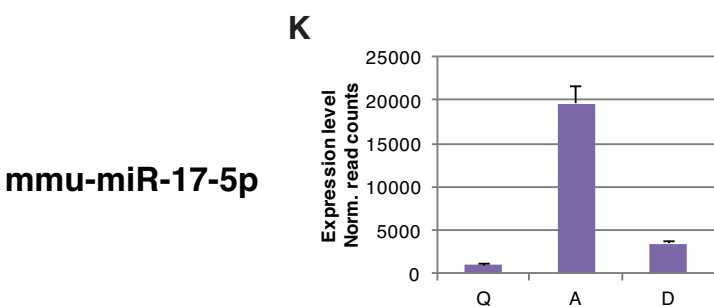
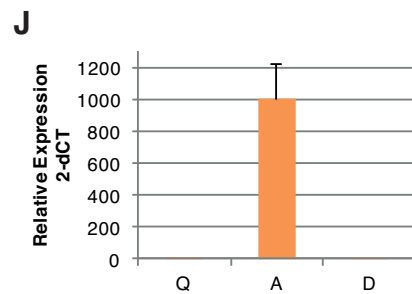
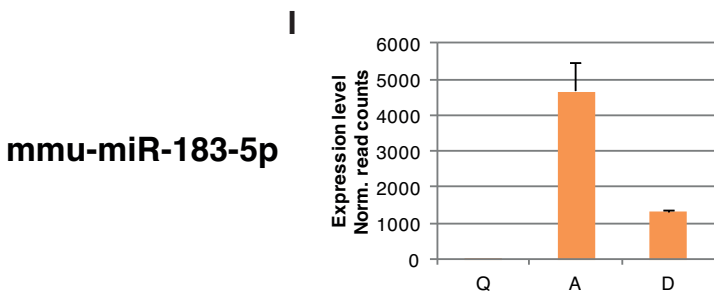
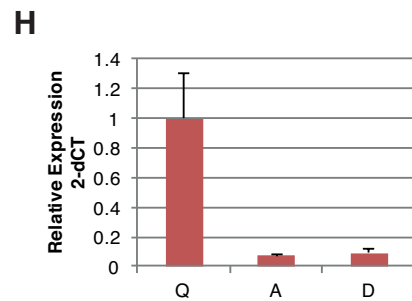
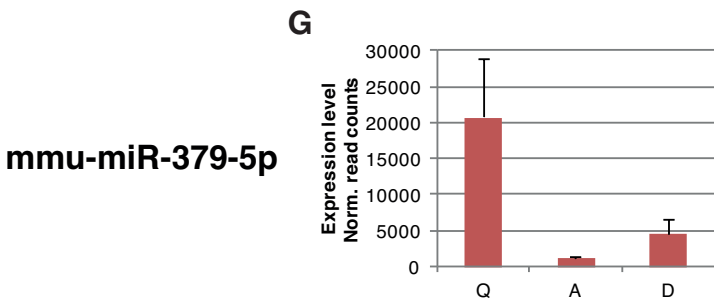
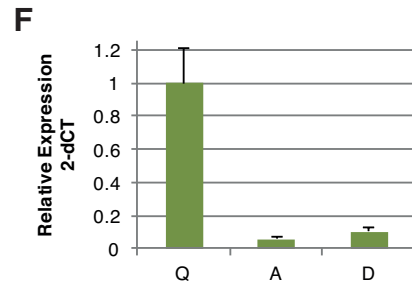
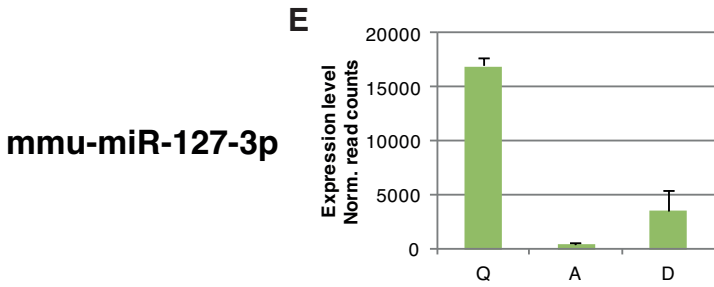
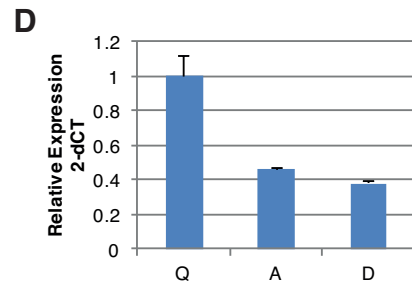
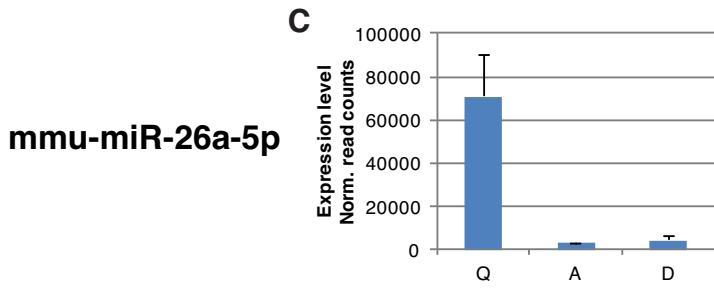
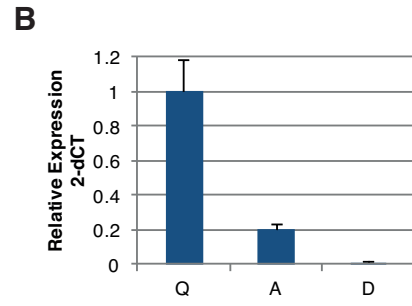
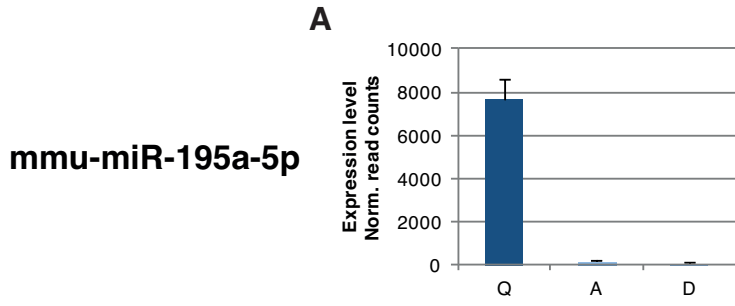
Threshold (Reads)	# detected miRNAs
>100	231
>10	412
>2	561
Total	1281

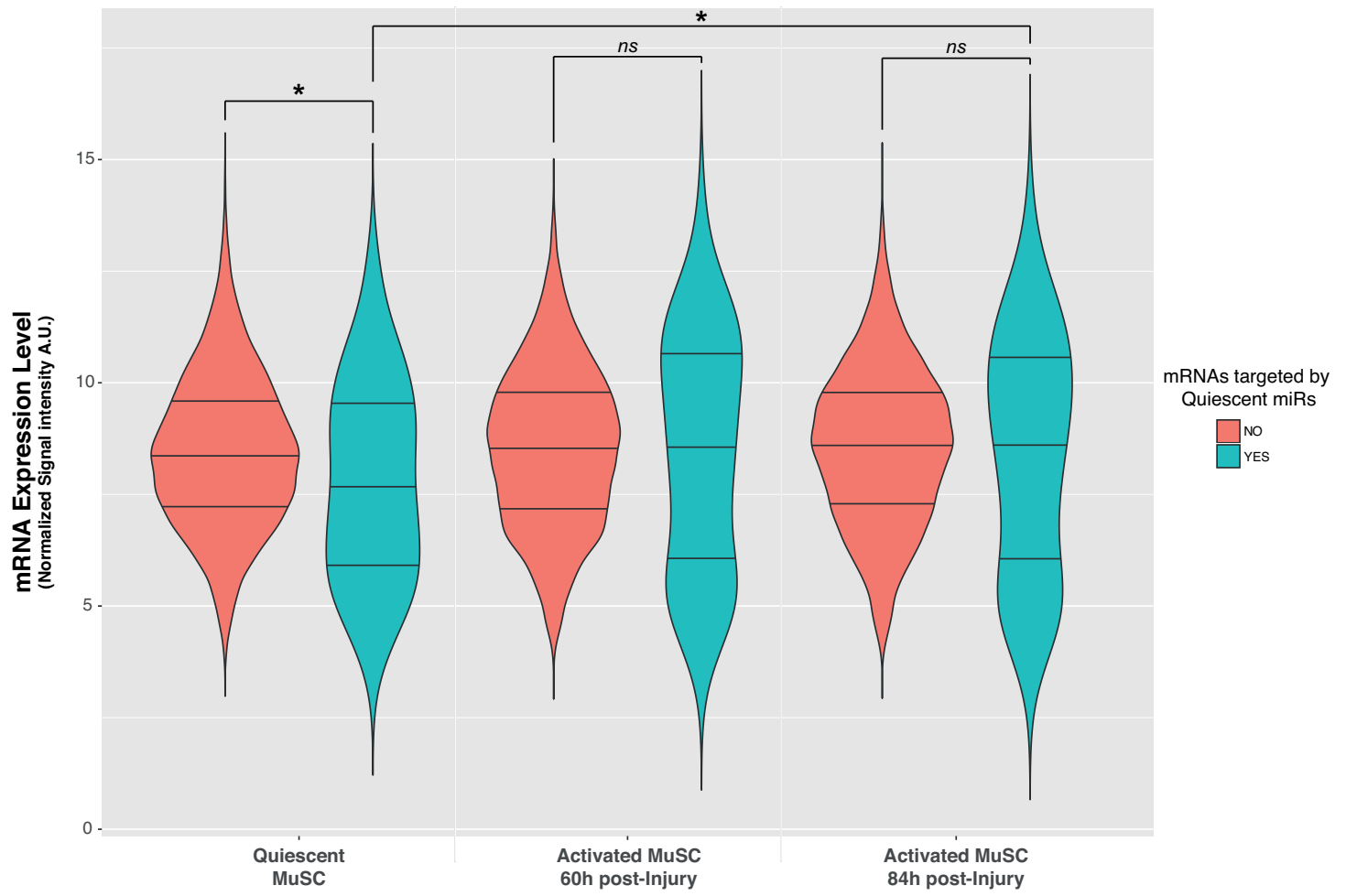


A**B****C****D**

miRNA-seq

RT-qPCR





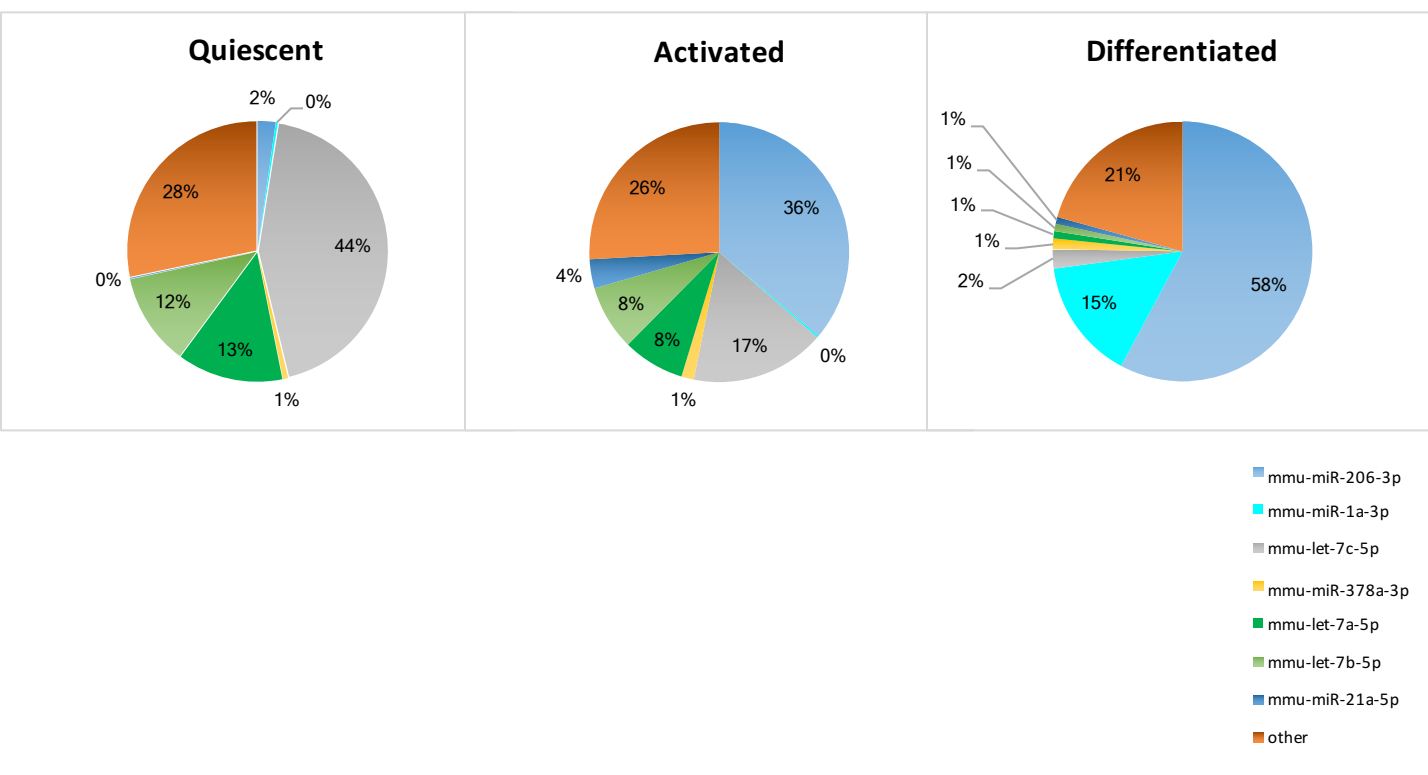


Figure S1. Comparison of expression of the seven most abundant miRNAs in quiescence during lineage progression.

Pie-charts display the percentage of reads of the mostly expressed miRNAs in differentiated cells in all 3 biological conditions. A wide variety of miRNAs are expressed in quiescent cells, whereas some miRNAs such as mir-21 (middle) or miR-1 and miR-206 account for increasing part of the detected miRNAs (around 60% of reads in differentiated samples). This points to wide modulation of miRNA expression in the muscle lineage and also raised the necessity of robust normalization of the data.

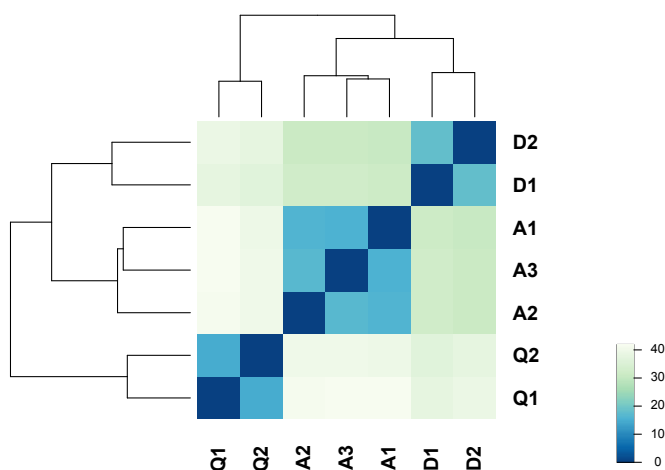


Figure S2. Assessment of overall similarities and dissimilarities between biological samples.

An unsupervised hierarchical clustering of biological samples was performed using the euclidian distance metrics based on rlog-transformed miRNAs expression counts. The heatmap displays the similarities between samples with dark blue color, together with a dendrogram. All samples regrouped according to the 3 each biological condition (quiescent, activated or differentiated) confirming the similitude of biological replicates. The activated and differentiated samples also appeared more closely related than the quiescent cells.

Castel *et al.*
Supplementary Figure S3

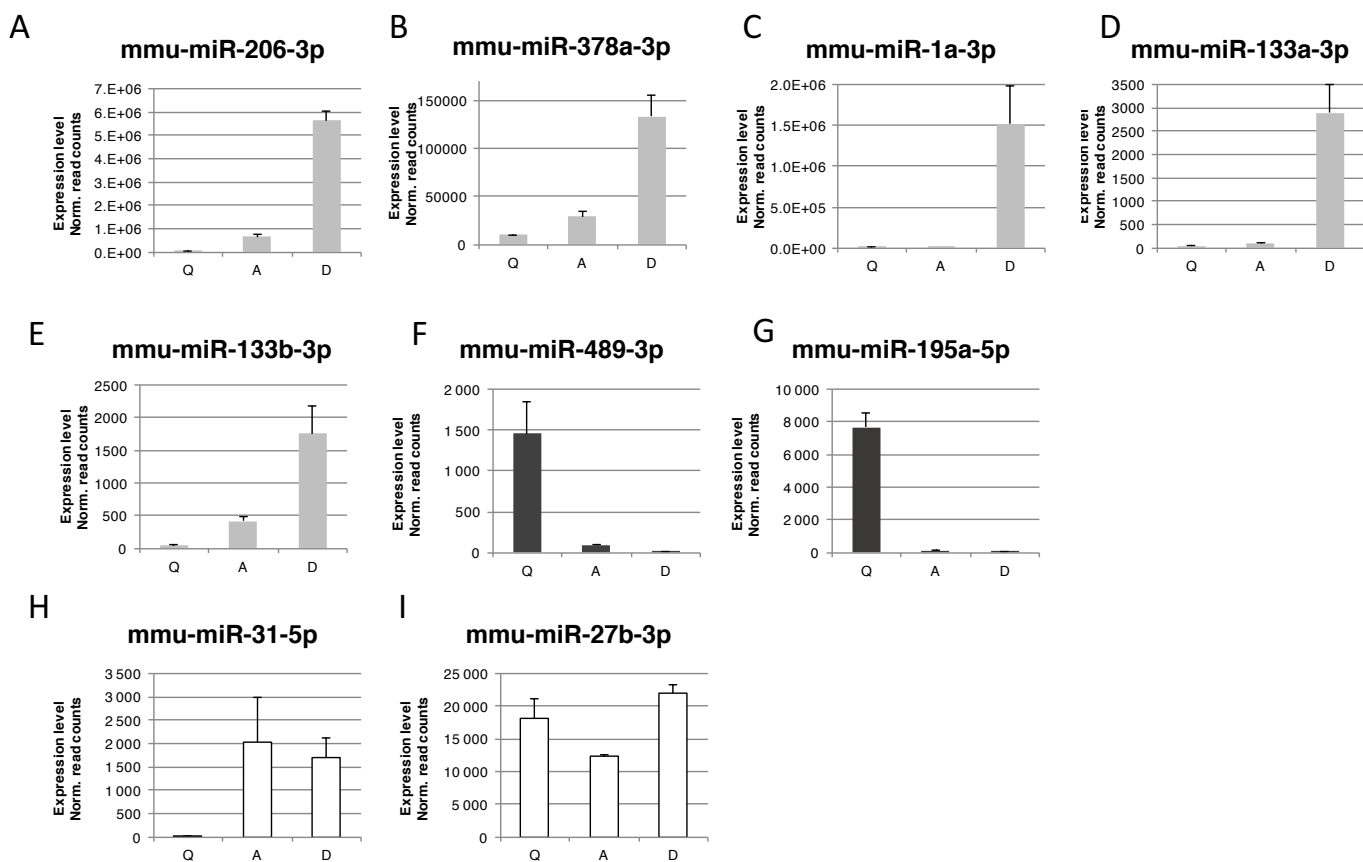


Figure S3. Expression profile of miRNAs previously identified in the muscle lineage.

Histogram of normalized miRNAs counts measured in quiescent, activated & differentiated MuSCs.

(A-E) Canonical myomiRs, i.e. miR-206, miR-378, miR-1 and miR-133, previously identified as upregulated during activation and differentiation show a robust induction in the small RNA-seq dataset.

(F,G) miR-489 and miR-195, previously associated with MuSCs quiescence are specifically expressed in quiescent samples.

(H, I) miR-31 and miR-27b expression profiles were discordant with the Pax-3 expressing MuSCs showing a down-regulation, or a high expression in quiescent cells, respectively.

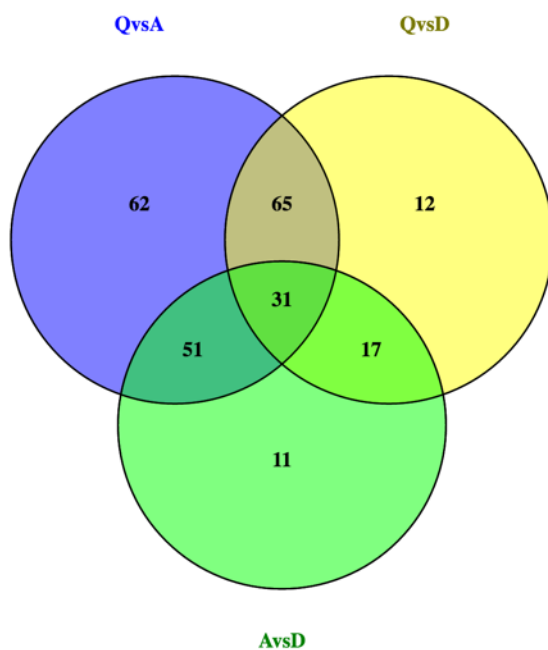


Figure S4. Comparison of differentially expressed miRNAs between the different cellular states. Many miRNAs identified as regulated during lineage progression concern the comparisons with the quiescent condition. Conversely, most miRNAs that are deregulated between activated and differentiated myoblasts are also deregulated between quiescent & activated MuSCs or quiescent MuSCs & differentiated myoblasts.

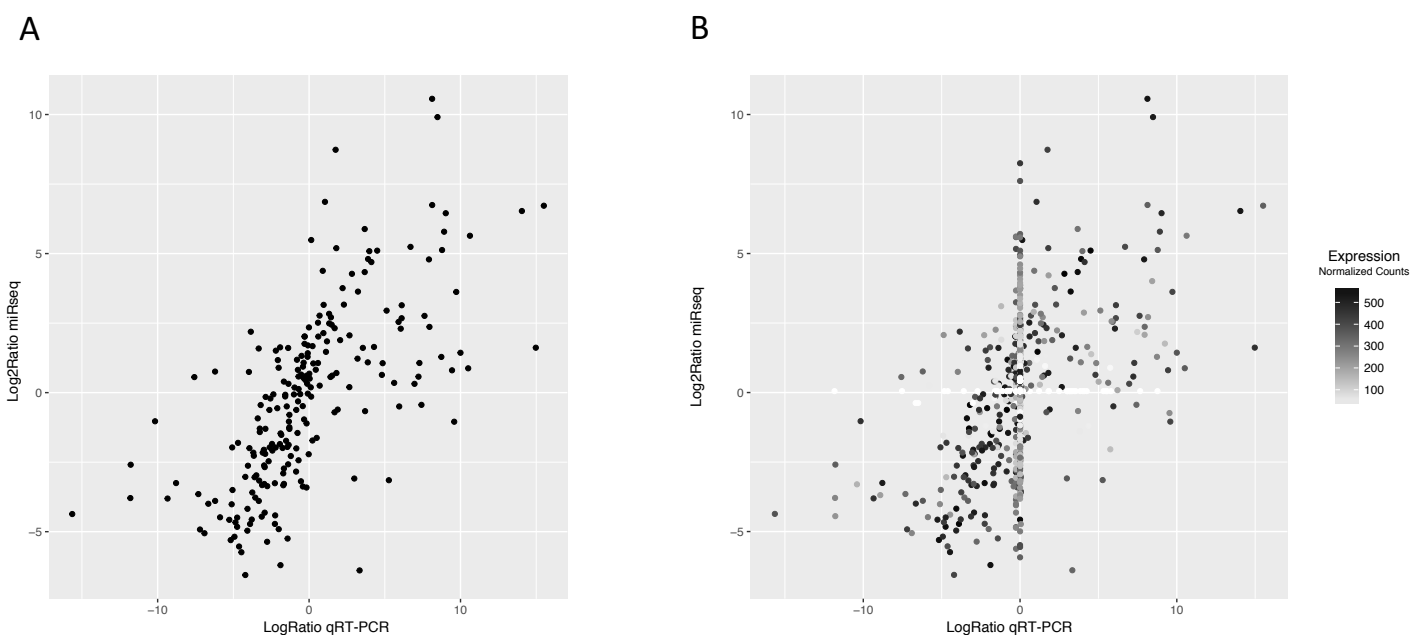


Figure S5. Comparison of data from the miR-seq study and from RT-qPCR profiling previously published by Cheung *and coll.*

A) The log-transformed ratios of [Activated/Quiescent] expression level were plotted to examine the concordance of data between the present dataset and those reported previously. Data were filtered for the 228 miRNAs detected by both methods, to highlight the identical trend in expression observed in the two datasets.

B) The same data as in panel A but unfiltered are presented. Circles were colored from white to black according to the average expression level in the miRseq dataset. A subset of miRNAs distributing on the X-axis (white circles) were not detected in the sequencing dataset as opposed to the PCR experiment constituting potential false-positive. Conversely, an important subset of miRNAs were not detected in the RT-qPCR experiment, were detected in the sequencing dataset and distribute on the Y-axis.

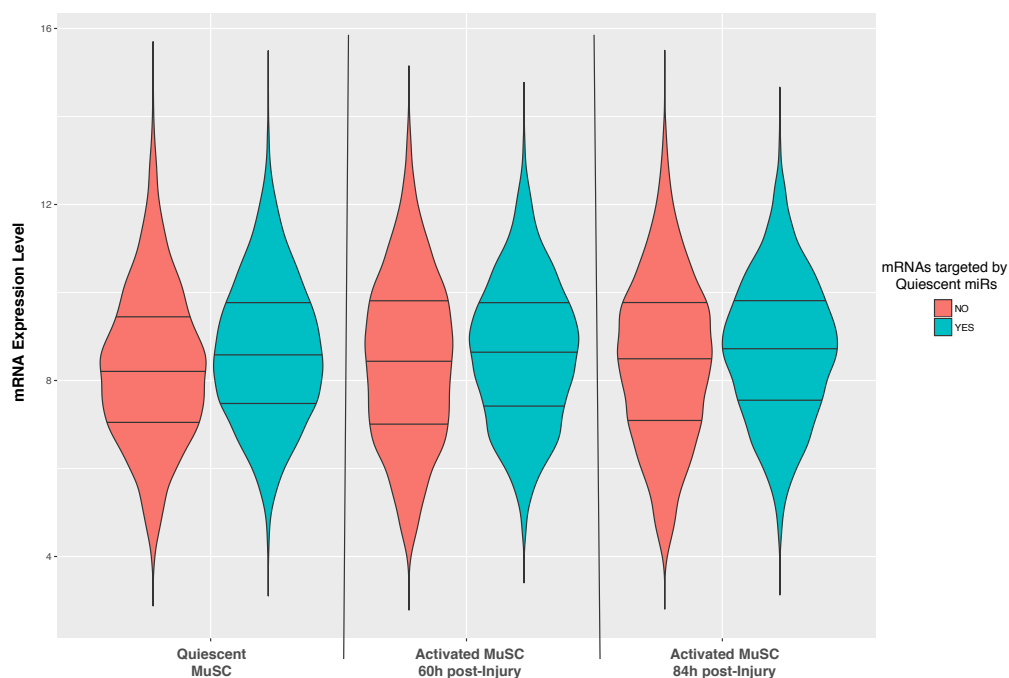


Figure S6. Comparative analysis of differentially expressed miRNAs and quiescent vs. activated MuSCs transcriptomes

High-confidence miRNA targets with either ≥ 2 conserved or ≥ 3 non-conserved target sites, and a Cumulative weighted context++ score < -0.2 were trimmed from TargetsScan 7 database. All transcripts targeted by the 59 quiescence-specific miRNAs were selected ($n = 8,013$). Violin plots display the expression level of targeted mRNAs (blue) vs. non-targeted mRNAs (red) in quiescent or *in vivo* activated MuSCs at 60 and 84 hours post-injury. No difference in the expression levels was observed between the two groups

REFERENCES

Abou-Khalil, R., Le Grand, F., and Chazaud, B. (2013). Human and murine skeletal muscle reserve cells. *Methods Mol Biol* *1035*, 165-177.

Agarwal, V., Bell, G.W., Nam, J.W., and Bartel, D.P. (2015). Predicting effective microRNA target sites in mammalian mRNAs. *eLife* *4*.

Ahmed, M., and Ffrench-Constant, C. (2016). Extracellular Matrix Regulation of Stem Cell Behavior. *Curr Stem Cell Rep* *2*, 197-206.

Alexander, M.S., Casar, J.C., Motohashi, N., Myers, J.A., Eisenberg, I., Gonzalez, R.T., Estrella, E.A., Kang, P.B., Kawahara, G., and Kunkel, L.M. (2011). Regulation of DMD pathology by an ankyrin-encoded miRNA. *Skeletal muscle* *1*, 27.

Allamand, V., Brinas, L., Richard, P., Stojkovic, T., Quijano-Roy, S., and Bonne, G. (2011). ColVI myopathies: where do we stand, where do we go? *Skeletal muscle* *1*, 30.

Ambros, V., Bartel, B., Bartel, D.P., Burge, C.B., Carrington, J.C., Chen, X., Dreyfuss, G., Eddy, S.R., Griffiths-Jones, S., Marshall, M., *et al.* (2003). A uniform system for microRNA annotation. *Rna* *9*, 277-279.

Ameres, S.L., and Zamore, P.D. (2013). Diversifying microRNA sequence and function. *Nature reviews Molecular cell biology* *14*, 475-488.

Anderson, C., Catoe, H., and Werner, R. (2006). MIR-206 regulates connexin43 expression during skeletal muscle development. *Nucleic Acids Res* *34*, 5863-5871.

Angermueller, C., Clark, S.J., Lee, H.J., Macaulay, I.C., Teng, M.J., Hu, T.X., Krueger, F., Smallwood, S., Ponting, C.P., Voet, T., *et al.* (2016). Parallel single-cell sequencing links transcriptional and epigenetic heterogeneity. *Nature methods* *13*, 229-232.

Armand, O., Boutineau, A.M., Mauger, A., Pautou, M.P., and Kieny, M. (1983). Origin of satellite cells in avian skeletal muscles. *Archives d'anatomie microscopique et de morphologie experimentale* *72*, 163-181.

Armulik, A., Genove, G., and Betsholtz, C. (2011). Pericytes: developmental, physiological, and pathological perspectives, problems, and promises. *Dev Cell* *21*, 193-215.

Arnaout, M.A., Goodman, S.L., and Xiong, J.P. (2007). Structure and mechanics of integrin-based cell adhesion. *Current opinion in cell biology* *19*, 495-507.

Arnold, L., Henry, A., Poron, F., Baba-Amer, Y., van Rooijen, N., Plonquet, A., Gherardi, R.K., and Chazaud, B. (2007). Inflammatory monocytes recruited after skeletal muscle injury switch into antiinflammatory macrophages to support myogenesis. *J Exp Med* *204*, 1057-1069.

Arora, R., Rumman, M., Venugopal, N., Gala, H., and Dhawan, J. (2017). Mimicking Muscle Stem Cell Quiescence in Culture: Methods for Synchronization in Reversible Arrest. *Methods Mol Biol* *1556*, 283-302.

Aster, J.C., Pear, W.S., and Blacklow, S.C. (2008). Notch signaling in leukemia. *Annual review of pathology* *3*, 587-613.

Bagutti, C., Forro, G., Ferralli, J., Rubin, B., and Chiquet-Ehrismann, R. (2003). The intracellular domain of teneurin-2 has a nuclear function and represses zic-1-mediated transcription. *J Cell Sci* *116*, 2957-2966.

Bajard, L., Relaix, F., Lagha, M., Rocancourt, D., Daubas, P., and Buckingham, M.E. (2006). A novel genetic hierarchy functions during hypaxial myogenesis: Pax3 directly activates Myf5 in muscle progenitor cells in the limb. *Genes Dev* *20*, 2450-2464.

Barczyk, M., Carracedo, S., and Gullberg, D. (2010). Integrins. *Cell and tissue research* *339*, 269-280.

- Bartel, D.P. (2004). MicroRNAs: genomics, biogenesis, mechanism, and function. *Cell* 116, 281-297.
- Bartel, D.P. (2009). MicroRNAs: target recognition and regulatory functions. *Cell* 136, 215-233.
- Beauchamp, J.R., Heslop, L., Yu, D.S., Tajbakhsh, S., Kelly, R.G., Wernig, A., Buckingham, M.E., Partridge, T.A., and Zammit, P.S. (2000). Expression of CD34 and Myf5 defines the majority of quiescent adult skeletal muscle satellite cells. *J Cell Biol* 151, 1221-1234.
- Ben-Yair, R., and Kalcheim, C. (2008). Notch and bone morphogenetic protein differentially act on dermomyotome cells to generate endothelium, smooth, and striated muscle. *J Cell Biol* 180, 607-618.
- Bentzinger, C.F., Wang, Y.X., von Maltzahn, J., Soleimani, V.D., Yin, H., and Rudnicki, M.A. (2013). Fibronectin regulates Wnt7a signaling and satellite cell expansion. *Cell stem cell* 12, 75-87.
- Berezikov, E. (2011). Evolution of microRNA diversity and regulation in animals. *Nature reviews Genetics* 12, 846-860.
- Bergstrom, D.A., Penn, B.H., Strand, A., Perry, R.L., Rudnicki, M.A., and Tapscott, S.J. (2002). Promoter-specific regulation of MyoD binding and signal transduction cooperate to pattern gene expression. *Mol Cell* 9, 587-600.
- Bernstein, B.E., Meissner, A., and Lander, E.S. (2007). The mammalian epigenome. *Cell* 128, 669-681.
- Bernstein, E., Caudy, A.A., Hammond, S.M., and Hannon, G.J. (2001). Role for a bidentate ribonuclease in the initiation step of RNA interference. *Nature* 409, 363-366.
- Bernstein, E., Kim, S.Y., Carmell, M.A., Murchison, E.P., Alcorn, H., Li, M.Z., Mills, A.A., Elledge, S.J., Anderson, K.V., and Hannon, G.J. (2003). Dicer is essential for mouse development. *Nat Genet* 35, 215-217.
- Bi, P., Yue, F., Sato, Y., Wirbisky, S., Liu, W., Shan, T., Wen, Y., Zhou, D., Freeman, J., and Kuang, S. (2016). Stage-specific effects of Notch activation during skeletal myogenesis. *eLife* 5.
- Birk, D.E., Fitch, J.M., Babiarz, J.P., and Linsenmayer, T.F. (1988). Collagen type I and type V are present in the same fibril in the avian corneal stroma. *J Cell Biol* 106, 999-1008.
- Bischoff, R. (1990). Interaction between satellite cells and skeletal muscle fibers. *Development* 109, 943-952.
- Bjornson, C.R., Cheung, T.H., Liu, L., Tripathi, P.V., Steeper, K.M., and Rando, T.A. (2012). Notch signaling is necessary to maintain quiescence in adult muscle stem cells. *Stem Cells* 30, 232-242.
- Blangy, A. (2017). Tensins are versatile regulators of Rho GTPase signalling and cell adhesion. *Biology of the cell* 109, 115-126.
- Blanpain, C., Lowry, W.E., Geoghegan, A., Polak, L., and Fuchs, E. (2004). Self-renewal, multipotency, and the existence of two cell populations within an epithelial stem cell niche. *Cell* 118, 635-648.
- Blanpain, C., Lowry, W.E., Pasolli, H.A., and Fuchs, E. (2006). Canonical notch signaling functions as a commitment switch in the epidermal lineage. *Genes Dev* 20, 3022-3035.
- Bonnemann, C.G. (2011). The collagen VI-related myopathies: muscle meets its matrix. *Nature reviews Neurology* 7, 379-390.

Boppart, M.D., Burkin, D.J., and Kaufman, S.J. (2006). Alpha7beta1-integrin regulates mechanotransduction and prevents skeletal muscle injury. *American journal of physiology Cell physiology* 290, C1660-1665.

Bouras, T., Pal, B., Vaillant, F., Harburg, G., Asselin-Labat, M.L., Oakes, S.R., Lindeman, G.J., and Visvader, J.E. (2008). Notch signaling regulates mammary stem cell function and luminal cell-fate commitment. *Cell stem cell* 3, 429-441.

Brack, A.S., Conboy, I.M., Conboy, M.J., Shen, J., and Rando, T.A. (2008). A temporal switch from notch to Wnt signaling in muscle stem cells is necessary for normal adult myogenesis. *Cell stem cell* 2, 50-59.

Bray, S.J. (2006). Notch signalling: a simple pathway becomes complex. *Nature reviews Molecular cell biology* 7, 678-689.

Brend, T., and Holley, S.A. (2009). Expression of the oscillating gene *her1* is directly regulated by Hairy/Enhancer of Split, T-box, and Suppressor of Hairless proteins in the zebrafish segmentation clock. *Dev Dyn* 238, 2745-2759.

Briskin, C., and Duss, S. (2007). Stem cells and the stem cell niche in the breast: an integrated hormonal and developmental perspective. *Stem cell reviews* 3, 147-156.

Brohl, D., Vasyutina, E., Czajkowski, M.T., Griger, J., Rassek, C., Rahn, H.P., Purfurst, B., Wende, H., and Birchmeier, C. (2012). Colonization of the satellite cell niche by skeletal muscle progenitor cells depends on Notch signals. *Dev Cell* 23, 469-481.

Brou, C., Logeat, F., Gupta, N., Bessia, C., LeBail, O., Doedens, J.R., Cumano, A., Roux, P., Black, R.A., and Israel, A. (2000). A novel proteolytic cleavage involved in Notch signaling: the role of the disintegrin-metalloprotease TACE. *Mol Cell* 5, 207-216.

Buas, M.F., Kabak, S., and Kadesch, T. The Notch effector *Hey1* associates with myogenic target genes to repress myogenesis. *J Biol Chem* 285, 1249-1258.

Buas, M.F., and Kadesch, T. (2010). Regulation of skeletal myogenesis by Notch. *Exp Cell Res* 316, 3028-3033.

Buczacki, S.J., Zecchini, H.I., Nicholson, A.M., Russell, R., Vermeulen, L., Kemp, R., and Winton, D.J. (2013). Intestinal label-retaining cells are secretory precursors expressing *Lgr5*. *Nature* 495, 65-69.

Byrd, D.T., and Kimble, J. (2009). Scratching the niche that controls *Caenorhabditis elegans* germline stem cells. *Seminars in cell & developmental biology* 20, 1107-1113.

Cacchiarelli, D., Legnini, I., Martone, J., Cazzella, V., D'Amico, A., Bertini, E., and Bozzoni, I. (2011). miRNAs as serum biomarkers for Duchenne muscular dystrophy. *EMBO molecular medicine* 3, 258-265.

Cai, X., Hagedorn, C.H., and Cullen, B.R. (2004). Human microRNAs are processed from capped, polyadenylated transcripts that can also function as mRNAs. *Rna* 10, 1957-1966.

Campo-Paysaa, F., Semon, M., Cameron, R.A., Peterson, K.J., and Schubert, M. (2011). microRNA complements in deuterostomes: origin and evolution of microRNAs. *Evolution & development* 13, 15-27.

Campos, L.S., Decker, L., Taylor, V., and Skarnes, W. (2006). Notch, epidermal growth factor receptor, and beta1-integrin pathways are coordinated in neural stem cells. *J Biol Chem* 281, 5300-5309.

Cao, Y., Kumar, R.M., Penn, B.H., Berkes, C.A., Kooperberg, C., Boyer, L.A., Young, R.A., and Tapscott, S.J. (2006). Global and gene-specific analyses show distinct roles for *Myod* and *Myog* at a common set of promoters. *Embo j* 25, 502-511.

Cao, Y., Yao, Z., Sarkar, D., Lawrence, M., Sanchez, G.J., Parker, M.H., MacQuarrie, K.L., Davison, J., Morgan, M.T., Ruzzo, W.L., *et al.* (2010). Genome-wide MyoD binding in skeletal muscle cells: a potential for broad cellular reprogramming. *Dev Cell* 18, 662-674.

Carlen, M., Meletis, K., Goritz, C., Darsalia, V., Evergren, E., Tanigaki, K., Amendola, M., Barnabe-Heider, F., Yeung, M.S., Naldini, L., *et al.* (2009). Forebrain ependymal cells are Notch-dependent and generate neuroblasts and astrocytes after stroke. *Nat Neurosci* 12, 259-267.

Carlson, M.E., Hsu, M., and Conboy, I.M. (2008). Imbalance between pSmad3 and Notch induces CDK inhibitors in old muscle stem cells. *Nature* 454, 528-532.

Carnac, G., Fajas, L., L'Honore, A., Sardet, C., Lamb, N.J., and Fernandez, A. (2000). The retinoblastoma-like protein p130 is involved in the determination of reserve cells in differentiating myoblasts. *Curr Biol* 10, 543-546.

Casali, A., and Batlle, E. (2009). Intestinal stem cells in mammals and *Drosophila*. *Cell stem cell* 4, 124-127.

Castel, D., Mourikis, P., Bartels, S.J., Brinkman, A.B., Tajbakhsh, S., and Stunnenberg, H.G. (2013). Dynamic binding of RBPJ is determined by Notch signaling status. *Genes Dev* 27, 1059-1071.

Cazzato, G. (1968). Considerations about a possible role played by connective tissue proliferation and vascular disturbances in the pathogenesis of progressive muscular dystrophy. *European neurology* 1, 158-179.

Chapouton, P., Skupien, P., Hesl, B., Coolen, M., Moore, J.C., Madelaine, R., Kremmer, E., Faus-Kessler, T., Blader, P., Lawson, N.D., *et al.* (2010). Notch activity levels control the balance between quiescence and recruitment of adult neural stem cells. *J Neurosci* 30, 7961-7974.

Chazaud, B., Sonnet, C., Lafuste, P., Bassez, G., Rimaniol, A.C., Poron, F., Authier, F.J., Dreyfus, P.A., and Gherardi, R.K. (2003). Satellite cells attract monocytes and use macrophages as a support to escape apoptosis and enhance muscle growth. *J Cell Biol* 163, 1133-1143.

Cheedipudi, S., Puri, D., Saleh, A., Gala, H.P., Rumman, M., Pillai, M.S., Sreenivas, P., Arora, R., Sellathurai, J., Schroder, H.D., *et al.* (2015). A fine balance: epigenetic control of cellular quiescence by the tumor suppressor PRDM2/RIZ at a bivalent domain in the cyclin gene. *Nucleic Acids Res* 43, 6236-6256.

Chen, J.F., Callis, T.E., and Wang, D.Z. (2009). microRNAs and muscle disorders. *J Cell Sci* 122, 13-20.

Chen, J.F., Mandel, E.M., Thomson, J.M., Wu, Q., Callis, T.E., Hammond, S.M., Conlon, F.L., and Wang, D.Z. (2006). The role of microRNA-1 and microRNA-133 in skeletal muscle proliferation and differentiation. *Nat Genet* 38, 228-233.

Chen, J.F., Tao, Y., Li, J., Deng, Z., Yan, Z., Xiao, X., and Wang, D.Z. (2010). microRNA-1 and microRNA-206 regulate skeletal muscle satellite cell proliferation and differentiation by repressing Pax7. *J Cell Biol* 190, 867-879.

Cheung, T.H., Quach, N.L., Charville, G.W., Liu, L., Park, L., Edalati, A., Yoo, B., Hoang, P., and Rando, T.A. (2012). Maintenance of muscle stem-cell quiescence by microRNA-489. *Nature* 482, 524-528.

Chiang, H.R., Schoenfeld, L.W., Ruby, J.G., Auyeung, V.C., Spies, N., Baek, D., Johnston, W.K., Russ, C., Luo, S., Babiarz, J.E., *et al.* (2010). Mammalian microRNAs: experimental evaluation of novel and previously annotated genes. *Genes Dev* 24, 992-1009.

Chinchilla, A., Lozano, E., Daimi, H., Esteban, F.J., Crist, C., Aranega, A.E., and Franco, D. (2011). MicroRNA profiling during mouse ventricular maturation: a role for miR-27 modulating Mef2c expression. *Cardiovascular research* 89, 98-108.

Christodoulou, F., Raible, F., Tomer, R., Simakov, O., Trachana, K., Klaus, S., Snyman, H., Hannon, G.J., Bork, P., and Arendt, D. (2010). Ancient animal microRNAs and the evolution of tissue identity. *Nature* 463, 1084-1088.

Christov, C., Chretien, F., Abou-Khalil, R., Bassez, G., Vallet, G., Authier, F.J., Bassaglia, Y., Shinin, V., Tajbakhsh, S., Chazaud, B., *et al.* (2007). Muscle satellite cells and endothelial cells: close neighbors and privileged partners. *Molecular biology of the cell* 18, 1397-1409.

Church, J.C., and Noronha, R.F. (1965). The use of the fruit bat in surgical research. *East African medical journal* 42, 348-355.

Coffman, C., Harris, W., and Kintner, C. (1990). Xotch, the Xenopus homolog of Drosophila notch. *Science* 249, 1438-1441.

Coffman, C.R., Skoglund, P., Harris, W.A., and Kintner, C.R. (1993). Expression of an extracellular deletion of Xotch diverts cell fate in Xenopus embryos. *Cell* 73, 659-671.

Collins, C.A., Olsen, I., Zammit, P.S., Heslop, L., Petrie, A., Partridge, T.A., and Morgan, J.E. (2005). Stem cell function, self-renewal, and behavioral heterogeneity of cells from the adult muscle satellite cell niche. *Cell* 122, 289-301.

Comai, G., Sambasivan, R., Gopalakrishnan, S., and Tajbakhsh, S. (2014). Variations in the efficiency of lineage marking and ablation confound distinctions between myogenic cell populations. *Dev Cell* 31, 654-667.

Conboy, I.M., Conboy, M.J., Smythe, G.M., and Rando, T.A. (2003). Notch-mediated restoration of regenerative potential to aged muscle. *Science* 302, 1575-1577.

Conboy, I.M., and Rando, T.A. (2002). The regulation of Notch signaling controls satellite cell activation and cell fate determination in postnatal myogenesis. *Dev Cell* 3, 397-409.

Conboy, M.J., Karasov, A.O., and Rando, T.A. (2007). High incidence of non-random template strand segregation and asymmetric fate determination in dividing stem cells and their progeny. *PLoS biology* 5, e102.

Concepcion, C.P., Bonetti, C., and Ventura, A. (2012). The microRNA-17-92 family of microRNA clusters in development and disease. *Cancer journal (Sudbury, Mass)* 18, 262-267.

Cooper, R.N., Tajbakhsh, S., Mouly, V., Cossu, G., Buckingham, M., and Butler-Browne, G.S. (1999). In vivo satellite cell activation via Myf5 and MyoD in regenerating mouse skeletal muscle. *J Cell Sci* 112 (Pt 17), 2895-2901.

Cornelison, D.D., Olwin, B.B., Rudnicki, M.A., and Wold, B.J. (2000). MyoD(-/-) satellite cells in single-fiber culture are differentiation defective and MRF4 deficient. *Dev Biol* 224, 122-137.

Cornelison, D.D., and Wold, B.J. (1997). Single-cell analysis of regulatory gene expression in quiescent and activated mouse skeletal muscle satellite cells. *Dev Biol* 191, 270-283.

Cox, D.M., Du, M., Marback, M., Yang, E.C., Chan, J., Siu, K.W., and McDermott, J.C. (2003). Phosphorylation motifs regulating the stability and function of myocyte enhancer factor 2A. *J Biol Chem* 278, 15297-15303.

Crist, C.G., Montarras, D., and Buckingham, M. (2012). Muscle satellite cells are primed for myogenesis but maintain quiescence with sequestration of Myf5 mRNA targeted by microRNA-31 in mRNP granules. *Cell stem cell* 11, 118-126.

Crist, C.G., Montarras, D., Pallafacchina, G., Rocancourt, D., Cumano, A., Conway, S.J., and Buckingham, M. (2009). Muscle stem cell behavior is modified by microRNA-27 regulation of Pax3 expression. *Proc Natl Acad Sci U S A* *106*, 13383-13387.

Dahlqvist, C., Blokzijl, A., Chapman, G., Falk, A., Dannaeus, K., Ibanez, C.F., and Lendahl, U. (2003). Functional Notch signaling is required for BMP4-induced inhibition of myogenic differentiation. *Development* *130*, 6089-6099.

de Cuevas, M., and Matunis, E.L. (2011). The stem cell niche: lessons from the *Drosophila* testis. *Development* *138*, 2861-2869.

De Strooper, B., Annaert, W., Cupers, P., Saftig, P., Craessaerts, K., Mumm, J.S., Schroeter, E.H., Schrijvers, V., Wolfe, M.S., Ray, W.J., *et al.* (1999). A presenilin-1-dependent gamma-secretase-like protease mediates release of Notch intracellular domain. *Nature* *398*, 518-522.

Deftos, M.L., He, Y.W., Ojala, E.W., and Bevan, M.J. (1998). Correlating notch signaling with thymocyte maturation. *Immunity* *9*, 777-786.

Demehri, S., Liu, Z., Lee, J., Lin, M.H., Crosby, S.D., Roberts, C.J., Grigsby, P.W., Miner, J.H., Farr, A.G., and Kopan, R. (2008). Notch-deficient skin induces a lethal systemic B-lymphoproliferative disorder by secreting TSLP, a sentinel for epidermal integrity. *PLoS biology* *6*, e123.

Derynck, R., and Zhang, Y.E. (2003). Smad-dependent and Smad-independent pathways in TGF-beta family signalling. *Nature* *425*, 577-584.

Dexter, J.S. (1914). The Analysis of a Case of Continuous Variation in *Drosophila* by a Study of Its Linkage Relations. *The American Naturalist* *48*, 712-758.

Dey, B.K., Gagan, J., and Dutta, A. (2011). miR-206 and -486 induce myoblast differentiation by downregulating Pax7. *Mol Cell Biol* *31*, 203-214.

Dey, B.K., Gagan, J., Yan, Z., and Dutta, A. (2012). miR-26a is required for skeletal muscle differentiation and regeneration in mice. *Genes Dev* *26*, 2180-2191.

Dey, B.K., Pfeifer, K., and Dutta, A. (2014). The H19 long noncoding RNA gives rise to microRNAs miR-675-3p and miR-675-5p to promote skeletal muscle differentiation and regeneration. *Genes Dev* *28*, 491-501.

Dontu, G., Jackson, K.W., McNicholas, E., Kawamura, M.J., Abdallah, W.M., and Wicha, M.S. (2004). Role of Notch signaling in cell-fate determination of human mammary stem/progenitor cells. *Breast cancer research : BCR* *6*, R605-615.

Dreesen, O., and Brivanlou, A.H. (2007). Signaling pathways in cancer and embryonic stem cells. *Stem cell reviews* *3*, 7-17.

DuFort, C.C., Paszek, M.J., and Weaver, V.M. (2011). Balancing forces: architectural control of mechanotransduction. *Nature reviews Molecular cell biology* *12*, 308-319.

Elbashir, S.M., Harborth, J., Lendeckel, W., Yalcin, A., Weber, K., and Tuschl, T. (2001a). Duplexes of 21-nucleotide RNAs mediate RNA interference in cultured mammalian cells. *Nature* *411*, 494-498.

Elbashir, S.M., Martinez, J., Patkaniowska, A., Lendeckel, W., and Tuschl, T. (2001b). Functional anatomy of siRNAs for mediating efficient RNAi in *Drosophila melanogaster* embryo lysate. *Embo j* *20*, 6877-6888.

Ellisen, L.W., Bird, J., West, D.C., Soreng, A.L., Reynolds, T.C., Smith, S.D., and Sklar, J. (1991). TAN-1, the human homolog of the *Drosophila* notch gene, is broken by chromosomal translocations in T lymphoblastic neoplasms. *Cell* *66*, 649-661.

Engler, A.J., Sen, S., Sweeney, H.L., and Discher, D.E. (2006). Matrix elasticity directs stem cell lineage specification. *Cell* *126*, 677-689.

Farina, N.H., Hausburg, M., Betta, N.D., Pulliam, C., Srivastava, D., Cornelison, D., and Olwin, B.B. (2012). A role for RNA post-transcriptional regulation in satellite cell activation. *Skeletal muscle* 2, 21.

Farnie, G., and Clarke, R.B. (2006). Breast stem cells and cancer. Ernst Schering Foundation symposium proceedings, 141-153.

Farnie, G., and Clarke, R.B. (2007). Mammary stem cells and breast cancer--role of Notch signalling. *Stem cell reviews* 3, 169-175.

Feng, Y., Niu, L.L., Wei, W., Zhang, W.Y., Li, X.Y., Cao, J.H., and Zhao, S.H. (2013). A feedback circuit between miR-133 and the ERK1/2 pathway involving an exquisite mechanism for regulating myoblast proliferation and differentiation. *Cell death & disease* 4, e934.

Fiore, D., Judson, R.N., Low, M., Lee, S., Zhang, E., Hopkins, C., Xu, P., Lenzi, A., Rossi, F.M., and Lemos, D.R. (2016). Pharmacological blockage of fibro/adipogenic progenitor expansion and suppression of regenerative fibrogenesis is associated with impaired skeletal muscle regeneration. *Stem cell research* 17, 161-169.

Fischer, A., and Gessler, M. (2007). Delta-Notch--and then? Protein interactions and proposed modes of repression by Hes and Hey bHLH factors. *Nucleic Acids Res* 35, 4583-4596.

Fiuza, U.M., and Arias, A.M. (2007). Cell and molecular biology of Notch. *The Journal of endocrinology* 194, 459-474.

Foudi, A., Hochedlinger, K., Van Buren, D., Schindler, J.W., Jaenisch, R., Carey, V., and Hock, H. (2009). Analysis of histone 2B-GFP retention reveals slowly cycling hematopoietic stem cells. *Nature biotechnology* 27, 84-90.

Fre, S., Hannezo, E., Sale, S., Huyghe, M., Lafkas, D., Kissel, H., Louvi, A., Greve, J., Louvard, D., and Artavanis-Tsakonas, S. (2011). Notch lineages and activity in intestinal stem cells determined by a new set of knock-in mice. *PloS one* 6, e25785.

Fre, S., Huyghe, M., Mourikis, P., Robine, S., Louvard, D., and Artavanis-Tsakonas, S. (2005). Notch signals control the fate of immature progenitor cells in the intestine. *Nature* 435, 964-968.

Friedman, R.C., Farh, K.K., Burge, C.B., and Bartel, D.P. (2009). Most mammalian mRNAs are conserved targets of microRNAs. *Genome research* 19, 92-105.

Fujiwara, H., Ferreira, M., Donati, G., Marciano, D.K., Linton, J.M., Sato, Y., Hartner, A., Sekiguchi, K., Reichardt, L.F., and Watt, F.M. (2011). The basement membrane of hair follicle stem cells is a muscle cell niche. *Cell* 144, 577-589.

Fukada, S., Uezumi, A., Ikemoto, M., Masuda, S., Segawa, M., Tanimura, N., Yamamoto, H., Miyagoe-Suzuki, Y., and Takeda, S. (2007). Molecular signature of quiescent satellite cells in adult skeletal muscle. *Stem Cells* 25, 2448-2459.

Fukada, S., Yamaguchi, M., Kokubo, H., Ogawa, R., Uezumi, A., Yoneda, T., Matev, M.M., Motohashi, N., Ito, T., Zolkiewska, A., *et al.* (2011). *Hesr1* and *Hesr3* are essential to generate undifferentiated quiescent satellite cells and to maintain satellite cell numbers. *Development* 138, 4609-4619.

Gagan, J., Dey, B.K., Layer, R., Yan, Z., and Dutta, A. (2012). Notch3 and Mef2c proteins are mutually antagonistic via Mkp1 protein and miR-1/206 microRNAs in differentiating myoblasts. *J Biol Chem* 287, 40360-40370.

Garcia-Prat, L., Martinez-Vicente, M., Perdiguero, E., Ortet, L., Rodriguez-Ubreva, J., Rebollo, E., Ruiz-Bonilla, V., Gutarra, S., Ballestar, E., Serrano, A.L., *et al.* (2016). Autophagy maintains stemness by preventing senescence. *Nature* 529, 37-42.

Gayraud-Morel, B., Chretien, F., Flamant, P., Gomes, D., Zammit, P.S., and Tajbakhsh, S. (2007). A role for the myogenic determination gene *Myf5* in adult regenerative myogenesis. *Dev Biol* 312, 13-28.

Gayraud-Morel, B., Chretien, F., Jory, A., Sambasivan, R., Negroni, E., Flamant, P., Soubigou, G., Coppee, J.Y., Di Santo, J., Cumano, A., *et al.* (2012). Myf5 haploinsufficiency reveals distinct cell fate potentials for adult skeletal muscle stem cells. *J Cell Sci* *125*, 1738-1749.

Gayraud-Morel, B., Chretien, F., and Tajbakhsh, S. (2009). Skeletal muscle as a paradigm for regenerative biology and medicine. *Regenerative medicine* *4*, 293-319.

Ge, W., Martinowich, K., Wu, X., He, F., Miyamoto, A., Fan, G., Weinmaster, G., and Sun, Y.E. (2002). Notch signaling promotes astroglialogenesis via direct CSL-mediated glial gene activation. *J Neurosci Res* *69*, 848-860.

George, R.M., Biressi, S., Beres, B.J., Rogers, E., Mulia, A.K., Allen, R.E., Rawls, A., Rando, T.A., and Wilson-Rawls, J. (2013). Numb-deficient satellite cells have regeneration and proliferation defects. *Proc Natl Acad Sci U S A* *110*, 18549-18554.

Gilbert, P.M., Havenstrite, K.L., Magnusson, K.E., Sacco, A., Leonardi, N.A., Kraft, P., Nguyen, N.K., Thrun, S., Lutolf, M.P., and Blau, H.M. (2010). Substrate elasticity regulates skeletal muscle stem cell self-renewal in culture. *Science* *329*, 1078-1081.

Gillespie, M.A., Le Grand, F., Scime, A., Kuang, S., von Maltzahn, J., Seale, V., Cuenda, A., Ranish, J.A., and Rudnicki, M.A. (2009). p38- γ -dependent gene silencing restricts entry into the myogenic differentiation program. *J Cell Biol* *187*, 991-1005.

Goetsch, S.C., Hawke, T.J., Gallardo, T.D., Richardson, J.A., and Garry, D.J. (2003). Transcriptional profiling and regulation of the extracellular matrix during muscle regeneration. *Physiological genomics* *14*, 261-271.

Goljanek-Whysall, K., Sweetman, D., and Munsterberg, A.E. (2012). microRNAs in skeletal muscle differentiation and disease. *Clinical science (London, England : 1979)* *123*, 611-625.

Gregory, R.I., Yan, K.P., Amuthan, G., Chendrimada, T., Doratotaj, B., Cooch, N., and Shiekhattar, R. (2004). The Microprocessor complex mediates the genesis of microRNAs. *Nature* *432*, 235-240.

Grimson, A., Srivastava, M., Fahey, B., Woodcroft, B.J., Chiang, H.R., King, N., Degnan, B.M., Rokhsar, D.S., and Bartel, D.P. (2008). Early origins and evolution of microRNAs and Piwi-interacting RNAs in animals. *Nature* *455*, 1193-1197.

Grishok, A., Pasquinelli, A.E., Conte, D., Li, N., Parrish, S., Ha, I., Baillie, D.L., Fire, A., Ruvkun, G., and Mello, C.C. (2001). Genes and mechanisms related to RNA interference regulate expression of the small temporal RNAs that control *C. elegans* developmental timing. *Cell* *106*, 23-34.

Gros, J., Manceau, M., Thome, V., and Marcelle, C. (2005). A common somitic origin for embryonic muscle progenitors and satellite cells. *Nature* *435*, 954-958.

Grun, D., Muraro, M.J., Boisset, J.C., Wiebrands, K., Lyubimova, A., Dharmadhikari, G., van den Born, M., van Es, J., Jansen, E., Clevers, H., *et al.* (2016). De Novo Prediction of Stem Cell Identity using Single-Cell Transcriptome Data. *Cell stem cell* *19*, 266-277.

Gutmann, E., Mares, V., and Stichova, J. (1976). Fate of 3H-thymidine labelled myogenic cells in regeneration of muscle isografts. *Cell and tissue research* *167*, 117-123.

Halder, G., Dupont, S., and Piccolo, S. (2012). Transduction of mechanical and cytoskeletal cues by YAP and TAZ. *Nature reviews Molecular cell biology* *13*, 591-600.

Hammond, S.M., Bernstein, E., Beach, D., and Hannon, G.J. (2000). An RNA-directed nuclease mediates post-transcriptional gene silencing in *Drosophila* cells. *Nature* *404*, 293-296.

Han, H., Tanigaki, K., Yamamoto, N., Kuroda, K., Yoshimoto, M., Nakahata, T., Ikuta, K., and Honjo, T. (2002). Inducible gene knockout of transcription factor recombination signal binding protein-J reveals its essential role in T versus B lineage decision. *Int Immunol* *14*, 637-645.

Han, J., Lee, Y., Yeom, K.H., Kim, Y.K., Jin, H., and Kim, V.N. (2004). The Drosha-DGCR8 complex in primary microRNA processing. *Genes Dev* *18*, 3016-3027.

Han, J., Lee, Y., Yeom, K.H., Nam, J.W., Heo, I., Rhee, J.K., Sohn, S.Y., Cho, Y., Zhang, B.T., and Kim, V.N. (2006). Molecular basis for the recognition of primary microRNAs by the Drosha-DGCR8 complex. *Cell* *125*, 887-901.

Hardy, D., Besnard, A., Latil, M., Jouvion, G., Briand, D., Thepenier, C., Pascal, Q., Guguin, A., Gayraud-Morel, B., Cavaillon, J.M., *et al.* (2016). Comparative Study of Injury Models for Studying Muscle Regeneration in Mice. *PLoS one* *11*, e0147198.

Hasty, P., Bradley, A., Morris, J.H., Edmondson, D.G., Venuti, J.M., Olson, E.N., and Klein, W.H. (1993). Muscle deficiency and neonatal death in mice with a targeted mutation in the myogenin gene. *Nature* *364*, 501-506.

Hawke, T.J., Meeson, A.P., Jiang, N., Graham, S., Hutcheson, K., DiMaio, J.M., and Garry, D.J. (2003). p21 is essential for normal myogenic progenitor cell function in regenerating skeletal muscle. *American journal of physiology Cell physiology* *285*, C1019-1027.

Hayashi, S., Manabe, I., Suzuki, Y., Relaix, F., and Oishi, Y. (2016). Klf5 regulates muscle differentiation by directly targeting muscle-specific genes in cooperation with MyoD in mice. *eLife* *5*.

Herman, P.K. (2002). Stationary phase in yeast. *Current opinion in microbiology* *5*, 602-607.

Hertel, J., Lindemeyer, M., Missal, K., Fried, C., Tanzer, A., Flamm, C., Hofacker, I.L., and Stadler, P.F. (2006). The expansion of the metazoan microRNA repertoire. *BMC genomics* *7*, 25.

Hollenberg, S.M., Cheng, P.F., and Weintraub, H. (1993). Use of a conditional MyoD transcription factor in studies of MyoD trans-activation and muscle determination. *Proc Natl Acad Sci U S A* *90*, 8028-8032.

Hosoyama, T., Nishijo, K., Prajapati, S.I., Li, G., and Keller, C. (2011). Rb1 gene inactivation expands satellite cell and postnatal myoblast pools. *J Biol Chem* *286*, 19556-19564.

Hu, P., Geles, K.G., Paik, J.H., DePinho, R.A., and Tjian, R. (2008). Codependent activators direct myoblast-specific MyoD transcription. *Dev Cell* *15*, 534-546.

Huang, G., Ge, G., Wang, D., Gopalakrishnan, B., Butz, D.H., Colman, R.J., Nagy, A., and Greenspan, D.S. (2011). alpha3(V) collagen is critical for glucose homeostasis in mice due to effects in pancreatic islets and peripheral tissues. *The Journal of clinical investigation* *121*, 769-783.

Huang, T.C., Sahasrabudhe, N.A., Kim, M.S., Getnet, D., Yang, Y., Peterson, J.M., Ghosh, B., Chaerkady, R., Leach, S.D., Marchionni, L., *et al.* (2012a). Regulation of lipid metabolism by Dicer revealed through SILAC mice. *Journal of proteome research* *11*, 2193-2205.

Huang, Z., Chen, X., Yu, B., He, J., and Chen, D. (2012b). MicroRNA-27a promotes myoblast proliferation by targeting myostatin. *Biochemical and biophysical research communications* *423*, 265-269.

Hutvagner, G., McLachlan, J., Pasquinelli, A.E., Balint, E., Tuschl, T., and Zamore, P.D. (2001). A cellular function for the RNA-interference enzyme Dicer in the maturation of the let-7 small temporal RNA. *Science* *293*, 834-838.

Hynes, R.O. (2002). Integrins: bidirectional, allosteric signaling machines. *Cell* *110*, 673-687.

Imayoshi, I., Sakamoto, M., Yamaguchi, M., Mori, K., and Kageyama, R. (2010). Essential roles of Notch signaling in maintenance of neural stem cells in developing and adult brains. *J Neurosci* *30*, 3489-3498.

Ishii, K., Suzuki, N., Mabuchi, Y., Ito, N., Kikura, N., Fukada, S., Okano, H., Takeda, S., and Akazawa, C. (2015). Muscle Satellite Cell Protein Teneurin-4 Regulates Differentiation During Muscle Regeneration. *Stem Cells* *33*, 3017-3027.

Isik, M., Korswagen, H.C., and Berezikov, E. (2010). Expression patterns of intronic microRNAs in *Caenorhabditis elegans*. *Silence* *1*, 5.

Iso, T., Kedes, L., and Hamamori, Y. (2003). HES and HERP families: multiple effectors of the Notch signaling pathway. *J Cell Physiol* *194*, 237-255.

Ito, M., Liu, Y., Yang, Z., Nguyen, J., Liang, F., Morris, R.J., and Cotsarelis, G. (2005). Stem cells in the hair follicle bulge contribute to wound repair but not to homeostasis of the epidermis. *Nature medicine* *11*, 1351-1354.

Izon, D.J., Aster, J.C., He, Y., Weng, A., Karnell, F.G., Patriub, V., Xu, L., Bakkour, S., Rodriguez, C., Allman, D., *et al.* (2002). Deltex1 redirects lymphoid progenitors to the B cell lineage by antagonizing Notch1. *Immunity* *16*, 231-243.

Jarriault, S., Brou, C., Logeat, F., Schroeter, E.H., Kopan, R., and Israel, A. (1995). Signalling downstream of activated mammalian Notch. *Nature* *377*, 355-358.

Jarriault, S., Le Bail, O., Hirsinger, E., Pourquie, O., Logeat, F., Strong, C.F., Brou, C., Seidah, N.G., and Israel, A. (1998). Delta-1 activation of notch-1 signaling results in HES-1 transactivation. *Mol Cell Biol* *18*, 7423-7431.

Jenuwein, T., and Allis, C.D. (2001). Translating the histone code. *Science* *293*, 1074-1080.

Jia, L., Li, Y.F., Wu, G.F., Song, Z.Y., Lu, H.Z., Song, C.C., Zhang, Q.L., Zhu, J.Y., Yang, G.S., and Shi, X.E. (2013). MiRNA-199a-3p regulates C2C12 myoblast differentiation through IGF-1/AKT/mTOR signal pathway. *International journal of molecular sciences* *15*, 296-308.

Joe, A.W., Yi, L., Natarajan, A., Le Grand, F., So, L., Wang, J., Rudnicki, M.A., and Rossi, F.M. (2010). Muscle injury activates resident fibro/adipogenic progenitors that facilitate myogenesis. *Nat Cell Biol* *12*, 153-163.

Jones, D.L., and Wagers, A.J. (2008). No place like home: anatomy and function of the stem cell niche. *Nature reviews Molecular cell biology* *9*, 11-21.

Jones, R.G., Li, X., Gray, P.D., Kuang, J., Clayton, F., Samowitz, W.S., Madison, B.B., Gumucio, D.L., and Kuwada, S.K. (2006). Conditional deletion of beta1 integrins in the intestinal epithelium causes a loss of Hedgehog expression, intestinal hyperplasia, and early postnatal lethality. *J Cell Biol* *175*, 505-514.

Juan, A.H., Kumar, R.M., Marx, J.G., Young, R.A., and Sartorelli, V. (2009). Mir-214-dependent regulation of the polycomb protein Ezh2 in skeletal muscle and embryonic stem cells. *Mol Cell* *36*, 61-74.

Kageyama, R., Niwa, Y., Shimojo, H., Kobayashi, T., and Ohtsuka, T. (2010). Ultradian oscillations in Notch signaling regulate dynamic biological events. *Curr Top Dev Biol* *92*, 311-331.

Kai, T., and Spradling, A. (2003). An empty *Drosophila* stem cell niche reactivates the proliferation of ectopic cells. *Proc Natl Acad Sci U S A* *100*, 4633-4638.

Kanatsu-Shinohara, M., Takehashi, M., Takashima, S., Lee, J., Morimoto, H., Chuma, S., Raducanu, A., Nakatsuji, N., Fassler, R., and Shinohara, T. (2008). Homing of mouse spermatogonial stem cells to germline niche depends on beta1-integrin. *Cell stem cell* *3*, 533-542.

Kassar-Duchossoy, L., Gayraud-Morel, B., Gomes, D., Rocancourt, D., Buckingham, M., Shinin, V., and Tajbakhsh, S. (2004). Mrf4 determines skeletal muscle identity in Myf5:Myod double-mutant mice. *Nature* *431*, 466-471.

Kassar-Duchossoy, L., Giacone, E., Gayraud-Morel, B., Jory, A., Gomes, D., and Tajbakhsh, S. (2005). Pax3/Pax7 mark a novel population of primitive myogenic cells during development. *Genes Dev* *19*, 1426-1431.

Kawamata, T., and Tomari, Y. (2010). Making RISC. *Trends in biochemical sciences* *35*, 368-376.

Kazanis, I., Lathia, J.D., Vadakkan, T.J., Raborn, E., Wan, R., Mughal, M.R., Eckley, D.M., Sasaki, T., Patton, B., Mattson, M.P., *et al.* (2010). Quiescence and activation of stem and precursor cell populations in the subependymal zone of the mammalian brain are associated with distinct cellular and extracellular matrix signals. *J Neurosci* *30*, 9771-9781.

Kenzelmann-Broz, D., Tucker, R.P., Leachman, N.T., and Chiquet-Ehrismann, R. (2010). The expression of teneurin-4 in the avian embryo: potential roles in patterning of the limb and nervous system. *The International journal of developmental biology* *54*, 1509-1516.

Ketting, R.F., Fischer, S.E., Bernstein, E., Sijen, T., Hannon, G.J., and Plasterk, R.H. (2001). Dicer functions in RNA interference and in synthesis of small RNA involved in developmental timing in *C. elegans*. *Genes Dev* *15*, 2654-2659.

Kherif, S., Lafuma, C., Dehaupas, M., Lachkar, S., Fournier, J.G., Verdiere-Sahuque, M., Fardeau, M., and Alameddine, H.S. (1999). Expression of matrix metalloproteinases 2 and 9 in regenerating skeletal muscle: a study in experimentally injured and mdx muscles. *Dev Biol* *205*, 158-170.

Khvorova, A., Reynolds, A., and Jayasena, S.D. (2003). Functional siRNAs and miRNAs exhibit strand bias. *Cell* *115*, 209-216.

Kim, H.K., Lee, Y.S., Sivaprasad, U., Malhotra, A., and Dutta, A. (2006). Muscle-specific microRNA miR-206 promotes muscle differentiation. *J Cell Biol* *174*, 677-687.

Kitamoto, T., and Hanaoka, K. (2010). Notch3 null mutation in mice causes muscle hyperplasia by repetitive muscle regeneration. *Stem Cells* *28*, 2205-2216.

Knapp, J.R., Davie, J.K., Myer, A., Meadows, E., Olson, E.N., and Klein, W.H. (2006). Loss of myogenin in postnatal life leads to normal skeletal muscle but reduced body size. *Development* *133*, 601-610.

Kokovay, E., Wang, Y., Kusek, G., Wurster, R., Lederman, P., Lowry, N., Shen, Q., and Temple, S. (2012). VCAM1 is essential to maintain the structure of the SVZ niche and acts as an environmental sensor to regulate SVZ lineage progression. *Cell stem cell* *11*, 220-230.

Konigsberg, I.R. (1963). Clonal analysis of myogenesis. *Science* *140*, 1273-1284.

Kopan, R., and Ilagan, M.X. (2009). The canonical Notch signaling pathway: unfolding the activation mechanism. *Cell* *137*, 216-233.

Kopan, R., Nye, J.S., and Weintraub, H. (1994). The intracellular domain of mouse Notch: a constitutively activated repressor of myogenesis directed at the basic helix-loop-helix region of MyoD. *Development* *120*, 2385-2396.

Kostallari, E., Baba-Amer, Y., Alonso-Martin, S., Ngoh, P., Relaix, F., Lafuste, P., and Gherardi, R.K. (2015). Pericytes in the myovascular niche promote post-natal myofiber growth and satellite cell quiescence. *Development* *142*, 1242-1253.

Kovanen, V., Suominen, H., Risteli, J., and Risteli, L. (1988). Type IV collagen and laminin in slow and fast skeletal muscle in rats--effects of age and life-time endurance training. *Collagen and related research* *8*, 145-153.

Krejci, A., Bernard, F., Housden, B.E., Collins, S., and Bray, S.J. (2009). Direct response to Notch activation: signaling crosstalk and incoherent logic. *Sci Signal* 2, ra1.

Krejci, A., and Bray, S. (2007). Notch activation stimulates transient and selective binding of Su(H)/CSL to target enhancers. *Genes Dev* 21, 1322-1327.

Krutzfeldt, J., Rajewsky, N., Braich, R., Rajeev, K.G., Tuschl, T., Manoharan, M., and Stoffel, M. (2005). Silencing of microRNAs in vivo with 'antagomirs'. *Nature* 438, 685-689.

Kuang, S., Kuroda, K., Le Grand, F., and Rudnicki, M.A. (2007). Asymmetric self-renewal and commitment of satellite stem cells in muscle. *Cell* 129, 999-1010.

Kuhl, U., Ocalan, M., Timpl, R., Mayne, R., Hay, E., and von der Mark, K. (1984). Role of muscle fibroblasts in the deposition of type-IV collagen in the basal lamina of myotubes. *Differentiation; research in biological diversity* 28, 164-172.

Kuroda, K., Tani, S., Tamura, K., Minoguchi, S., Kurooka, H., and Honjo, T. (1999). Delta-induced Notch signaling mediated by RBP-J inhibits MyoD expression and myogenesis. *J Biol Chem* 274, 7238-7244.

Lagos-Quintana, M., Rauhut, R., Yalcin, A., Meyer, J., Lendeckel, W., and Tuschl, T. (2002). Identification of tissue-specific microRNAs from mouse. *Curr Biol* 12, 735-739.

Lai, E.C. (2002). Micro RNAs are complementary to 3' UTR sequence motifs that mediate negative post-transcriptional regulation. *Nat Genet* 30, 363-364.

Lamar, E., Deblandre, G., Wettstein, D., Gawantka, V., Pollet, N., Niehrs, C., and Kintner, C. (2001). Nrarp is a novel intracellular component of the Notch signaling pathway. *Genes Dev* 15, 1885-1899.

Lau, N.C., Lim, L.P., Weinstein, E.G., and Bartel, D.P. (2001). An abundant class of tiny RNAs with probable regulatory roles in *Caenorhabditis elegans*. *Science* 294, 858-862.

Le Roux, I., Konge, J., Le Cam, L., Flamant, P., and Tajbakhsh, S. (2015). Numb is required to prevent p53-dependent senescence following skeletal muscle injury. *Nature communications* 6, 8528.

Lee, J., Basak, J.M., Demehri, S., and Kopan, R. (2007). Bi-compartmental communication contributes to the opposite proliferative behavior of Notch1-deficient hair follicle and epidermal keratinocytes. *Development* 134, 2795-2806.

Lee, R.C., Feinbaum, R.L., and Ambros, V. (1993). The *C. elegans* heterochronic gene *lin-4* encodes small RNAs with antisense complementarity to *lin-14*. *Cell* 75, 843-854.

Lee, Y., Ahn, C., Han, J., Choi, H., Kim, J., Yim, J., Lee, J., Provost, P., Radmark, O., Kim, S., *et al.* (2003). The nuclear RNase III Drosha initiates microRNA processing. *Nature* 425, 415-419.

Lee, Y., Jeon, K., Lee, J.T., Kim, S., and Kim, V.N. (2002). MicroRNA maturation: stepwise processing and subcellular localization. *Embo j* 21, 4663-4670.

Lee, Y., Kim, M., Han, J., Yeom, K.H., Lee, S., Baek, S.H., and Kim, V.N. (2004). MicroRNA genes are transcribed by RNA polymerase II. *Embo j* 23, 4051-4060.

Leitinger, B. (2011). Transmembrane collagen receptors. *Annual review of cell and developmental biology* 27, 265-290.

Lemos, D.R., Babaeijandaghi, F., Low, M., Chang, C.K., Lee, S.T., Fiore, D., Zhang, R.H., Natarajan, A., Nedospasov, S.A., and Rossi, F.M. (2015). Nilotinib reduces muscle fibrosis in chronic muscle injury by promoting TNF-mediated apoptosis of fibro/adipogenic progenitors. *Nature medicine* 21, 786-794.

Lepper, C., Conway, S.J., and Fan, C.M. (2009). Adult satellite cells and embryonic muscle progenitors have distinct genetic requirements. *Nature* 460, 627-631.

Lepper, C., Partridge, T.A., and Fan, C.M. (2011). An absolute requirement for Pax7-positive satellite cells in acute injury-induced skeletal muscle regeneration. *Development* 138, 3639-3646.

Lewis, J., Hanisch, A., and Holder, M. (2009). Notch signaling, the segmentation clock, and the patterning of vertebrate somites. *Journal of biology* 8, 44.

Li, L., and Clevers, H. (2010). Coexistence of quiescent and active adult stem cells in mammals. *Science* 327, 542-545.

Li, M., Liu, G.H., and Izpisua Belmonte, J.C. (2012). Navigating the epigenetic landscape of pluripotent stem cells. *Nature reviews Molecular cell biology* 13, 524-535.

Li, X., Li, Y., Zhao, L., Zhang, D., Yao, X., Zhang, H., Wang, Y.C., Wang, X.Y., Xia, H., Yan, J., *et al.* (2014). Circulating Muscle-specific miRNAs in Duchenne Muscular Dystrophy Patients. *Molecular therapy Nucleic acids* 3, e177.

Liu, J., Luo, X.J., Xiong, A.W., Zhang, Z.D., Yue, S., Zhu, M.S., and Cheng, S.Y. (2010). MicroRNA-214 promotes myogenic differentiation by facilitating exit from mitosis via down-regulation of proto-oncogene N-ras. *J Biol Chem* 285, 26599-26607.

Liu, L., Cheung, T.H., Charville, G.W., Hurgo, B.M., Leavitt, T., Shih, J., Brunet, A., and Rando, T.A. (2013a). Chromatin modifications as determinants of muscle stem cell quiescence and chronological aging. *Cell reports* 4, 189-204.

Liu, Y., Li, M., Ma, J., Zhang, J., Zhou, C., Wang, T., Gao, X., and Li, X. (2013b). Identification of differences in microRNA transcriptomes between porcine oxidative and glycolytic skeletal muscles. *BMC molecular biology* 14, 7.

Lodygin, D., Epanchintsev, A., Menssen, A., Diebold, J., and Hermeking, H. (2005). Functional epigenomics identifies genes frequently silenced in prostate cancer. *Cancer research* 65, 4218-4227.

Lu, H., Huang, D., Ransohoff, R.M., and Zhou, L. (2011a). Acute skeletal muscle injury: CCL2 expression by both monocytes and injured muscle is required for repair. *FASEB journal : official publication of the Federation of American Societies for Experimental Biology* 25, 3344-3355.

Lu, P., Takai, K., Weaver, V.M., and Werb, Z. (2011b). Extracellular matrix degradation and remodeling in development and disease. *Cold Spring Harbor perspectives in biology* 3.

Lukjanenko, L., Jung, M.J., Hegde, N., Perruisseau-Carrier, C., Migliavacca, E., Rozo, M., Karaz, S., Jacot, G., Schmidt, M., Li, L., *et al.* (2016). Loss of fibronectin from the aged stem cell niche affects the regenerative capacity of skeletal muscle in mice. *Nature medicine* 22, 897-905.

Lund, E., Guttinger, S., Calado, A., Dahlberg, J.E., and Kutay, U. (2004). Nuclear export of microRNA precursors. *Science* 303, 95-98.

Luo, R., Jeong, S.J., Jin, Z., Strokes, N., Li, S., and Piao, X. (2011). G protein-coupled receptor 56 and collagen III, a receptor-ligand pair, regulates cortical development and lamination. *Proc Natl Acad Sci U S A* 108, 12925-12930.

Lutolf, M.P., and Blau, H.M. (2009). Artificial stem cell niches. *Advanced materials (Deerfield Beach, Fla)* 21, 3255-3268.

Luz, M.A., Marques, M.J., and Santo Neto, H. (2002). Impaired regeneration of dystrophin-deficient muscle fibers is caused by exhaustion of myogenic cells. *Brazilian journal of medical and biological research = Revista brasileira de pesquisas medicas e biologicas* 35, 691-695.

Maciotta, S., Meregalli, M., Cassinelli, L., Parolini, D., Farini, A., Fraro, G.D., Gandolfi, F., Forcato, M., Ferrari, S., Gabellini, D., *et al.* (2012). Hmgb3 is regulated by microRNA-206 during muscle regeneration. *PloS one* 7, e43464.

Maillard, I., Koch, U., Dumortier, A., Shestova, O., Xu, L., Sai, H., Pross, S.E., Aster, J.C., Bhandoola, A., Radtke, F., *et al.* (2008). Canonical notch signaling is dispensable for the maintenance of adult hematopoietic stem cells. *Cell stem cell* 2, 356-366.

Malfait, F., Wenstrup, R.J., and De Paepe, A. (2010). Clinical and genetic aspects of Ehlers-Danlos syndrome, classic type. *Genetics in medicine : official journal of the American College of Medical Genetics* 12, 597-605.

Mammoto, T., and Ingber, D.E. (2010). Mechanical control of tissue and organ development. *Development* 137, 1407-1420.

Martynoga, B., Mateo, J.L., Zhou, B., Andersen, J., Achimastou, A., Urban, N., van den Berg, D., Georgopoulou, D., Hadjur, S., Wittbrodt, J., *et al.* (2013). Epigenomic enhancer annotation reveals a key role for NFIX in neural stem cell quiescence. *Genes Dev* 27, 1769-1786.

Massague, J., and Wotton, D. (2000). Transcriptional control by the TGF-beta/Smad signaling system. *Embo j* 19, 1745-1754.

Mauro, A. (1961). Satellite cell of skeletal muscle fibers. *The Journal of biophysical and biochemical cytology* 9, 493-495.

McCarthy, J.J., and Esser, K.A. (2007). MicroRNA-1 and microRNA-133a expression are decreased during skeletal muscle hypertrophy. *Journal of applied physiology (Bethesda, Md : 1985)* 102, 306-313.

McLatchie, L.M., Fraser, N.J., Main, M.J., Wise, A., Brown, J., Thompson, N., Solari, R., Lee, M.G., and Foord, S.M. (1998). RAMPs regulate the transport and ligand specificity of the calcitonin-receptor-like receptor. *Nature* 393, 333-339.

Meadows, E., Cho, J.H., Flynn, J.M., and Klein, W.H. (2008). Myogenin regulates a distinct genetic program in adult muscle stem cells. *Dev Biol* 322, 406-414.

Megeney, L.A., Kablar, B., Garrett, K., Anderson, J.E., and Rudnicki, M.A. (1996). MyoD is required for myogenic stem cell function in adult skeletal muscle. *Genes Dev* 10, 1173-1183.

Milasincic, D.J., Dhawan, J., and Farmer, S.R. (1996). Anchorage-dependent control of muscle-specific gene expression in C2C12 mouse myoblasts. *In vitro cellular & developmental biology Animal* 32, 90-99.

Mizutani, K., Yoon, K., Dang, L., Tokunaga, A., and Gaiano, N. (2007). Differential Notch signalling distinguishes neural stem cells from intermediate progenitors. *Nature* 449, 351-355.

Mohan, A., and Asakura, A. (2017). CDK inhibitors for muscle stem cell differentiation and self-renewal. *The journal of physical fitness and sports medicine* 6, 65-74.

Mohr, O.L. (1919). Character Changes Caused by Mutation of an Entire Region of a Chromosome in *Drosophila*. *Genetics* 4, 275-282.

Montarras, D., Morgan, J., Collins, C., Relaix, F., Zaffran, S., Cumano, A., Partridge, T., and Buckingham, M. (2005). Direct isolation of satellite cells for skeletal muscle regeneration. *Science* 309, 2064-2067.

Moss, F.P., and Leblond, C.P. (1970). Nature of dividing nuclei in skeletal muscle of growing rats. *J Cell Biol* 44, 459-462.

Motohashi, N., and Asakura, A. (2014). Muscle satellite cell heterogeneity and self-renewal. *Frontiers in cell and developmental biology* 2, 1.

Mourikis, P., Gopalakrishnan, S., Sambasivan, R., and Tajbakhsh, S. (2012a). Cell-autonomous Notch activity maintains the temporal specification potential of skeletal muscle stem cells. *Development* *139*, 4536-4548.

Mourikis, P., Sambasivan, R., Castel, D., Rocheteau, P., Bizzarro, V., and Tajbakhsh, S. (2012b). A critical requirement for notch signaling in maintenance of the quiescent skeletal muscle stem cell state. *Stem Cells* *30*, 243-252.

Mourikis, P., and Tajbakhsh, S. (2014). Distinct contextual roles for Notch signalling in skeletal muscle stem cells. *BMC Dev Biol* *14*, 2.

Mouw, J.K., Ou, G., and Weaver, V.M. (2014). Extracellular matrix assembly: a multiscale deconstruction. *Nature reviews Molecular cell biology* *15*, 771-785.

Mumm, J.S., Schroeter, E.H., Saxena, M.T., Griesemer, A., Tian, X., Pan, D.J., Ray, W.J., and Kopan, R. (2000). A ligand-induced extracellular cleavage regulates gamma-secretase-like proteolytic activation of Notch1. *Mol Cell* *5*, 197-206.

Muroya, S., Taniguchi, M., Shibata, M., Oe, M., Ojima, K., Nakajima, I., and Chikuni, K. (2013). Profiling of differentially expressed microRNA and the bioinformatic target gene analyses in bovine fast- and slow-type muscles by massively parallel sequencing. *Journal of animal science* *91*, 90-103.

Murphy, M.M., Lawson, J.A., Mathew, S.J., Hutcheson, D.A., and Kardon, G. (2011). Satellite cells, connective tissue fibroblasts and their interactions are crucial for muscle regeneration. *Development* *138*, 3625-3637.

Nabeshima, Y., Hanaoka, K., Hayasaka, M., Esumi, E., Li, S., Nonaka, I., and Nabeshima, Y. (1993). Myogenin gene disruption results in perinatal lethality because of severe muscle defect. *Nature* *364*, 532-535.

Naguibneva, I., Ameyar-Zazoua, M., Poleskaya, A., Ait-Si-Ali, S., Groisman, R., Souidi, M., Cuvellier, S., and Harel-Bellan, A. (2006). The microRNA miR-181 targets the homeobox protein Hox-A11 during mammalian myoblast differentiation. *Nat Cell Biol* *8*, 278-284.

Nakayama, K.H., Batchelder, C.A., Lee, C.I., and Tarantal, A.F. (2010). Decellularized rhesus monkey kidney as a three-dimensional scaffold for renal tissue engineering. *Tissue engineering Part A* *16*, 2207-2216.

Nowell, C., and Radtke, F. (2013). Cutaneous Notch signaling in health and disease. *Cold Spring Harbor perspectives in medicine* *3*, a017772.

Nowell, C.S., and Radtke, F. (2017). Corneal epithelial stem cells and their niche at a glance. *J Cell Sci* *130*, 1021-1025.

O'Reilly, A.M., Lee, H.H., and Simon, M.A. (2008). Integrins control the positioning and proliferation of follicle stem cells in the *Drosophila* ovary. *J Cell Biol* *182*, 801-815.

O'Rourke, J.R., Georges, S.A., Seay, H.R., Tapscott, S.J., McManus, M.T., Goldhamer, D.J., Swanson, M.S., and Harfe, B.D. (2007). Essential role for Dicer during skeletal muscle development. *Dev Biol* *311*, 359-368.

Okuyama, R., Tagami, H., and Aiba, S. (2008). Notch signaling: its role in epidermal homeostasis and in the pathogenesis of skin diseases. *Journal of dermatological science* *49*, 187-194.

Olguin, H.C., and Olwin, B.B. (2004). Pax-7 up-regulation inhibits myogenesis and cell cycle progression in satellite cells: a potential mechanism for self-renewal. *Dev Biol* *275*, 375-388.

Ordentlich, P., Lin, A., Shen, C.P., Blaumueller, C., Matsuno, K., Artavanis-Tsakonas, S., and Kadesch, T. (1998). Notch inhibition of E47 supports the existence of a novel signaling pathway. *Mol Cell Biol* *18*, 2230-2239.

Oustanina, S., Hause, G., and Braun, T. (2004). Pax7 directs postnatal renewal and propagation of myogenic satellite cells but not their specification. *Embo j* 23, 3430-3439.

Ozsolak, F., Poling, L.L., Wang, Z., Liu, H., Liu, X.S., Roeder, R.G., Zhang, X., Song, J.S., and Fisher, D.E. (2008). Chromatin structure analyses identify miRNA promoters. *Genes Dev* 22, 3172-3183.

Paavola, K.J., Sidik, H., Zuchero, J.B., Eckart, M., and Talbot, W.S. (2014). Type IV collagen is an activating ligand for the adhesion G protein-coupled receptor GPR126. *Sci Signal* 7, ra76.

Pallafacchina, G., Francois, S., Regnault, B., Czarny, B., Dive, V., Cumano, A., Montarras, D., and Buckingham, M. (2010). An adult tissue-specific stem cell in its niche: a gene profiling analysis of in vivo quiescent and activated muscle satellite cells. *Stem cell research* 4, 77-91.

Palomero, T., Lim, W.K., Odom, D.T., Sulis, M.L., Real, P.J., Margolin, A., Barnes, K.C., O'Neil, J., Neubergh, D., Weng, A.P., *et al.* (2006). NOTCH1 directly regulates c-MYC and activates a feed-forward-loop transcriptional network promoting leukemic cell growth. *Proc Natl Acad Sci U S A* 103, 18261-18266.

Parekh, T.V., Wang, X.W., Makri-Werzen, D.M., Greenspan, D.S., and Newman, M.J. (1998). Type V collagen is an epithelial cell cycle inhibitor that is induced by and mimics the effects of transforming growth factor beta1. *Cell growth & differentiation : the molecular biology journal of the American Association for Cancer Research* 9, 423-433.

Parker, R., and Sheth, U. (2007). P bodies and the control of mRNA translation and degradation. *Mol Cell* 25, 635-646.

Paroush, Z., Finley, R.L., Jr., Kidd, T., Wainwright, S.M., Ingham, P.W., Brent, R., and Ish-Horowitz, D. (1994). Groucho is required for Drosophila neurogenesis, segmentation, and sex determination and interacts directly with hairy-related bHLH proteins. *Cell* 79, 805-815.

Pascoal, S., Carvalho, C.R., Rodriguez-Leon, J., Delfini, M.C., Duprez, D., Thorsteinsdottir, S., and Palmeirim, I. (2007). A molecular clock operates during chick autopod proximal-distal outgrowth. *Journal of molecular biology* 368, 303-309.

Pasquinelli, A.E., Reinhart, B.J., Slack, F., Martindale, M.Q., Kuroda, M.I., Maller, B., Hayward, D.C., Ball, E.E., Degnan, B., Muller, P., *et al.* (2000). Conservation of the sequence and temporal expression of let-7 heterochronic regulatory RNA. *Nature* 408, 86-89.

Pasut, A., Chang, N.C., Gurriaran-Rodriguez, U., Faulkes, S., Yin, H., Lacaria, M., Ming, H., and Rudnicki, M.A. (2016). Notch Signaling Rescues Loss of Satellite Cells Lacking Pax7 and Promotes Brown Adipogenic Differentiation. *Cell reports* 16, 333-343.

Pear, W.S., and Radtke, F. (2003). Notch signaling in lymphopoiesis. *Semin Immunol* 15, 69-79.

Peerani, R., and Zandstra, P.W. (2010). Enabling stem cell therapies through synthetic stem cell-niche engineering. *The Journal of clinical investigation* 120, 60-70.

Pellegrinet, L., Rodilla, V., Liu, Z., Chen, S., Koch, U., Espinosa, L., Kaestner, K.H., Kopan, R., Lewis, J., and Radtke, F. (2011). Dll1- and Dll4-mediated Notch signaling is required for homeostasis of intestinal stem cells. *Gastroenterology*.

Petcherski, A.G., and Kimble, J. (2000). Mastermind is a putative activator for Notch. *Curr Biol* 10, R471-473.

Pinho, S., and Niehrs, C. (2007). Dkk3 is required for TGF-beta signaling during *Xenopus* mesoderm induction. *Differentiation; research in biological diversity* 75, 957-967.

Porpiglia, E., Samusik, N., Van Ho, A.T., Cosgrove, B.D., Mai, T., Davis, K.L., Jager, A., Nolan, G.P., Bendall, S.C., Fantl, W.J., *et al.* (2017). High-resolution myogenic lineage mapping by single-cell mass cytometry. *Nat Cell Biol* 19, 558-567.

Potocnik, A.J., Brakebusch, C., and Fassler, R. (2000). Fetal and adult hematopoietic stem cells require beta1 integrin function for colonizing fetal liver, spleen, and bone marrow. *Immunity* 12, 653-663.

Prochnik, S.E., Rokhsar, D.S., and Aboobaker, A.A. (2007). Evidence for a microRNA expansion in the bilaterian ancestor. *Development genes and evolution* 217, 73-77.

Qian, H., Tryggvason, K., Jacobsen, S.E., and Ekblom, M. (2006). Contribution of alpha6 integrins to hematopoietic stem and progenitor cell homing to bone marrow and collaboration with alpha4 integrins. *Blood* 107, 3503-3510.

Rantanen, J., Hurme, T., Lukka, R., Heino, J., and Kalimo, H. (1995). Satellite cell proliferation and the expression of myogenin and desmin in regenerating skeletal muscle: evidence for two different populations of satellite cells. *Laboratory investigation; a journal of technical methods and pathology* 72, 341-347.

Relaix, F., Montarras, D., Zaffran, S., Gayraud-Morel, B., Rocancourt, D., Tajbakhsh, S., Mansouri, A., Cumano, A., and Buckingham, M. (2006). Pax3 and Pax7 have distinct and overlapping functions in adult muscle progenitor cells. *J Cell Biol* 172, 91-102.

Relaix, F., Rocancourt, D., Mansouri, A., and Buckingham, M. (2005). A Pax3/Pax7-dependent population of skeletal muscle progenitor cells. *Nature* 435, 948-953.

Reznik, M. (1969). Thymidine-3H uptake by satellite cells of regenerating skeletal muscle. *J Cell Biol* 40, 568-571.

Rezza, A., Sennett, R., and Rendl, M. (2014). Adult stem cell niches: cellular and molecular components. *Curr Top Dev Biol* 107, 333-372.

Rios, A.C., Serralbo, O., Salgado, D., and Marcelle, C. (2011). Neural crest regulates myogenesis through the transient activation of NOTCH. *Nature* 473, 532-535.

Rizvi, T.A., Huang, Y., Sidani, A., Atit, R., Largaespada, D.A., Boissy, R.E., and Ratner, N. (2002). A novel cytokine pathway suppresses glial cell melanogenesis after injury to adult nerve. *J Neurosci* 22, 9831-9840.

Rocheteau, P., Gayraud-Morel, B., Siegl-Cachedenier, I., Blasco, M.A., and Tajbakhsh, S. (2012). A subpopulation of adult skeletal muscle stem cells retains all template DNA strands after cell division. *Cell* 148, 112-125.

Rodriguez, A., Griffiths-Jones, S., Ashurst, J.L., and Bradley, A. (2004). Identification of mammalian microRNA host genes and transcription units. *Genome research* 14, 1902-1910.

Ronchini, C., and Capobianco, A.J. (2001). Induction of cyclin D1 transcription and CDK2 activity by Notch(ic): implication for cell cycle disruption in transformation by Notch(ic). *Mol Cell Biol* 21, 5925-5934.

Rozo, M., Li, L., and Fan, C.M. (2016). Targeting beta1-integrin signaling enhances regeneration in aged and dystrophic muscle in mice. *Nature medicine* 22, 889-896.

Ruby, J.G., Jan, C.H., and Bartel, D.P. (2007). Intronic microRNA precursors that bypass Drosha processing. *Nature* 448, 83-86.

Rudnicki, M.A., Schnegelsberg, P.N., Stead, R.H., Braun, T., Arnold, H.H., and Jaenisch, R. (1993). MyoD or Myf-5 is required for the formation of skeletal muscle. *Cell* 75, 1351-1359.

Rumman, M., Dhawan, J., and Kassem, M. (2015). Concise Review: Quiescence in Adult Stem Cells: Biological Significance and Relevance to Tissue Regeneration. *Stem Cells* 33, 2903-2912.

Russell, F.A., King, R., Smillie, S.J., Kodji, X., and Brain, S.D. (2014). Calcitonin gene-related peptide: physiology and pathophysiology. *Physiological reviews* 94, 1099-1142.

Sabourin, L.A., Girgis-Gabardo, A., Seale, P., Asakura, A., and Rudnicki, M.A. (1999). Reduced differentiation potential of primary MyoD^{-/-} myogenic cells derived from adult skeletal muscle. *J Cell Biol* 144, 631-643.

Sacco, A., Doyonnas, R., Kraft, P., Vitorovic, S., and Blau, H.M. (2008). Self-renewal and expansion of single transplanted muscle stem cells. *Nature* 456, 502-506.

Saclier, M., Yacoub-Youssef, H., Mackey, A.L., Arnold, L., Ardjoune, H., Magnan, M., Sailhan, F., Chelly, J., Pavlath, G.K., Mounier, R., *et al.* (2013). Differentially activated macrophages orchestrate myogenic precursor cell fate during human skeletal muscle regeneration. *Stem Cells* 31, 384-396.

Saha, K., Keung, A.J., Irwin, E.F., Li, Y., Little, L., Schaffer, D.V., and Healy, K.E. (2008). Substrate modulus directs neural stem cell behavior. *Biophysical journal* 95, 4426-4438.

Sambasivan, R., Comai, G., Le Roux, I., Gomes, D., Konge, J., Dumas, G., Cimper, C., and Tajbakhsh, S. (2013). Embryonic founders of adult muscle stem cells are primed by the determination gene Mrf4. *Dev Biol* 381, 241-255.

Sambasivan, R., Gayraud-Morel, B., Dumas, G., Cimper, C., Paisant, S., Kelly, R.G., and Tajbakhsh, S. (2009). Distinct regulatory cascades govern extraocular and pharyngeal arch muscle progenitor cell fates. *Dev Cell* 16, 810-821.

Sambasivan, R., Kuratani, S., and Tajbakhsh, S. (2011a). An eye on the head: the development and evolution of craniofacial muscles. *Development* 138, 2401-2415.

Sambasivan, R., and Tajbakhsh, S. (2007). Skeletal muscle stem cell birth and properties. *Seminars in cell & developmental biology* 18, 870-882.

Sambasivan, R., Yao, R., Kissenpfennig, A., Van Wittenberghe, L., Paldi, A., Gayraud-Morel, B., Guenou, H., Malissen, B., Tajbakhsh, S., and Galy, A. (2011b). Pax7-expressing satellite cells are indispensable for adult skeletal muscle regeneration. *Development* 138, 3647-3656.

Sanes, J.R. (2003). The basement membrane/basal lamina of skeletal muscle. *J Biol Chem* 278, 12601-12604.

Sarkar, S., Dey, B.K., and Dutta, A. (2010). MiR-322/424 and -503 are induced during muscle differentiation and promote cell cycle quiescence and differentiation by down-regulation of Cdc25A. *Molecular biology of the cell* 21, 2138-2149.

Sato, T., Yamamoto, T., and Sehara-Fujisawa, A. (2014). miR-195/497 induce postnatal quiescence of skeletal muscle stem cells. *Nature communications* 5, 4597.

Schiaffino, S., Dyar, K.A., Ciciliot, S., Blaauw, B., and Sandri, M. (2013). Mechanisms regulating skeletal muscle growth and atrophy. *The FEBS journal* 280, 4294-4314.

Schofield, R. (1978). The relationship between the spleen colony-forming cell and the haemopoietic stem cell. *Blood cells* 4, 7-25.

Schultz, E. (1984). A quantitative study of satellite cells in regenerated soleus and extensor digitorum longus muscles. *The Anatomical record* 208, 501-506.

Schultz, E. (1996). Satellite cell proliferative compartments in growing skeletal muscles. *Dev Biol* 175, 84-94.

Schultz, E., Gibson, M.C., and Champion, T. (1978). Satellite cells are mitotically quiescent in mature mouse muscle: an EM and radioautographic study. *J Exp Zool* 206, 451-456.

Schuster-Gossler, K., Cordes, R., and Gossler, A. (2007). Premature myogenic differentiation and depletion of progenitor cells cause severe muscle hypotrophy in Delta1 mutants. *Proc Natl Acad Sci U S A* 104, 537-542.

Schwarz, D.S., Hutvagner, G., Du, T., Xu, Z., Aronin, N., and Zamore, P.D. (2003). Asymmetry in the assembly of the RNAi enzyme complex. *Cell* 115, 199-208.

Schworer, S., Becker, F., Feller, C., Baig, A.H., Kober, U., Henze, H., Kraus, J.M., Xin, B., Lechel, A., Lipka, D.B., *et al.* (2016). Epigenetic stress responses induce muscle stem-cell ageing by Hoxa9 developmental signals. *Nature* 540, 428-432.

Seale, P., Sabourin, L.A., Girgis-Gabardo, A., Mansouri, A., Gruss, P., and Rudnicki, M.A. (2000). Pax7 is required for the specification of myogenic satellite cells. *Cell* 102, 777-786.

Sellathurai, J., Cheedipudi, S., Dhawan, J., and Schroder, H.D. (2013). A novel in vitro model for studying quiescence and activation of primary isolated human myoblasts. *PloS one* 8, e64067.

Sempere, L.F., Cole, C.N., McPeck, M.A., and Peterson, K.J. (2006). The phylogenetic distribution of metazoan microRNAs: insights into evolutionary complexity and constraint. *Journal of experimental zoology Part B, Molecular and developmental evolution* 306, 575-588.

Seok, H.Y., Tatsuguchi, M., Callis, T.E., He, A., Pu, W.T., and Wang, D.Z. (2011). miR-155 inhibits expression of the MEF2A protein to repress skeletal muscle differentiation. *J Biol Chem* 286, 35339-35346.

Shawber, C., Nofziger, D., Hsieh, J.J., Lindsell, C., Bogler, O., Hayward, D., and Weinmaster, G. (1996). Notch signaling inhibits muscle cell differentiation through a CBF1-independent pathway. *Development* 122, 3765-3773.

Shen, H., McElhinny, A.S., Cao, Y., Gao, P., Liu, J., Bronson, R., Griffin, J.D., and Wu, L. (2006). The Notch coactivator, MAML1, functions as a novel coactivator for MEF2C-mediated transcription and is required for normal myogenesis. *Genes Dev* 20, 675-688.

Shen, Q., Wang, Y., Kokovay, E., Lin, G., Chuang, S.M., Goderie, S.K., Roysam, B., and Temple, S. (2008). Adult SVZ stem cells lie in a vascular niche: a quantitative analysis of niche cell-cell interactions. *Cell stem cell* 3, 289-300.

Sherr, C.J., and Roberts, J.M. (1999). CDK inhibitors: positive and negative regulators of G1-phase progression. *Genes Dev* 13, 1501-1512.

Shimojo, H., Ohtsuka, T., and Kageyama, R. (2008). Oscillations in notch signaling regulate maintenance of neural progenitors. *Neuron* 58, 52-64.

Shinin, V., Gayraud-Morel, B., Gomes, D., and Tajbakhsh, S. (2006). Asymmetric division and cosegregation of template DNA strands in adult muscle satellite cells. *Nat Cell Biol* 8, 677-687.

Siegel, A.L., Atchison, K., Fisher, K.E., Davis, G.E., and Cornelison, D.D. (2009). 3D timelapse analysis of muscle satellite cell motility. *Stem Cells* 27, 2527-2538.

Sinha-Hikim, I., Roth, S.M., Lee, M.I., and Bhasin, S. (2003). Testosterone-induced muscle hypertrophy is associated with an increase in satellite cell number in healthy, young men. *American journal of physiology Endocrinology and metabolism* 285, E197-205.

Smith, C.K., 2nd, Janney, M.J., and Allen, R.E. (1994). Temporal expression of myogenic regulatory genes during activation, proliferation, and differentiation of rat skeletal muscle satellite cells. *J Cell Physiol* 159, 379-385.

Snow, M.H. (1977). Myogenic cell formation in regenerating rat skeletal muscle injured by mincing. II. An autoradiographic study. *The Anatomical record* 188, 201-217.

Soleimani, V.D., Punch, V.G., Kawabe, Y., Jones, A.E., Palidwor, G.A., Porter, C.J., Cross, J.W., Carvajal, J.J., Kockx, C.E., van, I.W.F., *et al.* (2012). Transcriptional dominance of Pax7 in adult myogenesis is due to high-affinity recognition of homeodomain motifs. *Dev Cell* 22, 1208-1220.

Song, X., Zhu, C.H., Doan, C., and Xie, T. (2002). Germline stem cells anchored by adherens junctions in the Drosophila ovary niches. *Science* 296, 1855-1857.

Spitzer, M.H., and Nolan, G.P. (2016). Mass Cytometry: Single Cells, Many Features. *Cell* 165, 780-791.

Struhl, G., and Greenwald, I. (1999). Presenilin is required for activity and nuclear access of Notch in Drosophila. *Nature* 398, 522-525.

Stuelsatz, P., Shearer, A., Li, Y., Muir, L.A., Ieronimakis, N., Shen, Q.W., Kirillova, I., and Yablonka-Reuveni, Z. (2015). Extraocular muscle satellite cells are high performance myo-engines retaining efficient regenerative capacity in dystrophin deficiency. *Dev Biol* 397, 31-44.

Sun, D., Li, H., and Zolkiewska, A. (2008). The role of Delta-like 1 shedding in muscle cell self-renewal and differentiation. *J Cell Sci* 121, 3815-3823.

Sun, Y., Chen, C.S., and Fu, J. (2012). Forcing stem cells to behave: a biophysical perspective of the cellular microenvironment. *Annual review of biophysics* 41, 519-542.

Suzuki, N., Fukushi, M., Kosaki, K., Doyle, A.D., de Vega, S., Yoshizaki, K., Akazawa, C., Arikawa-Hirasawa, E., and Yamada, Y. (2012). Teneurin-4 is a novel regulator of oligodendrocyte differentiation and myelination of small-diameter axons in the CNS. *J Neurosci* 32, 11586-11599.

Tajbakhsh, S. (2009). Skeletal muscle stem cells in developmental versus regenerative myogenesis. *Journal of internal medicine* 266, 372-389.

Tajbakhsh, S., Rocancourt, D., and Buckingham, M. (1996). Muscle progenitor cells failing to respond to positional cues adopt non-myogenic fates in myf-5 null mice. *Nature* 384, 266-270.

Teta, M., Choi, Y.S., Okegbe, T., Wong, G., Tam, O.H., Chong, M.M., Seykora, J.T., Nagy, A., Littman, D.R., Andl, T., *et al.* (2012). Inducible deletion of epidermal Dicer and Drosha reveals multiple functions for miRNAs in postnatal skin. *Development* 139, 1405-1416.

Thomas, K., Engler, A.J., and Meyer, G.A. (2015). Extracellular matrix regulation in the muscle satellite cell niche. *Connective tissue research* 56, 1-8.

Thorsteinsdottir, S., Deries, M., Cachaco, A.S., and Bajanca, F. (2011). The extracellular matrix dimension of skeletal muscle development. *Dev Biol* 354, 191-207.

Tierney, M.T., Gromova, A., Sesillo, F.B., Sala, D., Spenle, C., Orend, G., and Sacco, A. (2016). Autonomous Extracellular Matrix Remodeling Controls a Progressive Adaptation in Muscle Stem Cell Regenerative Capacity during Development. *Cell reports* 14, 1940-1952.

Tucker, R.P., Kenzelmann, D., Trzebiatowska, A., and Chiquet-Ehrismann, R. (2007). Teneurins: transmembrane proteins with fundamental roles in development. *Int J Biochem Cell Biol* 39, 292-297.

Tumbar, T., Guasch, G., Greco, V., Blanpain, C., Lowry, W.E., Rendl, M., and Fuchs, E. (2004). Defining the epithelial stem cell niche in skin. *Science* 303, 359-363.

Uezumi, A., Fukada, S., Yamamoto, N., Takeda, S., and Tsuchida, K. (2010). Mesenchymal progenitors distinct from satellite cells contribute to ectopic fat cell formation in skeletal muscle. *Nat Cell Biol* *12*, 143-152.

Umansky, K.B., Gruenbaum-Cohen, Y., Tsoory, M., Feldmesser, E., Goldenberg, D., Brenner, O., and Groner, Y. (2015). Runx1 Transcription Factor Is Required for Myoblasts Proliferation during Muscle Regeneration. *PLoS genetics* *11*, e1005457.

Urciuolo, A., Quarta, M., Morbidoni, V., Gattazzo, F., Molon, S., Grumati, P., Montemurro, F., Tedesco, F.S., Blaauw, B., Cossu, G., *et al.* (2013). Collagen VI regulates satellite cell self-renewal and muscle regeneration. *Nature communications* *4*, 1964.

van Rooij, E., Quiat, D., Johnson, B.A., Sutherland, L.B., Qi, X., Richardson, J.A., Kelm, R.J., Jr., and Olson, E.N. (2009). A family of microRNAs encoded by myosin genes governs myosin expression and muscle performance. *Dev Cell* *17*, 662-673.

Vasyutina, E., Lenhard, D.C., Wende, H., Erdmann, B., Epstein, J.A., and Birchmeier, C. (2007). RBP-J (Rbpsi) is essential to maintain muscle progenitor cells and to generate satellite cells. *Proc Natl Acad Sci U S A* *104*, 4443-4448.

Vauclair, S., Majo, F., Durham, A.D., Ghyselinck, N.B., Barrandon, Y., and Radtke, F. (2007). Corneal epithelial cell fate is maintained during repair by Notch1 signaling via the regulation of vitamin A metabolism. *Dev Cell* *13*, 242-253.

Ventura, A., Young, A.G., Winslow, M.M., Lintault, L., Meissner, A., Erkeland, S.J., Newman, J., Bronson, R.T., Crowley, D., Stone, J.R., *et al.* (2008). Targeted deletion reveals essential and overlapping functions of the miR-17 through 92 family of miRNA clusters. *Cell* *132*, 875-886.

Venuti, J.M., Morris, J.H., Vivian, J.L., Olson, E.N., and Klein, W.H. (1995). Myogenin is required for late but not early aspects of myogenesis during mouse development. *J Cell Biol* *128*, 563-576.

Viatour, P., Somervaille, T.C., Venkatasubrahmanyam, S., Kogan, S., McLaughlin, M.E., Weissman, I.L., Butte, A.J., Passegue, E., and Sage, J. (2008). Hematopoietic stem cell quiescence is maintained by compound contributions of the retinoblastoma gene family. *Cell stem cell* *3*, 416-428.

Visvader, J.E., and Stingl, J. (2014). Mammary stem cells and the differentiation hierarchy: current status and perspectives. *Genes Dev* *28*, 1143-1158.

von Maltzahn, J., Jones, A.E., Parks, R.J., and Rudnicki, M.A. (2013). Pax7 is critical for the normal function of satellite cells in adult skeletal muscle. *Proc Natl Acad Sci U S A* *110*, 16474-16479.

Voog, J., and Jones, D.L. (2010). Stem cells and the niche: a dynamic duo. *Cell stem cell* *6*, 103-115.

Walker, C.S., Conner, A.C., Poyner, D.R., and Hay, D.L. (2010). Regulation of signal transduction by calcitonin gene-related peptide receptors. *Trends in pharmacological sciences* *31*, 476-483.

Wang, H., Garzon, R., Sun, H., Ladner, K.J., Singh, R., Dahlman, J., Cheng, A., Hall, B.M., Qualman, S.J., Chandler, D.S., *et al.* (2008). NF-kappaB-YY1-miR-29 regulatory circuitry in skeletal myogenesis and rhabdomyosarcoma. *Cancer cell* *14*, 369-381.

Wang, L., Chen, X., Zheng, Y., Li, F., Lu, Z., Chen, C., Liu, J., Wang, Y., Peng, Y., Shen, Z., *et al.* (2012). MiR-23a inhibits myogenic differentiation through down regulation of fast myosin heavy chain isoforms. *Exp Cell Res* *318*, 2324-2334.

Wang, Y., Medvid, R., Melton, C., Jaenisch, R., and Blelloch, R. (2007). DGCR8 is essential for microRNA biogenesis and silencing of embryonic stem cell self-renewal. *Nat Genet* *39*, 380-385.

Webster, M.T., Manor, U., Lippincott-Schwartz, J., and Fan, C.M. (2016). Intravital Imaging Reveals Ghost Fibers as Architectural Units Guiding Myogenic Progenitors during Regeneration. *Cell stem cell* *18*, 243-252.

Weerkamp, F., Luis, T.C., Naber, B.A., Koster, E.E., Jeannotte, L., van Dongen, J.J., and Staal, F.J. (2006). Identification of Notch target genes in uncommitted T-cell progenitors: No direct induction of a T-cell specific gene program. *Leukemia* *20*, 1967-1977.

Wei, W., He, H.B., Zhang, W.Y., Zhang, H.X., Bai, J.B., Liu, H.Z., Cao, J.H., Chang, K.C., Li, X.Y., and Zhao, S.H. (2013). miR-29 targets Akt3 to reduce proliferation and facilitate differentiation of myoblasts in skeletal muscle development. *Cell death & disease* *4*, e668.

Weinberg, R.A. (1995). The retinoblastoma protein and cell cycle control. *Cell* *81*, 323-330.

Weng, A.P., Ferrando, A.A., Lee, W., Morris, J.P.t., Silverman, L.B., Sanchez-Irizarry, C., Blacklow, S.C., Look, A.T., and Aster, J.C. (2004). Activating mutations of NOTCH1 in human T cell acute lymphoblastic leukemia. *Science* *306*, 269-271.

Wenstrup, R.J., Florer, J.B., Brunskill, E.W., Bell, S.M., Chervoneva, I., and Birk, D.E. (2004). Type V collagen controls the initiation of collagen fibril assembly. *J Biol Chem* *279*, 53331-53337.

Wenstrup, R.J., Florer, J.B., Davidson, J.M., Phillips, C.L., Pfeiffer, B.J., Menezes, D.W., Chervoneva, I., and Birk, D.E. (2006). Murine model of the Ehlers-Danlos syndrome. col5a1 haploinsufficiency disrupts collagen fibril assembly at multiple stages. *J Biol Chem* *281*, 12888-12895.

Wheeler, B.M., Heimberg, A.M., Moy, V.N., Sperling, E.A., Holstein, T.W., Heber, S., and Peterson, K.J. (2009). The deep evolution of metazoan microRNAs. *Evolution & development* *11*, 50-68.

White, J.D., Scaffidi, A., Davies, M., McGeachie, J., Rudnicki, M.A., and Grounds, M.D. (2000). Myotube formation is delayed but not prevented in MyoD-deficient skeletal muscle: studies in regenerating whole muscle grafts of adult mice. *The journal of histochemistry and cytochemistry : official journal of the Histochemistry Society* *48*, 1531-1544.

White, R.B., Bierinx, A.S., Gnocchi, V.F., and Zammit, P.S. (2010). Dynamics of muscle fibre growth during postnatal mouse development. *BMC Dev Biol* *10*, 21.

Wightman, B., Ha, I., and Ruvkun, G. (1993). Posttranscriptional regulation of the heterochronic gene *lin-14* by *lin-4* mediates temporal pattern formation in *C. elegans*. *Cell* *75*, 855-862.

Williams, A.H., Liu, N., van Rooij, E., and Olson, E.N. (2009). MicroRNA control of muscle development and disease. *Current opinion in cell biology* *21*, 461-469.

Wilson, A., Laurenti, E., Oser, G., van der Wath, R.C., Blanco-Bose, W., Jaworski, M., Offner, S., Dunant, C.F., Eshkind, L., Bockamp, E., *et al.* (2008). Hematopoietic stem cells reversibly switch from dormancy to self-renewal during homeostasis and repair. *Cell* *135*, 1118-1129.

Wilson, A., and Trumpp, A. (2006). Bone-marrow haematopoietic-stem-cell niches. *Nature reviews Immunology* *6*, 93-106.

Wilson-Rawls, J., Molkenin, J.D., Black, B.L., and Olson, E.N. (1999). Activated notch inhibits myogenic activity of the MADS-Box transcription factor myocyte enhancer factor 2C. *Mol Cell Biol* *19*, 2853-2862.

Winbanks, C.E., Wang, B., Beyer, C., Koh, P., White, L., Kantharidis, P., and Gregorevic, P. (2011). TGF-beta regulates miR-206 and miR-29 to control myogenic differentiation through regulation of HDAC4. *J Biol Chem* *286*, 13805-13814.

Wolfe, M.S., Xia, W., Ostaszewski, B.L., Diehl, T.S., Kimberly, W.T., and Selkoe, D.J. (1999). Two transmembrane aspartates in presenilin-1 required for presenilin endoproteolysis and gamma-secretase activity. *Nature* 398, 513-517.

Wong, C.F., and Tellam, R.L. (2008). MicroRNA-26a targets the histone methyltransferase Enhancer of Zeste homolog 2 during myogenesis. *J Biol Chem* 283, 9836-9843.

Wu, Z., Woodring, P.J., Bhakta, K.S., Tamura, K., Wen, F., Feramisco, J.R., Karin, M., Wang, J.Y., and Puri, P.L. (2000). p38 and extracellular signal-regulated kinases regulate the myogenic program at multiple steps. *Mol Cell Biol* 20, 3951-3964.

Yablonka-Reuveni, Z., and Rivera, A.J. (1994). Temporal expression of regulatory and structural muscle proteins during myogenesis of satellite cells on isolated adult rat fibers. *Dev Biol* 164, 588-603.

Yaffe, D. (1969). Cellular aspects of muscle differentiation in vitro. *Curr Top Dev Biol* 4, 37-77.

Yaffe, D., and Saxel, O. (1977). Serial passaging and differentiation of myogenic cells isolated from dystrophic mouse muscle. *Nature* 270, 725-727.

Yamaguchi, M., Watanabe, Y., Ohtani, T., Uezumi, A., Mikami, N., Nakamura, M., Sato, T., Ikawa, M., Hoshino, M., Tsuchida, K., *et al.* (2015). Calcitonin Receptor Signaling Inhibits Muscle Stem Cells from Escaping the Quiescent State and the Niche. *Cell reports* 13, 302-314.

Yavropoulou, M.P., and Yovos, J.G. (2014). The role of Notch signaling in bone development and disease. *Hormones (Athens, Greece)* 13, 24-37.

Yekta, S., Shih, I.H., and Bartel, D.P. (2004). MicroRNA-directed cleavage of HOXB8 mRNA. *Science* 304, 594-596.

Yennek, S., Burute, M., Thery, M., and Tajbakhsh, S. (2014). Cell adhesion geometry regulates non-random DNA segregation and asymmetric cell fates in mouse skeletal muscle stem cells. *Cell reports* 7, 961-970.

Yennek, S., and Tajbakhsh, S. (2013). DNA asymmetry and cell fate regulation in stem cells. *Seminars in cell & developmental biology* 24, 627-642.

Yi, R., Qin, Y., Macara, I.G., and Cullen, B.R. (2003). Exportin-5 mediates the nuclear export of pre-microRNAs and short hairpin RNAs. *Genes Dev* 17, 3011-3016.

Zammit, P.S., Heslop, L., Hudon, V., Rosenblatt, J.D., Tajbakhsh, S., Buckingham, M.E., Beauchamp, J.R., and Partridge, T.A. (2002). Kinetics of myoblast proliferation show that resident satellite cells are competent to fully regenerate skeletal muscle fibers. *Exp Cell Res* 281, 39-49.

Zammit, P.S., Relaix, F., Nagata, Y., Ruiz, A.P., Collins, C.A., Partridge, T.A., and Beauchamp, J.R. (2006). Pax7 and myogenic progression in skeletal muscle satellite cells. *J Cell Sci* 119, 1824-1832.

Zetterberg, A., and Larsson, O. (1985). Kinetic analysis of regulatory events in G1 leading to proliferation or quiescence of Swiss 3T3 cells. *Proc Natl Acad Sci U S A* 82, 5365-5369.

Zhang, D., Li, X., Chen, C., Li, Y., Zhao, L., Jing, Y., Liu, W., Wang, X., Zhang, Y., Xia, H., *et al.* (2012). Attenuation of p38-mediated miR-1/133 expression facilitates myoblast proliferation during the early stage of muscle regeneration. *PloS one* 7, e41478.

Zou, P., Yoshihara, H., Hosokawa, K., Tai, I., Shinmyozu, K., Tsukahara, F., Maru, Y., Nakayama, K., Nakayama, K.I., and Suda, T. (2011). p57(Kip2) and p27(Kip1) cooperate to maintain hematopoietic stem cell quiescence through interactions with Hsc70. *Cell stem cell* 9, 247-261.

Zou, Y., Zhang, R.Z., Sabatelli, P., Chu, M.L., and Bonnemann, C.G. (2008). Muscle interstitial fibroblasts are the main source of collagen VI synthesis in skeletal muscle: implications for congenital muscular dystrophy types Ullrich and Bethlem. *Journal of neuropathology and experimental neurology* 67, 144-154.

Abstract

Adult skeletal muscles can regenerate after repeated trauma, yet our understanding of how adult muscle satellite (stem) cells (MuSCs) restore muscle integrity and homeostasis after regeneration is limited. In the adult mouse, MuSCs are quiescent and located between the basal lamina and the myofibre. After injury, they re-enter the cell cycle, proliferate, differentiate and fuse to restore the damaged fibre. A subpopulation of myogenic cells then self-renews and replenishes the stem cell pool for future repair. The paired/homeodomain transcription factor Pax7 is expressed all skeletal muscle stem and progenitor cells and various genetically modified mice have exploited this locus for isolation and analysis of MuSCs. When MuSCs are removed from their niche, they rapidly express the commitment marker Myod and proliferate. The basal lamina that ensheaths MuSCs is rich in collagens, non-collagenous glycoproteins and proteoglycans. Whether these and other extracellular matrix (ECM) proteins constitute functional components of MuSCs niche remains unclear. Moreover, although signalling pathways that maintain MuSCs quiescence have been identified, how these regulate stem cell properties and niche composition remains largely unknown. Sustained, high activity of the Notch signalling pathway is critical for the maintenance of MuSCs in a quiescence state. Of interest, whole-genome ChIP for direct Notch/Rbpj transcriptional targets identified specific micro-RNAs and collagen genes in satellite cells. Using genetic tools to conditionally activate or abrogate Notch signalling, we demonstrate that the expression of these target genes is controlled by the Notch pathway *in vitro* and *in vivo*. Further, we propose that Collagen V and miR708 can contribute cell-autonomously to the generation of the MuSC niche via a Notch signalling-regulated mechanism.

Key words: Muscle stem cells – Niche - Notch signaling – Quiescence – micro-RNA – Extracellular matrix

Résumé

Le muscle squelettique adulte est capable de se régénérer à plusieurs reprises après blessure grâce à sa population de cellules souches résidentes : les cellules satellites. Cependant, les mécanismes impliquant les cellules satellite dans la recouvrement de l'homéostasie et de l'intégrité musculaire ne sont toujours pas clairs. Chez l'adulte, les cellules satellites sont quiescentes et localisées dans une niche entre la lame basale et la fibre musculaire. Après blessure, elles entrent à nouveau dans le cycle cellulaire, prolifèrent, se différencient et fusionnent afin de restaurer les fibres endommagées. Le pair-homeo domaine facteur de transcription Pax7 marque les cellules souches périnatales et postnatales et permet l'isolation de ces cellules à l'état souche et activé. Lorsque la niche des cellules satellite est altérée elles expriment rapidement le marqueur d'activation *Myod* puis prolifèrent. La lame basale des cellules souches est riche en collagène, glycoprotéines qui ne font pas partie de la famille des collagènes et de protéoglycan. Cependant, le mécanisme de fonction de ces protéines de la matrice extracellulaire (MEC) dans le maintien de la cellule satellite dans sa niche est toujours inconnu. De plus, l'interaction entre la MEC et des voies de signalisation cellulaire essentielles au maintien des cellules souches quiescentes sont toujours un mystère. Nous avons identifiés la voie Notch comme effecteur indispensable à la quiescence des cellules satellites. Un ChIP screening dans des cellules musculaires nous a permis d'identifier des micro-RNAs et collagènes spécifiques comme des gènes cibles de la voie Notch. L'utilisation d'outils génétiques permettant de moduler l'activité de la voie Notch démontrent que ces micro-RNAs et collagènes sont régulés transcriptionnellement par la voie Notch *in vitro* et *in vivo*. Nous proposons que le Collagène de type V et miR-708, induits par Notch, peuvent autoréguler la niche des cellules souches.

Mots clés : Cellules souches – Muscle – Niche – Voie Notch – Quiescence – micro-ARN – Matrice extracellulaire